東京帝國大學

地震研究所彙報

第 五 號

昭和三年八月發行

目 次

論 文

最近の二三の大地震の觀測及其走時曲線（第一回）（英文）……所員 松澤武雄
昭和二年十月二十七日長岡市西方の强震調査報告（邦文）……所員 松澤武雄
關東大地震並に丹後大地震に表はれたる斷層の横ずれに就いて（邦文）……所員 今村明恒／所員 岸上冬彦
關東に於ける氣壓勾配の長週期變化と地震發生との關係（英文）……所員 井上宇胤
彈性波の廻折に就て（英文）……所員 妹澤克惟
半無限體上の震動の擴散に就て（英文）……所員 妹澤克惟
彈性體の內部層に傳はるレーレー型波（英文）……所員 妹澤克惟／所員 西村源六郎
不規則なる衝撃に因る振動系の運動に關する實驗（英文）……所員 寺田寅彦／理化學研究所 中谷宇吉郎
奥丹後半島の地形發達史（邦文）……所員 多田文男
支壁式鐵筋混凝土堰堤の耐震法に就て（邦文）……所員 物部長穂
新築中の議院建築物の震動驗測（第二回）（邦文）……所員 今村明恒／所員 岸上冬彦

報 告

日本海溝の形（邦文）（轉載）……海軍水路部
丹後震災地一等水準測量第二回及第三回檢測成果比較要圖……陸地測量部

所 報

(The titles in occidental languages are given on the back cover.)

本彙報ハ不定期ニ發行ス.

本彙報掲載ノ報告ニ關シテハ著者ノミニ其責任アルモノトス.

本彙報ニ關スル照會通信ハ東京帝國大學地震研究所長ヘ宛テラレタシ.

The bulletin is published at irregular intervals.

The authors of the papers alone are responsible for the statements and opinions.

All communications relating to this bulletin should be addressed to the Director of the Earthquake Research Institute, Tokyo Imperial University.

地震研究所彙報 第五號 目次

論　文

頁

最近の二三の大地震の觀測及其走時曲線（第一回）（英文）……所員　松澤武雄‥ 1

昭和二年十月二十七日長岡市西方の强震調査報告（邦文）……所員　松澤武雄‥ 29

關東大地震並に丹後大地震に表はれたる斷層の横ずれに就いて（邦文）……所員　今村明恒‥ 所員　岸上冬彦 35

關東に於ける氣壓勾配の長週期變化と地震發生との關係（英文）……所員　井上宇胤‥ 43

彈性波の廻折に就て（英文）……所員　妹澤克惟‥ 59

半無限體上の震動の擴散に就て（英文）……所員　妹澤克惟‥ 71

彈性體の内部層に傳はるレーレー型波（英文）……所員　妹澤克惟‥ 所員　西村源六郎 85

不規則なる衝撃に因る振動系の運動に關する實驗（英文）……所員（理化學研究所）　寺田寅彦　中谷宇吉郎 93

奥丹後半島の地形發達史（邦文）……所員　多田文男 111

支壁式鐵筋混凝土堰堤の耐震法に就て（邦文）　所員　物部長穂‥ 123

新築中の議院建築物の震動驗測（第二回）（邦文）　所員　今村明恒‥ 所員　岸上冬彦 143

報　告

日本海溝の形（邦文）（轉載）……海軍水路部‥ 163

丹後震災地一等水準測量第二回及第三回檢測成果比較要圖‥陸地測量部‥ 165

所　報……167

CONTENTS OF VOLUME V

Papers Contributed

		Page
Observations of some of recent Earthquakes and their Time-Distance Curves. (Part I)(in English)	T. Matuzawa	1
Report of Inspection of the Strong Etigo Earthquake, Oct. 27, 1927. (in Japanese)	T. Matuzawa	29
On the Horizontal Shift of the Dislocation accompanied by the Recent Destructive Earthquakes in the Kwantô District and in Tango Province. (in Japanese)	A. Imamura F. Kishinouye	35
On the Correlation between the Long Period Fluctuation of Barometric Grandient and the Occurrence of Earthquakes in Kwantô District, Japan. (in English)	W. Inouye	43
On the Diffraction of Elastic Waves. (in English)	K. Sezawa	59
On the Diffusion of Tremors on the Surface of a Semi-infinite Solid Body. (in English)	K. Sezawa	71
Rayleigh-type Waves propagated along an Inner Stratum of a Body. (in English)	K. Sezawa G. Nishimura	85
Experiments on the Effect of an Irregular Succession of Impulses upon a Simple Vibrating System. (in English)	T. Terada U. Nakaya	93
Physiographic History of the Oku-Tango Peninsula. (in Japanese)	F. Tada	111
New Method of Improving the Seismic Stability of Reinforced Concrete Dams. (in Japanese)	N. Mononobe	123
On the vibration of the Imperial Diet Building. (Second report) (in Japanese)	A. Imamura F. Kishinouye	143

Reports

Form of the Japan Trench. (in Japanese) (Reproduction)	Hydrographic Department	163
Comparison of the Results of the Second and Third Precise Levelling in the Region Disturbed by the Tango Earthquake. (in Japanese)	Land Survey Department	165

Institute Notes 167

東京帝國大學

地震研究所彙報

第　五　號

Observation of some of recent Earthquakes and their Time-Distance Curves. (Part 1)

By

Takeo MATUZAWA.

Aramasi no Kotogara (Abstract in Japanese.)

(1) Etigo no Zisin (1927 nen 10 gt 27 nt) wo Tôkyô de kwansokusita Kekkwa ni yoruto Singen-Kyori ni taisite Syokibidô no Keizoku-Zikan ga itumo yori medatte sukunakatta.

(2) Ue no Kotogara wo akirakani suru Tame ni Zisin-ha no Tôtyaku-Zikan to Kyori tono Kwankei wo sirabeta.

(3) Hyômen de Tihen wo tomonau yôna ookii Zisin no Baai niwa Nippon demo P, P,* $\overline{P}$ ni ataru Nami no aru Kotoga wakatta.

(4) Etigo no Zisin dewa P Nami wa mattaku miusinawareta rasii.

(5) Ippanni ono-ono no Sô (phase) wa Singen no Iti ya sono Okorikata ni kwankeisite aru Basyo dewa taihen mitomegatai.

(6) $\overline{P}$ Nami no Hayasa wa 5.0 km/sec., P* wa 6.1 km/sec., gurai, Hyômen no Sô no Atusa wa 20 km. gurai ni naru.

(7) Oozisin no Baai niwa $\overline{P}$ Nami wa Hyômen ni taihen tikai Tokoro kara okoru yôni mieru. P Nami wa musiro Betu na Tokoro, sarani hukai Tokoro kara hiki-okosareru to kangaerareru. Sosite P Nami ni taisitewa "Epicentre" naru hitotu no Ten wo sadameru koto wa aru Tôkei-teki no Heikin yori hoka no Imi ga nai to omowareru.

(8) Oozisin no *Energy* no takuwaerareru Basyo wo P oyobi $\overline{P}$ wo okosu hutatu no Basyo ni wakete kangaeruto Zisin-hassei no Zikanteki-Bunpu no Riron no aru Konnan-na Ten ga sukosiku torinozokareru yôni omowareru.

I. Introduction.

On Oct. 27, 1927 a strong earthquake took place in Etigo Province, the geographic coordinates of which were $\varphi=37^\circ\ 27'N$ and $\lambda=138^\circ\ 46'E$. The author was appointed by the Director of this institute, Professor K. Suyehiro, to study this earthquake, and some phenomena directly accompanied with it are explained in another paper.[1] By way of instrumental study of this earthquake, the author came to a fact that the ratio of the epicentral distance to the duration of the preliminary tremor at Tôkyô was 8.6 and much greater than the ordinary value 7.44. For elucidation of this fact, it was necessary to study time-distance relation of the propagation of seismic waves, and instrumental records.

In addition to that, the time-distance curve within a small epicental distance, say less than 2000 km., in general is not yet very clear, although that of greater distance has been precisely studied by many authorities. The precise study of it is very important for investigation of the earth's crust.

Principal aim of this paper consists in promotion of precision of numerical values already obtained by senior authorities, so that nothing original may be found.

II. Investigation of the Etigo Earthquake,[2] Oct. 27, 1927.

This earthquake was very local, so that its epicentre was determined precisely. Thus the principal merit of this case in studying the propagation of seismic waves consists in the accurate determination of epicentral distances. A pair of seismograms obtained at Hongô (Tôkyô) is as shown in Pl. I. Fig. 1. The time of commencement of the phase marked "1" was $10^h\ 54^m\ 17.^s5$ (L. M. T of $\lambda=135^\circ E$) and is very consistent to that reported by the Central Meteorological Observatory. The duration of the preliminary tremor (1–3) is 25 sec and that by the Central Meteorological Observatory is 24.7 sec., which is also very consistent. Slow motions between "mark 2" and "3" may perhaps be a manifestation of pulsatory motions then prevailing, for such waves could not be identified at other stations such as Titibu (Pl. II. Fig. 2), Kamakura, Misaki, Kiyosumi-yama, etc.

In the next place, the time-distance relation of seismic waves is plotted in Fig. 3.

(1) T. Matuzawa, this Bull. **5** (1928), 29.

(2) During the preparation of this paper, the author came across a paper by Dr. S. I. Kunitomi on the same earthquake (Journ. Meteor. Soc. Japan. [ii] **6** (1928) 59–85), and yet my paper contains somewhat different views.

Time-distance curve of Etigo Earthquake, Oct. 27, 1927.

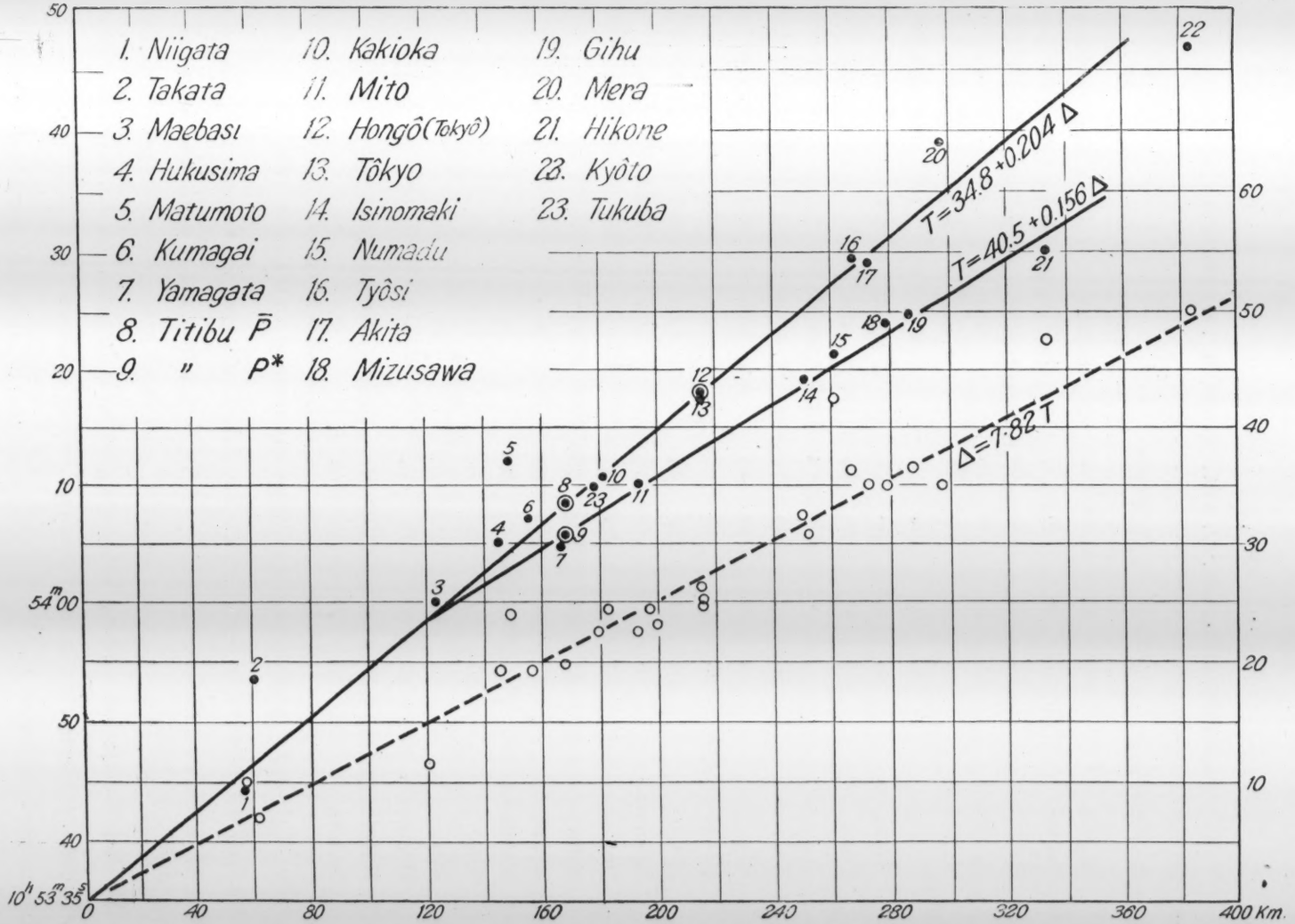

Dot: Time of commencement. Circle: Duration of preliminary tremor.
Origin of time for empirical formula, 10^h53^m (L.M.T. of $\lambda = 135°$ E)

Fig. 3.

The data were adopted from the report of the Central Meteorological Observatory and tabulated below. (Table I.)

TABLE I.

Etigo Earthquake, Oct. 27, 1927. ($\varphi=37°\ 27'$, $\lambda=138°\ 46'$)

No.	Station	Latitude	Longitude	T. of Comm. L.M.T of $\lambda=135°E$	*P. T.* sec.	Δ km.
				h m s		
1	Niigata	37° 55′	139° 03′	10 53 44.2	9.8	57.5
2	Takata	37 06	138 15	53.7	7.2	60.2
3	Maebasi	36 24	139 04	54 00.0	27.0	122.4
4	Hukusima	37 45	140 24	05.0	19.4	144.7
5	Matumoto	36 14	137 59	12.0	24.0	148.4
6	Kumagai	36 09	139 24	07.1	19.1	155.8
7	Yamagata	38 15	140 21	04.6	19.6	167.0
8	Titibu (P^*)	35 59	139 05	05.6		168.4
9	,, ($\bar{P}$)	,,	,,	08.0		
10	Kakioka	36 14	140 11	10.6	24.3	181.8
11	Mito	36 23	140 28	10.0	22.7	193.0
12	Hongô (Tôkyô)	35 43	139 46	17.5	25.0	215.
13	Tôkyô	35 41	139 46	17.9	24.7	215.
14	Isinomaki	38 26	141 19	19.0	32.3	250.4
15	Numazu	35 06	138 51	21.5	42.6	261.6
16	Tyôsi	35 44	140 51	29.7	36.3	267.1
17	Akita	39 41	140 06	29.0	35.1	272.7
18	Mizusawa	39 08	141 08	24.0	35.0	278.3
19	Gihu	35 24	136 46	24.9	36.5	287.5
20	Mera	34 55	139 50	38.9	34.9	296.8
21	Hikone	35 16	136 15	30.0	47.5	334.0
22	Kyôto	35 01	135 44	46.6	50.2	384.0
23	Tukuba	36 13	140 06	10.0	22.5	178.1

Remark: The time of commencement at Titibu was assumed on the curve (Fig. 3.)

As apparent from the figure, two branches of straight lines can clearly be seen one of which is characterised by $d\Delta/dT=4.99$ km/sec. and the other by $d\Delta/dT=6.4$ km/sec. The values observed at Tôkyô belong to the upper branch. From the distribution of stations belonging to each branch, no directional effect can be found. Moreover, it is remarkable that stations belonging to the upper branch are mainly those in the Kwantô plain. Thus a supposition is at hand that the forerunning part belonging to the lower branch was masked by the pulsatory motion of the earth's crust then having been prevailing and missed

from observation, or rather could not be identified. Indeed, at Titibu the two phases were clearly observed. (Pl. II. Fig. 2).

The next point to be considered is that to which phase of waves each branch of curves belongs. This point can easily be explained by assuming a mechanism similar to that of Mohorovičić. Then the velocity in the upper layer becomes 4.99 km/sec. and that in the lower layer is 6.4 km/sec. The former value seems too small compared with the current value 5.56 km/sec. of P waves by European authorities, but is very near to that obtained by G. Krumbach.[1]

The latter value 6.4 km/sec. is near to the European value of P^* waves,[2] 6.2 km/sec. Thus assuming tentatively as such, the depth of the first discontinuity can be calculated. The time difference of P and P^*, τ, is given by

$$\tau=\frac{\sqrt{\Delta^2+f_1^2}}{v_1}-(2d_1-f_2)\frac{\cos i}{v_1}-\frac{\Delta}{v_2},$$

where d_1 is the depth of the first discontinuity,

v_1 ,, ,, velocity of P waves,

v_2 ,, ,, ,, ,, P^* ,, ,

f_1 ,, ,, depth of the origin of P waves,

f_2[3] ,, ,, ,, ,, ,, ,, ,, P^* ,, ,

Δ ,, ,, epicentral distance

and i is defined such that $\sin i=v_1/v_2$.

The distance for which $\tau=0$ is $\Delta=118$ km. Therefore,

$$d_1=18.2+f_2/2+f_1^2/125 \text{ in km.}$$

The depth of the seismic origin is not very clear but is doubtlessly not deep. Perhaps d_1 may plausibly be 20 km. or so.

III. Review of Some of Recent Great Earthquakes.

The values experienced in the foregoing example are much different from current values. And moreover, no literature with regard to the existence of the P^* phase in Japan can be found. Besides these, if each branch of curves in the above example is interpreted as above, another question arises that why the phase P was not present in that case. It may remain doubtfull that the phase interpreted here as P^* might correspond to the P phase, but this is not the case as discussed later. The reason why the P phase was missed is supposed as follows:

(1) G. Krumbach, über die Fortpflanzungsgeschwindigkeit der direkten Longitudinalwellen bei künstliche Beben, Zeits. f. Geophys. **2** (1926) 30-33.

(2) See B. Gutenberg, Der Aufbau der Erdkruste; Zeits. f. Geophys. **3** (1927) Hft. 7.

(3) The reason why distinguishing f_1 and f_2 will be discussed later.

that is, that earthquake was a very local shock and its energy was not sufficient to transmit P waves as detected by ordinary instruments. In addition to this, the pulsatory motion then having been prevailing disturbed much some of instrumental records and identification of the phase was much unfavourable.

If such consideration is not wrong, investigation of earthquakes of vast scale will reveal some evidence concerning the above stated inferences.

In doing so, earthquakes to be chosen must be those of distinct epicentre, because an error of epicentral distances even within a few tens of kilometers, which value is often probable in some cases, will produce a serious mistake with regard to the classification of waves.

Review of the Great Tango Earthquake, March 7, 1927.

Full reports concerning this earthquake instrumentally observed have been already published by such authorities as Dr. S. I. Kunitomi[1] and Professor A.Imamura.[2] Hence in this paper precise description will be omitted.

Indeed, instrumental records at Hongô (Tôkyô) (Pl. III. Fig. 4)[3] and at Kamakura (Pl. IV. Fig. 5)[4] will show very clearly three steps as marked P, P^* and $\bar{P}$. The time of commencement of the P phase can be determined by much sensitive instruments such as shown in Fig. 1 of Prof. Imamura's paper. The commencement of P was $18^h\ 28^m\ 43^s$ (L. M. T of $\lambda=135°$) on March 7, 1927 and the duration $P-P^*$ was $10.^s3$ and that of $P-\bar{P}$ was $22.^s5$ ($\Delta=427$ km). The time of commencement at Kamakura was not certain because the time keeping was not sufficient. The duration of each phase, however, could be determined very well such that $P-P^*$ was $9.^s2$ and $P-\bar{P}$, $19.^s2$ ($\Delta=410$ km).

Thus, existence of three phases in the preliminary tremor is almost beyond doubt, but for interpretation of these phases their time-distance relations must be carefully examined, for such a characteristic appearance may also be produced by step-wise occurrence of earthquake. In Pl. V. Fig. 6, reported values of time of commencement are plotted taking the epicentral distance as the abscissa. The values of time of commencement were adopted from Dr. S. I. Kunitomi's paper,[5] and tabulated below with some modifications of epicentral distances taking the epicentre as $\varphi=35°\ 38'N$, $\lambda=135°\ 03'E$.

(1) S. I. Kunitomi, Journ. Meteor. Soc. Japan [ii] **5** (1927) 8.
(2) A. Imamura, This Bull. **4** (1928) 179–202.
(3), (4). These figures are the same as those of Prof. Imamura's paper (ibid. Fig. 3 and Fig. 4), but with slight modifications of notations.
(5) l. c.

TABLE II.

Tango Earthquake, March 7, 1927. ($\varphi = 35°\ 38'N.$ $\lambda = 135°\ E.$)

No.	Station	Latitude	Longitude	T. of Comm. L.M.T of $\lambda = 135°\ E$	PP	P T	Epicentral Dist. km.
				h m			
1	Miyazu	35° 32′	135° 12	18 27 43.5			17.5
2	Toyooka	,,	134 49	43.8			24.6
3	Kyôto	35° 01	135 44	56.9			92.5
4	Kôbe	34 41	135 11	58.1			106.
5	Oosaka	34 39	135 26	56.8			114.
6	Hikone	35° 16′	136° 15′	28 00.0			116.
7	Hukui	36° 03	136 16′	27 59.0			125.7
8	Yagi	34 31	135 48	28 02.6			140.5
9	Sumoto	34 21	134 53	27 58.0			148.
10	Okayama	34 40	133 54	28 08.7			149.
11	Gihu	35 24	136 46	00.7			157.2
12	Wakayama	34 14	135 09	05.			160.
13	Sakai	35 33	133 14	03.0			163.
14	Tu	34 44	136 31	07.2			170.
15	Nagoya	35 10	136 58	10.0			176.
16	Tokusima	34 04	134 33	19.			179.
17	Tadotu	34 17	133 46	18.0			193.
18	Takayama	36 09	137 15	04.9			209.
19	Husiki	36 47	137 03	15.9			223.
20	Hirosima	34 23	132 27	19.2			231.
21	Sisakazima	34 06	133 11	15.0			239.
22	Niihama	33 58	133 16	14.0			246.
23	Iida	35 31	137 50	19.2			255.
24	Siomisaki	33 27	135 46	30.			255.
25	Kôti	33 33	133 32	18.1			267.
26	Hamamatu	34 43	137 43	40.			267.
27	Kure	34 14	132 33	32.0			273.
28	Matumoto	36 14	137 59	27.0			274.
29	Hamada	34 54	132 04	19.	3.9		280.
30	Matuyama	33 50	132 45	28.	4.3		285.
31	Nagano	36 40	138 12	24.7	6.2		306.
32	Kôhu	35 38	138 34	40.			320.
33	Takada	37 06	138 15	31.2	6.8		332.
34	Numazu	35 06	138 51	31.8	6.8		352.
35	Maebasi	36 24	139 04	34.6			376.

to be continued.

(Continued.)

No.	Station	Latitude		Longitude		T. of Comm. L.M.T of $\lambda=135°E$			$P\bar{P}$	$P.\ T.$	Epicentral Dist.
						h	m	s			
36	Kumagai	36	09	139	23		28	39.3	8.2	52.3	399.
37	Ooita	33	14	131	37			38.7		56.0	411.
38	Yokohama	35	27	139	39			47.2			421.
39	Yokosuka	35	17	139	40			39.			423.
40	Hongô (Tôkyô)	35	43	139	46			43.0			427.
41	Tôkyô	35	41	139	46			42.2	9.9	53.7	431.
42	Niigata	37	55	139	03			35.5	15.6	54.0	441.
43	Mera	34	55	139	50			46.6		49.0	444.
44	Utunomiya	36	34	139	53			57.9			446.
45	Tukuba	36	13	140	06			48.4		65.0	469.
46	Kakioka	36	14	140	11			46.	14.4	67.2	472.
47	Hukuoka	33	35	130	25			43.2		68.8	480.
48	Mito	36	23	140	28			50.		57.0	500.
49	Kumamoto	32	49	130	42			54.6		73.	505.
50	Hatizyô	33	06	139	50		29	27.			521.
50	Miyazaki	31	55	131	26		28	57.9		77.1	527.
51	Tyôsi	35	44	140	51			50.6		70.3	530.
52	Unzen	32	44	130	15		29	00.0		71.8	545.
53	Onahama	36	56	140	54			26.0			548.
54	Izuhara	34	12	129	17		28	50.0		72.0	546.
55	Husan	35	06	129	01			49.		66.0	546.
56	Yamagata	38	15	140	21			57.5		68.4	556.
57	Nagasaki	32	44	129	52		29	06.0			573.
58	Sendai	38	16	140	54			00.3			596.
59	Saga	33	12	130	18		28	59.6			609.
60	Kagosima	31	34	130	33		29	02.8			612.
61	Akita	39	41	140	06			06.0		78.5	633.
62	Isinomaki	38	26	141	19			07.8			636.
63	Mizusawa	39	08	141	08			12.8			662.
64	Morioka	39	42	141	10			13.8		78.0	703.
65	Miyako	39	38	141	59			51.			754.
66	Zinsen	37	29	126	37			23.1		89.0	780.
67	Hakodate	41	47	140	43			35.2			840.
68	Muroran	42	20	140	57		30	29.			901.
69	Nase	28	23	129	30		29	25.0			957.
70	Sapporo	43	04	141	21		29	46.5			986.

to be continued.

(Continued.)

No.	Station	Latitude		Longitude		T. of Comm. L.M.T of $\lambda=135°E$			$P\bar{P}$	$P.\ T$	Epicentral Dist.
						h	m	s			
71	Obihiro	42	55	143	12			59.			1073.
72	Asahigawa	43	47	142	22		30	05.			1099.
73	Kusiro	42	59	144	24			07.			1132.
74	Titizima	27	05	142	10			23.6			1162.
75	Dairen	38	54	121	38			12.			1238.
76	Nemuro	43	20	145	35		30	29.5			1240.
77	Ootomari	46	39	142	46			43.			1414.

Remark: Seismometrical elements were adopted (except Hongô) from Dr. S. Kunitomi's paper (Journ. Meteor. Soc. Japan [ii] **5** (1927) no. 8). The reported time of commencement at Onahama and Nemuro seems too earlier by one minute perhaps by accidental mistake of calculation of time marks. Therefore, in the table values with the correction are adopted.

In Fig. 6, the dot represents the reported time of commencement, the circle is plotted such that to represent the value of $P\bar{P}$ of Dr. Kunitomi's paper measured from the corresponding point on the P curve. Values obtained at Hongô and at Kamakura (represented by the concentric circle) were carefully measured by the present author. As to be seen from the figure, the distribution of the time of commencement can be classified into three groups in this case also. The upper curve (straight line) is characterised by $d\Delta/dT=5.0$ km/sec. and the middle is by $d\Delta/dT=5.9$ km/sec. The former value is quite consistent with that experienced in the case of the Etigo Earthquake. The latter value is somewhat smaller than the value in that case. The value 6.4 km/sec. may, however, be perhaps somewhat too large. In Fig. 3, if the point marked " 21 " is omitted, a smaller value will be obtained. At any rate, it is almost beyond doubt that the curve characterised by 6.4 km/sec. in the case of the Etigo earthquake will correspond to the middle branch of curves in this case. Besides these, the lowest curve which seems to belong to P waves has been obtained as expected. Thus the supposition that the P waves of the Etigo earthquake were missed from observation turns out highly probable. It is also almost doubtless that P, P^* and $\bar{P}$ phases are observed in Japan also as in the continent. The phase reported by Mr. Kunitomi as $\bar{P}$ waves seems to correspond to that of P^* waves. It may seem queer that at certain stations the P phase or both P and P^* phases are missed from observation in such a great earthquake. Many factors can, however, be considered for explaining such a fact, for examples, sensitivity of instrument, mechanism of occurrence of earth-

quake, disturbance of earth's crust other than seismic waves at those stations etc. Among these factors, the author is inclined to believe that the mechanism at the seismic origin may play an essential rôle as once discussed by the author.[1] Thus we must be very circumspect in discussing any thing concerning directional properties of propagation of seismic waves.

From these two earthquakes, the velocity of propagation of dilatational waves in the uppermost layer in Japan is very probably 5.0 km/sec. and that of the next layer is 6.1 km/sec. or so. Taking these values, the depth of the discontinuity will be re-examined. In this case the distance Δ at which the P^* and $\bar{P}$ arrive simultaneously is 62 km. Therefore

$$d_1 = 9.8 + f_2/2 + 0.00705\, f_1^2 \text{ in km.}$$

In this case also values of f_1 and f_2 are not exactly known. If $f_2 = 15$ km.[2] and $f_1 = 10$ km. tentatively (these values are very probable), then $d_1 = 18.0$ km. Thus the depth of the first discontinuity will be taken as some 20 km in a round number.

The curve P will be discussed later.

Review of the Great Tazima Earthquake, May 23, 1925.

This earthquake occurred also in the land and its epicentre could be determined well. The seismograms recorded at Hongô are shown in Pl. VI. Fig. 7. On the case of this earthquake Dr. K. Wadati[3] drew attention for the first time in Japan the existence of the P and $\bar{P}$ waves. In this case also the three phases P, P^* and $\bar{P}$ can be identified in Fig. 7, especially clear in the vertical component. The time of commencement at Hongô was $11^h\ 10^m\ 49^s$ (L. M. T of $\lambda = 135°E$) on May 23, 1925. The duration $P - P^*$ was 10 sec and that of $P - \bar{P}$ was 20 sec. $P - (S^*) = 59.0$, $P - (\bar{S})$ or $P - (L) = 75.5$. Again the time-distance relation of propagation of seismic waves will be examined using mainly the reported values of the time of commencement at certain stations. The data are tabulated in Table III.

The values are plotted in Fig. 8.

The broken lines representing the time-distance curve are so drawn that the uppermost line coincides with that of the Tango earthquake (Fig. 6) and

(1) T. Matuzawa, Japanese Journ. Astr. Geophy. **4** (1926) no. 1.

(2) Dr. N. Nasu read a paper at the colloquium of this Institute that the depth of aftershocks of this earthquake was mainly distributed within this value.

(3) K. Wadati, Journ. Meter. Soc. Japan [ii] **3** (1925) 201–211.

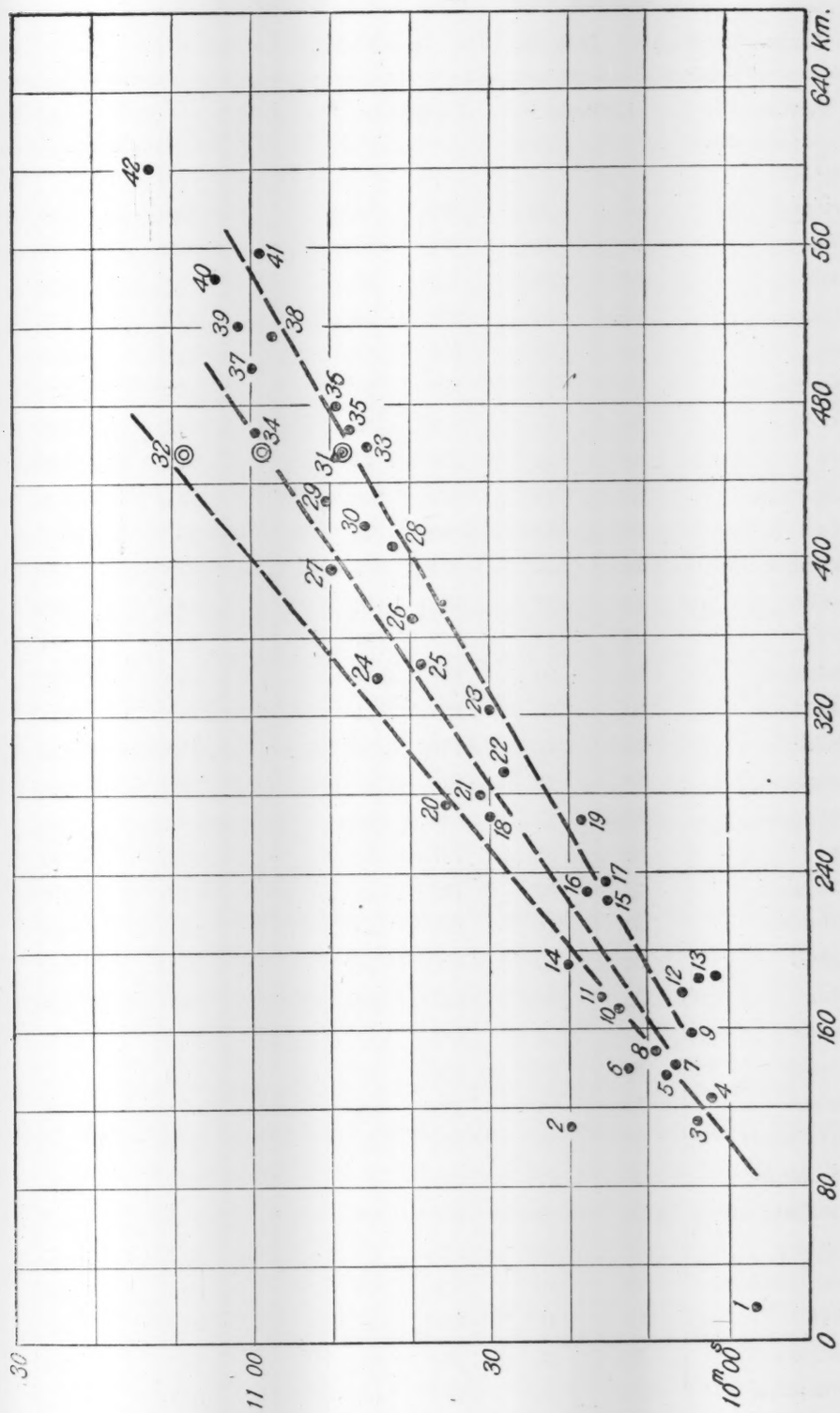

Time-distance curves (broken lines) are tentatively drawn comparing with those of the Great Tango earthquake.

Fig. 8.

TABLE III.

Tazima Earthquake, May 23, 1925. ($\varphi = 35° 38'.5$, $\lambda = 134° 50'$)

No.	Station	Latitude		Longitude		T. of Comm. L.M.T of $\lambda = 135°E$			Δ
						h	m	s	
1	Toyooka					11	9	57.0	
2	Turuga	35	38	136	03		10	20.0	110
3	Kôbe	34	41	135	11			04.4	112
4	Oosaka	34	39	135	26			01.8	124
5	Hikone	35	16	136	15			08.2	137
6	Hukui	36	03	136	16			12.0	138
7	Okayama	34	40	133	54			07.4	140
8	Sumoto	34	21	134	53			09.2	149
9	Yagi	34	31	135	48			05.0	158
10	Wakayama	34	14	135	09			14.0	169
11	Gihu	35	24	136	46			16.7	177
12	Tokusima	34	04	134	33			06.0	178
13	Tadotu	34	17	133	46			04.0	185
14	Kure	34	14	132	33			20.6	194
15	Takayama	36	09	137	15			15.6	225
16	Sisakazima	34	06	133	11			18.0	231
17	Husiki	36	47	137	03			15.8	235
18	Hirosima	34	23	132	27			30.4	265
19	Siomisaki	33	27	135	46			18.6	266
20	Iida	35	31	137	50			35.9	273
21	Matuyama	33	50	132	45			31.0	279
22	Matumoto	36	14	137	59			28.0	291
23	Nagano	36	40	132	12			30.0	322
24	Kôhu	35	38	138	34			44.0	338
25	Takada	37	06	138	15			38.2	346
26	Numazu	35	06	138	51			39.1	371
27	Maebasi	36	24	139	04			50.2	393
28	Simonoseki	33	57	130	56			42.0	405
29	Yokohama	35	27	139	39			50.5	430
30	Kumagai	36	09	139	23			45.8	416
31	Niigata	37	55	139	03			49.3	453
32	Hongô (Tôkyô)	35	43	139	46			49.0	455
33	Tôkyô	35	41	139	46			45.5	455
34	Hukuoka	33	35	130	25			59.7	464
35	Utunomiya	36	34	139	53			47.8	466

to be continued.

(Continued.)

No.	Station	Latitude		Longitude		T. of Comm. L.M.T of $\lambda=135°E$	Δ
						h m s	
36	Mito	36	23	140	28	10 57.0	514
37	Miyazaki	31	55	131	26	11 02.1	520
38	Tyôsi	35	44	140	51	04.8	543
39	Nagasaki	32	44	129	52	10 59.0	556
40	Kagosima	31	34	130	33	11 13.0	601
41	Tukuba	36	13	140	06	49.6	479
42	Saga	33	12	130	18	11 00.0	497

Remark: The reported value of time of commencement at Tokusima seems to be too small by one minute, perhaps being due to a mistake of calculation of time marks.

other lines are drawn in just the same position relative to the uppermost one as in Fig. 6. In this case, points representing time of commencement scatter somewhat irregular, and yet are included well between the P and the $\bar{P}$ curve. This fact can easily be explained by considering that the energy of producing the P wave was not sufficient to be observed everywhere. Indeed, the observed values at Hongô are quite reconcilable in this case also. Moreover, the P and the $\bar{P}$ curve are clearly defined by drawing the boundary of the domain of the distributed points. This will also furnish an evidence of the above stated idea. It may be remarked that the P wave seems to be rather well defined at a remote stations beyond 400 km. compared with the nearer stations ($280<\Delta<400$ km.) in this case. Closer examination of distribution of stations will show that most stations with later commencement are situated almost in the $E-W$ direction relative to the epicentre, as stated by Dr. S. I. Kunitomi.[1] A contrary proposition that stations distributed in the $E-W$ direction show later commencement than that represented by the lowest curve (Fig. 8) without exception is not the case. For example, Nagano (23), Simonoseki (28), Niigata (31) Tôkyô (32, 33) etc. This point will be discussed later. Here it will only be remarked that the P phase was quite small compared with the principal part observed at Hongô (See Fig. 7) which is situated almost in the East direction.

Tango earthquake on April 1, 1927.

This is one of after-shocks of the Great Tango earthquake on March 7.

(1) S. Kunitomi, Journ. Meteor. Soc. Japan [ii] **3** (1925) no. 7.

According to Dr. N. Nasu, its epicentre was determined as $\varphi=35°\ 28'N$ and $\lambda=135°\ 07'$ by seismic triangulation. Instrumental records at Hongô are shown in Pl. VII. Fig. 9. The time of commencement at Hongô was $6^h\ 9^m\ 37^s.3$ (L.M.T $\lambda=135°E$) Careful study of the records will also reveal the existence of three phases P, P^* and $\bar{P}$. The duration of $P-P^*$ was $6^s.75$ and $P-\bar{P}$ was $18^s.1$. $P-(S)=42^s$, $P-(S^*)=54^s$, and $P-(\bar{S})=73^s$. It is remarkable that magnitude of the preliminary phase of this earthquake observed at Hongô was quite small compared with the principal part.

In the next place, the time-distance relation of propagation of seismic waves will be examined as before. The values of time of commencement were adopted from "Kisyô-Yôran" published by the Central Meteorological Observatory, and tabulated below.

TABLE IV.

Tangô Earthquake, April 1, 1927. ($\varphi=35°\ 28'$, $\lambda=135°\ 07'$)

No.	Station	Latitude		Longitude		T. of Comm. L.M.T of $\lambda=135°E$			P. T sec.	Δ km.
						h	m	s		
1	Miyaz	35	32	135	12	6	08	29.3		10.6
2	Toyooka	"		134	49			42.6	3.8	40.2
3	Kyôto	35	01	135	44			49.9	9.8	75.2
4	Kôbe	34°	41	135	11			52.0	13.0	87.1
5	Oosaka	34	39	135	26			51.3	15.5	95.1
6	Hikone	35	16	136	15			57.6	13.2	105.4
7	Yagi	34	31	135	48		09	00.0		122.5
8	Hukui	36	03	136	16		08	52.5	13.0	123.
9	Sumoto	34	21	134	53			57.2	17.4	126.
10	Wakayama	34	14	135	09			59.0	22.5	136.9
11	Okayama	34	40	133	54		09	00.0	17.1	140.5
12	Gihu	35	24	136	46		08	54.7	18.6	148.0
13	Tu	34	44	136	31		09	10.7	20.0	151.1
14	Tokusima	34	04	134	33		08	54.0	23.0	164.
15	Sakai	35	33	133	14		09	20.7	22.8	168.3
16	Nagoya	35	10	136	58			6.8	22.3	170.1
17	Tadotu	34	17	133	46			28.0	19.0	175.7
18	Kanazawa	36	32	136	39			21.0	23.0	181.2
19	Takayama	36	09	137	15			9.0	25.9	205.3
20	Husiki	36	47	137	03			10.9	35.6	225.6
21	Siomisaki	33	27	135	46			2.0	35.0	231.5
22	Iida	35	31	137	50			13.7	32.6	244.1

to be continued.

(Continued.)

No.	Station	Latitude		Longitude		T. of Comm. L.M.T of $\lambda=135°E$	P. T	Δ
						h m s		
23	Kôti	33	33	133	32	09 14.6	33.2	253.3
24	Hirosima	34	23	132	27	19.9	39.0	268.1
25	Matumoto	36	14	137	59	10.0	39.0	268.1
26	Kure	34	14	132	33	29.3	52.4	270.0
27	Matuyama	33	50	132	45	39.8	41.7	283.
28	Hamada	34	54	132	04	19.7	37.3	283.0
29	Nagano	36	40	138	12	24.9	40.2	307.0
30	Kôhu	35	38	138	34	10 4.0	14.0	323.6
31	Takada	37	06	138	15	09 34.2	38.8	333.0
32	Numazu	35	06	138	51	31.5	48.3	340.2
33	Kumagai	36	09	139	23	39.6	56.4	390.2
34	Yokohama	35	27	139	39	48.7	40.3	408.6
35	Tôkyô	35	41	139	46	42.8	54.6	420.
35′	Hongô (Tôkyô)	35	43	135	46	9 37.3		419.
36	Maebasi	36	24	139	04	41.2	38.9	426.
37	Mera	34	55	139	50	48.5	50.4	429.
38	Utunomiya	36	34	139	53	38.1	55.0	444.
39	Niigata	37	55	139	03	50.1	56.5	444.
40	Tukuba	36	13	140	06	31.3	51.8	453.7
41	Kakioka	36	14	140	11	41.5	1m 11.5	462.
42	Ooita	33	14	131	37	37.0	56.0	465.
43	Hukuoka	33	35	130	25	47.2	1m 03.8	477.
44	Mito	36	23	140	28	49.0	1m 00.0	479.
45	Kumamoto	32	49	130	42	10 4.3	1m 16.6	501.
46	Miyazaki	31	55	131	26	09 53.0	1m 16.0	519.
47	Tyôsi	35	44	140	51	10 2.1		518.
48	Onahama	36	56	140	54	09 55.6	1m 11.1	544.
49	Izuhara	34	12	129	17	10 2.3	1m 00.0	551.
50	Nagasaki	32	44	129	52	7.7	1m 19.4	569.
51	Kagosima	31	34	130	33	1.9	1m 32.9	603.
52	Akita	39	41	140	06	27.3	1m 25.2	640.
53	Isinomaki	38	26	141	19	6.4	1m 41.9	639.
54	Mizusawa	39	08	141	08	10.0	1m 12.0	669.6
55	Morioka	39	42	141	10	9.2	1m 30.7	708.
56	Hakodate	41	47	140	43	58.8	1m 27.3	850.

Remark: The reported values at Kôhu and Onahama may be too small by one minute.

These values are plotted in Fig. 10.

Time-distance curve of one of after-shocks of the Great Tango Earthquake, Apil 1, 1927.

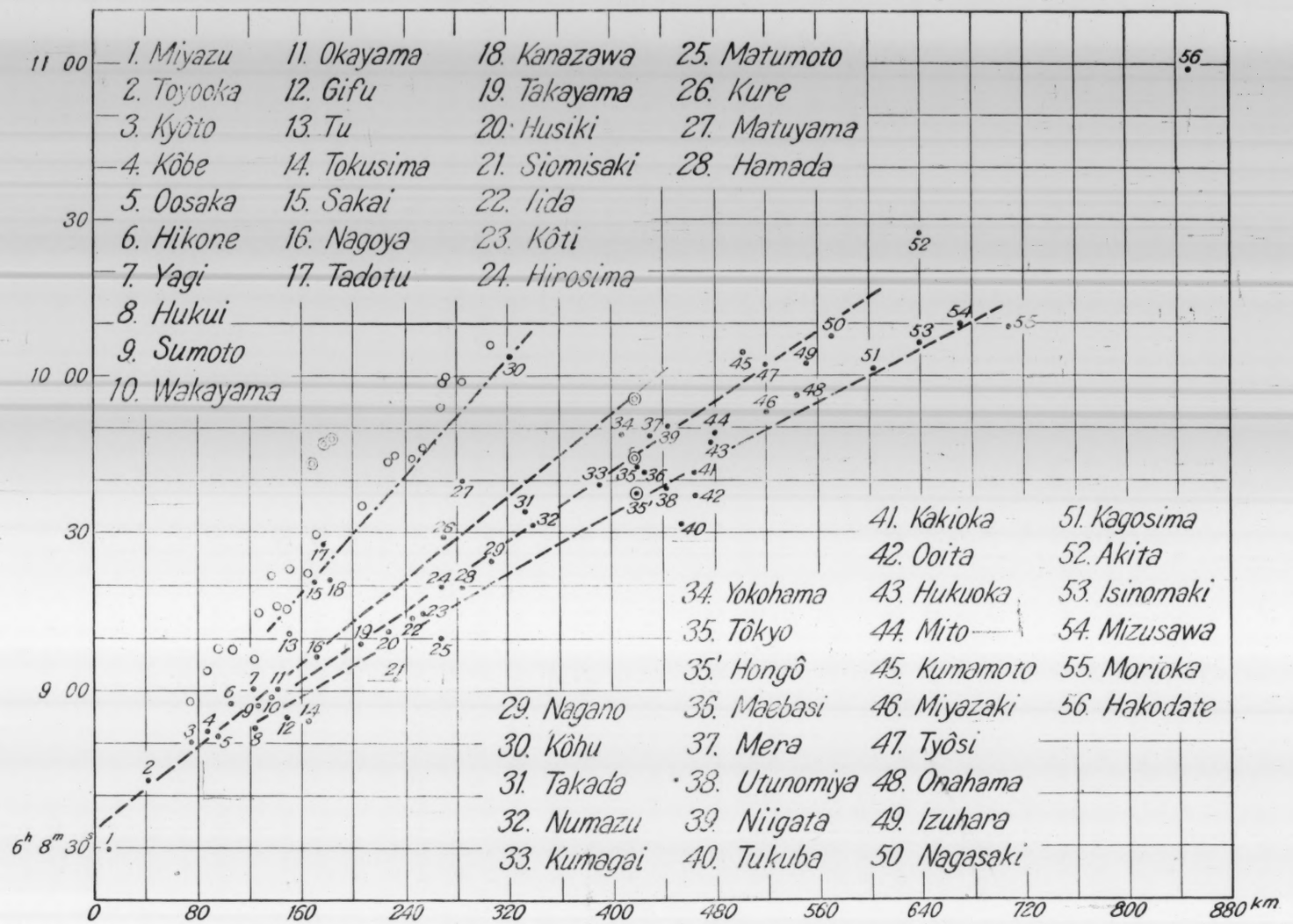

Time curves (broken lines) are tentatively drawn comparing with those of the Great Tango Earthquake. Circles denote the time of commencement of the principal phase.

Fig. 10.

Broken lines are drawn in a similar manner as in the case of the Tazima Earthquake. Essential characters to be remarked are almost the same as in that case. In this case, however, the distributed points can be grouped in three sets of curves somewhat better compared with the case of the Tango earthquake, March 7, 1927. At stations situated between 280 km. and 400 km., it seems that the P phase was missed out of observation and the P^* phase was observed as the commencement. The stations included within this range are distributed almost in the east-west direction relative to the origin of the earthquake. Thus, a consideration is at hand that in such directions the dilatational waves presented themselves quite small in magnitude and the P phase was missed from observation. This point can be inferred from the record at Hongô (Pl. VII. Fig. 9). Indeed, the phase between P and P^* is quite liable to be missed. The value of the time of commencement observed at the Central Meteorological Observatory differed from that at Hongô by just the same amount as $P-P^*$ difference.

Another point to be remarked is the phase characterised by the one dot chain line in the figure (Fig. 10). The distribution of stations is too systematic to be rejected as due to observational errors. The direction of the stations from the epicentre is almost in $E-W$ except Tadotu (marked 17). If the commencement of (S^*) at Hongô is plotted, it will just fall on the line. Moreover this chain line borders approximately the lower limit of points representing the commencement of the principal phase (denoted by circles in Fig. 10). Thus the author is inclined to explain that at such stations all the dilatational part was gone out of observation. Indeed, from Pl. VII. Fig. 9, it will be seen that the magnitude of the preliminary part is quite small compared with that of the principal part. The reported values of duration of preliminary tremor (denoted by concentric circle in Fig. 10) may be some other phase such as $S-L$ or the like.

Even in Fig. 9, after several tens of seconds from (S) larger motions can be seen.

IV. Review of the Great Kwantô Earthquake, Sept. 1, 1923.

This earthquake has been investigated from many points of view and even now its investigation is being carried on from several sides by many authorities. Accordingly, instrumental studies have also been published by many authorities,

for examples, T. Hirano,[1] K. Suda,[2] A. Imamura,[3] S. T. Nakamura,[4] K. Siratori[5] S. I. Kunitomi[6] et. al.

This earthquake was of a considerable scale and had considerable energy for transmitting seismic waves. Moreover, the epicentral region was apparent, so that the time-distance curve within a considerable distance, say 3000 km., could be determined with a small probable error as shown in Pl. VIII. Fig. 11. The value of time of commencement is adopted from Professor Imamura's report,[7] and tabulated below.

TABLE V.

Kwantô Earthquake, Sept. 1, 1923. ($\varphi = 35°\ 16'$, $\lambda = 139°\ 20'$)

No.	Station	Latitude		Longitude		T. of Comm. I.M.T of $\lambda = 135°E$			Δ km.
						h	m	s	
1	Numazu	35°	06′	138°	51′	11	58	39	47.8
2	Tôkyô (Hongô)	35	41	139	46			44	60.8
3	Kumagai	36	09	139	23			51	98.1
4	Tukuba	36	13	140	06			53	126.5
5	Tyôsi	35	44	140	51			57	147.8
6	Matumoto	36	14	137	59		59m	04	163.
7	Mito	36	23	140	28		58	56	163.
8	Nagano	36	40	138	12			56	187.
9	Takayama	36	09	137	15		59	03	214.5
10	Takada	37	06	138	15			10	226.
11	Gihu	35	24	136	46			02	235.
12	Tu	34	44	136	31			11	263.
13	Hikone	35	16	136	15			14	283.
14	Niigata	37	55	139	03			14	298.
15	Kyôto	35	01	135	44			33	329.
16	Yagi	34	31	135	48			21	331.
17	Yamagata	38	15	140	21			39	344.
18	Sendai	38	16	140	54			21	361.
19	Oosaka	34	39	135	26			24	362.
20	Kôbe	34	41	135	11			26	383.
21	Isinomaki	38	26	141	19			30	392.

to be continued.

(1) T. Hirano, Journ. Meteor. Soc. Japan (in Japanese) [ii] **2** (1924) 116-121.
(2) K. Suda, Memoirs Imp. Marine Obs. Kôbe, **1** (1924) 137-239.
(3) A. Imamura, Rep. Imp. Earthq. Invest. Comm. **100** A (1925) 21-65.
(4) S. T. Nakamura, ibid, 67-140.
(5) K. Siratori, Jap. Journ. Astro. Geophy. **2** (1925) 173-192.
(6) S. I. Kunitomi, Journ. Meteor. Soc. Japan [ii] **3** (1925) 281-293.
(7) A. Imamura, Rep. Imp. Earthq. Invest. Comm. **100** A (1925) 31, 32.

(Continued)

No.	Station	Latitude		Longitude		T. of Comm. L.M.T of $\lambda=135°E$			Δ
						h	m	s	
22	Mizusawa	39	8	141	8			40	459.
23	Tadotu	34	17	133	46			42	519.5
24	Okayama	34	40	133	54			55	501.
25	Matuyama	33	50	132	45			58	623.
26	Hamada	34	54	132	04	12	00	06	662.
27	Hakodate	41	47	140	43			13	734.
28	Ooita	33	14	131	37			24	742.
29	Simonoseki	33	57	130	56			22	780.
30	Hukuoka	33	35	130	25			22	837.5
31	Kagosima	31	34	130	33			36	910.
32	Nagasaki	32	44	129	52			30	915.
33	Kusiro	42	59	144	24			33	960.
34	Oodomari	46	59	142	46		01	20	1334.
35	Naha	26	13	127	41			19	1494.
36	Dairen	38°	54	121	38		01	48	1615.
37	Shanghai	31	11.5	121	25.8		02	15	1719.
38	Taihoku	25	02	121	31		01	49	2045.
39	Hongkong	22	18.2	114	10.5		04	00	2822.
40	Manila	14	34.7	120	58.6		04	11	2930.

Remark: Time of commencement is adopted from Professor A. Imamura's Paper (Rep. Imp. Earthq. Invest. Commit. (in Japanese) **100** A (1925) 31). The time of commencement at Taihoku was too earlier by one minute, perhaps being due to mistake ef calculation of minute-marks.

The author tentatively assumed the epicentre of this earthquake as $\varphi=35°$ 16′ and $\lambda=139°$ 20′ which is somewhat different from that determined by Professor Imamura and rather near to that determined by Professor S. T. Nakamura.[1] This assumed epicentre is not inconsistent even with the seismogram at Hongô, if the duration of the preliminary tremor is taken as $9.^s8$ which can be clearly seen from the record.[2]

From Fig. 11 it is almost beyond doubt that in this case also the phase exactly corresponding to $\bar{P}$ existed. If the epicentre determined by Professor Imamura is adopted, $d^2T/d\Delta^2$ for the $\bar{P}$ phase has considerable positive value within 120 km. or so, so that the depth of the origin generating $\bar{P}$ waves must be 40 km. or more which would not give rise to the $\bar{P}$ waves as apparent from

(1) S. T. Nakamura, l. c. p. 18.

(2) See Fig. 1 of Prof. Imamura's report, l. c. p. 18.

the mechanism of occurrence of that phase. This is another reason why the author assumed the above stated origin. With regard to the P^* waves, discussion will be found later.

It is remarkable that the P curve is situated far below the $\bar{P}$ curve and seems not to intersect with each other. This point will also be discussed in the next section.

V. Concluding Remarks.

From the foregoing examples, it is almost doubtless that three phases P, P^* and $\bar{P}$ are observed in Japan too, at least in cases shown above. In the following, some remarks will be given with respect to each phase and other allied problems.

The $\bar{P}$ phase.

In all the five cases above shown, a time-distance curve characterised by $d\Delta/dT=5.0$ km/sec. has been observed clearly. This fact implies that the origin of this phase of waves is situated in a shallow place less than some twenty kilometres deep, that is to say that the depth of origin must be shallower than that of the first discontinuity. In addition to this, closer study of its time-distance curve will show that it is practically a straight line even in the region very near to the epicentre. Usually, curves are drawn so that $d^2T/d\Delta^2>0$ near the epicentre. In present cases, however, such is not the case within the limit of observational errors. H. Jeffreys stated in his paper,(1) " ....I have called attention, ..., to the possibility that the compressional movement originally sent out from the focus may be inappreciable and that the observed movement arises only by reflection of S_g(2) movement at the outer surface. If this is true the apparent depth of the focus found from the compressional waves is zero...." Whether or no his case corresponds to these cases is not certain for I have not yet come across to his full paper. And yet, these cases seem formally correspond to his one. Indeed, such a case may be probable in a special mechanism of occurrence of earthquakes. In general, however, such a consideration is beyond author's comprehension. Moreover the author does not know how such a consideration reconciles with the P or other phase.

Returning to the original problem, these earthquakes were all severe ones

(1) H. Jeffreys, Gerlands Beitr. z. Geophys. **17** (1927) 424–425.
(2) S_g stands for current notation $\bar{S}$.

with remarkable terrestrial disturbances such as fault etc. It may be quite natural that elastic vibrations will be excited with the formation of such disturbances. To what depth such disturbances extend is not certain generally. Their extension, however, may very probably be confined within several kilometers deep in ordinary cases. Indeed, Dr. N. Nasu[1] has found that origins of aftershocks of the great Tango earthquake, March 7, 1927 are almost confined within some fifteen kilometers, thus furnishing a supposition that the origin of the waves directly accompanied with a fracture would also be at a certain point within such a depth.

If the $\bar{P}$ waves is interpreted as a wave of such an origin, the observed fact may very naturally be understood. This view is very akin to that of certain authors mainly of geological school, who implicitly suppose that formation of faults is nothing but an earthquake phenomenon.

The P phase.

From Figs. 6, 8, 10 and 11, it will be seen that a dot representing the P phase seems to appear for the first time at an epicentral distance 120 km. or so. A more remarkable fact is, however, that the appearance of the P phase is much earlier than $\bar{P}$ ordinarily expected. This point is especially clear in the case of the Kwantô earthquake (Pl. VIII. Fig. 11). Even if the P curve were prolonged, it would not intersect with the $\bar{P}$ curve. In ordinary text-figures explaining them, the time of the first appearance of the P phase is so situated that it is later than that of the $\bar{P}$ phase corresponding to that distance. The present experience seems to be irreconcilable to it. Therefore, it is necessary to examine this point carefully.

Assuming that all P, P^* and $\bar{P}$ waves are emitted from a point source and their respective velocity of propagation is constant in each layer, their time-distance relations will be given as follows:[2]

for $\bar{P}$, $$\tau_1=\frac{\sqrt{\Delta^2+f_1^2}}{v_1},$$

,, P^*, $$\tau_2=(2d_1-f_2)\frac{\cos i_1}{v_1}+\frac{\Delta}{v_2},\quad \Delta>(2d_1-f_2)\tan i_1,$$

and

for P, $$\tau_3=(2d_1-f_3)\frac{\cos i}{v_1}+2d_2\frac{\cos i_2}{v_2}+\frac{\Delta}{v_3},$$

(1) N. Nasu l. c. p. 10.

(2) Effect of curvature of the earth's surface can be neglected for near stations.

$$\Delta > (2d_1 - f_3)\tan i' + 2d_2 \tan i_2,$$

where $\sin i_1 = \frac{v_1}{v_2}$, $\sin i' = \frac{v_1}{v_3}$ and $\sin i_2 = \frac{v_2}{v_3}$.

The meaning of notations will be understood by the next figure. (Fig. 12.)

Fig. 12.

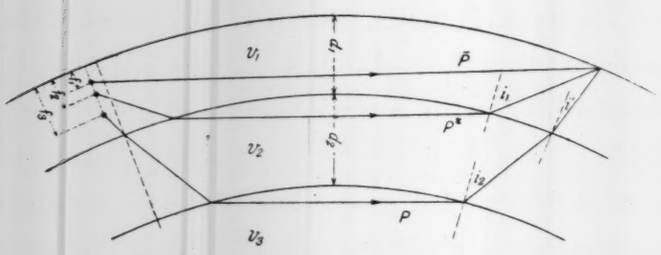

The above shown expressions hold good when f_1, f_2 and f_3 are all less than d_1. If $d_1 + d_2 > f_3 > d_1$, then

$$\tau_3 = (d_1 + 2d_2 - f_3)\frac{\cos i_2}{v_2} + d_1 \frac{\cos i'}{v_1} + \frac{\Delta}{v_3},$$

$$\Delta > (d_1 + 2d_2 - f_3)\tan i_2 + d_1 \tan i'.$$

When $d_1 + d_2 > f_1 > d_1$, the expression for τ_1 will be much complicated as was given in our former paper.(1) By the way it will easily be shown from expressions for τ's that $\partial^2\tau_1/\partial\Delta^2$ may be positive for a shorter distance, however, $\partial^2\tau_2/\partial\Delta^2$ or $\partial^2\tau_3/\partial\Delta^2$ cannot be so, which fact is sometimes mistaken carelessly.

Returning to the present problem, it will be sufficient if attention will be payed for the distance $\Delta_0 = (2d_1 - f_3)\tan i' + 2d_2 \tan i_2$ for the case $d_1 > f_3$, and $\Delta_0 = (d_1 + 2d_2 - f_3)\tan i_2 + d_1 \tan i'$, for the case $d_1 + d_2 > f_3 > d_1$. In the following, τ's corresponding to that distance will be denoted by adding prefix, 0, such as ${}_0\tau_3$. For the P^* waves, $\Delta_0 = (2d_1 - f_2)\tan i_1$ and ${}_0\tau_2 = (2d_1 - f_2)\frac{1}{v_1 \cos i_1}$.

Thus ${}_0\tau_1 - {}_0\tau_2 = (2d_1 - f_2)\frac{1}{v_1 \cos i_1}(\sin i_1 - 1) + \frac{f_1^2}{2v_1\Delta_0}$. From assumption, as $f_1 < d_1$, the last term is small, so that ${}_0\tau_1 - {}_0\tau_2$ is negative. This is not inconsistent with the observed cases.

For the P waves

$${}_0\tau_3 = (2d_1 - f_3)\frac{1}{v_1 \cos i'} + \frac{2d_2}{v_2 \cos i_2},$$

and

$${}_0\tau_1 = (2d_1 - f_3)\frac{\tan i'}{v_1} + \frac{2d_2}{v_1}\tan i_2 + \frac{f_1^2}{2v_1\Delta_0}, \quad \text{when } f_3 < d_1,$$

(1) T. Matuzawa, K. Hasegawa and S. Haeno, this Bull. **4** (1928) 96.

where $\Delta_0=(2d_1-f_3)\tan i'+2d_2\tan i_2$.

Thus

$$ {}_0\tau_1-{}_0\tau_3=\frac{2d_1-f_3}{v_1\cos i'}\left(\frac{v_1}{v_3}-1\right)+\frac{2d_2}{\cos i_2}\frac{v_2^2-v_1v_3}{v_1v_2v_3}+\frac{f_1^2}{2v_1\Delta_0}. $$

If $f_1<d_1$ and $d_1+d_2>f_3>d_1$,

then

$$ {}_0\tau_3=(d_1+2d_2-f_3)\frac{1}{v_2\cos i_2}+\frac{d}{v_1\cos i'}, $$

and

$$ {}_0\tau_1=(d_1+2d_2-f_3)\frac{\sin i_2}{v_1\cos i_2}+\frac{d_1\sin i'}{v_1\cos i'}+\frac{f_1^2}{2v_1\Delta_0}, $$

$$ \Delta_0=(d_1+2d_2-f_3)\tan i_3+d_1\tan i'. $$

Thus

$$ {}_0\tau_1-{}_0\tau_3=(d_1+2d_2-f_3)\frac{1}{\cos i_2}\left(\frac{v_2^2-v_1v_3}{v_1v_2v_3}\right)+\frac{d_1}{v_1\cos i'}\left(\frac{v_1}{v_3}-1\right)+\frac{f_1^2}{2v_1\Delta_0}. $$

The values of v_3 and d_2 are not exactly certain in the present case. Even if $v_3=6.5$ km/sec. is tentatively assumed as apparently to be seen from Fig. 6, and $d_2=30$ km. which value is supposed to be probable from some of other phenomena, ${}_0\tau_1-{}_0\tau_3$ is negative.

Thus the observed fact cannot be explained by only such a consideration. This point will be examined from somewhat different consideration.

Assuming that P wave is emitted from the seismic origin simultaneously with the P waves, from Fig. 6, ${}_0\tau_3=18.^s5$ and $\Delta_0=116$ km. are measured. Thus following simultaneous equations are obtained.

$$ \left.\begin{aligned}(2d_1-f_3)\frac{1}{v_1\cos i'}+\frac{2d_2}{v_2\cos i_2}&=18.5,\\ (2d_1-f_3)\tan i'+2d_2\tan i_2&=116.\end{aligned}\right\} $$

$d_1=20$ km., $v_1=5.0$ km/sec., $v_2=6.1$ km/sec. have been already determined. Taking into account of these values, values of v_3 and d_2 satisfying these equations cannot be found within the domain $f_3<20$ and $v_3>v_2$.

If $d_1+d_2>f_3>d_1$,

then

$$ \left.\begin{aligned}(d_1+2d_2-f_3)\tan i_2+d_1\tan i'&=116\\ \frac{d_1+2d_2-f_3}{v_2\cos i_2}+\frac{d_1}{v_1\cos i'}&=18.5.\end{aligned}\right\} $$

Taking the former values, an equation for dertermining v_3 can be obtained,

$$116\,v_3 - 689 = -\frac{49}{\sqrt{1-\frac{v_1^2}{v_3^2}}}.$$

This equation has not such a solution as $v_3 > v_2$. Therefore, another way of explanation must be attempted.

In short, the observed fact seems to be very naturally explained by taking into account of a certain kind of effective dimension of the hypocentral region generating the P waves. If this is the case, *effective* epicentral distances of near stations must be smaller than those measured from an approximate middle point of epicentral region. This idea was already elucidated by Mr. T. Hirano[1] in his elegant paper on the velocity of propagation of the preliminary tremors of the great Kwantô earthquake and the area of the Seismic Origin (written in Japanese), though his method of treating the data was, I think, somewhat unsatisfactory. In fact the great Kwantô earthquake, Sept. 1, 1923 was of a much greater scale than that of the Tango earthquake or others. This fact seems to be seen by comparison of Fig. 6 with Fig. 11, or Fig. 13, though not very distinct owing to some uncertainty of observed data.

Comparison of two Great Earthquakes.
The Tango Earthquake and The Kwanto Earthquake.

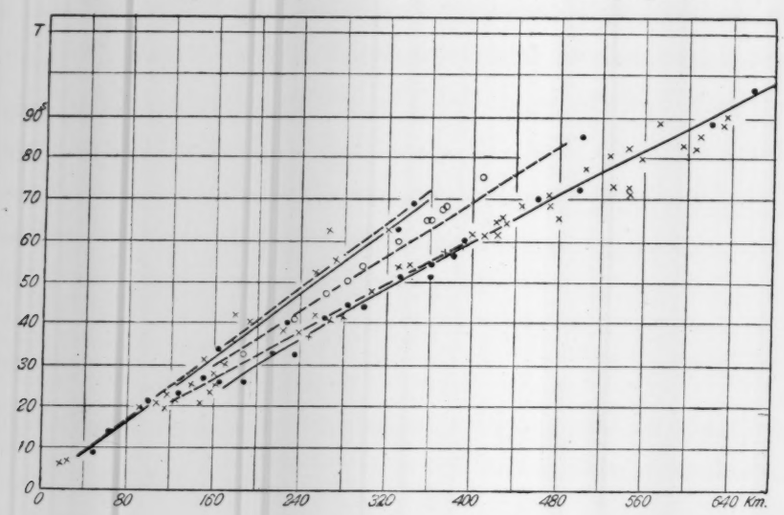

Cross: Tango Earthquake
Dot: Kwantô Earthquake
Fig. 13.

Thus a consideration is at hand that a hypocentral *point* of an earthquake could not be determined by observing the P wave, but only a hypocentral

(1) l. c. p. 18.

region may be determined with accuracy of the order of magnitude of wave length of disturbances. This consideration may be very akin to that of the wave mechanics by Schrödinger in quantum theory. Thus the time-distance curve of the P phase in a definite meaning may be determined by observation of very intense and very local shocks. The Etigo earthquake Oct. 27, 1927 was unfortunately in too shallow depth to produce the P movement.

From above considerations, a supposition with regard to generation of P waves follows. In discussion of the $\bar{P}$ movement, it was supposed that the movement may be very probably emitted from a point (of course in a statistical sense but may be far definite compared with the case of P) very near to the surface. On the other hand, with respect to the P movement somewhat wider range must be considered as its origin. Thus the origin of each kind of waves must be taken as different, as was implicitly assumed in the foregoing discussions. This point must be more closely examined, from the point of view of occurrence of such great earthquakes as to produce superficial terrestrial disturbances. It is very probably considered that destruction of earth's crust such as to produce the $\bar{P}$ movement is a result of accumulation of potential energy not only in that part but also in a much wider part connected in a certain manner with the former part. The author is inclined to believe that the accumulation of energy producing the $\bar{P}$ movement takes place in the superficial layer mainly in the form of strain energy and that producing the P movement will do in the lower layer. The origin of energy may be gravitational or endogen dynamical. Some kind of endogen dynamical process may play an important rôle in converting the gravitational energy into the kinetic energy. Of course, strain energy caused by endogen dynamical process itself will also not be excluded.

Thus at a certain stage of accumulation of strain, by destruction of material at a certain point, release of accumulated strain will take place, generating the P and $\bar{P}$ waves almost simultaneously. In such a case, the accumulation of energy corresponding to the $\bar{P}$ movement may be more localised as a result of the mosaic structure of the superficial crust than that of the P in a deep region. The mechanism of emission of the movement which can be observed as P with sufficient magnitude at a remote station is perhaps a certain mode[1] of motion of somewhat *large* part as a whole of the upper layer directly trans-

(1) It may be bodily movement of the so-called crustal block or elastic vibration of a certain oscillator. It seems to me. however, that the latter may be more probable.

mitted to the lower layer or of the lower layer itself. The fact that the period of the P movement is long[1] (very often nearly equal to that of pulsatory motion) may be very naturally understood by such a mechanism.

The following factor must also be taken into account. The velocity of propagation of elastic waves when they are propagated releasing initial elastic strain is given in the elegant paper of K. Uller[2] as follows:

For the dilatational wave

$$v_p^2=\frac{\left(\varepsilon_v+\frac{4}{3}\varepsilon_g\right)(\mathfrak{N},\ \mathrm{grad\ div}\ \mathfrak{S})}{\rho\,(1-\mathrm{div}\ \mathfrak{S}_0)\,(\mathfrak{N},\ \mathrm{grad\ div}\ (\mathfrak{S}-\mathfrak{S}_0))}+\text{higher terms},$$

and for distortional waves

$$v_s^2=\frac{\varepsilon_g\,[\mathfrak{N},\ \mathrm{rot\ rot}\ \mathfrak{S}]}{\rho\,(1-\mathrm{div}\ \mathfrak{S}_0)\,[\mathfrak{N},\ \mathrm{rot\ rot}\,(\mathfrak{S}-\mathfrak{S}_0)]}+\text{higher terms},$$

where ε_v is the bulk modulus

ε_g ,, ,, rigidity ,,

ρ ,, ,, density

$\mathfrak{S}$,, ,, strain vector

$\mathfrak{S}_0$,, ,, initial strain vector

$\mathfrak{N}$ is the unit vector normal to wave front

( ) means the scalar product of vectors

and [ ] ,, ,, vector ,, ,, ,, .

Therefore in a region where $\mathfrak{S}_0 \neq 0$, that is, in the hypocentral region, waves may be propagated very quickly, thus apparently showing a finite dimension of source even if waves are originated from a point. Hence the P wave appears somewhat earlier than expected.

By specifying regions where the energy of such an earthquake as stated above is stored, the mode of time-distribution of earthquakes related to a main shock may naturally be understood.

After-shocks of small intensity may be understood as a kind of irreversible process of somewhat gradual release of residual strain through the region destructed severely. The result of Mr. N. Nasu[3] will furnish an evidence of this

(1) Dissipation of quick motion only cannot explain the fact. Indeed very deep earthquakes show superposition of quick vibrations from the commencement even observed at a remote station.

(2) K. Uller, Gerlands Beitr. z. Geophys. **15** (1926) Hft. 2.

(3) N. Nasu, l. c. p. 18.

theory. The reason why the process of release takes place intermittently can easily be understood as the process is irreversible. Thus in such a region, a theory of after-shocks such as that of F. Omori[1] or of S. Kusakabe[2] will be applied. S. Kusakabe's idea that the number of after-shocks in a unit time may be proportional to the rate of recovery of elastic after-effect may naturally be understood by supposing such a mechanism.

On the other hand, we have experienced some examples of successive occurrence of strong earthquakes of nearly equal intensity at nearly the same region.[3] One of the most remarkable examples may be that of the great Tazima earthquake, May 23, 1925 and the great Tango earthquake, March 7, 1927. Such process of occurrence is difficult to understand if the region of accumulation of a certain kind of potential energy is confined only in a superficial layer of crust where remarkable terrestrial disturbances take place. On the contrary, if storage of energy somewhat deeprooted is released by a local fracture of the superficial crust, such process of successive occurrence may result with high probability. Change of topography with a vast scale will also be a natural consequence. In the above reasoning, fracture in the lower layer, too, is not denied of course.

Indeed, in the Kwantô District, the distribution[4] of seismic hypocentre has been found mainly between twenty and fifty kilometres deep which is the prabable thickness of the second layer.

On the case of such a great earthquake as that of Kwantô and in such a geologically week region as Kwantô, it may very naturally be understood that fracture may proceed very quickly to a deeper region.

The P^* phase.

Existence of this phase was clearly seen on the occasions of the Etigo earthquake, Oct. 27, 1927, the great Tazima earthquake, May 23, 1925, the great Tango earthquake, March 7, 1927, and the Tango earthquake April 1, 1927. Even in the case of the Great Kwantô earthquake, Sept. 1, 1923, its existence is inferred though somewhat vaguely. In Fig. 13, the circle is plotted according to the data of Mr. S. Kunitomi,[5] reported as the $P-\bar{P}$ difference.

(1) F. Omori, Rep. Imp. Earthq. Invest. Comm. (in Japanese) **2** (1893) 103.
(2) S. Kusakabe, Publ. Imp. Earthq. Invest. Comm. **17** (1904) 1-48.
(3) For example, see F. Omori's paper. Rep. Imp. Earthq. Comm. **94** (1921) 16.
(4) T. Matuzawa, K. Hasegawa, S. Haeno, this Bull. **4** (1928) 101.
(5) S. Kunitomi, Journ. Meteor. Soc. Japan [ii] **3** (1925) 291.

From the present view point, they are rather interpreted as the $P-P^*$ difference.

The time-distance curve of the P^* movement is nearly straight, and the effect of dimension of source of energy can hardly be detected. From this reason, the place where that movement is emitted may not be far different from that of the $\bar{P}$ phase, or rather be regarded the same in usual cases,[1] and accordingly is started in the uppermost layer. Even if the origin of this phase is situated in the second layer, a phase can be detected corresponding to the P^* phase, although the mechanism becomes rather similar to that of the $\bar{P}$ phase.[2] In such a case the time of appearance of the P^* phase will be somewhat earlier than the former case, and $d^2T/d\Delta^2$ may be positive. In cases of earthquakes such that destruction of material takes place only at a very deeper place than the thickness of the first layer, the $\bar{P}$ phase characterised by $d\Delta/dT=5.0$ km/sec. will disappear. Thus it may very naturally be expected that the apparent velocity of propagation of $\bar{P}$ waves determined by taking mean values takes an intermediate value between 5.0 and 6.1 km/sec.

April, 1928.

Seismological Institute, Imperial University, Tokyô.

(1) The case of the Etigo earthquake may be regarded as such.

(2) Examples of such a case will be shown in the next paper which will be published in the next volume of this bulletin.

Seismograms of the Etigo earthquake, Oct. 27, 1927.
(Observed at Hongô)

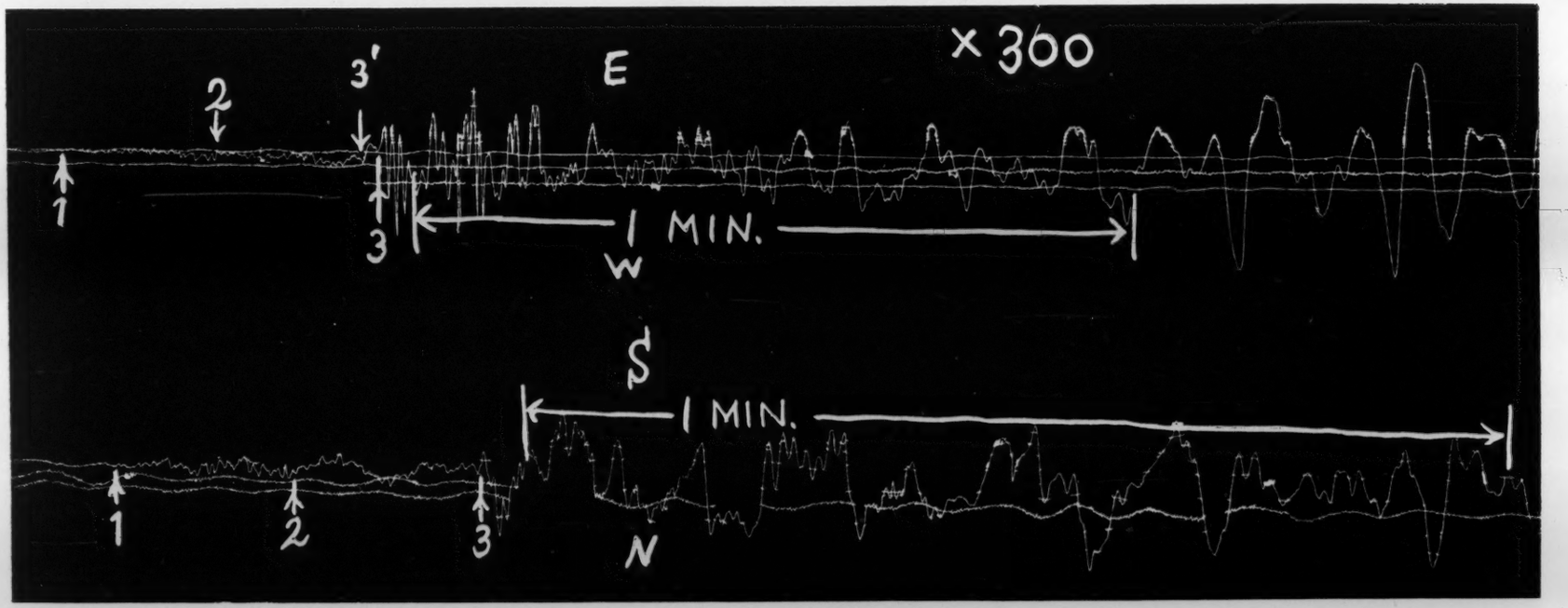

The slow motion between 2-3 may be the pulsatory motion then prevailing.

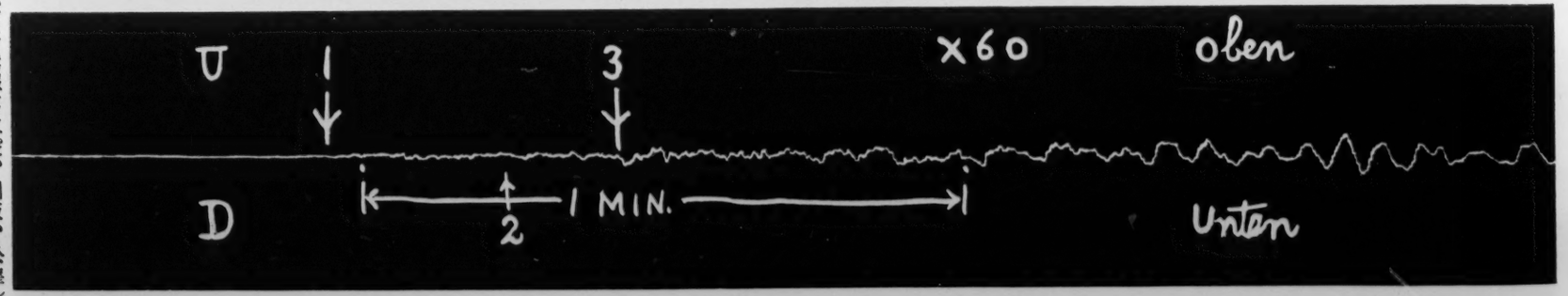

（震研彙報第五號、圖版、松澤）

Fig. 1.

Seismogram of the Etigo earthquake, Oct. 27, 1927.
(Observed at Titibu)

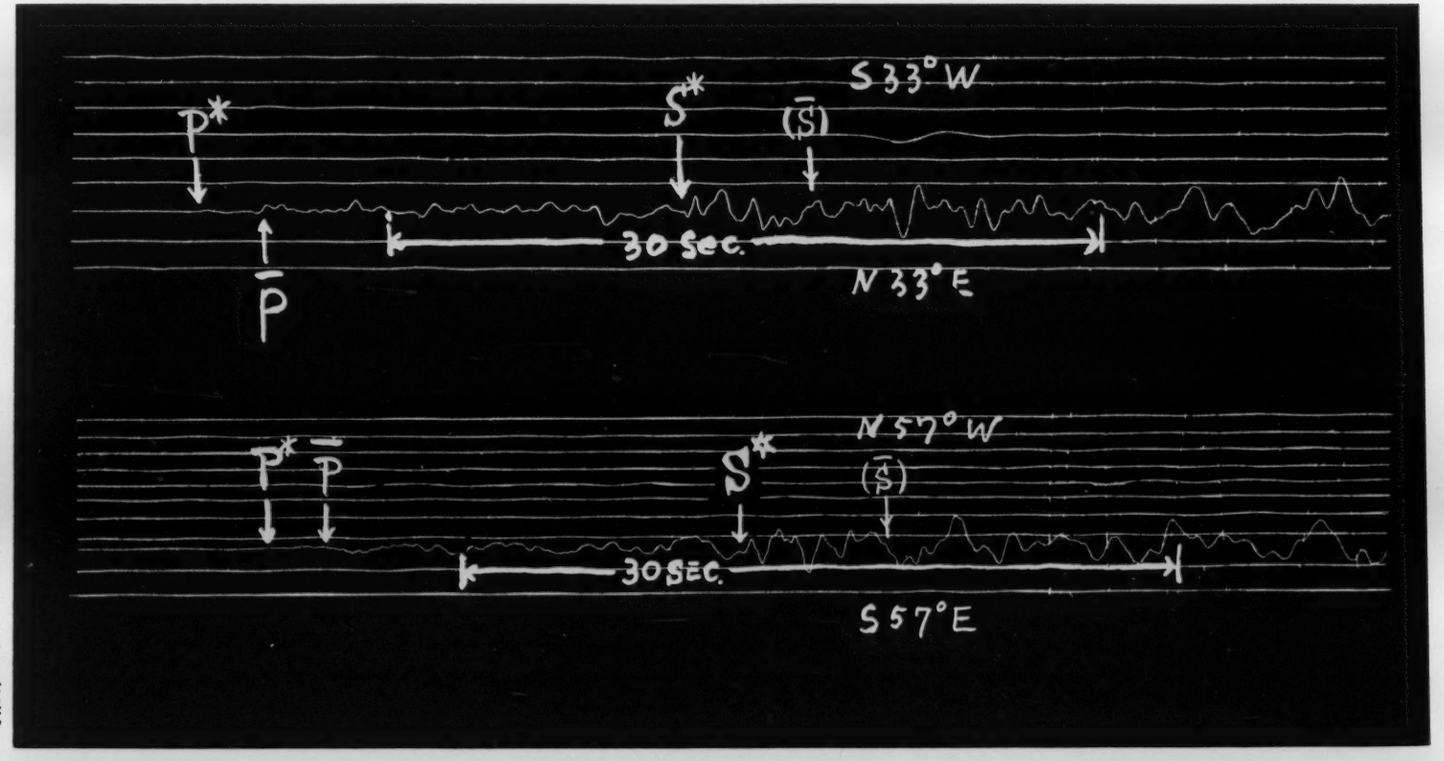

（震研彙報第五號、圖版、松澤）

Fig. 2

Tango Earthquake, March 7, 1927.
(Observed at Hongô)

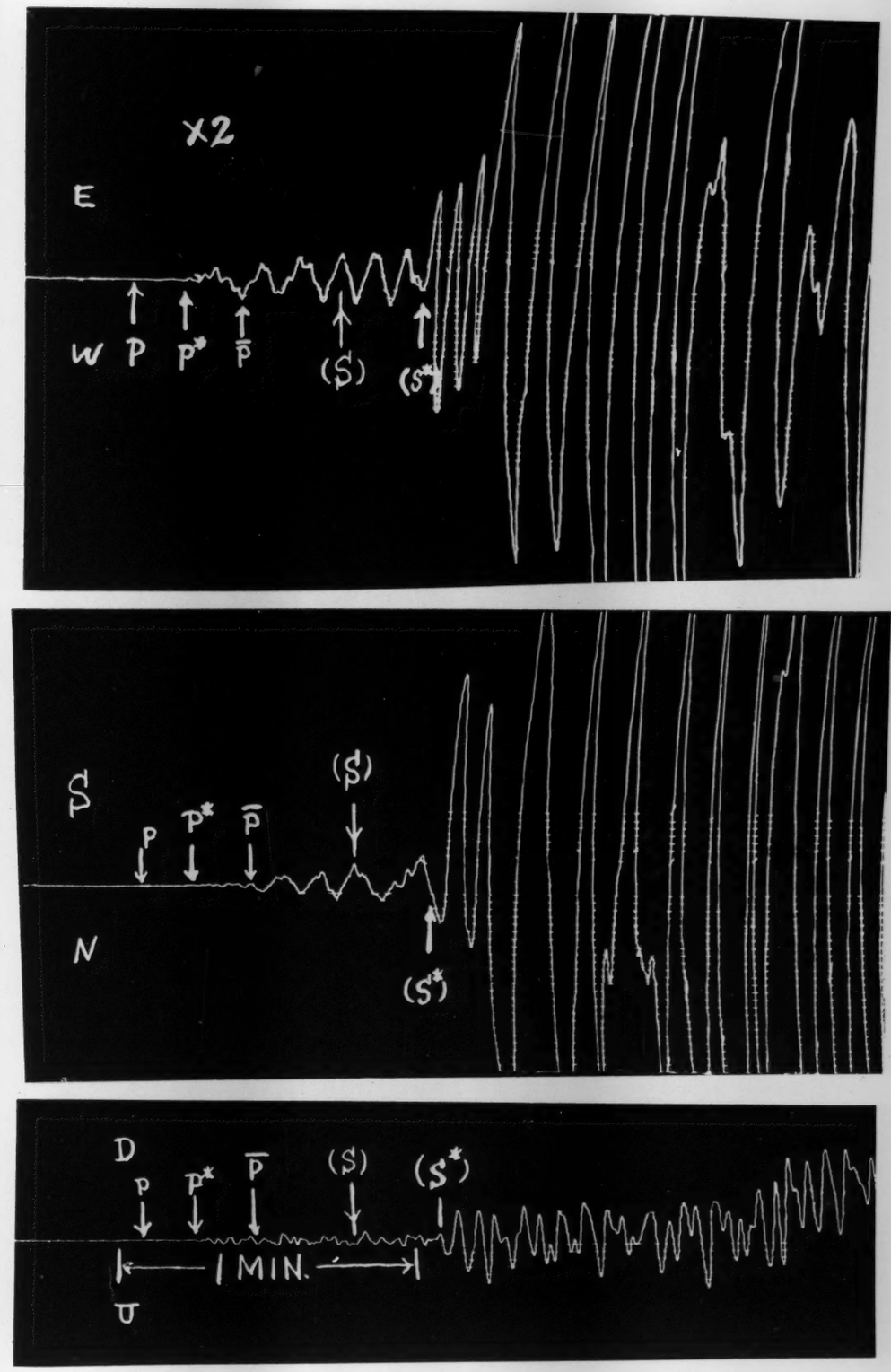

Phase P was determined by more sensitive instruments.

Fig. 4.

（震研彙報第五號、圖版、松澤）

Tango Earthquake, March 7, 1927.
(Observed at Kamakura)

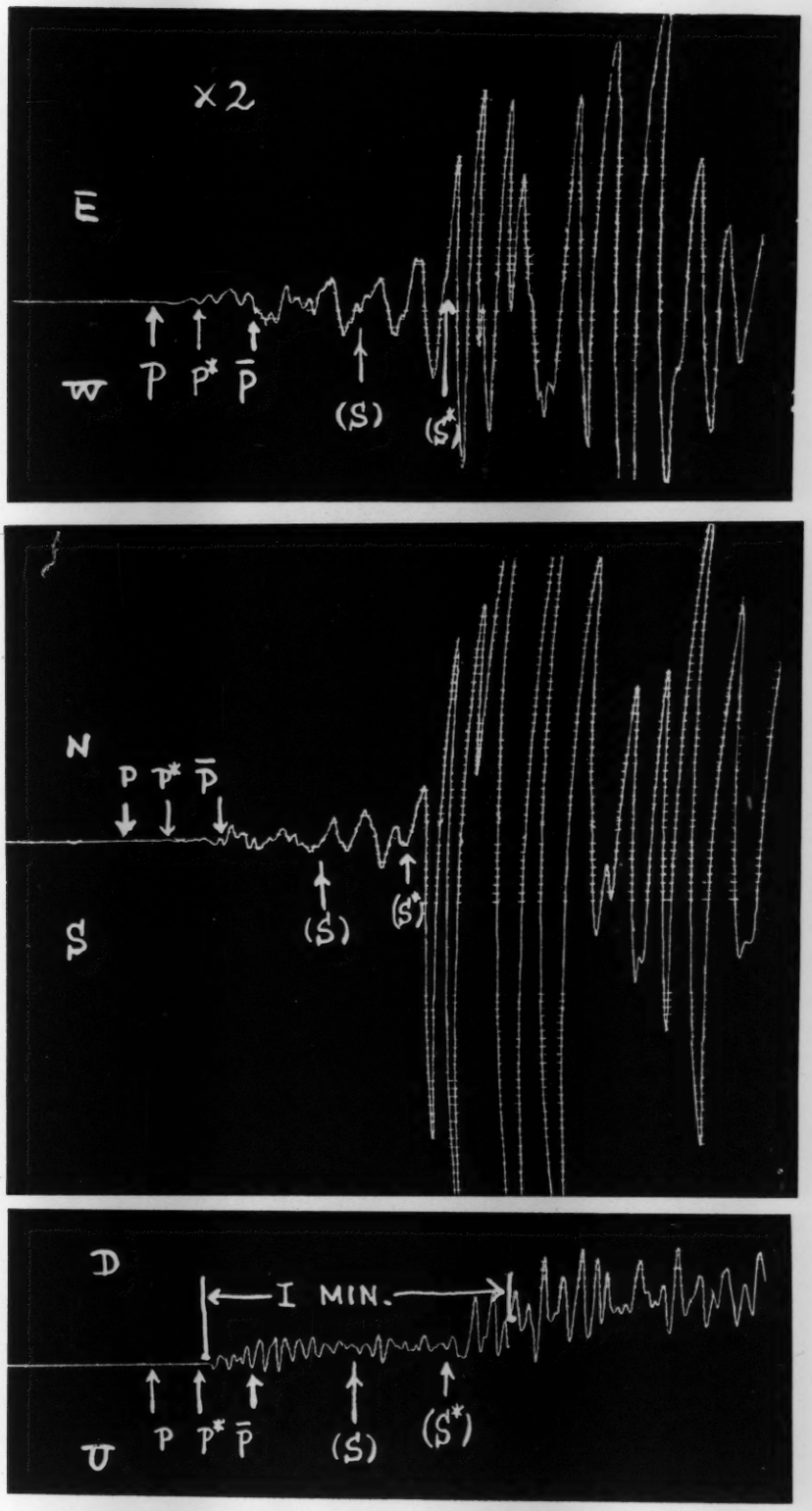

Phase P was accurately determined by more sensitive instruments.

Fig. 5.

（震研彙報第五號、圖版、松澤）

Time-distance curve of the Great Tango Earthquake, March 7, 1927.

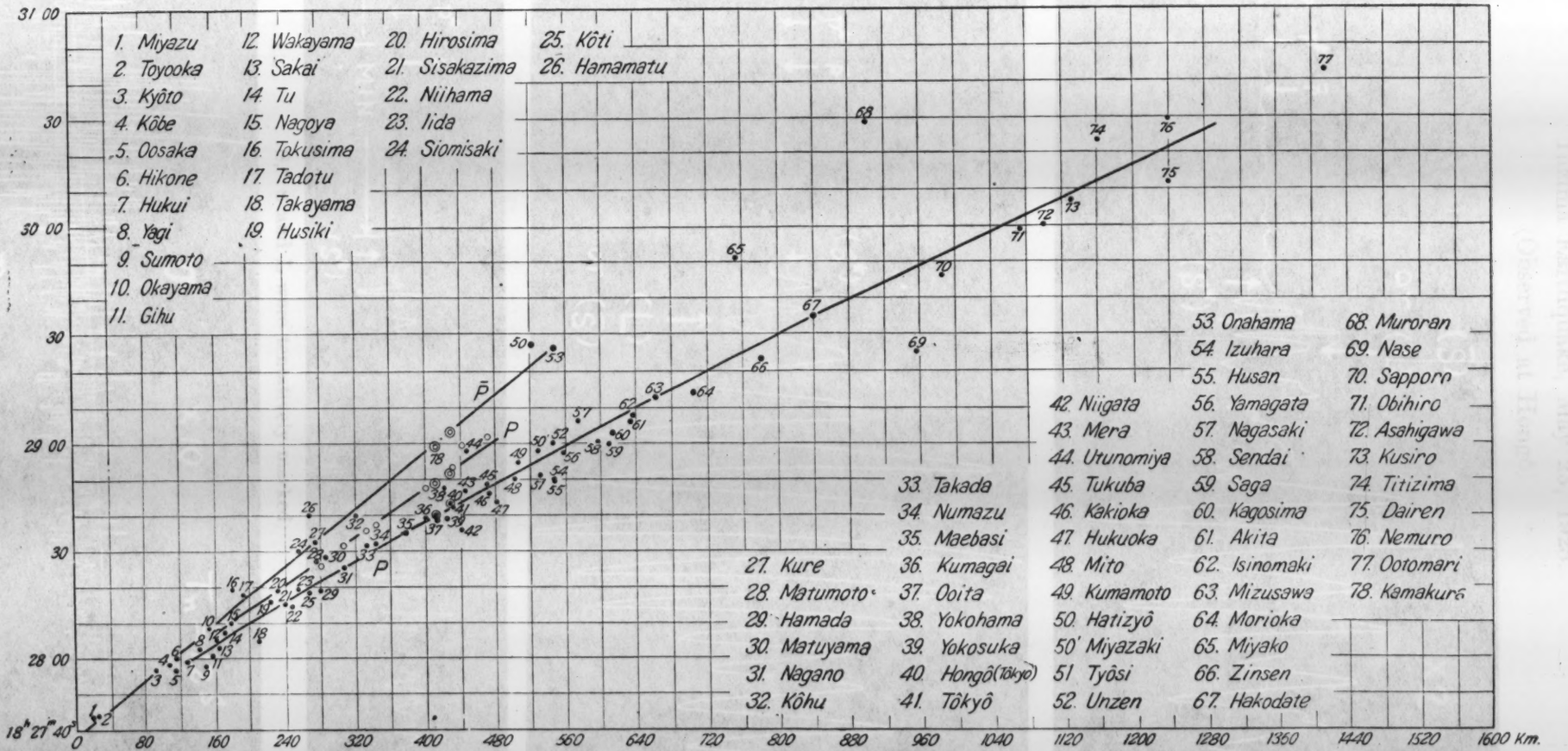

Curve $\bar{P}$: $T = -2.0 + 0.20\Delta$

,, P^*: $T = -0.075 + 0.169\Delta$

,, P : $T = -0.43 + 0.1539\Delta - 2.08 \times 10^{-5}\Delta^2$ $(120 < \Delta < 400)$; $-1.08 + 0.1522\Delta - 1.875 \times 10^{-5}\Delta^2$ $(400 < \Delta < 600)$; $8.0 + 0.1275\Delta$ $(600 < \Delta < 800)$.

Fig. 6.

（震研彙報第五號、圖版、松澤）

Tazima Earthquake, May 23, 1925.
(Observed at Hongô)

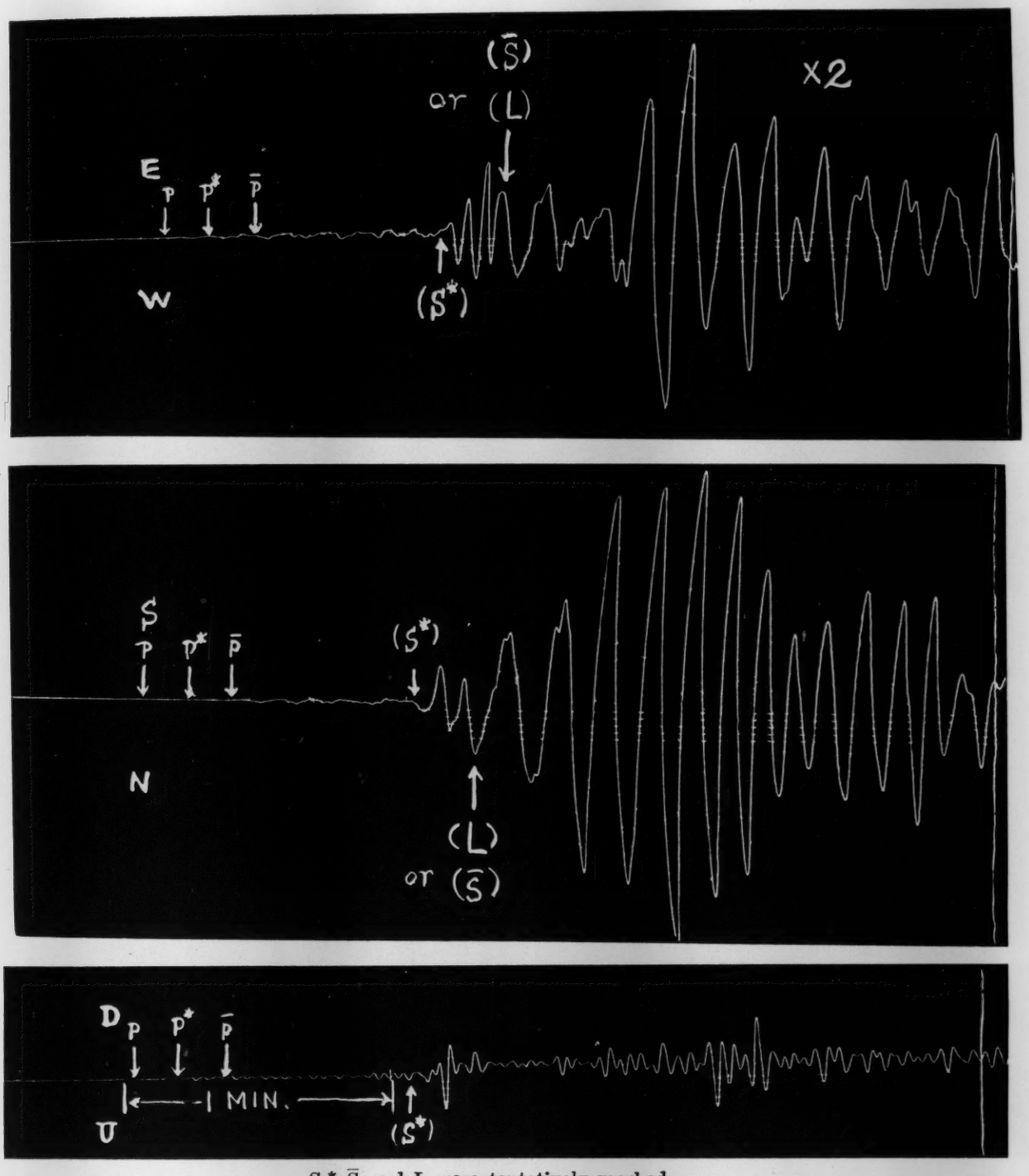

S,* S̄ and L were tentatively marked.

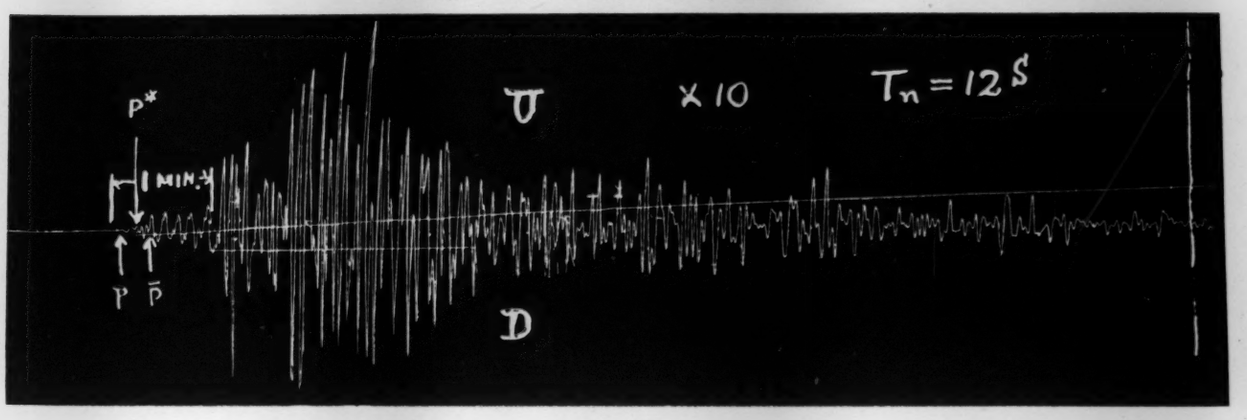

Fig. 7.

（震研彙報第五號、圖版、松澤）

Tango Earthquake, April 1, 1927.
(Observed at Hongô)

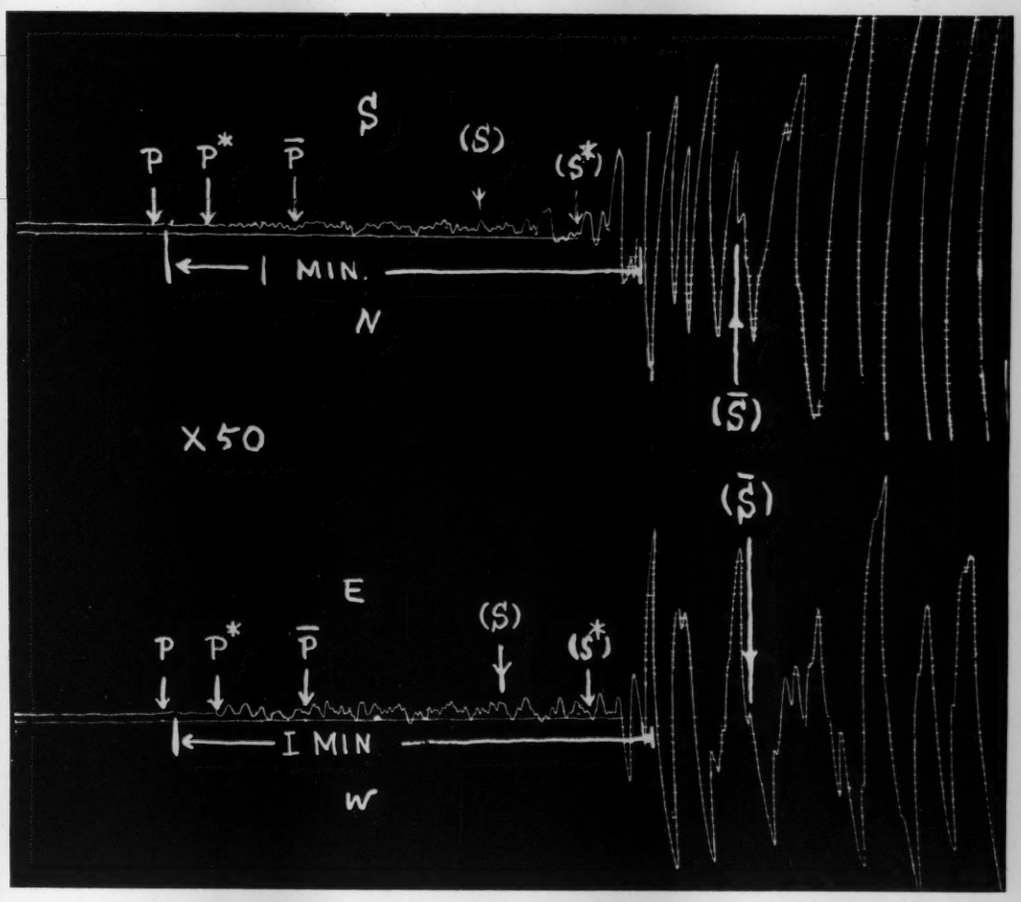

The S phase was tentatively classified, but is not certain accuraetly.

Fig. 9.

（震研彙報第五號、圖版、松澤）

Time-distance curve of the Great Kwantô Earthquake, Sept. 1, 1923.

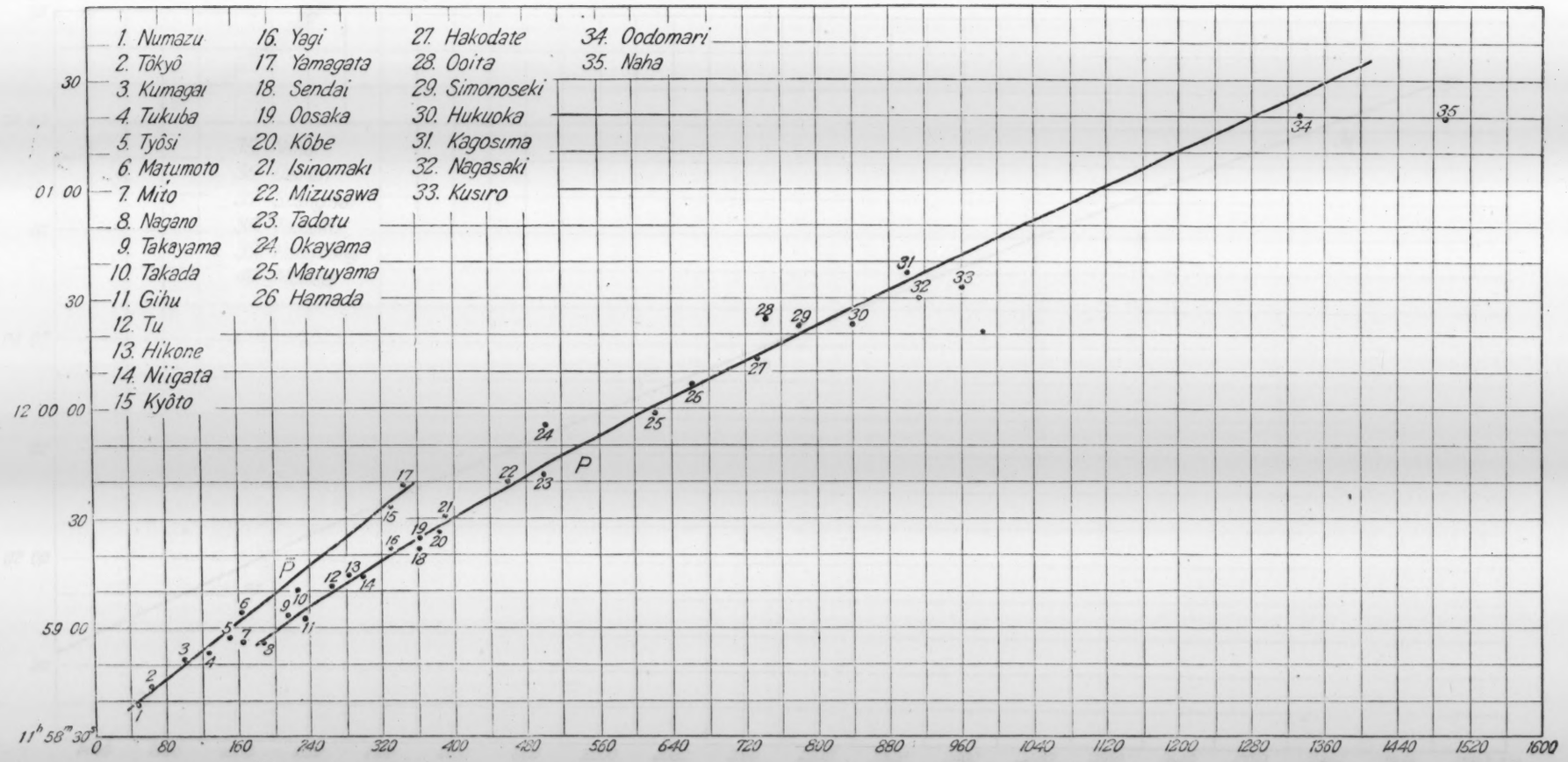

Curve $\bar{P}$: $T = 0.48 + 0.194\triangle$

P: $T = -2.81 + 0.163\triangle - 3.9\times10^{-6}\triangle^2 - 2.8\times10^{-8}\triangle^3$ $(200 < \triangle < 600)$

$T = 12.538 + 0.1270\triangle - 3.31\times10^{-6}\triangle^2$ $(600 < \triangle < 1400)$

} origin of time. $11^h58^m30^s$ (L. M. T. of $\lambda = 135°$E)

(To be continued to the next sheet.)

Fig. 11.

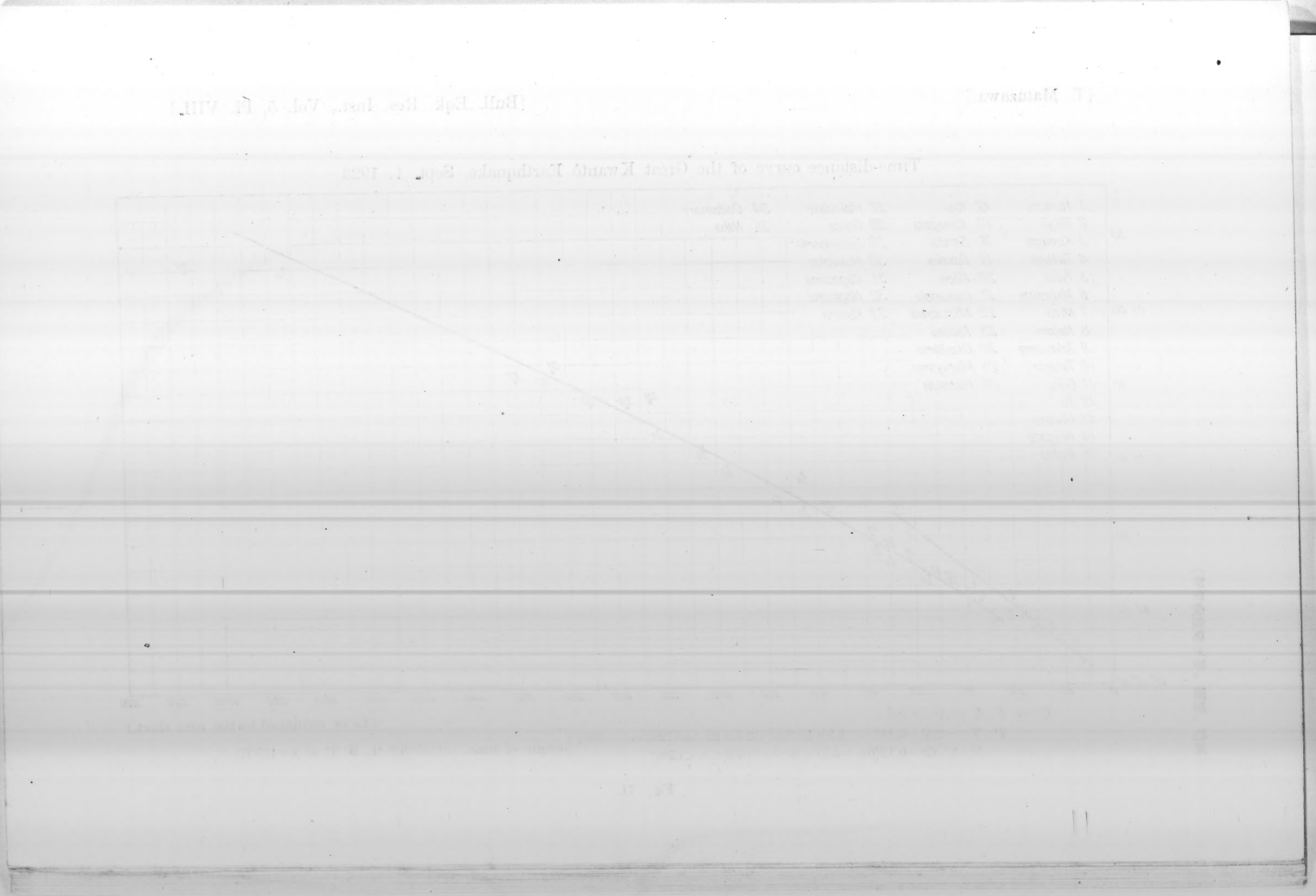

Time-distance curve of the Great Kwantô Earthquake, Sept. 1, 1923.

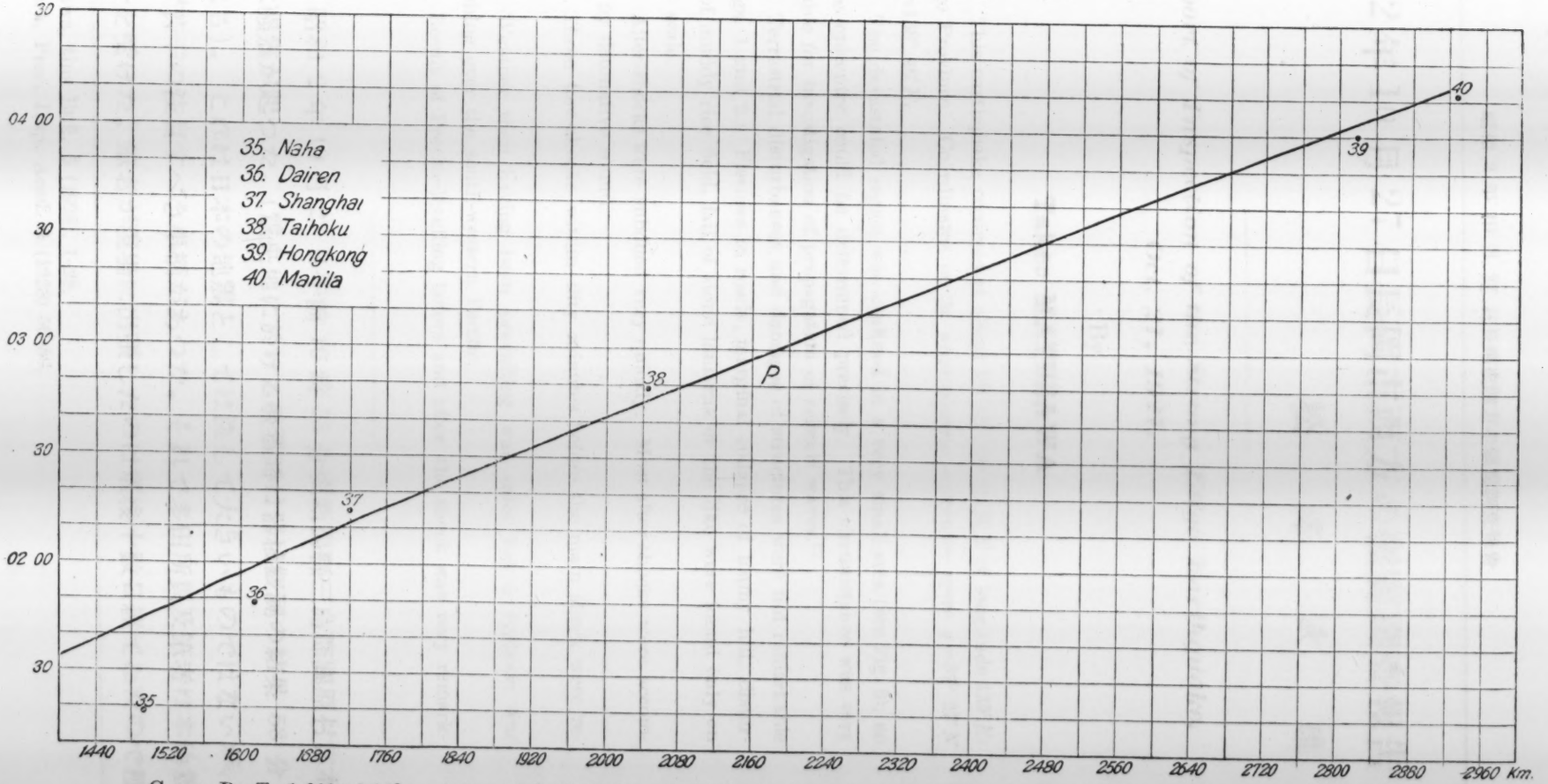

Curve P: $T = 1.000 + 0.143\triangle - 9.01 \times 10^{-6}\triangle^2$ $(1400 < \triangle < 3000)$; origin of time. $11^h58^m30^s$ (L. M. T. of Long. 135°E) (continued)

Fig. 11.

（震研彙報第五號、圖版、松澤）

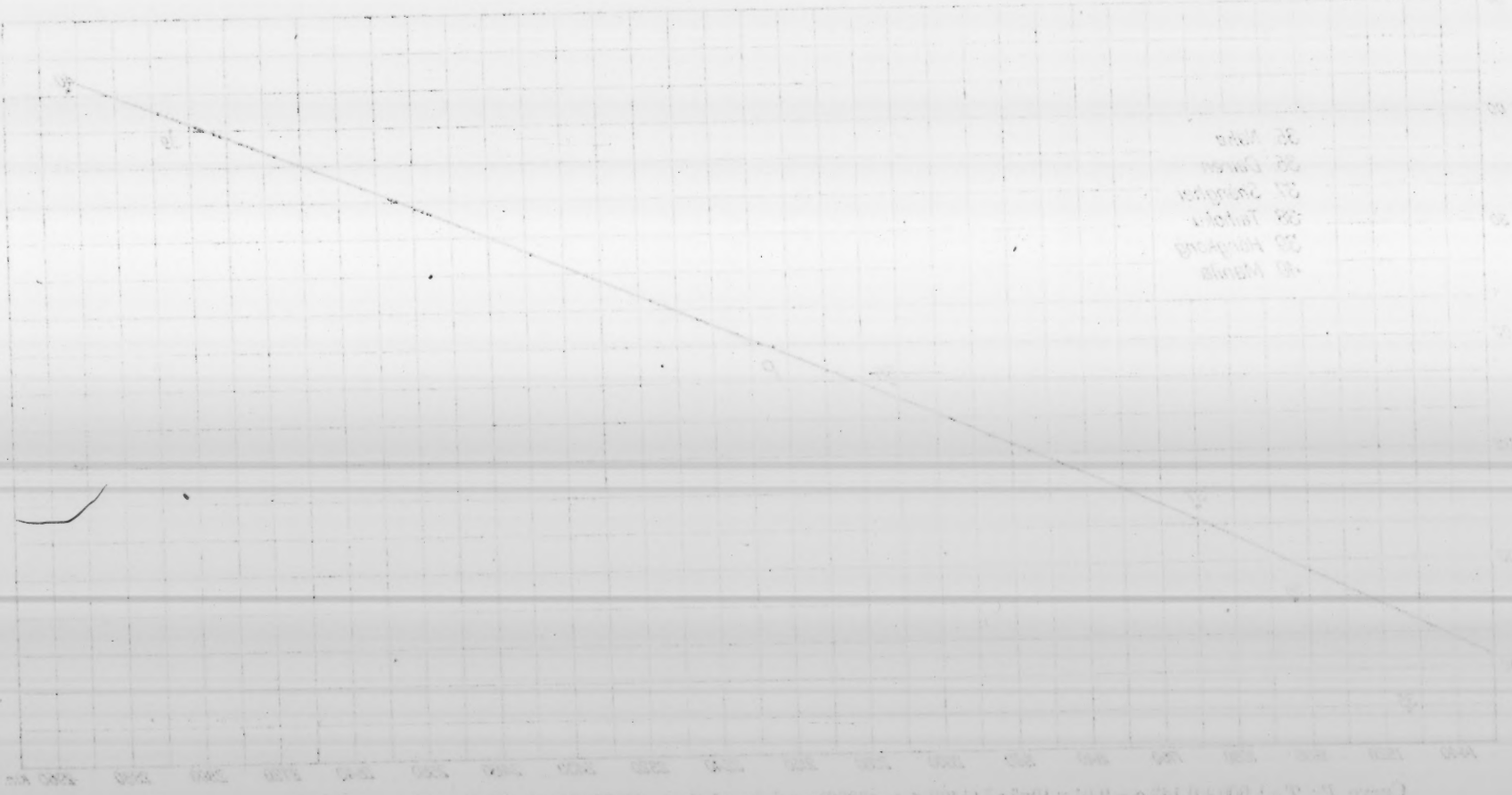

Fig. 11.

昭和2年10月27日長岡市西方の強震調査報告

松 澤 武 雄

Report of Inspection of the Strong Etigo Earthquake, Oct. 27, 1927.

By

Takeo MATUZAWA.

(1) This earthquake occurred at about $10^h\ 53^m\ 35^s$ (L.M.T of longitude $135°E$) in Etigo Province. Coördinates of its approximate epicentre were $\varphi = 37°\ 27'N$ and $\lambda = 138°\ 46'E$.

(2) The devastated region was confined in a very small area (See Fig. 3), so that the epicentre could be determined precisely. This circumstance was very favourable for investigation of propagation of seismic waves.[1)]

(3) Terrestrial disturbances and damages of structures were not remarkable (See Figs. 1 and 2.) Fissures in roads, marginal collapse of loamy hill, disturbance of muddy rice field, fall of stone lanterns or the like were found only on a small scale.

(4) After-shocks were subdued very quickly. Most after-shocks were accompanied by detonative sound.

(5) Three fore-shocks within fifty minutes before the main shock were reported.

(6) Weather then having been prevailing was calm but a typhoon was approaching over the south-western Pacific.

(7) Result of Precise-levelling before and after the shock was very remarkable.[2)]

緒 言。 昭和 2 年 10 月 27 日午前 10 時 53 分頃新潟縣三島郡關原村宮本村日吉村附近に強震が起つた。(震央地に於ける發震時は器械觀測の結果 53 分 35 秒頃と見られる)。これは日本の地震としては決して大きいものではないが、それにも拘らず若干の注目すべき事柄があつた。それで多田所員及筆者は本地震の取調べの命令を受けた。筆者が現場に出張したのは震後十數日經てゐたので種々

1) T. Matuzawa, this Bull. **5** (1928). 1-28.
2) A. Imamura, Proc. Imp. Acad. **4** (1928) 56-59.

な證據物件が煙滅して居たので調査甚だ不充分となつたのは遺憾の次第である。尙本地震に關しては國富中央氣象臺技師の詳報[1] がある故玆にはなるべく重複を避ける積りである。

該地方の地震。 今回の地震の起つた所は信濃川流域越後平原の西南隅であつて全く所謂信濃川流域大地震帶[2] なるものゝ一部である。然るに本地震帶に起る地震頻度は決して多いものではないから一寸した强震も世人の注意を惹起した次第である。舊記に現はれた大震はさて措き、明治以後に起つた弱震程度のものまで數へあげても十數回に過ぎない。卽ち次表の如きものである。

番號	日附	震動著しき地方
1	明治 19 年 7 月 23 日午前 11 時	水內郡及東頸城郡
2	〃 20 年 7 月 22 日午後 8 時半	* 古志、三島、南蒲原、諸郡强震
3	〃 23 年 1 月 7 日	上水內、東筑摩、北安曇、更級、諸郡
4	〃 31 年 1 月 17 日	上高井、上水內、諸郡
5	〃 31 年 5 月 26 日午前 3 時及 5 時	六日町强震
6	〃 32 年 1 月 22 日	諏訪、上伊野、東筑摩
7	〃 35 年 5 月 15 日午後 9 時	* 長岡町强震
8	〃 〃 〃 16 日午前 9 時半	小千谷弱震
9	〃 37 年 5 月 8 日午前 4 時半	六日町强震
10	〃 38 年 7 月 23 日午後 5 時半	安塚町强震
11	〃 43 年 1 月 22 日午後 3 時	上田弱震
12	大正元年 12 月 11 日午後 3 時半	信濃飯山强震
13	〃 4 年 11 月 16 日午前 1 時	魚沼郡弱震
14	〃 7 年 11 月 11 日	大町激震

表中 * を附したるものは今回のものに極めて近きものである。尙文政11年(1928) 11 月 12 日三條大地震なるものゝ震央地方の一部は今回のものと大差なきものと思はれる。

地震の發生及餘震。 地震發生の順序といふものは時により所により實に區々たる經過を取るものであつて如何にも捕捉し難い。今回の場合には午前 10 時 53

1) 國富信一： 氣象集誌第二輯第六卷第二號（昭和三年）59-85.
2) 大森房吉： 大正七年信州大町地方激震調査報告、震災豫防調査會報告 **94** (1922) 16-69.

分の最強なるものに先だつて 10 時 10 分、同 35 分及 36 分の三回微震が感じられて居つたやうである。之等は躊躇なく前震と認めてよい場合であらう。

又今回のやうな局部的強震にはよく數十時間經て同樣若くはそれ以上の強さの地震が起る場合が報告されてゐるが、[1]今回は幸に續發強震は無かつた。

餘震の狀況は、27 日午後2時頃より同 11 時頃まで 20 分乃至 30 分毎に一回位の割合、同 11 時 40 分頃より翌 28 日午前1時 30 分頃まで 27 回。同 2 時 46 分より同午前 9 時頃まで 26 回、日吉村南西地下より遠雷の如き爆音を聞いたと云はれる。[2] 其後は極めて急速に沈靜したようである。

地震發生當時の氣壓配置の狀況は二三日前より本州の大部分 765 ミリ內外の高氣壓に覆はれて居つて、したがつて氣壓傾度も極めて緩かであつた。そして臺灣の東方大平洋上には 740 ミリ位の可成り廣範圍の颱風が迫つて來て居つて東京邊では例によつて脈動が發現し初めてゐる。尤も低氣壓は大抵の場合何處かに一つ位存在するけれども然し大地震の發生の當時低氣壓が近づき脈動が出現しつゝあつた例は甚だ多いことは注目すべきである。

被害狀況及地變。　現場調査に於て最も有力な參考物件となるものは構造物や自然物の變位變形等の狀況であること論を待たないが、今回は幸にして震害は世評程甚だしく無かつたことや餘震が急速に沈靜したことなどで、極めて速に人心平靜に歸したらしい。その爲に破損物の整理も極めて速に行はれたらしく十數日の後では調査材料は豐富といふわけには參らなかつた。

先新潟縣當局よりの報告を摘錄する。

種別 ＼ 村別		日吉村	關原村	宮本村	合計
傷	男	1			1
	女	1			1
住家	半潰	9	8	6	23
	大破	190	13	31	234
非住家	大破	10	8		18

（續く）

1) 大森房吉：震災豫防調査會報告 **94** (1921) 16.
2) 新潟縣知事報告。

（續き）

道路	個所	龜裂 3 缺潰 1	龜裂 3		7
	延長	105 25	28		158
堤防	個所			1	1
	延長			8	8

尙被害の內容は次の如き種類である。

1. 宮本村
   (1) 烏越雲出間縣道約 100 間深さ約 6 尺位陷沒。中央 50 間位は 3, 4 寸の龜裂。交通杜絕。
   (2) 住家 5 戶土台を外し爲に相當傾斜。
   (3) 新潟水力電氣高壓線の變壓器一ヶ墜落。
2. 關原村
   (1) 同村某女避難せんとする際荷馬車に衝突、又某男も同樣避難の際屋根石墜落負傷せるも何れも生命には支障なし。
   (2) 戶障子破損土臺の外れたるもの五戶。
3. 宮本村
   (1) 村道の龜裂を生じたる個所七ヶ所、決潰一ヶ所、何れも延長 2 間位。
   (2) 戶障子破損土臺の一部外れたるもの約百戶。

以上の如き狀況であれば震動の强さといふものも蓋し大したものではなかつたであらう。實際此邊の家屋は實に粗造のもが多いやうである。それにも拘らず損害の程度は極めて微少であつたやうである。(Pl. IX. Figs. 1a–1e).

地變の主なるものは路面の龜裂決潰、及び田面の搔亂である。道路の決潰の尤なるものは烏越雲出間のものである (Pl. IX. Figs. 2c, 2d)。これは兩ローム臺地の間に狹まれた底地から堤防狀に積み上げた道路であつて崩れたことそれ自身には餘り珍らしい事は無ささうである。但しその崩れ方には注目すべきものがある。崩土が橫に廣がつた量は高さに比して著しく大きい。そして崩れ方の性質は全く寺田先生等[1] の砂の崩れ方の實驗と同樣なことが見られる。卽ち崩れないで、全體として固體の如く形を保つて居る部分、それから、上表の辷り乍ら變形はしてゐるが始めの物質部分の配列順序は餘り變つて居ない部分卽ち彈性體のやうな部

1) T. Terada and N. Miyabe, Proc. Imp. Acad. **3** (1927); This Bull. **4** (1928) 33-56.

分、それから此等兩部分を界する部分卽ち液體のやうな部分を區別することが出來るやうである (Pl. IX. Fig. 2d.)。かう考へれば、地震の時よく出會ふ所の水平に驚くべき距離を辷つてゐる地辷り現象は好都合に說明出來るやうである。それにはどうしても前述彈性體に似た部分と名づけた部分の分量の多い事がどうしても必要條件だと思ふ。[1] それは運動量が少くては遠方まで行き得ぬからである。事實一握りの土塊を傾斜に沿つて落した所で如何に地震の場合と雖も百米も二百米も辷るものではあるまい。中間の擬液層部分は車の如く、或は減摩油の如く働くに相違ない。どうも崩れた土の全體が液體の如く流下するといふ考へ方は隨分漠然たるものの樣に思はれる。(十勝嶽の場合の如く事實液體になつた場合は別)

關原地方の圖
(約 1:75000)

Fig. 3.

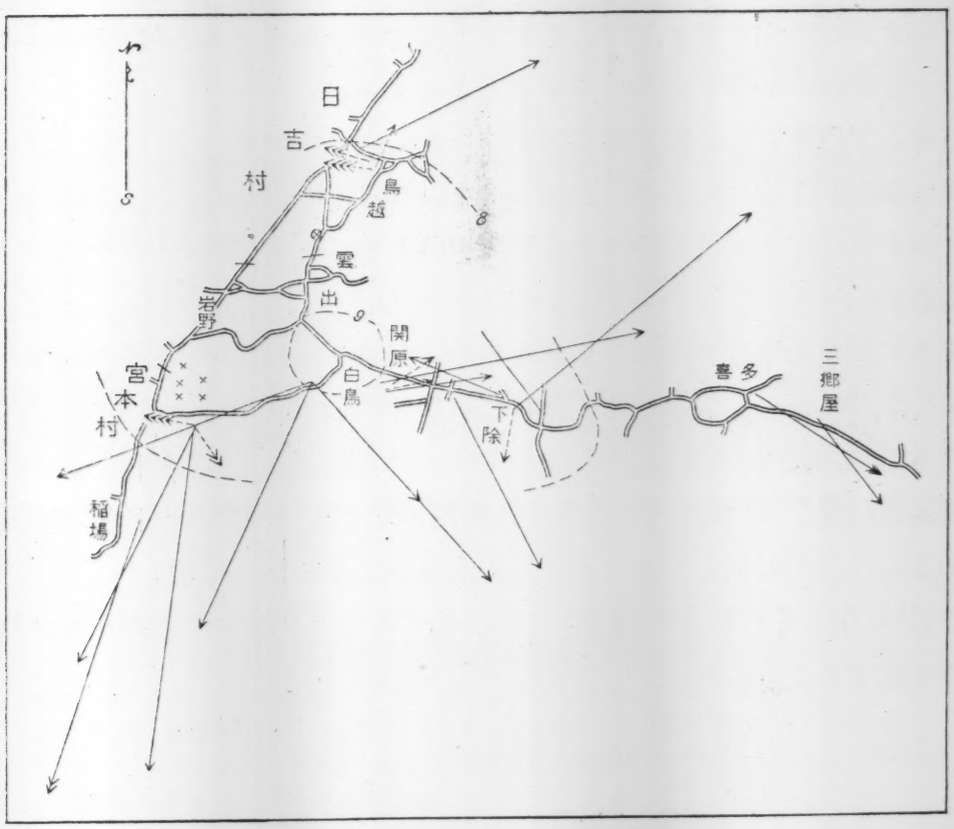

⊗ 道路缺潰　— 路面龜裂　×× 田面搔亂多し
破線はロツシ，フォレル氏震度區域を示す。實線矢印は移動方向及大いさ (縮尺 $\frac{2}{3}$)
破線矢印は轉落方向を示す

1) 松澤武雄： 根府川山津浪調査報告、震災豫防調査會報告 **100** (1925) 乙、83.

前述の場所の雲出臺地の緣邊部は著しく崩れ落ちてゐる(Pl. IX. Fig. 2a)。ローム臺地の緣邊が地震の際被害をよく受けるといふことは小藤先生から御注意を受けた。ロームでなくても粗質な臺地の端は崩れ易いやうである。丹後の地震の際峰山から鄕へ通ずる中間の霞爛し切つた花剛岩の山の端も大分崩れてゐた。

宮本村白鳥邊の田面に略南北に龜裂を生じて砂を噴出し同時に油狀のものを出したといふことである。不幸筆者が踏査した時には明瞭なるものを認め兼ねた。但し此邊の田面はかなりの搔亂を受けて居た。

尙地變に就て著しいことは今村、山崎兩先生の委託によつて陸地測量部で行つた水準測量の結果[1]である。地震の略々直前直後の測量結果を比較し得たのは恐らく嚆矢であらうがその結果關原村邊が2センチ餘り上昇したことになる、これが地震の原因であつたか結果であつたかは俄に斷じ難いが何れかと云へば地震を起したと共通の原因で起つたと見る方が考へ易い。それは狹いとは雖も4キロにも及ぶ部分が振動丈で震り上げらるゝと云ふことは極めて不自然である。尙地變と震動との關係は別稿[2]に於て論ずることにする。

尙石碑、石燈籠の類の轉落移動等を受けたものに未だ整理されなかつたものを若干調べ得た。(Fig. 3)。(Pl. IX. Figs. 1a—1d)。圖の如く極めて區々たる移動狀況を示すけれども大體に於て宮本村西田邊を中心に放射狀の傾向が見える。

最强震動區域は Rossi Forrel の尺度で 8 乃至 9 位のものである。(Fig. 3)

要するに激動區域が極めて狹く而も中心と目さるゝ地方の振動がともかく地變や破壞を生ずる程であつたことを見れば、震動の發現點は地下餘り深くないものと思れる。

器械觀測結果。本地震は震央地が比較的明瞭であつたが故に器械觀測結果を吟味するには甚だ好都合であつた。その上他の場合に比して著しい二三の事柄があつた。然し乍らそれを論ずることは勢ひ他の場合と比較するを要するが故に稿[3]を更めて論ずることにする。

昭和3年4月。

1) l, c. p. 29.
2) T. Matuzawa, this Bull. **5** (1928). 1-28.
3) Ibid.

石燈轉落（關原西端）
Fig. 1 a

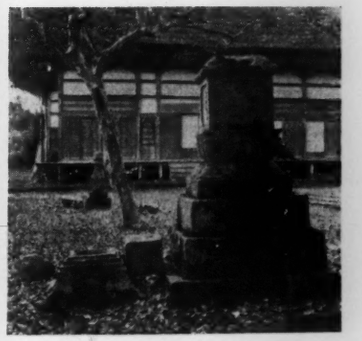

關　原
Fig. 1 c

關　原
Fig. 1 b

小祠のの移動（三郷屋）
Fig. 1 d

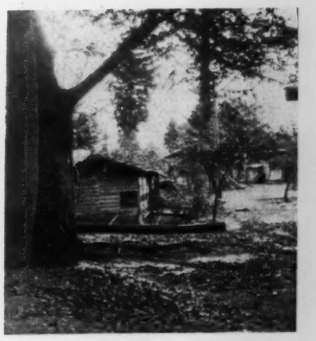

粗造家屋損害を見ず（關原西端）
Fig. 1 e

雲出臺地北端の崩壞（ローム）
Fig. 2 a

雲出縣道の段違ひ（南方 4 センチ 落ちる）
Fig. 2 b

雲出鳥越間縣道の缺壞及龜裂
Fig. 2 c

雲出鳥越間縣道の缺壞及龜裂
Fig. 2 d

（震研彙報第五號、圖版、松澤）

關東大地震並に丹後大地震に表はれたる斷層の横ずれに就いて

所員 今村明恒
助手 岸上冬彦

On the Horizontal Shift of the Dislocation accompanied by the Recent Destructive Earthquakes in the Kwanto District and in Tango Province.

By

Akitune IMAMURA and Fuyuhiko KISHINOUYE.

(Abstract.)

It is well known that the Go-mura fault, the larger of the two dislocations accompanied by the recent destructive Tango earthquake, actually shifted horizontally as much as 270 cm. The present writers have devised a method other than that of direct measurement for the estimation of the amount of shift by taking into consideration the relation which may exist between the distance of each geodetic station from the fault and the horizontal displacement assumed at the corresponding station by the earthquake. For this purpose, they selected only such stations as were situated on, or near, the straight line drawn at right angles to the fault through the point of its maximum shift. (See Fig. 1.) In Tables I and II, x indicates the distance of each station from the fault line, and y the displacement of same parallel to the fault. The diplacements here adopted were computed from the results of trigonometrical observations carried out both before and after the earthquake under the assumption that the two southernmost stations in the surveyed area suffered no displacement. The values of y in Table I are deduced from the observations of 1884-1888 and June, 1927, while those in Table II are based on those made in 1884-1888 and Aug., 1927. Plotting them as in Fig. 2, the data in the second table give more satisfactory results. The curve showing the relation between x and y has two branches; the intercept of the axis of y by these branches corresponds to the shift of the fault and is found to be in fair agreement with the actual measurements.

The same method has been applied to the case of the destructive Kwanto earthquake of 1923. Here the great fault across the bottom of the Sagami Bay from NW to SE is concealed under water; its existence was first revealed as

the result of the elaborate surveys carried out by the Naval Hydrographers. According to Prof. N. Yamasaki, the situation of that fault is likely to be in the place as shown in Fig. 3, its active centre being located somewhere near a point equidistant from Misaki, Mera and Oosima. Selecting the trigonometrical points, which are situated on, or near, the straight line drawn at right angles to the fault line through the active centre, the distance x from the fault to, and the horizontal displacement y parallel to that line of, each station come out as in Table III. Plotting these data as before, and then drawing the curve which shows their mutual relationship (Fig. 3), the intercept of the axis of y by the two branches of that curve, i. e., the horizontal shift of the fault, comes out as 8 meters.

去る大正十二年の關東大地震に就いては、震原が相模灣の海底にありしが爲に、地形變化の正確な狀況を知ることが頗る難事であつた。曩に海軍水路部では此方面に於ける綿密な水深測量を實施し、猶ほ其結果について山崎博士は地形學的講究を加へ、相模灣底を北西から南東へ横切る大斷層の存在を推定せられて、此問題も解決がついた様に見えたけれども、研究者仲間には猶ほ疑問を懷く人もあつて、今一度水深測量を繰返して貰ひたいなどと希望する人もある位である。勿論相模灣の再測量は別な意味に於て吾々も希望する所であるけれども、論者の如き意味に於ては、無條件に同意する譯には行かぬ。

最近の丹後大地震に於ては陸地に著しい斷層が出現して、之に關係せる地形變動中垂直の移動は精密水準測量により計測せられたが水平移動については觀測者によりて直接に計測せられたのみであつた。然るに其後三角測量によりて各測點の水平移動が氣附かれたが自分等は之を應用して、該斷層の横ずれの分量を推定し得る方法を考究して見た。此事項は丹後大地震の研究に對しては、大した効能もないかも知れないが、然しながら之を關東大地震の場合に適用することに於て、相當な價値のあることが認められるであらう。自分等は其結果を以て、相模灣底に於ける大斷層存在の一證左ともなし、又其斷層に沿うて生じた横ずれの數量について或る具體的の觀念を與ふるものと思ふのである。

丹後大地震に於ける主要な斷層は郷村斷層と名づけられた。其上下の變位は、水準測量の結果、峰山町附近に於て 75 糎に達したことが明かになつたが、水平の變位については郷村高橋に於て 2.5 米に達した處が處々にあり、2.7 米を示した處もあつたので、此最後の値を以て最大値とすべきである。今一二等三角測量

の結果（第一圖）を大觀して見るに、斷層の東方にある測點は北方に移動し（震域中最南の二測點たる床之尾山と烏ヶ岳を不動と假定して）、西方にあるものは南方に移動し、而も其移動の分量は斷層に近きもの程大きく、之を遠ざかるに隨

第　一　圖

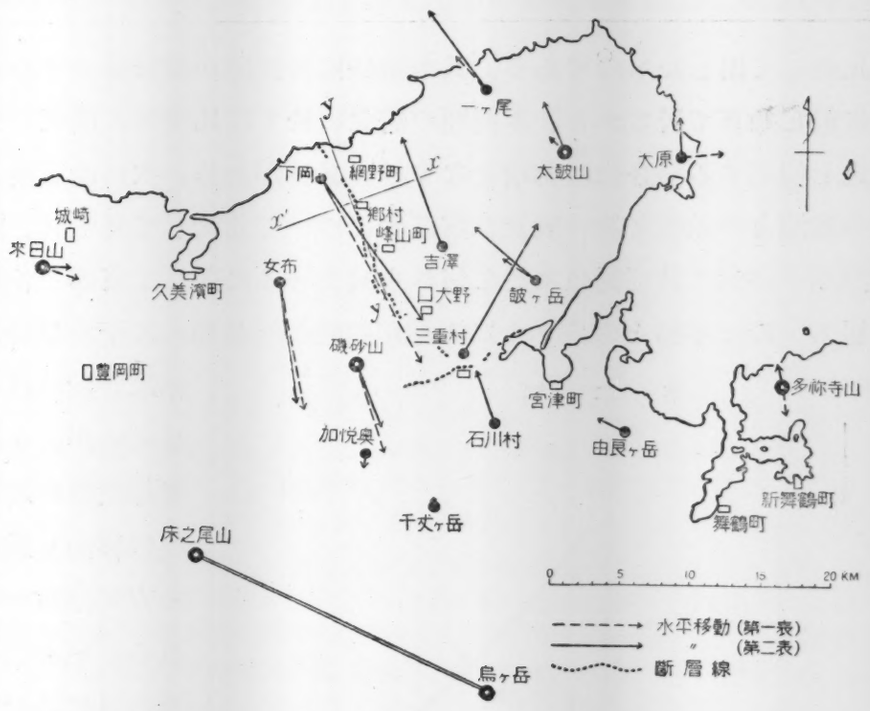

Fig. 1.

つて次第に小さくなる傾向を示して居る。今郷村斷層の最も著しき中央部を取りて此部分を直線と看做し、各測點の此線からの距離を x とし、それが東にあるを正、西にあるを負とし、又各測點の斷層線に平行な水平移動量を y とし、それが北へ向へるを正、南に向へるを負とするならば次の様な結果が得られる。

但し右の移動量につき第一表の結果は明治十七年乃至二十一年實測と昭和二年六月實測とを比較して出したもの、第二表のものは最初の實測と昭和二年八月の

第　一　表　Table. I.

測　點	城　崎	女　布	磯砂山	下　岡	吉　澤	一ヶ尾	大鼓山	大　原
x	−21.5km	−7.0	−4.7	−0.7	5.0	10.6	14.8	20.4
y	−21cm	−91	−65	−153	—	31	16	−13

第二表　Table. II.

測點	城崎	女布	磯砂山	下岡	吉澤	一ヶ尾	大鼓山	大原
x	−21.5km	−7.0	−4.7	−0.7	5.0	10.6	14.8	20.4
y	−10cm	−87	−48	−127	86	70	38	25

ものとを比較して出したものである。其中磯砂山は位置が斷層線の中心に對し、少しく南に偏し過ぎて居るから、本問題の研究に於ては比較的に價値の少い値であつて、之を使用する場合には割增をなすべき必要がある。次に地震後第一の實測と第二の實測との差違を第一表及び第二表について比較して見るに、斷層西部にある諸測點の移動は其絕對値に於て何れも減少せるに對して東部の各點は增加を示して居る。此は不動と假定した二測點が前記の三月間に若干の移動をなした結果と疑はれないこともないが、それよりも東部諸點が此間に更に反撥移動を進めたと見る方が穩當の樣に思はれる。昭和二年五月乃至八月に於ける餘震分布が此考方にも調和する。今此等の結果を圖示（第二圖）するときは第二圖の實測値（第二表）の方が原點に對して寧ろ對稱に近く現はれて來るから、此方の諸點を縫ふて曲線を引いて見ると、大體圖示されたものになる。之を少しく延長すると、y 軸との交點の縱

第二圖

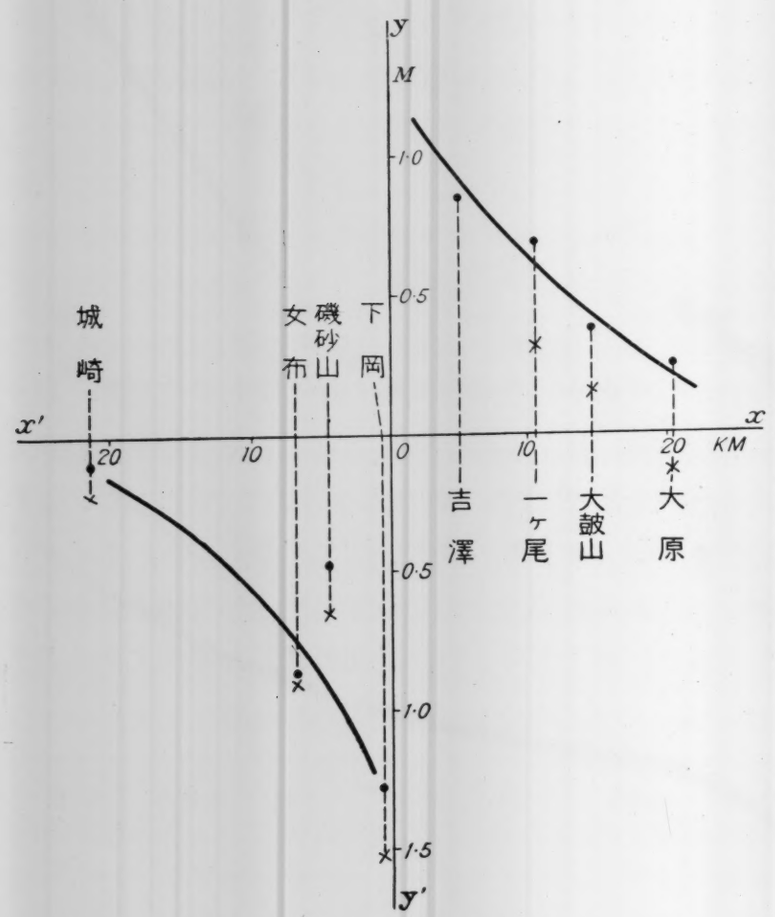

Fig. 2.

座標として 130 cm と −140 cm とが得られる。卽ち兩方の枝線による y 軸の截部が 270 cm と出て來るので、實際に計測した斷層の最大横ずれに全く一致することになるのである。

次に同様の方法を大正十二年の關東大地震の場合に應用して見る。(第三圖參照) 相模灣底に於ける大斷層線を山崎博士の推定せる位置に取り、其中央部に直

第　三　圖

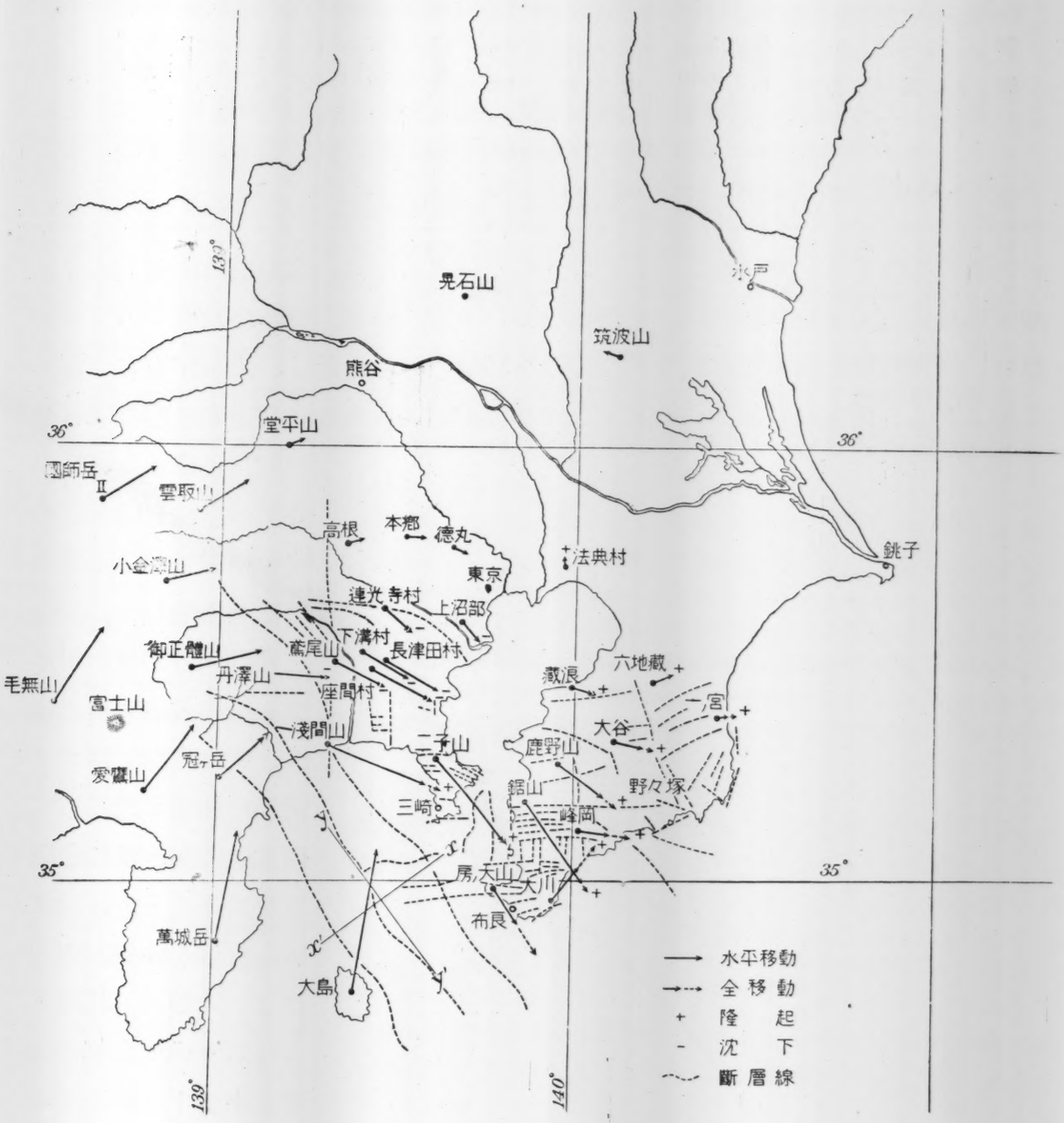

Fig. 3.

角に引いた線の上若しくはそれに近き位置にある測點を選び、斷層線からの距離 x と斷層線に平行な水平移動 y とを前と同様に定めるときは次の様な値が得られる。但し水平移動量を算出するには明治十七年乃至三十二年と大正十三年乃至十四年との三角測量の結果につき、最北點の晃石山及び此點と筑波山とを連ねる方位が不動と假定された。

第三表　Table. III.

測點	萬城岳	大島	淺間山	(房の大山)	二子山	大川	鋸山	(峰岡)	鹿野山	藏浪	(野々塚)	大谷	六地藏	(一の宮)
x	km. −41.5	−20.0	8.9	24.7	30.2	34.6	44.1	50.5	56.1	69.1	71.0	71.0	87.1	95.7
y	cm. −216	254	−221	−116	−267	34	−256	−57	−139	−37	−70	−50	−7	−19

x の値の負數なるは萬城岳と大島との二點だけであつて、本問題の研究上不足を感ずるけれども止むを得ない。又房の大山、大川、蜂岡、野々塚及び一の宮の五點は、所謂外房に屬する諸點であつて水平移動の中心に對し、位置が南方に偏して居るから、此等は差別的の取扱をなす必要がある。今表に於ける各點を圖（第四圖）に盛込み、先づ外房の諸點を除き、丹後大地震について得た結果を參酌して、距離と移動との關係を示す線を第四象限に於て畫き、次に原點に對する對稱の關係を適用して同意味の線を第二象限に於て畫くとき、圖に示した様な曲線が得られる。此等の二枝線によれる y 軸の截部は如何に小さく見積つても 8 米はあるらしく思は

第四圖

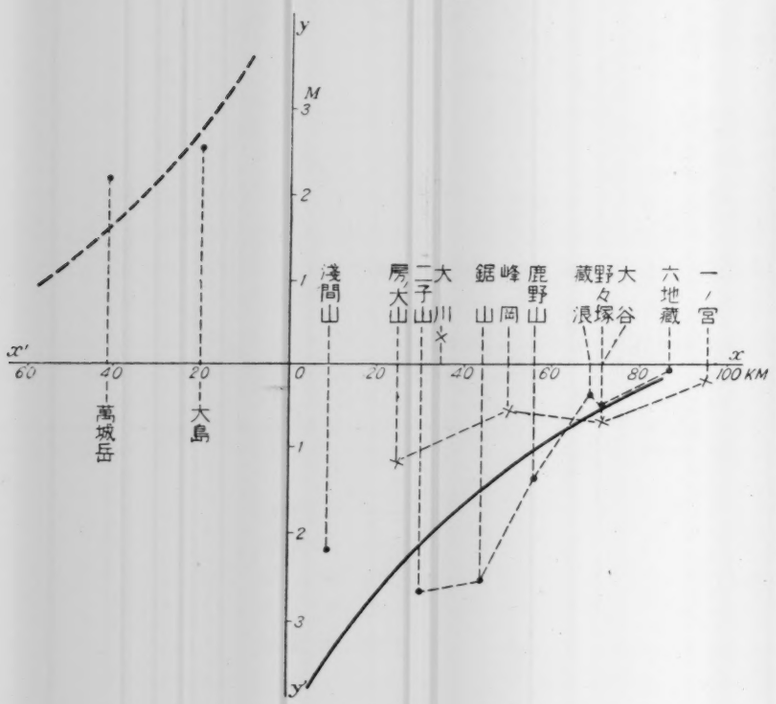

Fig. 4.

れる。卽ち相模灣底に於ける大斷層の存在が認められるならば、其斷層の横ずれは8米の程度に達したらうといふことになるのである。此は海底並に陸地が同様の物理學的性質を有するものとしての計算であるが、實際は海底を構成して居る部分は比較的に粘性に富むものらしいから、横ずれはもつと大きいものであるかも知れない。

外房の諸點中、最も南に偏したものは大川であるが、此點の移動は附近の諸點の移動と方向を異にして居る。恐らくは灣底に於ける大斷層の南東の終點か或は方向轉換を暗示するものであらう。此等の諸點の垂直移動が比較的に大きいことによりてもさう想像せられるのである。國府津附近の湘南沿岸に現はれた垂直の大移動も同様の意味を有するかも知れない。

上の結果は相模灣底に於ける斷層の存在を假定して得られたものであるが、斯様な斷層の存在は第四圖に示した諸座標の配置から見ても、之を否定することは頗る不自然の様に思はれる。實際再檢査の爲め海深測量の再施を希望せられる向きも、海底變動に關する分量の餘りに偉大なるに疑を挾まれるのであつて、言はば單に數量的の疑問である。之に對しては寺田教授の解說によりて納得が出來ることと信ずるのであるが、然しながら自分等の本講究の結果は該斷層の垂直移動の分量とは全く獨立して成立するものと考へる。

On the Correlation between the Long Period Fluctuation of Barometric Gradient and the Occurrence of Earthquakes in Kwatô District, Japan.

By

Win INOUYE.

關東に於ける氣壓勾配の長週期變化と地震發生との關係

所員　井上宇胤

宇都宮と布良及び銚子と甲府の毎日午前六時の氣壓の差を大正十五年一月から九月迄の九ケ月間中央氣象臺から發表して居る天氣圖の裏面の氣壓の價から求めそれ等を適當になだらかにしてから組合せて關東地方の氣壓勾配の長週期變化を求めました。

それに依ると圖一に見られる樣に東北一西南の方向の約九十日の變化と西北一東南の方向の約一年の變化とがあります。

そこで今村所員が震研彙報第三號に發表された此の當時の地震の中から五十五ケの有感地震を選び出して氣壓勾配の九十日の變化と比較しました。

氣壓勾配がその平均値より東北に偏しておるときに發生した地震を十の組とし西南に傾いて居るときに發生した分を一の組とし殆んど平均値に近いときに發生した分を？の組として圖二に各々の震央の上にそれ等の屬する組の符號を書き込みました。

此れに依ると同じ組の地震は互に集まつて地方的な集團をなす樣であります。

結局氣壓勾配の九十日の變化と共に地震が發生する地方が異なるかの樣になつて居ります。此の事實を一層確かめ且その意味を理解するために今村所員、中村左衞門太郎教授、松澤助教授、故大森教授の此の地方の地震に關する御研究及び矢部教授、東木氏の地質に關する御研究及び此の地方で行はれた重力測定、地磁氣測定の結果及び最近の陸地測量部の此の地方の構造線に關する御研究等と比較致しました。

尙又著者が陸地測量部に依つて確定された關東大地震後の此の地方の水平並びに垂直變位の結果を取り扱つたもの（圖三參照）、及び此の地方の數十ケの地震の震源の深さを決定したものをも參考致しました。

その上寺田所員が御親切にも上記の現象の一つの可能性ある模型的說明を御教示下さいましたが、遺憾ながら今日の狀態では此の問題並びにそれに類似の問題の眞の意味を了得する事が出來ない樣に思はれます。

然しとにかく氣壓勾配の長週期變化は地殼の傾斜運動を通して地震の發生と相關する樣に思はれますし、又其處には多少物質の粘性が要求されてるのではないかと思はれます。尙以上列擧した多くの他の成果と比較する事に依つてここに求めた有感地震の地理的集團と云ふものは可なり實在性のあるものと思はれます。

I. Introduction.

The question regarding the relation between the occurrence of earthquakes and certain quantities connected with the barometric pressures had already been investigated by many authorities.

Among them, late Prof. F. Omori[1] made a classical study of the relation between the earthquakes originating in different localities widely distributed in entire Japan and the barometric pressures at the corresponding stations.

Later Prof. T. Terada[2] made an investigation of the relation between the seismic frequencies and the barometric gradients in many parts of Japan for the first time, and then Dr. K. Hasegawa[3] studied the relations between the local earthquakes which took place near Gihu, central part of Japan, and the barometric gradients existing there at the epoch thirty minutes before the occurrence of the earthquake; still later, Prof. Saemontarô Nakamura[4] studied the same problem using the data of the local earthquakes which took place in Kwantô District, near Mt. Tukuba. They all agreed in concluding that the barometric gradients shortly before the occurence of earthquakes are generally perpendicular to the tectonic lines or weak lines already known by geological and seismological investigations in the localities in question.

Next, Prof. T. Terada[5] and Mr. Sadazumi Masuzawa determined the local distribution of the barometric gradients predominating at the time of occurence of the earthquakes for each of a number of districts in the main island of Japan, and came to attribute some definite type of stresses in the earth's crust to be the probable cause of these earthquakes.

Moreover, there are several other results of investigation of the allied problems obtained by Messrs. Daizô Nukiyama and Masayuki Mukai,[6] Prof. Saemontarô Nakamura,[7] Mr. T. Ishikawa[8] of the Central Meteorological Observatory, Tokyo, and Mr. K. Suda[9] of the Marine Meteorological Observatory, Kobe.

They have all studied the problem concerning certain quantities related to the barometric pressures at the time of the occurrence of earthquakes, but they, except Mr. T. Ishikawa, did not take into consideration any integral effect of these quantities prevailing before the time of earthquake for a certain duration.

Recently, Prof. M. Ishimoto[10] of our Institute expressed his view that the sensible after-shocks of the Tango earthquake of May 7, 1927, occurred mostly when the difference of the barometric pressures at Kyôto and Miyadu had been

increasing for several days preceding the time of occurrence of the earthquake.

With the encouragement and advices by Prof. M. Ishimoto the present author studied the relation between the occurrence of the sensible earthquakes in Kwantô district and the long period variation of the barometric gradients prevailing there.

2. In the first place, the author calculated the difference of the barometric pressures between Utunomiya and Mera, Tyôsi and Kôhu and several other pairs of Stations, at 6 o'clock every morning, for the three months from July to September, 1926, using the data of the barometric pressures at the stations in question printed on the back page of the daily weather chart published by the Central Meteorological Observatory.

Smoothing these differences by using the formula

$$\overline{H}_n=\frac{H_{n-2}+2H_{n-1}+3H_n+2H_{n+1}+H_{n+2}}{9}$$

the author found that there exist several kinds of periodic variations i.e. with the periods of about 7 days, 15 days, 20–40 days and 90 days.

Using the usual method of eliminating the periodic variation with n day period in the case when such a periodic term exists in the observed phenomena i.e. by taking the mean values for successive overlapping intervals of n day, the author eliminated the short period fluctuation from the differences of the barometric pressures at Utunomiya and Mera as one group and at Tyôsi and Kôhu as another group, using the data of the barometric pressures during 9 months between January and September, 1926, by putting $n=5$ days, putting $n=15$ days and $n=27$ days I could eliminate the more or less longer period fluctuation, and could find that the long period variations amount to about 90 days and one year.

As the two lines connecting respectively the stations Tyôsi-Kôhu and Utunomiya-Mera are situated perpendicularly to each other in Kwantô district and the distance between the two stations of each pair are about 200 km., the barometric gradients could be determined by combining the two differences as shown graphically in fig. 1.

As seen from the figure, the appearance of the vector diagram of the barometric gradients looks like a Lissajou's figure, and is composed of the two variation one in NW-SE direction with a period of one year, and another in NE-SW direction with a period of $\frac{1}{4}$ year or 90 days.

Fig. 1. Long Period Fluctuation of the Barometric Gradient in Kwantô District between January and September, 1926.

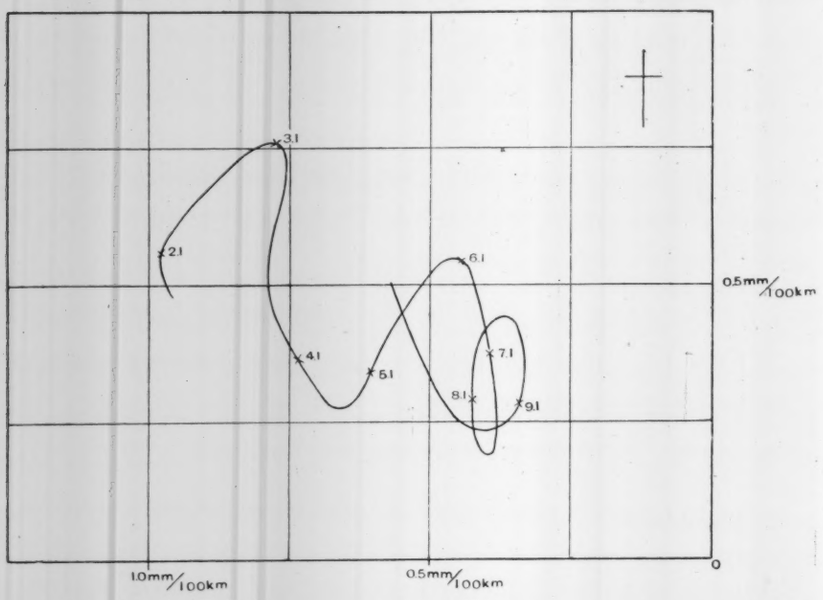

The amplitudes of these variations, corrected for the decrease due to the process of smoothing, are 7.5 μ/km. or 1.5 mm. Hg per 200 km. for the longer period variation and 5 μ/km. or 1 mm. per 200 km. for the shorter one.

The above results are quite similar to that obtained by Prof. T. Terada in his paper above referred to. In the latter the barometric gradients in Kwantô district were determined by the monthly means of the barometric pressures at four stations lying at the four corners of a rectangle, namely Wajima, Niigata, Tyôsi and Nagaturo.

3. Next, the author compared the long period fluctuation of the barometric gradients thus obtained with the occurrence of the sensible earthquakes.

The data of earthquakes are taken as far as possible from the list reported by Prof. A. Imamura[11] of the earthquakes which occurred during the nine months between January and September, 1926, in Kwantô district. I could use 55 sensible earthquakes for the purpose.

As for the barometric gradient, only its variation with the period of 90 days was taken into consideration. The barometric gradients at the beginning of January could not be obtained on account of the method of procedure here used and the lack of the data, but the value was assumed according to the result of Prof. T. Terada above cited.

These earthquakes will be classified into three classes according to the

direction of the barometric gradient vector at the time of their respective occurrences. When the barometric gradient vector at the time of occurrence of a certain earthquake deviates to NE or SW from its mean position, we will indicate the epicentre of the earthquake with the mark + or − respectively on the map as shown in fig. 2. The epicentres indicated with a mark ? in the map are those of the earthquakes, at the time of occurrence of which the vector scarcely deviated from its mean position.

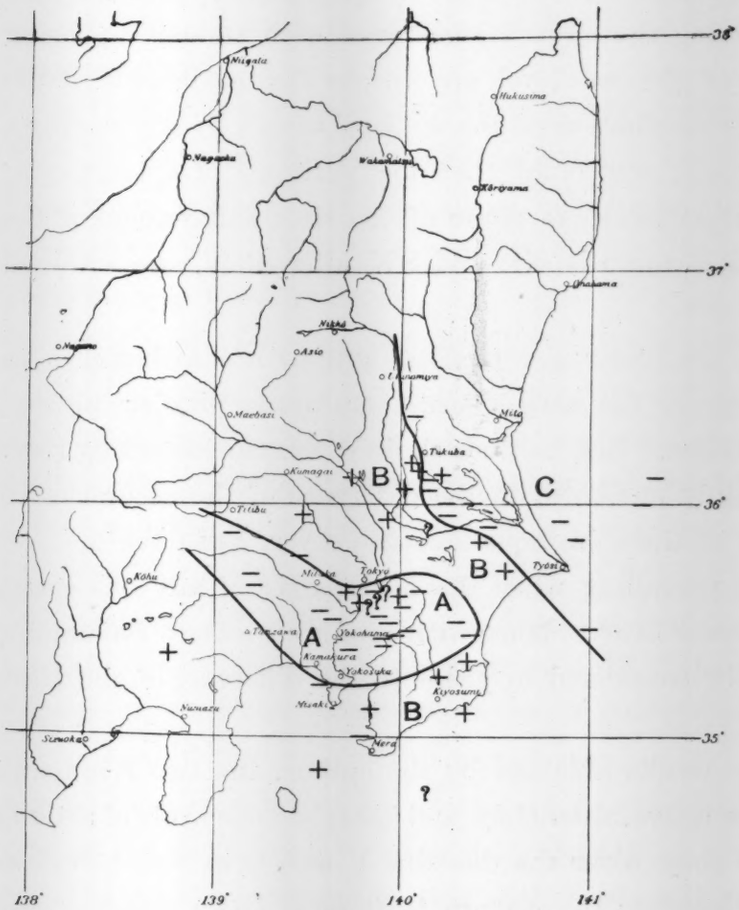

Fig. 2.

The number of earthquakes which fall into the groups with the mark +, −, and ? are 18, 32 and 5 respectively. Thus it appears that the earthquake occurs rather frequently when the vector of the barometric gradient is deviated to SW.

The geographical distribution of the epicentres of the earthquake seems to be more or less systematic, the epicentres specified with the same mark swarming together into rather definite local groups.

The geotectonic significances of the boundaries of these groups may be mentioned later in more or less detail.

By the way, Prof. Saemontarô Nakamura[12] compared the mean anomaly of the sea level determined from the records of the tide-gauges at Tyôsi, Mera and Yokosuka mareographical stations, during two days before the occurrence of the earthquakes, on the day when they occured and duringtwo day s after

the occurrence of them, with the time of occurrence of after-shocks of the great Kwantô earthquake of September 1, 1923, and he obtained the result that the positions of epicentres of the earthquakes, which occurred when the mean anomalies of the sea level at a given station had been positive and negative respectively, were distributed in groups. Moreover, when we take into consideration the assumed tilting of the earth's crust in the district, which may be obtained by combining the mean anomalies at each station supposing that the mean anomalies of the sea level are due to the movements of the earth's crust and not to the fluctuation of the sea level caused by any meteorological or astronomical causes, we found that the positions of epicentres of earthquakes which occurred at the same phase of the tilting movement of the earth's crust in the direction towards NE and SW alternately, are crowded together within a definite area.

In the main feature, the latter geographical groups of earthquakes as regards the assumed tilting of the earth's crust are quite similar to that obtained by the present author. But he finds slight discrepancies among these groups, which may be mainly attributed to the difference of the accuracies in determining the epicentres of these earthquakes. Moreover, as to the mode of tilting of the earth's crust prevailing when the earthquakes of any one group take place, the author is quite in accordance with Prof. Saemontarô Nakamura, if the earth's crust could be considered to yields to the difference of the barometric pressures.

Now, according to the results obtained by the author, the two Kinugawa seismic zones must become active alternately and complete one cycle of activity within 3 months, because they cover the domains B and C in fig. 2. and as the Tama seismic zone enters into the domain A, it must be in action during the early part of each cycle and be dormant during the later half.

Prof. A. Imamura mentioned in his report (in Japanese), above cited, as follows, which I will here quote translating into English.

"We have two seismic zones along the drainage basin of the River Kinu, and the activity has migrated from one to another of these zones within these three months, and this cycle of minor activity became more and more clear in the succeeding three months."

He also says in his English abstract of his report, "The most conspicuous feature may be a completion of cycle or epoch of minor activity in the Tama

seismic zone. It became rather active in January about the middle point of the zone: the activity migrated a little eastwards in February, but was less active in March. Similar movement was repeated during the subsequent three months, but in July the activity was revived with augmented energy in the western part and at last it calminated on Aug. 3 about the middle point of the zone causing slight damages in Yokohama and Tokyo. Afterwards, more or less after-shocks were experienced for a few days, but finally the whole zone became quiet.''

4. The author determined the amount of dilatation and contraction of the distances between the neighbouring stations, reduced to per 1 km., using the data of the horizontal displacements in the area disturbed by the great Kwantô earthquake, which had been revealed by the triangulation carried out by the Land Survey Department.[13]

The values are written down in the annexed fig. 3. on the middle points of the lines connecting the neighbouring two stations with positive and negative sign according to elongation and contraction respectively. As seen from the figure, even if there are some regions where positive and negative signs occur mixed together probably on account of some local shearings, the same signs, are found as a whole, grouped together in definite areas. When these features are compared with the mode of distribution of the vertical displacements in Kwantô district detected by the leveling work of the Land Survey Department[14] carried out after the great catastrophe, it seems that in the elongated portion, the surface of the earth's crust was stretched in its horizontal extention smoothing its furrows more or less in way of its subsidence, and in the contracted portion the earth's crust shrinked horizontaly in the process of its elevation.

The boundary of the portion with horizontal dilatation are quite similar to that of the seismic domain A in fig. 2. along the drainage basin of the River Tama, which I obtained as the result of my investigation of the relation between the barometric gradients and the time of the occurrence of the earthquakes. It seems that they are physically connected with each other.

5. To determine the geological meaning of these boundaries of regions with different feature of seismic activity, the author studied some papers dealing with the geology of the district.

According to the opinion of Prof. H. Yabe and Mr. R. Aoki[15] the boundary between the portions A and B in fig. 2. along the southern part of the

Bôsô peninsula and Sagami seems to have a geological meaning as follows.

The main part of the Bôsô and Miura peninsulas and Ôiso block, which had been forming the horst extending in E-W direction, were disturbed by the Post-Narita disturbances, the latest one in the district, opening a channel in the intermediate portion.

Next, according to Mr. R. Tôki's[16] chronological researchs on the fluctuation of the level of the eroded surfaces in Kwantô district, the drainage basin of the River Kinu, along which is extended the boundary between the portion B and C, had been repeating the tilting motions sometimes eastwards and sometimes westwards in the geological era, and it may thus be assumed to be in activity even now.

6. Next, the author examined the results of the gravity observation and the magnetic survey in the district.

According to the result obtained by Prof. M. Matuyama[17] the anomalies of gravity in the region A seems to be smaller than in the neighbouring regions though the complete corrections for the neighbouring topography and isostasy are not yet porformed. W. Heiskanen,[18] applying isostatic correction according to Hayford's method, found that the gravity anomalies of this portion are negative.

According to the results of the magnetic survey, reduced to the epoch 1895.0 which was carried out by many able physicists of our country under the guidance of Prof. A. Tanakadate,[19] the rocks consisting the lithosphere of the portion A seems to be less magnetic than that consisting the neighbouring portions, because an apparent valley line of the magnetic disturbing force, though its existence is not quite certain, lies just in this district. Recently, the Hydrographic Department, Imperial Japanese Navy[20] carried out the magnetic survey several times all over Japan, but the results cannot be here utilized, as the number of stations in this district are too scarce for this purpose.

7. Next, the author calculated the focal depths for 33 among the 55 earthquakes in question, as they could be determined more or less distinctly using Omori's formula for the focal distance. Moreover, the focal depths of ten earthquakes which occured during 1927, were determined by the ratios of duration of the preliminary tremors at more than 4 stations taken among Tokyo, Kamakura, Misaki, Kiyosumi, Titibu and some other meteorological stations. For

the details regarding these earthquakes Prof. K. Suehiro's[21] paper may be referred to.

The values of the focal depths thus obtained range from 15 km. to 85 km., and most of them are within 60 km. . The author found that the focal depth of the earthquake of domain A might not much exceed 60 km.

Moreover, the author could verify this result by the result of an allied investigation of one of my colleague Mr. R. Takahashi. The significance of this result shall be mentioned later.

8. Next, studying the paper by late Prof. F. Omori[22] "Macro-seismic Measurement in Tokyo," the author found that the domain F of the "insensible earthquake" in Pl. II. "Map showing the distribution of the origin of the earthquakes in Central Japan, which were not felt in Tokyo, Sept. 1887 to July 1889" is quite similar in its form to our domain A, except the western portion which in the case of Prof. F. Omori is extended to as far as Matumoto, Nagano and Niigata but in the author's case the boundary is ambiguous.

De Montessus de Ballore mentioned on P. 339 of his book "La Science Seismologique" regarding the domaine F as follows.

"Inversement, il se forme aussi des zones portant ombre séimique, ou faisant pont, comme on dit, et dont il a déjà été question; elles trouvent leur raison d'être de la même manière dans l'agencement relatif, près de la surface terrestre, des couches anciennes à grands modules d'élasticité et de rigidité par rapport aux couches plus récentes au sein desquelles le mouvement séismique se propage moins rapidement et, partant, moins énergiquement. Kusakabe tire argument, en faveur de ces intéressantes considérations, de la distribution des origines des tremblements de terre qui, de Septembre 1887 à Juillet 1889, n'ont pas été ressentis à Tokyo, en dépit de la proximité de leurs origines et même de l'intensité parfois assez grande de ces secousses. La curieuse disposition de la carte de ces origines, établie par Omori, peut certainement s'expliquer, dans une certaine mesure, au moyen de ces conséquences des recherches de Kusakabe."

It is a question whether this results may be attributed to the difference of the rocks composing the lithosphere of different parts of the district in the sense above quoted or to the hypothetical secular change of the activity of the insensible earthquakes. At the time when Prof. F. Ômori investigated the insensible earthquakes, they occurred only in some separated domains; which

may be attributed to the secular change in the activity of this kind of earthquake.

Moreover, examining the space distribution of the direction of major axis of the disturbed area in the cases of 47 earthquakes given in Table II. of the paper by Prof. F. Omori, above quoted the author found that the epicentres of the earthquakes which have more or less similar, direction of the major axis are grouped in some definite localities quite similar to those which the author here obtained, namely the domains where the major axis take NE-SW direction are quite in accordance with the domains A and C, and where they take from E-W to NW-SE direction the domain are quite similar to the domain B. The authour thinks that the direction of the major axis of the area of disturbance, though they cannot be determined very accurate, is connected in some ways with the tectonie lines or weak lines in the district.

Further, very recently, Messrs. Mutô and Atumi, the experts of the Land Survey Department, determined the trends of the tectonic lines in Kwantô district very accurately, utilizing the data of the precise leveling performed several times in the district. According to their result, the predominating directions of the tectonic lines in the portion A and B are quite different; namely in the portion A they take N-S and E-W directions, and in the portion B they take NE-SW and NW-SE directions.

9. Recently, Prof. T. Matuzawa, Messrs. K. Hasegawa and S. Haeno[23] investigated the forerunners of earthquake-motions of certain earthquakes, and it seems to the author that the region bordered by chain lines in fig. 7 of their work, where those earthquakes occurred in which the development of each of the three phases due, according to them, to the refraction of seismic waves at the boundary between the surface layer 7 km thick and substratum, is remarkably observed at Tokyo, may be quite in accordance with the eastern portion of the domain B.

Moreover, as quoted by the above authors late Prof. F. Ômori confirmed that the earthquakes accompanied with detonative sounds had occurred nearly in the same region as those considered here.

10. Next, as to the correlation of the mutual activity of seismic zones or domains it was late Prof. F. Ômori[24] who has made investigation for the first time. Afterward, Prof. A. Imamura[25] studied the alternation of activity in the two seismic zones with the minor activity in Kyûsyû.

According to Mr. R. Hirano's[26] investigation the after-shocks of the great

Kwantô earthquake have become ative alternately in two regions with a period of 19 days, and Mr. K. Suda says that these earthquakes could be separated in two domains namely Bôsô and Sakawa-Sagami domain, exhibiting an alternate activity.

Moreover, K. Siratori[27] have made a study on the same problem. Mr. K. Wadati[28] of the Central Meteorological Observatory studied the fluctuation of the activity of the outer zones in recent years. Recently, Prof. T. Terada,[29] Mr. N. Miyabe[30] and Mr. T. Takayama[31] also investigated the similar problems.

Nevertheless, to the author's great regret, the true meaning of these phenomena seems to be yet unknown.

II. Discussion.

Let us consider the mechanism by which the variation of the barometric gradients may bring about the occurrence of the earthquake.

The earthquakes occur in the region on the one side of any boundary at the epoch when the barometric gradients deviate to a certain direction from the mean position, and on the other side they take place when the gradients deviate to the opposite direction. Thus, we must consider the mechanism as such that the earthquakes in any one seismic domain occur at the epoch when the barometric gradients deviate to a certain direction from the mean position in the course of their fluctuation with a period of 90 days.

The author is at present not yet in a position to express anything definite on this point, but may be allowed to mention here one of the possible mechanisms which was suggested to him by Prof. T. Terada, in the following.

Suppose two adjacent blocks of the crust be in somewhat loose contact with each other at an inclined faut plane forming the boundary between the blocks. If the atmospheric pressure be higher on the block on the upper side of the inclined boundary plane than on the other, the contact between the two blocks will be tightened, whereas if the pressure distribution be in opposite sense there will ensue a tendency to loosen the junction between them and thence to facilitate a dislocation along the weak plane of fault.

12. At any rate, according to the author's opinion, the variation of the barometric gradients cannot be the primary cause of earthquakes though it may act under some favourable conditions as a secondary cause or serve as a trigger action of earthquakes.

According to the author's result that the long period variation of the barometric gradients has some effects upon the occurrence of earthquakes, the author is led to assume the existence of some plastic material in the mechanism of the trigger action in question.

The assumption of such a plastic material may be found in several instances. For example, the elegant work of A. Wegener on the theory of the continental drift, and the theory of isostasy are powerful enough to make many eminent geophysicists believe the existence of a plastic material between the solid earth's crust and the dense core. As to the remarkable displacements in vertical direction which took place in the bottom of the Sagami Bay, which has been revealed by the sounding carried out by the Hydrographic Department, Imperial Japanese Navy, Prof. T. Terada[32] of our institute attributed it to the high plasticity of the substance composing the deep sea bottom in that region; moreover, he expressed his opinion, recently, that the material beneath the lithosphere of our country is more or less rich in fluidity, which he infers from the results of the precise leveling carried out by the Land Survey Department in the disturbed area of the Tango earthquake of March 7, 1927. Next, the plastic material may be assumed in the portion of the solid part of the earth's crust suffering enormous stresses.

Moreover, many folded structures, especially of the famous overthrust in the Alps, exhibit a fairly plastic nature of the material. It is needless to cite the plasticity of the magmas and lavas of volcanoes.

13. A further consideration about the geological structure of the district may here be added. According to the results of the gravity observation it seems that the earth's crust in the seismic domain A may consist of a more light material than the neighbouring regions; moreover, the rocks consisting the lithosphere of that portion may be less magnetic than the neighbouring rocks as seen from the results of the magnetic survey.

The density of the more or less acidic rock or some kind of granitic rock may be less than the ordinary rock consisting the sial part of the earth's crust; moreover, it is quite probable that the former may also be less magnetic than the latter.

The author is thus led to suppose that the portion A is composed of some such granitic rock, so that the gravity anomaly and the intensity of the terrestrial magnetism are all less than the neighbouring portion.

By the way, the fact that the focal depths of the earthquakes which took place in the portion A did not exceed 60 km., and forms a striking contrast to the neighbouring portions where the earthquakes occur more or less frequently with the focal depths amounting to 100 km., suggest that the thickness of the lithosphere of the portion A is smaller than that of others, moreover, it suggests that in these portions fairly good isostatic compensation exists. As there seems to exist the isostatic compensation in those two portions having the same height above sea level, the one in which the thickness of the sial part is rather small will be composed of more light material, and the other in which the thickness of the sial part is rather great must be composed of more dense substance.

14. Probably, the boundaries of the seismic domains determined by the above investigation are not of a permanent nature, because it is a question whether the apparent boundar may differ to some extent from time to time or not, owing to a secular variation of the effects of the primary and the secondary causes of earthquakes and of some mechanism connecting the domains with one another.

As seen from the author's investigation, at the epoch here in consideration, there were several seismic domains of the sensible earthquakes in Kwantô district, and some of them became active simultaneously and some of them alternately, and the cycle of their minor activity was completed within three months quite in accordance with the periodic variation of the barometric gradients with the period of about three months existing there simultaneously.

Further, the author hopes that the reader will keep in mind that this relation between the two phenonena now in question may be disturbed by some more effective agents under some unknown conditions.

It seems to the author that there are some phenomena of kindred nature; for instance, Mr. T. Takayama recently found that some seismic domains became active simultaneouly in some epoch and alternately in the other epoch. Again, it is a well known fact that some volcanoes exhibit several phases in their activities. In meteorology also may be found many examples of such phenomena. Moreover, it is a question whether the apparent parallelism between the variations of the seismic activity and the barometric gradients may be caused by some one and the same fundamental cause or not.

Nevertheless, it is quite significant that the seismic domains revealed by

the present investigation are connected with the phenomena such as gravity, terrestrial magnetism, again with the orogenic events in geological era and even in the present time, with the mean anomaly of the sea level, focal depths, forerunner, earthquake sound, direction of the major axis of a disturbed area, tectonic lines and the space distribution of the epicentre of the insensible earthquakes. After all, the author is of opinion that the variation of the barometric gradient shows some apparent correlation with the occurence of earthquakes as the variation is related with the tilting motion of the earth's crust.

15. In conclusion, the author expresses his cordial thanks to Professors Torahiko Terada, Sakuhei Fujiwhara, Misio Isimoto, Messrs. Chuji Tsuboi, Ryûtaro Takahasi and Chuji Yasuda in our Institute for their kind advices and encouragements, and to Mr. Minoru Ôtuka for his kind assistance in preparing the figures in the present paper.

References.

(1) F. Omori, Pub. E. I. C., in Foreign Languages No. 8.
(2) T. Terada, Journ. Met. Soc., 28 (1909), 1.
(3) K. Hasegawa, Proc. Tokyo Math.-Phys. Soc., 1913. p. 181.
(4) Saemontarô Nakamura, Proc. Tokyo Math.-Phys. Soc., 1915. p. 69.
(5) T. Terada, Proc. Physico Math. Soc. Japan, 3rd Ser., Vol. 1. No. 10-11.
(6) D. Nukiyama & M. Mukai, Jap. Journ. Astro. Geophys., Vol. 1. No. 2. 1922.
(7) Saemontarô Nakamura, Japanese Journ. Astro. Geophys., Vol. III. No. 2, 1925.
(8) T. Ishikawa, Journ. Meteoro. Soc. (11), 3 (1925) p. 255.
(9) K. Suda, Mem. Imp. Mar. Obs., 1, No. 4. (1924).
(10) M. Ishimoto, Bull. Earthq. Research Inst., Vol. 4.
(11) A. Imamura, Bull. Earthq. Research Inst., Vol. 3.
(12) Saemontarô Nakamura, Jap. Journ. Astro. Geophys., Vol. 4. No. 3, 1927.
(13) Bull. Earthq. Reseach Inst., Vol. 1.
(14) Sinsai-yobô-tyôsakai-hôkoku, 100, B.
(15) H. Yabe & R. Annual Report Saito Gratitude Foundation, No. 1, May, 1926.
(16) R. Tôki, Tirigaku-hyôron, Vol. 4, No. 2, Feb., 1928.
(17) M. Matsuyama, Pub. Bureau Centr. Seism, Intern. Sériè A. Traveau Scient. 2 (1925) pp. 1-24.
(18) W. Heiskanen, Zeitschr. f. Geophys., III. (1927) Heft 5.
(19) A. Tanakadate, Journ. College Seience, Imperial Univ. Tokyo., Vol. 14.
(20) Bull. Hydrographic Depart., Imperal Japanes Navy, Vol. 5.

(21) K. Suehiro, Pro. Imp. Acad., Feb., 1928.
(22) F. Omori, Pub. E. I. C., No. 11.
(23) K. Matuzawa, K. Hasegawa & S. Haeno, Bull. Ekque Reseach Inst., Vol. 4.
(24) F. Omori, Bull. Imp. E. I. C., Vol. 1. No. 1.
(25) A. Imamura, Sinsai-yobô-tyôsakai-hôkoku, 92. (1920).
(26) R. Hirano, Journ. Meteoro. Soc., Ser. 2. Vol. 2. No. 3.
(27) K. Siratori, Jap. Journrn. Astro. Geophys., Vol. 2 p. 182.
(28) K. Wadati, Journ. Meteoro. Soc., Ser. 2. Vol. 4. No. 7.
(29) T. Terada & N. Miyabe. Proc. Imp. Acad., 3 (1927), No. 5.
(30) N. Miyabe, Poc. Imp. Acad., 3 (1927), No. 10.
(31) T. Takayama, Bull. Earthq. Reseach Inst., Vol. 4.
(32) T. Terada, Pro. Imp. Acad., Feb, 1928.

Fig. 3. Changes in the Mutual Distances of the Triangulation Points in Kwantô District.

[W. Inouye]

關東震災地一等三角點移動要圖

[Bull. Eqk. Res. Inst., Vol. 5. Pl.XI.]

説　明

1. 本圖ハ大正十二年關東地方震災地復舊測量作業中一等三角測量計算ノ結果ヲ圖示セルモノニシテ舊測量成果ニ對スル水平移動ノ狀態ヲ通覽スル爲ノ概リニ調製シタルモノナリ
2. 本圖ノ構成上計算ノ基礎ニ於テ一等三角點晃石山ヲ不動トシ又晃石山筑波山ノ方位ヲ移動セキモノトス故ニ各點ノ移動ハ何等絶對ノモノニアラス見解上注意ヲ望ム
3. 圖上ニ於ケル見例次ノ如シ
   - ○ 基線增大點及一等三角本點
   - ● 一等三角補點
   - ○—○ 相模野基線
   - ○—→ 舊位置ニ對スル新位置ノ移動量ニシテ北ヨリ東廻リ93°方向ニ1.″28移動シタルコトヲ示ス（93°, 1.″28）
   - 縮尺　三角點ノ位置ハ 1/400000，移動量ハ約 1/100
4. 新舊測量年度次ノ如シ
   - 基線測量　舊 明治十五年(1882)　新 大正十三年(1924)
   - 三角測量　舊 明治十七年—同三十二年(1884-1899)　新 大正十三年—同十四年(1924-1925)
5. 相模野基線長ハ明治十五年 Bilgard 基線尺ヲ用ヒテ測定シタル結果 5209.″969 6 ナリシガ大正十三年 Jäderin 式基線尺ヲ用ヒテ改測シタル結果ハ 5210.″212 5 ニシテ 0.″242 9 伸長セリ
   角觀測ニ用ヒタル機械及觀測回數ハ新舊共ニ同一ナリ
6. 平均計算ニ於テ舊位置ヲ求ムル爲メニハ舊基線長ト舊觀測角トヲ用ヒ、新位置ヲ求ムル爲メニハ基線改測値ト改測角トヲ用ヒタリ而シテ新舊計算ニ於テ觀測方向及條件式ヲ全ク同一ナラシメ基線增大邊ハ基線網ノ平均法ニ依リ、本點ハ獨立三角網ノ平均法ニ依リ、補點ハ鎖横線ノ平均法ニ依リ夫々計算セリ、但シ補點大島ニ對シテハ與點方向ヲ同一ナラシムルコト能ハサリキ、

陸地測量部

+elongation
−contraction (unit in cm./km.)

T and C represent the horizontally elongated and contracted regions respectively.

On the Diffraction of Elastic Waves.

By

Katsutada SEZAWA.

Member of the Institute.

彈性波の廻折に就て

所員 妹澤克惟

間隙による音波の廻折に就てはレーレー卿などによつて其の解を與へられてゐるが、彈性波に於ける同問題は今日に到るまで遂に提出を見なかつた樣である。近年マシュー函數の發展は可なり著しい樣に思はれるが、それを適當に利用して、著者は彈性波が障碍の間隙を通つてから廻折する理論を計算した。マシュー函數が未だ極く完全な發達の領域に達して居らぬから、多少の欠陷はあるが、大體其の廻折の性質を極め得る樣に見える。

理論的に面白い結果を摘錄すれば

(1) 間隙を通しての廻折は種々の場合があり、波長、間隙の幅、入射波の性質、障碍の應力狀態によつて其の性質を異にする。

(2) 入射波が縱波とし、障碍が自由な爲に應力を受けぬ時は、間隙からの廻折波は縱橫二種があり、且つ其の二種の勢力は同じ程度のものである。

(3) 障碍が固定されて居る時は廻折波は主として縱波のみから成る。

The theory of the scattering of elastic waves by some kinds of obstacles was given by the present author[1] in this Bull. III. Although these obstacles were of some idealized kinds, yet it seems that the theory was an important guidance for the confirmation of the behaviours of seismic waves. This can be clearly known in the light of other branches of physical sciences, in which highly idealized models contribute very often to the determination of the natures.

An important problem arising in connection with the theory of scattering is the treatment of the diffraction of elastic waves by an aperture of a screen. So far as the author is aware, this problem has not yet been studied for the reason that it involves mathematical difficulty. The diffraction of sound waves by an apperture of a screen was successfully investigated by Lord Rayleigh[2];

(1) *Bull.* III *of the Institute* (1927), p. 19.
(2) Lord Rayleigh, *Scientific Papers*, Vol. 4, p. 283.

the method employed by him, however, can never be applied to the problem of elastic waves. No effort, that might have been made by means of ordinary mathematics to the analysis of the diffraction of elastic waves by an aperture of a screen, would have given any successful solution of the problem.

As the recent development[1] of Mathieu's functions enables us that a few complicated problems in physics are attacked analytically, it reveals that Mathieu's functions will also be applied to the problem of the diffraction of elastic waves. The author's attempt to apply Mathieu's functions to such a problem is not, of course, sufficient for the complete solutions; but it appears that the investigation by means of such functions has answered the purpose of the elucidation of the nature of the present problem.

In this paper an attempt is made to study the way in which the waves are diffracted by an apperture of an infinitely extended screen, when the primary waves are of plane type with wave fronts parallel to the screen. The primary waves, which are transmitted in a purely elastic medium, are reflected at the screen, while the diffracted waves are formed at the aperture so as to make the stresses and the displacements continuous there. As to the breadth of the aperture, we consider it very narrow, because of the easy application of Mathieu's functions. The secondary waves are composed of two kinds of waves, that is, diffracted dilatational and distortional waves. The effects of barriers, which form the screen, on the secondary waves are neglected for the reason that their energy is very small compared with that of the normally reflected waves.

General Solutions.

1. When the axis of x is taken coincident with the screen in an elastic body and the axis of y, passing through the middle point of the slit, is directed perpendicularly to the x-axis, the equations of motion of the body are expressed by

$$\left.\begin{aligned} \rho\frac{\partial^2 \Delta}{\partial t^2} &= (\lambda+2\mu)\left(\frac{\partial^2 \Delta}{\partial x^2}+\frac{\partial^2 \Delta}{\partial y^2}\right), \\ \rho\frac{\partial^2 \bar{\omega}}{\partial t^2} &= \mu\left(\frac{\partial^2 \bar{\omega}}{\partial x^2}+\frac{\partial^2 \bar{\omega}}{\partial y^2}\right), \end{aligned}\right\} \quad \cdots\cdots\cdots\cdots\cdots\cdots (1)$$

(1) H. Jeffreys, *LondonMath. Soc. Proc.* (1925).
Humbert, *Fonctions de Mathieu et de Lamé* (1926).
Goldstein, *Cambridge Phil. Soc. Trans.* Vol. 23 (1927).
M. J. O. Strutt, *Ann. d. Phys. & Phil. Mag.* (1927 & 1928).

where

$$\Delta=\frac{\partial u}{\partial x}+\frac{\partial v}{\partial y},$$

$$2\varpi=\frac{\partial v}{\partial x}-\frac{\partial u}{\partial y},$$

u, v=components of displacement parallel to x- and y-axes respectively,

ρ=density of the medium,

λ, μ=Lamé's elastic constants.

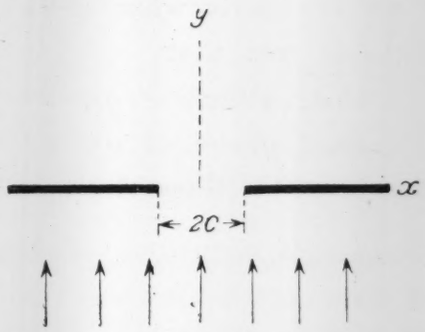

The expression of the primary waves, when they are dilatational, and directed parallel to y-axis, are deduced from the equation (1) as follows:—

$$\Delta_0'=Ae^{i(hy-pt)}, \quad \ldots\ldots\ldots\ldots\ldots\ldots\ldots\ldots (2)$$

in which

$$h^2=\frac{\rho p^2}{\lambda+2\mu},$$

$\frac{2\pi}{p}$=period of waves,

$\frac{2\pi}{h}$=wave length.

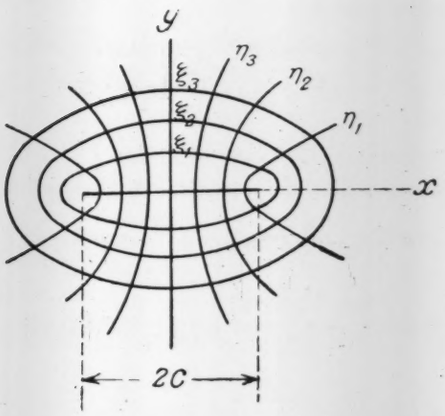

The equation (2), when we refer to the orthogonal curvilinear co-ordinates constituting a series of confocal ellipses and hyperbolas, is written by

$$\Delta_0' = Ae^{i(h c \mathrm{sh}\xi \sin\eta - pt)}$$
$$= e^{-ipt}\left[\sum_{n=0}^{\infty} A_n Ce_n(\xi, q)\, ce_n(\eta, q) + \sum_{1=n}^{\infty} A_n' Se_n(\xi, q)\, se_n(\eta, q)\right], \quad \ldots(3)$$

where $2c$=breadth of the apperture and

$$q^2 = \frac{h^2 c^2}{32}.$$

In the equation (3), $ce_n(\eta, q)$, $sc_n(\eta, q)$ are Mathieu's functions that reduce to constant multiples of $\cos nx$, $\sin nx$ when $q \to 0$. $Ce_n(\xi, q)$, $Se_n(\xi, q)$ are associated[1] Mathieu's functions, such that

$$\left.\begin{aligned} Ce_n(\xi, q) &= ce_n(i\xi, q), \\ Se_n(\xi, q) &= sc_n(i\xi, q). \end{aligned}\right\} \quad \ldots\ldots\ldots\ldots\ldots\ldots (4)$$

2. Mathieu's functions have the integral properties which are given by

$$\left.\begin{aligned} &\int_0^{2\pi} ce_n(x, q)\, cc_m(x, q)\, dx = 0, \qquad [n \neq m] \\ &\int_0^{2\pi} se_n(x, q)\, se_m(x, q)\, dx = 0, \qquad [n \neq m] \\ &\int_0^{2\pi} ce_n(x, q)\, se_m(x, q)\, dx = 0, \end{aligned}\right\} \quad \ldots\ldots\ldots\ldots (5)$$

and, when $q \to 0$,

$$\left.\begin{aligned} &\int_0^{2\pi} [ce_0(x, q)]^2 dx = 2\pi, \qquad \int_0^{2\pi} [ce_n(x, q)]^2 dx = \pi, \\ &\int_0^{2\pi} [se_n(x, q)]^2 dx = \pi. \end{aligned}\right\} \quad \ldots\ldots\ldots (6)$$

Now $ce_n(\eta, q)$, $se_n(\eta, q)$ can be expanded in the forms,[2]

$$\left.\begin{aligned} ce_0(\eta, q) &= 1 + 4q\cos 2\eta + 2q^4 \cos 4\eta \\ &\quad + 8^3 q^6 \left\{\frac{\cos 6\eta}{2^7 . 3^2} - \frac{7\cos 2\eta}{3^2}\right\} + 8^4 q^8 \left\{\frac{\cos 8\eta}{2^{13} . 3^2} - \frac{5\cos 4\eta}{2^7 . 3^2}\right\} + \cdots, \\ ce_1(\eta, q) &= \cos\eta + q^2 \cos 3\eta + q^4 \left(\frac{1}{3}\cos 5\eta - \cos 3\eta\right) \\ &\quad + q^6 \left(\frac{1}{18}\cos 7\eta - \frac{4}{9}\cos 5\eta + \frac{1}{3}\cos 3\eta\right) \\ &\quad + q^8 \left(\frac{1}{180}\cos 9\eta - \frac{1}{12}\cos 7\eta + \frac{1}{6}\cos 5\eta + \frac{11}{9}\cos 3\eta\right) \\ &\quad + \cdots, \end{aligned}\right\}$$

(1) H. Jeffreys, *London Math. Soc. Proc.* (1925).
(2) Whittaker, *Modern Analysis*, p. 427.

$$
\left.\begin{aligned}
se_1(\eta, q) &= \sin\eta + q^2\sin 3\eta + q^4\left(\frac{1}{3}\sin 5\eta + \sin 3\eta\right) \\
&\quad + q^6\left(\frac{1}{18}\sin 7\eta + \frac{4}{9}\sin 5\eta + \frac{1}{3}\sin 3\eta\right) \\
&\quad + q^8\left(\frac{1}{180}\sin 9\eta + \frac{1}{12}\sin 7\eta + \frac{1}{6}\sin 5\eta - \frac{11}{9}\sin 3\eta\right) \\
&\quad + \cdots, \\
c_2(\eta, q) &= \cos 2\eta + q^2(\cos 4\eta - 2) + \frac{1}{6}q^4\cos 6\eta \\
&\quad + q^6\left(\frac{1}{45}\cos 8\eta + \frac{43}{27}\cos 4\eta + \frac{40}{3}\right) \\
&\quad + q^8\left(\frac{1}{540}\cos 10\eta + \frac{293}{540}\cos 6\eta\right) + \cdots.
\end{aligned}\right\} \quad (7)
$$

3. In the case of expansion in (3), the approximate values of the associated Mathieu's functions with constant coefficients are given by the forms[1] below:—

$$
\left.\begin{aligned}
&[A_0 Ce_0(\xi, q)]_{q\to 0} = AJ_0(h\operatorname{cch}\xi), \\
&A_1 = 0, \\
&[A_2 Ce_2(\xi, q)]_{q\to 0} = 2AJ_2(h\operatorname{cch}\xi), \\
&A_3 = 0, \\
&[A_4 Ce_4(\xi, q)_{q\to 0} = 2AJ_4(h\operatorname{cch}\xi), \\
&A_5 = 0, \\
&\cdots\cdots\cdots
\end{aligned}\right\} \quad \cdots\cdots\cdots\cdots (8)
$$

$$
\left.\begin{aligned}
&[A_1' Se_1(\xi, q)]_{q\to 0} = 2iAJ_1(h\operatorname{cch}\xi), \\
&A_2' = 0, \\
&[A_3' Se_3(\xi, q)]_{q\to 0} = 2iAJ_3(h\operatorname{cch}\xi), \\
&A_4' = 0, \\
&\cdots\cdots\cdots
\end{aligned}\right\} \quad \cdots\cdots\cdots\cdots (9)
$$

4. Returning to the original solution (3), the displacement corresponding to Δ_0' is expressed by

$$
\left.\begin{aligned}
u_0' = -e^{-ipt}\Bigg[&\sum_{n=0}^{\infty}\frac{A_n}{h^2c\sqrt{\operatorname{ch}^2\xi - \cos^2\eta}}\frac{\partial Ce_n(\xi, q)}{\partial\xi}ce_n(\eta, q) \\
&+ \sum_{n=1}^{\infty}\frac{A_n'}{h^2c\sqrt{\operatorname{ch}^2\xi - \cos^2\eta}}\frac{\partial Se_n(\xi, q)}{\partial\xi}se_n(\eta, q)\Bigg],
\end{aligned}\right\} \quad \cdots\cdots (10)
$$

(1) Heine, *Kugelfunktionen*, Bd. I, § 106.

$$v_0' = -e^{-ipt}\left[\sum_{n=0}^{\infty}\frac{A_n}{h^2c\sqrt{\mathrm{ch}^2\xi-\cos^2\eta}}Ce_n(\xi,q)\frac{\partial ce_n(\eta,q)}{\partial\eta}\right.$$
$$\left.+\sum_{n=1}^{\infty}\frac{A_n'}{h^2c\sqrt{\mathrm{ch}^2\xi-\cos^2\eta}}Se_n(\eta,q)\frac{\partial se_n(\eta,q)}{\partial\eta}\right].$$

5. The reflected waves at the screen are readily obtained in the following forms:—

When the screen is free from stress, the dilatation is expressed by

$$\Delta_0'' = -Ae^{-i(hy+pt)}, \quad \cdots\cdots\cdots\cdots\cdots\cdots (11)$$

so that the resultant dilatation composed of Δ_0' and Δ_0'' is expressed by

$$\Delta_0 = \Delta_0' + \Delta_0'' = 2\sum_{n=1}^{\infty}A_n'Se_n(\xi,q)se_n(\eta,q)e^{-ipt}, \quad \cdots\cdots\cdots (12)$$

The corresponding displacement is expressed by

$$\left.\begin{aligned} u_0 &= -\sum_{n=1}^{\infty}\frac{2A_n'}{h^2c\sqrt{\mathrm{ch}^2\xi-\cos^2\eta}}\frac{\partial Se_n(\xi,q)}{\partial\xi}se_n(\eta,q)e^{-ipt},\\ v_0 &= -\sum_{n=1}^{\infty}\frac{2A_n'}{h^2c\sqrt{\mathrm{ch}^2\xi-\cos^2\eta}}Se_n(\xi,q)\frac{\partial se_n(\eta,q)}{\partial\eta}e^{-ipt}, \end{aligned}\right\} \quad \cdots\cdots (13)$$

When the screen is composed of infinitely rigid barriers, at which $u_0'+u_0''=v_0'+v_0''=0$ must satisfy, the dilatation of the reflected waves is expressed by

$$\Delta_0'' = Ae^{-i(hy+pt)}, \quad \cdots\cdots\cdots\cdots\cdots\cdots (14)$$

so that

$$\Delta_0 = \Delta_0' + \Delta_0'' = 2\sum_{n=0}^{\infty}A_nCe_n(\xi,q)ce_n(\eta,q)e^{-ipt}, \quad \cdots\cdots\cdots (15)$$

and the corresponding displacement is written by

$$\left.\begin{aligned} u_0 &= -\sum_{n=0}^{\infty}\frac{2A_n}{h^2c\sqrt{\mathrm{ch}^2\xi-\cos^2\eta}}\frac{\partial Ce_n(\xi,q)}{\partial\xi}ce_n(\eta,q)e^{+ipt},\\ v_0 &= -\sum_{n=0}^{\infty}\frac{2A_n}{h^2c\sqrt{\mathrm{ch}^2\xi-\cos^2\eta}}Ce_n(\xi,q)\frac{\partial ce_n(\eta,q)}{\partial\eta}e^{-ipt}. \end{aligned}\right\} \quad \cdots\cdots (16)$$

6. The equations of motion of the secondary waves generated from the aperture, where the elastic bodies on both sides of the screen has a narrow communication, are expressed by

$$\left.\begin{aligned} \rho\frac{\partial^2\Delta}{\partial t^2} &= \frac{\lambda+2\mu}{c^2(\mathrm{ch}^2\xi-\cos^2\eta)}\left(\frac{\partial^2\Delta}{\partial\xi^2}+\frac{\partial^2\Delta}{\partial\eta^2}\right),\\ \rho\frac{\partial^2\bar{\omega}}{\partial t^2} &= \frac{\mu}{c^2(\mathrm{ch}^2\xi-\cos^2\eta)}\left(\frac{\partial^2\bar{\omega}}{\partial\xi^2}+\frac{\partial^2\bar{\omega}}{\partial\eta^2}\right), \end{aligned}\right\} \quad \cdots\cdots\cdots (17)$$

where

$$\left.\begin{aligned} \Delta &= h_1^2\left\{\frac{\partial}{\partial\xi}\left(\frac{u}{h_1}\right)+\frac{\partial}{\partial\eta}\left(\frac{v}{h_1}\right)\right\}, \\ 2\varpi &= h_1^2\left\{\frac{\partial}{\partial\xi}\left(\frac{v}{h_1}\right)+\frac{\partial}{\partial\eta}\left(\frac{u}{h_1}\right)\right\}, \\ \frac{1}{h_1^2} &= c^2(\mathrm{ch}^2\xi-\cos^2\eta). \end{aligned}\right\} \quad \cdots\cdots\cdots\cdots (18)$$

Writing

$$\Delta=\Delta_1 e^{-ipt}, \qquad \varpi=\varpi_1 e^{-ipt},$$

we get

$$\left.\begin{aligned} &\frac{\partial^2\Delta_1}{\partial\xi^2}+\frac{\partial^2\Delta_1}{\partial\eta^2}+h^2c^2(\mathrm{ch}^2\xi-\cos^2\eta)\,\Delta_1=0, \\ &\frac{\partial^2\varpi_1}{\partial\xi^2}+\frac{\partial^2\varpi_1}{\partial\eta^2}+k^2c^2(\mathrm{ch}^2\xi-\cos^2\eta)\,\varpi_1=0, \end{aligned}\right\} \quad \cdots\cdots\cdots (19)$$

in which

$$\frac{\rho p^2}{\lambda+2\mu}=h^2, \qquad \frac{\rho p^2}{\mu}=k^2.$$

The solutions of (17) are, thus, given by

$$\left.\begin{aligned} \Delta &= \sum_{n=0}^{\infty} B_n He_n^{(1)}(\xi,q)\begin{Bmatrix} ce_n(\eta,q) \\ se_n(\eta,q)\end{Bmatrix} e^{-ipt}, \\ 2\varpi &= \sum_{n=0}^{\infty} C_n He_n^{(1)}(\xi,q')\begin{Bmatrix} ce_n(\eta,q') \\ se_n(\eta,q')\end{Bmatrix} e^{-ipt}, \end{aligned}\right\} \quad \cdots\cdots\cdots (20)$$

where $He_n^{(1)}(\xi,q)$ are solutions of Mathieu's differential equations in the forms of Hankel's type and

$$q'^2=\frac{k^2c^2}{32},$$

$$\left.\begin{aligned} &[He_0^{(1)}(\xi,q)]_{q\to 0}=H_0^{(1)}(hc\,\mathrm{ch}\xi), \\ &[He_1^{(1)}(\xi,q)]_{q\to 0}=H_1^{(1)}(hc\,\mathrm{ch}\xi), \\ &[He_2^{(1)}(\xi,q)]_{q\to 0}=H_2^{(1)}(hc\,\mathrm{ch}\xi), \\ &\cdots\cdots\cdots\cdots\cdots\cdots\cdots \end{aligned}\right\} \quad \cdots\cdots\cdots\cdots (21)$$

Displacement (u_1, v_1) answering to Δ in (20) and satisfying, $\varpi=0$, is expressed by the forms,

$$\left.\begin{aligned} u_1 &= -\sum_{n=0}^{\infty}\frac{B_n}{h^2c\sqrt{\mathrm{ch}^2\xi-\cos^2\eta}}\frac{\partial He_n^{(1)}(\xi,q)}{\partial\xi}\begin{Bmatrix} ce_n(\eta,q) \\ se_n(\eta,q)\end{Bmatrix} e^{-ipt}, \\ v_1 &= -\sum_{n=1}^{\infty}\frac{B_n}{h^2c\sqrt{\mathrm{ch}^2\xi-\cos^2\eta}}He_n^{(1)}(\xi,q)\begin{Bmatrix} \dfrac{\partial ce_n(\eta,q)}{\partial\eta} \\ \dfrac{\partial se_n(\eta,q)}{\partial\eta}\end{Bmatrix} e^{-ipt}. \end{aligned}\right\} \quad \cdots (22)$$

Displacement (u_2, v_2) derived from the value of ϖ in (20) under the condition, $\Delta=0$, is expressed by

$$\left.\begin{aligned} u_2 &= \sum_{n=1}^{\infty} \frac{C_n}{k^2 c\sqrt{\mathrm{ch}^2\xi-\cos^2\eta}} He_n^{(1)}(\xi, q') \left\{ \begin{matrix} \dfrac{\partial ce_n(\eta, q')}{\partial \eta} \\ \dfrac{\partial se_n(\eta, q')}{\partial \eta} \end{matrix} \right\} e^{-ipt} \\ v_2 &= -\sum_{n=1}^{\infty} \frac{C_n}{k^2 c\sqrt{\mathrm{ch}^2\xi-\cos^2\eta}} \frac{\partial He_n^{(1)}(\xi, q')}{\partial \xi} \left\{ \begin{matrix} ce_n(\eta, q') \\ se_n(\eta, q') \end{matrix} \right\} e^{-ipt} \end{aligned}\right\} \quad \ldots (23)$$

Free Barrier.

7. At the aperture of the screen the stresses and the displacements must be continuous. These conditions are given by the following four relations.

When $\xi=0$, we must have

$$\left.\begin{aligned} &\text{(a)} \quad u_0=u_1+u_2, \\ &\text{(b)} \quad v_0=v_1+v_2, \\ &\text{(c)} \quad \lambda\Delta_0+2\mu\left[\frac{1}{c\sqrt{\mathrm{ch}^2\xi-\cos^2\eta}}\frac{\partial u_0}{\partial \xi}+\frac{v_0}{c^2(\mathrm{ch}^2\xi-\cos^2\eta)}\frac{\partial}{\partial \eta}(c\sqrt{\mathrm{ch}^2\xi-\cos^2\eta})\right] \\ &\qquad =\lambda\Delta+2\mu\left[\frac{1}{c\sqrt{\mathrm{ch}^2\xi-\cos^2\xi}}\frac{\partial(u_1+u_2)}{\partial \xi}\right. \\ &\qquad\qquad \left.+\frac{(v_1+v_2)}{c^2(\mathrm{ch}^2\xi-\cos^2\eta)}\frac{\partial}{\partial \eta}(c\sqrt{\mathrm{ch}^2\xi-\cos^2\eta})\right], \\ &\text{(d)} \quad \frac{\partial}{\partial \xi}\left[\frac{v_0}{\sqrt{\mathrm{ch}^2\xi-\cos^2\eta}}\right]+\frac{\partial}{\partial \eta}\left[\frac{u_0}{\sqrt{\mathrm{ch}^2\xi-\cos^2\eta}}\right] \\ &\qquad =\frac{\partial}{\partial \xi}\left[\frac{v_1+v_2}{\sqrt{\mathrm{ch}^2\xi-\cos^2\eta}}\right]+\frac{\partial}{\partial \eta}\left[\frac{u_1+u_2}{\sqrt{\mathrm{ch}^2\xi-\cos^2\eta}}\right]. \end{aligned}\right\} \quad (24)$$

8. When the screen is free from stress and when we superpose some stationary vibration on the side of the secondary waves, we have to apply only the relations of (a) and (b). Thus we get,

$$\left.\begin{aligned} &-\sum_{n=1}^{\infty}\frac{2A_n'}{h^2c\sqrt{\mathrm{ch}^2\xi-\cos^2\eta}}\frac{\partial Se_n(\xi, q)}{\partial \xi}se_n(\eta, q) \\ &\quad =-\sum_{n=1}^{\infty}\frac{B_n}{h^2c\sqrt{\mathrm{ch}^2\xi-\cos^2\eta}}\frac{\partial He_n^{(1)}(\xi, q)}{\partial \xi}se_n(\eta, q) \\ &\qquad +\sum_{n=1}^{\infty}\frac{C_n}{k^2c\sqrt{\mathrm{ch}^2\xi-\cos^2\eta}}He_n^{(1)}(\xi, q')\frac{\partial ce_n(\eta, q')}{\partial \eta}, \\ &-\sum_{n=1}^{\infty}\frac{2A_n'}{h^2c\sqrt{\mathrm{ch}^2\xi-\cos^2\eta}}Se_n(\xi, q)\frac{\partial se_n(\eta, q)}{\partial \eta} \end{aligned}\right\} \quad \ldots . (25)$$

$$= -\sum_{n=1}^{\infty} \frac{B_n}{h^2 c\sqrt{\mathrm{ch}^2\xi - \cos^2\eta}} He_n^{(1)}(\xi, q) \frac{\partial se_n(\eta, q)}{\partial \eta}$$
$$-\sum_{n=1}^{\infty} \frac{C_n}{k^2 c\sqrt{\mathrm{ch}^2\xi - \cos^2\eta}} \frac{\partial He_n^{(1)}(\xi, q')}{\partial \xi} ce_n(\eta, q') \Bigg\}$$

at $\xi = 0$.

Solving (25) for $q \to 0$, we get approximately

$$\left.\begin{aligned} B_1 &= -4iA \begin{vmatrix} \frac{H_1^{(1)}(kc)}{c}, & \frac{\partial J_1(hc)}{\partial c} \\ \frac{\partial H_1^{(1)}(kc)}{\partial c}, & \frac{J_1(kc)}{c} \end{vmatrix} \Bigg/ \begin{vmatrix} \frac{\partial H_1^{(1)}(hc)}{\partial c}, & \frac{H_1^{(1)}(kc)}{c} \\ \frac{H_1^{(1)}(hc)}{c}, & \frac{\partial H_1^{(1)}(kc)}{\partial c} \end{vmatrix}, \\ C_1 &= 4i\frac{k^2}{h^2} A \begin{vmatrix} \frac{\partial H_1^{(1)}(hc)}{\partial c}, & \frac{\partial J_1(hc)}{\partial c} \\ \frac{H_1^{(1)}(hc)}{c}, & \frac{J_1(hc)}{c} \end{vmatrix} \Bigg/ \begin{vmatrix} \frac{\partial H_1^{(1)}(hc)}{\partial c}, & \frac{H_1^{(1)}(kc)}{c} \\ \frac{H_1^{(1)}(hc)}{c}, & \frac{\partial H_0^{(1)}(kc)}{\partial c} \end{vmatrix}, \end{aligned}\right\} \quad \ldots (26)$$

and generally for odd n,

$$\left.\begin{aligned} B_n &= -4iA \begin{vmatrix} \frac{nH_n^{(1)}(kc)}{c}, & \frac{\partial J_n(hc)}{\partial c} \\ \frac{\partial H_n^{(1)}(kc)}{\partial c}, & \frac{nJ_n(hc)}{c} \end{vmatrix} \Bigg/ \begin{vmatrix} \frac{\partial H_n^{(1)}(hc)}{\partial c}, & \frac{nH_n^{(1)}(kc)}{c} \\ \frac{nH_n^{(1)}(hc)}{c}, & \frac{\partial H_n^{(1)}(kc)}{\partial c} \end{vmatrix}, \\ C_n &= 4iA\frac{k^2}{h^2} A \begin{vmatrix} \frac{\partial H_n^{(1)}(hc)}{\partial c}, & \frac{\partial J_n(hc)}{\partial c} \\ \frac{nH_n^{(1)}(hc)}{c}, & \frac{nJ_n(hc)}{c} \end{vmatrix} \Bigg/ \begin{vmatrix} \frac{\partial H_n^{(1)}(hc)}{\partial c}, & \frac{nH_n^{(1)}(kc)}{c} \\ \frac{nH_n^{(1)}(hc)}{c}, & \frac{\partial H_n^{(1)}(kc)}{\partial c} \end{vmatrix}. \end{aligned}\right\} \quad (27)$$

For relatively large values of hc and kc, we have

$$\left.\begin{aligned} B_1 &= 4iA \frac{\left\{\frac{1}{c^2}\cos\left(hc - \frac{3\pi}{4}\right) + ihk \sin\left(hc - \frac{3\pi}{4}\right)\right\} e^{i\left(kc - \frac{3\pi}{4}\right)}}{\left(hk - \frac{1}{c^2}\right) e^{i\left(hc + kc - \frac{3\pi}{2}\right)}}, \\ C_1 &= -4i\frac{k^2}{h^2} A \frac{\frac{h}{c}\left\{i\cos\left(hc - \frac{3\pi}{4}\right) + \sin\left(hc - \frac{3\pi}{4}\right)\right\} e^{i\left(hc - \frac{3\pi}{4}\right)}}{\left(hk - \frac{1}{c^2}\right) e^{i\left(hc + kc - \frac{3\pi}{2}\right)}}, \end{aligned}\right\} \quad \ldots (26')$$

and generally for $n = \text{odd}$,

$$B_n = 4iA \frac{\left\{\frac{n^2}{c^2}\cos\left(hc - \frac{2n+1}{4}\pi\right) + ihk \sin\left(hc - \frac{2n+1}{4}\pi\right)\right\} e^{i\left(kc - \frac{2n+1}{4}\pi\right)}}{\left(hk - \frac{n^2}{c^2}\right) e^{i\left(hc + kc - \frac{2n+1}{2}\pi\right)}}, \quad \ldots (27')$$

$$C_n=-4i\frac{k^2}{h^2}A\frac{\frac{hn}{c}\left\{i\cos\left(hc-\frac{2n+1}{4}\pi\right)+\sin\left(hc-\frac{2n+1}{4}\pi\right)\right\}e^{i\left(hc-\frac{2n+1}{4}\pi\right)}}{\left(hk-\frac{n^2}{c^2}\right)e^{i\left(hc+kc-\frac{2n+1}{2}\pi\right)}}.$$

B_n and C_n for even values of n vanish.

The diffracted waves are, thus, given by

$$\left.\begin{aligned}\Delta&=\sum_{n=1}^{\infty}B_nHe_n^{(1)}(\xi,q)se_n(\eta,q)e^{-ipt},\\ 2\varpi&=\sum_{n=1}^{\infty}C_nHe_n^{(1)}(\xi,q')ce_n(\eta,q')e^{-ipt},\end{aligned}\right\}\quad\cdots\cdots\cdots\cdots(28)$$

$$n=1,3,5,\ \ldots,$$

together with the coefficients written in (26) and (27).

These solutions tell the fact that, when the barriers are free from stress, the diffracted waves are composed of dilatational and distortional waves of the first order distribution and those of higher orders. The principal waves are seen from the determinantal forms of B_n and C_n in (26) and (27) to be of the types,

$$\left.\begin{aligned}\Delta&=B_1He_1^{(1)}(\xi,q)se_1(\eta,q)e^{-ipt},\\ 2\varpi&=C_1He_1^{(1)}(\xi,q)ce_1(\eta,q')e^{-ipt}.\end{aligned}\right\}\quad\cdots\cdots\cdots\cdots(29)$$

These two kinds of waves are, thus, principally diffracted from an aperture of a screen.

Rigid Barrier.

9. When the screen is composed of very rigid barriers and when we superpose some stationary vibration on the side of the secondary waves, we have to apply the relations (c) and (d). As these relations, however, are very complicated, we may be contented with the following simplified formulae:—

When $q\to0$, $\xi=0$,

$$\left.\begin{aligned}&\lambda\Delta_0+2\mu\frac{\partial u_0}{\partial\xi_1}=\lambda\Delta+2\mu\frac{\partial(u_1+u_2)}{\partial\xi_1},\\ &\frac{\partial v_0}{\partial\xi_1}-\frac{v_0}{\xi_1}+\frac{1}{\xi_1}\frac{\partial u_0}{\partial\eta}=\frac{\partial(v_1+v_2)}{\partial\xi_1}-\frac{1}{\xi_1}(v_1+v_2)+\frac{1}{\xi_1}\frac{\partial(u_1+u_2)}{\partial\eta},\end{aligned}\right\}\quad..(30)$$

in which $\xi_1=\mathrm{ch}\xi$.

These give us

$$B_0=\frac{\left[\frac{\lambda}{2\mu}J_0(hc)-\frac{1}{h^2}\frac{\partial^2 J_0(hc)}{\partial c^2}\right]2A}{\frac{\lambda}{2\mu}H_0^{(1)}(hc)-\frac{1}{h^2}\frac{\partial^2 H_0^{(1)}(hc)}{\partial c^2}},$$

or

$$B_0=\cos\left(hc-\frac{\pi}{4}\right)e^{-\left(hc-\frac{\pi}{4}\right)}2A \qquad \left.\begin{array}{l}\\ \\ \\ \end{array}\right\} \quad \ldots\ldots\ldots\ldots (31)$$

for relatively large value of hc; and generally for even n we have

$$B_n=4A\frac{\begin{vmatrix} \frac{n}{k^2}\frac{\partial}{\partial c}\frac{H_n^{(1)}(kc)}{c}, & \frac{\lambda}{2\mu}J_n(hc)-\frac{1}{h^2}\frac{\partial^2 J_n(hc)}{\partial c^2} \\ -\frac{n^2}{k^2c^2}H_n^{(1)}(kc)-\frac{1}{k^2}\frac{\partial^2 H_n^{(1)}(kc)}{\partial c^2}+\frac{1}{k^2c}\frac{\partial H_n^{(1)}(kc)}{\partial c}, & \\ & \frac{n}{h^2c}\frac{\partial J_n(hc)}{\partial c}+\frac{n}{h^2}\frac{\partial}{\partial c}\frac{J_n(hc)}{c}-\frac{n}{h^2}\frac{J_n(hc)}{c^2} \end{vmatrix}}{\begin{vmatrix} \frac{\lambda}{2\mu}H_n^{(1)}(hc)-\frac{1}{h^2}\frac{\partial^2 H_n^{(1)}(hc)}{\partial c^2}, & \frac{n}{k^2}\frac{\partial}{\partial c}\frac{H_n^{(1)}(kc)}{c} \\ \frac{n}{h^2c}\frac{\partial H_n^{(1)}(hc)}{\partial c}+\frac{n}{h^2}\frac{\partial}{\partial c}\frac{H_n^{(1)}(hc)}{c}-\frac{n}{h^2}\frac{H_n^{(1)}(hc)}{c^2}, & \\ & -\frac{n^2}{k^2c^2}H_n^{(1)}(kc)-\frac{1}{k^2}\frac{\partial^2 H_n^{(1)}(kc)}{\partial c^2}+\frac{1}{k^2c^2}\frac{\partial H_n^{(1)}(hc)}{\partial c} \end{vmatrix}},$$

$$C_n=-4A\frac{\begin{vmatrix} \frac{\lambda}{2\mu}H_n(hc)-\frac{1}{h^2}\frac{\partial^2 H_n(hc)}{\partial c^2}, & \frac{\lambda}{2\mu}J_n(hc)-\frac{1}{h^2}\frac{\partial^2 J_n(hc)}{\partial c^2} \\ \frac{n}{h^2c}\frac{\partial H_n^{(1)}(hc)}{\partial c}+\frac{n}{h^2}\frac{\partial}{\partial c}\frac{H_n^{(1)}(hc)}{c}-\frac{n}{h^2}\frac{H_n^{(1)}(hc)}{c^2}, & \\ & \frac{n}{h^2c}\frac{\partial J_n(hc)}{\partial c}+\frac{n}{h^2}\frac{\partial}{\partial c}\frac{J_n(hc)}{c}-\frac{n}{h^2}\frac{J_n(hc)}{c^2} \end{vmatrix}}{\begin{vmatrix} \frac{\lambda}{2\mu}H_n^{(1)}(hc)-\frac{1}{h^2}\frac{\partial^2 H_n^{(1)}(hc)}{\partial c^2}, & \frac{n}{k^2}\frac{\partial}{\partial c}\frac{H_n(kc)}{c} \\ \frac{n}{h^2c}\frac{\partial H_n^{(1)}(hc)}{\partial c}+\frac{n}{h^2}\frac{\partial}{\partial c}\frac{H_n^{(1)}(hc)}{c}-\frac{n}{h^2}\frac{H_n^{(1)}(hc)}{c^2}, & \\ & -\frac{n^2}{k^2c^2}H_n^{(1)}(kc)-\frac{1}{k^2}\frac{\partial^2 H_n^{(1)}(kc)}{\partial c^2}+\frac{1}{k^2c}\frac{\partial H_n^{(1)}(kc)}{\partial c} \end{vmatrix}}. \quad \ldots\ldots\ldots\ldots\ldots\ldots (32)$$

In these $n=2, 4, 6, \ldots$

The diffracted waves are, thus, given by

$$\Delta=\sum_{n=0}^{\infty}B_nHe_n^{(1)}(\xi, q)ce_n(\eta, q)e^{-ipt}, \qquad \left.\begin{array}{l}\\ \end{array}\right\} \quad \ldots\ldots\ldots\ldots (33)$$

$$2\varpi = \sum_{n=1}^{\infty} C_n H_n^{(1)}(\xi, q') se_n(\eta, q') e^{-ipt}, \Big]$$

together with coefficients written in (31) and (32).

The determinantal forms of B_n and C_n show that the principal diffracted waves from an aperture of a rigid screen are given by

$$\Delta = B_0 He_0^{(1)}(\xi, q) ce_0(\eta, q) e^{-ipt} \quad \ldots\ldots\ldots\ldots\ldots\ldots (34)$$

The principal waves diffracted from an aperture of a rigid screen are, thus, purely dilatational waves. We have in this case a fair resemblance to the sound waves.

Summary.

We have thus obtained some results having theoretical interest on seismology by the use of Mathieu's functions: the principal results are enumerated as follows:—

1. Elastic waves passing through an aperture of a screen are diffracted in complex manners.

2. When the barriers are free from stress and the primary waves, propagated perpendicularly to the barriers, are purely dilatational, the diffracted waves are of two kinds, that is, dilatational and distortional types, energy of each kind of waves being of comparable magnitude.

3. When the barriers are very rigid and the primary waves are of the same nature as the above case, the principal diffracted waves are of the dilatational kind, resembling to the diffraction phenomena of sound waves.

In concluding this paper the author's thanks are due to Professor Nagaoka for his kind advice.

February 1928.

On the Diffusion of Tremors on the Surface of a Semi-infinite Solid Body.

By

Katsutada SEZAWA.

Member of the Institute.

半無限體上の震動の擴散に就て

所員　妹　澤　克　惟

本問題の目的として、勝手な初動による老衰表面波の算出法を求める事と、高粘性體中で震動部が擴散する有樣の研究とを擧げる事が出來る。こゝに老衰表面波の算出法とは表面の性質のみを與へる樣な積分法を得た事である。次に擴散の問題として研究し得た主要點を列記すれば

1. 粘彈性體中を減衰しつゝ進む波動と高粘性體中の震動の擴散とは、物理的要素としては全然同一のものに支配されるが、現象としては可なり異なる筈である。計算の結果も明かに之を示す。

2. 高粘性體上に加へられた震動は、殆ど波動する事なく擴散される。

3. 斯る物體上の初期の變位による震動は次第に擴散する。初めの變位速度による震動は漸次大きくなるが、しかし、時が經過すると共に此も亦擴散する。

4. 二次元の或場合に別の場所で起つた震動が始めの內は互に擴散する。其結果此等が一つの震動部の如くなつて兩者の區別がつかぬ樣になる。然し少しすると、この一つの震動部の中央が次第に低くなり、遂に左右兩震動部に分れ、之等は互に反對の方向に極めて遲く波動する。この二つの山が初期の二つの震動部と全然相當せぬ事は明かである。

Methods of the kind considered in a previous paper[1], concerning the decay of waves in visco-elastic solid bodies, may be employed also in the problem of diffusion of tremors on the surface of a body. The behaviour of waves in an elastic body having high solid viscosity shows scarcely the damped progressive nature. It seems that in such a case the waves are found to be diffused without any sensible transmission. In spite of its importance in connection with the vibration of extremely viscous medium and with the impact of materials, this problem of diffusion has escaped so far the notice of the investigators.

We have already had occasion to discover the fundamental equations of

1) On the Decay of Waves in Visco-Elastic Solid Bodies, *Bull.* III *of the Institute* (1927).

motion of a visco-elastic solid body, which are, too, adequately available to the problem of diffusion. Though the clear distinction between the the decay of waves and the diffusion of tremors cannot be made in the formal expressions of mathematical equations, yet the physical natures of both cases are quite different. Accordingly the mathematical solutions of each problem take different types. Besides, a few problems of integration of the equations of surface waves left untouched in the previous paper have been solved in this paper without difficulty.

The method employed in this paper is the application of Fourier's double integral, which seems to be adequate to the investigation of arbitrary tremors occurring in limited regions of the medium. The difficulty of the evaluation of the definite integrals has been avoided fortunately by the nature of the high solid viscosity of the medium. Another successful device carried out in the course of this paper is on the problem of integration relating to the surface tremors. Complexity of integration occurring in the case, that the whole medium of the semi-infinite solid body is taken into consideration, has been avoided successfully by taking merely the coordinates of the surface in the evaluation of Fourier's double integral. The results thus obtained are, of course, applicable only to the points on the surface of the body.

The paper consists of two sections; the first is on the tremors in a semi-infinite body and the second on that in two-dimensional body.

Diffusion in Three Dimensions.

The equations of motion of a visco-elastic solid body in cylindrical coordinates, when the circumferential component of the motion is omitted, are expressed by

$$\frac{\partial^2 \Delta}{\partial t^2}=\left(\frac{\lambda+2\mu}{\rho}+\frac{\lambda'+2\mu'}{\rho}\frac{\partial}{\partial t}\right)\left(\frac{\partial^2 \Delta}{\partial r^2}+\frac{1}{r}\frac{\partial \Delta}{\partial r}+\frac{\partial^2 \Delta}{\partial y^2}\right), \quad \ldots(1)$$

$$\frac{\partial^2 \bar{\omega}}{\partial t^2}=\left(\frac{\mu}{\rho}+\frac{\mu'}{\rho}\frac{\partial}{\partial t}\right)\left(\frac{\partial^2 \bar{\omega}}{\partial r^2}+\frac{1}{r}\frac{\partial \bar{\omega}}{\partial r}-\frac{\bar{\omega}}{r^2}+\frac{\partial^2 \bar{\omega}}{\partial y^2}\right), \quad (2)$$

where

$$\left.\begin{aligned}\Delta&=\frac{1}{r}\frac{\partial (ru)}{\partial r}+\frac{\partial v}{\partial y},\\ 2\bar{\omega}&=\frac{\partial u}{\partial y}-\frac{\partial v}{\partial r},\end{aligned}\right\} \quad \ldots\ldots\ldots\ldots(3)$$

u, v=radial and vertical components of displacement respectively,

ρ=density of isotropic solid,

λ, μ=Lamé's elastic constants,

λ', μ'=voluminal and equivoluminal viscosity.

Writing Δ and ϖ of (1) and (2) in the forms,

$$\Delta=\Delta_1 e^{-\alpha y}\begin{cases}\cos pt\\ \sin pt\end{cases} \quad \text{and} \quad \varpi=\varpi_1 e^{-\beta y}\begin{cases}\cos pt\\ \sin pt\end{cases}$$

respectively and solving the resulting equations, we obtain,

$$\Delta=Ae^{-w_1h^2t-\alpha y}J_0(fr)\begin{cases}\cos pt\\ \sin pt\end{cases}, \quad \cdots\cdots\cdots\cdots\cdots\cdots(4)$$

$$2\varpi=Be^{-w_2k^2t-\beta y}J_1(fr)\begin{cases}\cos pt\\ \sin pt\end{cases}, \quad \cdots\cdots\cdots\cdots\cdots\cdots(5)$$

in which

$$f^2=\alpha^2+h^2=\beta^2+k^2,$$

$$w_1=\frac{\lambda'+2\mu'}{2\rho}, \quad w_2=\frac{\mu'}{2\rho}, \quad h^2=\frac{\rho p^2}{\lambda+2\mu}, \quad k^2=\frac{\rho p^2}{\mu},$$

$$r^2=f^2-h^2, \quad s^2=f^2-k^2,$$

$$\frac{2\pi}{p}=\text{period of vibration.}$$

Displacement (u_1, v_1) answering to Δ in (4) and satisfying $\varpi=0$ is given by the forms,

$$u_1=A\frac{f}{f^2-\alpha^2}e^{-w_1h^2t-\alpha y}J_1(fr)\begin{cases}\cos pt\\ \sin pt\end{cases}, \quad \cdots\cdots\cdots\cdots(6)$$

$$v_1=A\frac{\alpha}{f^2-\alpha^2}e^{-w_1h^2t-\alpha y}J_0(fr)\begin{cases}\cos pt\\ \sin pt\end{cases}. \quad \cdots\cdots\cdots\cdots(7)$$

Displacement (u_2, v_2) derived from the value of ϖ in (5) under the condition, $\Delta=0$, is expressed by

$$u_2=B\frac{\beta}{f^2-\beta^2}e^{-w_2k^2t-\beta y}J_1(fr)\begin{cases}\cos pt\\ \sin pt\end{cases}, \quad \cdots\cdots\cdots\cdots(8)$$

$$v_2=B\frac{f}{f^2-\beta^2}e^{-w_2k^2t-\beta y}J_0(fr)\begin{cases}\cos pt\\ \sin pt\end{cases}. \quad \cdots\cdots\cdots\cdots(9)$$

The surface $y=0$ being free from traction, the equations

$$\lambda\Delta+2\mu\frac{\partial v}{\partial y}+\frac{\partial}{\partial t}\left(\lambda'\Delta+2\mu'\frac{\partial v}{\partial y}\right)=0, \quad \cdots\cdots\cdots(10)$$

$$\mu\left(\frac{\partial u}{\partial y}+\frac{\partial v}{\partial r}\right)+\mu'\frac{\partial}{\partial t}\left(\frac{\partial u}{\partial y}+\frac{\partial v}{\partial r}\right)=0, \quad \cdots\cdots\cdots\cdots(11)$$

in which $u=u_1+u_2$ and $v=v_1+v_2$ must hold on that surface.

If
$$\frac{\lambda}{\mu}=\frac{\lambda'}{\mu'}, \quad \cdots\cdots\cdots\cdots\cdots\cdots\cdots\cdots (12)$$
these equations give
$$\left.\begin{aligned}\frac{B/(f^2-\beta^2)}{A/(f^2-\alpha^2)}&=\frac{\lambda}{2\mu}\frac{f^2-\alpha^2}{\alpha f}-\frac{\alpha}{f},\\ \frac{B/(f^2-\beta^2)}{A/(f^2-\alpha^2)}&=-\frac{2f\beta}{f^2+\beta^2}.\end{aligned}\right\} \quad \cdots\cdots\cdots\cdots (13)$$
Eliminating $\dfrac{B/(f^2-\beta^2)}{A/(f^2-\alpha^2)}$, we obtain
$$j^8-8j^6+24j^4-16(1+g^2)j^2+16h^2=0, \quad \cdots\cdots\cdots\cdots (14)$$
where
$$g^2=\frac{\rho p^2}{(\lambda+2\mu)f^2} \quad \text{and} \quad j^2=\frac{\rho p^2}{\mu f^2}.$$

The relation (14) is a characteristic equation to determine the velocity of propagation of Rayleigh waves.

From (13) and (14), we find the expressions for displacement (taking $\lambda=\mu$) as written below:—
$$\left.\begin{aligned}u=u_1+u_2&=C\{3\cdot55\,e^{-\cdot847fy}-2\cdot04\,e^{-\cdot393fy}\}e^{-\cdot845w_2f^2t}J_1(fr)\begin{Bmatrix}\cos fv_0t\\ \sin fv_0t\end{Bmatrix},\\ v=v_1+v_2&=C\{3\cdot01e^{-\cdot847fy}-5\cdot21e^{-\cdot393fy}\}e^{-\cdot845w_2f^2t}J_0(fr)\begin{Bmatrix}\cos fv_0t\\ \sin fv_0t\end{Bmatrix},\end{aligned}\right\} \quad \cdots (15)$$
where C=constant multiplier,

v_0=velocity of propagation of Rayleigh-waves.

Generalising this, we obtain for an initial surface displacement $v=\varphi(r)$ and an initial surface velocity $\dfrac{\partial v}{\partial t}=\psi(r)$ on $y=0$,
$$\left.\begin{aligned}u=&\int_0^\infty e^{-\cdot845w_2f^2t}\left\{\frac{-3\cdot55e^{-\cdot847fy}+2\cdot04e^{-\cdot393fy}}{2\cdot20}\right\}\cos fv_0tJ_1(fr)\,fdf\\ &\times\int_0^\infty\varphi(\lambda)J_0(f\lambda)\lambda d\lambda\\ &+\int_0^\infty e^{-\cdot845w_2f^2t}\left\{\frac{-3\cdot55e^{-\cdot847fy}+2\cdot04e^{-\cdot393fy}}{2\cdot20}\right\}\frac{\sin fv_0t}{v_0}J_1(fr)\,df\\ &\times\int_0^\infty\psi(\lambda)J_0(f\lambda)\lambda d\lambda,\\ v=&\int_0^\infty e^{-\cdot845w_2f^2t}\left\{\frac{-3\cdot01e^{-\cdot847fy}+5\cdot21e^{-\cdot393fy}}{2\cdot20}\right\}\cos fv_0tJ_0(fr)\,fdf\\ &\times\int_0^\infty\varphi(\lambda)J_0(f\lambda)\lambda d\lambda\end{aligned}\right\} \quad (16)$$

$$+\int_0^\infty e^{-\cdot 845\, w_2 f^2 t}\left\{\frac{-3\cdot 01\, e^{-\cdot 847 fy}+5\cdot 21\, e^{-\cdot 393 fy}}{2\cdot 20}\right\}\frac{\sin fv_0 t}{v_0}J_0(fr)\,df \times\int_0^\infty \psi(\lambda)\,J_0(f\lambda)\,\lambda\,d\lambda$$

Putting $\varphi(\lambda)=Be^{-\frac{\lambda^2}{b^2}}$, $\psi(\lambda)=Ce^{-\frac{\lambda^2}{c^2}}$ and using the formula

$$\int_0^\infty e^{-\frac{\lambda^2}{x^2}}J_0(f\lambda)\,\lambda\,d\lambda=\frac{x^2}{2}e^{-\frac{f^2x^2}{4}},$$

we find,

$$\left.\begin{aligned}
u_0&=\frac{Bb^2}{2}\int_0^\infty\left\{\frac{-3\cdot 55\, e^{-\cdot 847 fy}+2\cdot 04\, e^{-\cdot 393 fy}}{2\cdot 20}\right\}e^{-\left(\cdot 845\, w_2 t+\frac{b^2}{4}\right)f^2}\times J_1(fr)\,f\cos fv_0 t\,df\\
&+\frac{Cc^2}{2}\int_0^\infty\left\{\frac{-3\cdot 55\, e^{-\cdot 842 fy}+2\cdot 04\, e^{-\cdot 393 fy}}{2\cdot 20}\right\}e^{-\left(\cdot 845\, w_2 t+\frac{b^2}{4}\right)f^2}\times J_1(fr)\,\frac{\sin fv_0 t}{v_0}\,df,\\
v_0&=\frac{Bb^2}{2}\int_0^\infty\left\{\frac{-3\cdot 01\, e^{-\cdot 847 fy}+5\cdot 21\, e^{-\cdot 393 fy}}{2\cdot 20}\right\}e^{-\left(\cdot 848\, w_2 t+\frac{b^2}{4}\right)f^2}\times J_0(fr)\,f\cos fv_0 t\,df\\
&+\frac{Cc^2}{2}\int_0^\infty\left\{\frac{-3\cdot 01\, e^{-\cdot 847 fy}+5\cdot 21\, e^{-\cdot 393 fy}}{2\cdot 20}\right\}e^{-\left(\cdot 845\, w_2 t+\frac{b^2}{4}\right)f^2}\times J_0(fr)\,\frac{\sin fv_0 t}{v_0}\,df.
\end{aligned}\right\}\quad(17)$$

The forms of $\varphi(\lambda)$ and $\psi(\lambda)$ here given seem to be sufficient as the expressions of the initial disturbances. Taking different values of each of B, C, b^2, c^2, we will obtain various cases of symmetrical disturbances.

As the integration of (17) is very difficult, the special case $y=0$ has been taken in this paper; this does not lose the generality of integration in a sense that the resulting formulae give only the values of the surface displacements.

Expanding $\cos fv_0 t$, $\sin fv_0 t$ in series, we get

$$\left.\begin{aligned}
u_0&=-\frac{1\cdot 51}{2\cdot 20}\frac{Bb^2}{2}\sum_{n=0}^\infty\frac{(v_0t)^{2n}}{(2n)!}\int_0^\infty f^{2n+1}J_1(fr)\,e^{-\left(\cdot 845\, w_2 t+\frac{b^2}{4}\right)f^2}df\\
&-\frac{1\cdot 51}{2\cdot 20}\frac{Cc^2}{2}\sum_{n=0}^\infty\frac{v_0^{2n}t^{2n+1}}{(2n+1)!}\int_0^\infty f^{2n+1}J_1(fr)\,e^{-\left(\cdot 845\, w_2 t+\frac{b^2}{4}\right)f^2}df,\\
v_0&=\frac{Bb^2}{2}\sum_{n=0}^\infty\frac{(v_0t)^{2n}}{(2n)!}\int_0^\infty f^{2n+1}J_0(fr)\,e^{-\left(\cdot 845\, w_2 t+\frac{b^2}{4}\right)f^2}df
\end{aligned}\right\}\quad..(18)$$

$$+\frac{Cc^2}{2}\sum_{n=0}^{\infty}\frac{{v_0}^{2n}t^{2n+1}}{(2n+1)!}\int_0^{\infty}f^{2n+1}J_0(fr)\,e^{-\left(\cdot 845\,w_2t+\frac{b^2}{4}\right)f^2}df. \qquad \Big)$$

Now by Kummer's transformation,

$$\int_0^{\infty}J_\nu(fr)\,e^{-\alpha^2f^2}f^{\mu-1}df=\frac{\Gamma\left(\frac{\nu+\mu}{2}\right)\left(\frac{1}{2}\frac{r}{\alpha}\right)^\nu}{2\alpha^\mu\Gamma(\nu+1)}$$
$$\times e^{-\frac{r^2}{4\alpha^2}}{}_1F_1\left(\frac{\nu-\mu}{2}+1;\ \nu+1;\ \frac{r^2}{4\alpha^2}\right), \quad \ldots\ldots(19)$$

in which ${}_1F_1(\gamma;\ \rho;\ z)$ is generalised hypergeometric function due to Pochhammer and Barnes and is expressed by the form,

$${}_1F_1(\gamma;\ \rho;\ z)=\sum_{m=0}^{\infty}\frac{(\gamma)_m}{m!\,(\rho)_m}z^m,$$

where

$$(\gamma)_m=\gamma(\gamma+1)(\gamma+2)\ldots(\gamma+m-1),$$
$$(\gamma)_0=1.$$

Applying these relations, we find

$$\left.\begin{aligned}
u_0=&-\frac{1\cdot 51}{2\cdot 20}\cdot\frac{Bb^2}{8}\sum_{n=0}^{\infty}e^{-\frac{r^2}{4\times\cdot 845\,w_2t+b^2}}\frac{\Gamma\left(n+\frac{3}{2}\right)r\,(v_0t)^{2n}}{(2n)!\left(\cdot 845\,w_2t+\frac{b^2}{4}\right)^{n+\frac{3}{2}}}\\
&\times{}_1F_1\left(1-n;\ 2;\ \frac{r}{4\times\cdot 845\,w_2t+b^2}\right)\\
&-\frac{1\cdot 51}{2\cdot 20}\cdot\frac{Cc^2}{8}\sum_{n=0}^{\infty}\frac{t}{(2n+1)}e^{-\frac{r^2}{4\times\cdot 845\,w_2t+c^2}}\frac{\Gamma\left(n+\frac{3}{2}\right)r\,(v_0t)^{2n}}{(2n)!\left(\cdot 845\,w_2t+\frac{c^2}{4}\right)^{n+\frac{3}{2}}}\\
&\times{}_1F_1\left(1-n;\ 2;\ \frac{r^2}{4\times\cdot 845\,w_2t+c^2}\right),\\
v_0=&\frac{Bb^2}{4}\sum_{n=0}^{\infty}e^{-\frac{r^2}{4\times\cdot 845\,w_2t+b^2}}\frac{n!\,(v_0t)^{2n}}{(2n)!\left(\cdot 845\,w_2t+\frac{b^2}{4}\right)^{n+1}}\\
&\times{}_1F_1\left(-n;\ 1;\ \frac{r^2}{4\times\cdot 845\,w_2t+b^2}\right)\\
&+\frac{Cc^2}{4}\sum_{n=0}^{\infty}\frac{t}{(2n+1)}e^{-\frac{r^2}{4\times\cdot 845\,w_2t+c^2}}\frac{n!\,(v_0t)^{2n}}{(2n)!\left(\cdot 845\,w_2t+\frac{c^2}{4}\right)^{n+1}}\\
&\times{}_1F_1\left(-n;\ 1;\ \frac{r^2}{4\times\cdot 845\,w_2t+c^2}\right).
\end{aligned}\right\}$$
$$\ldots\ldots(20)$$

FIG. I

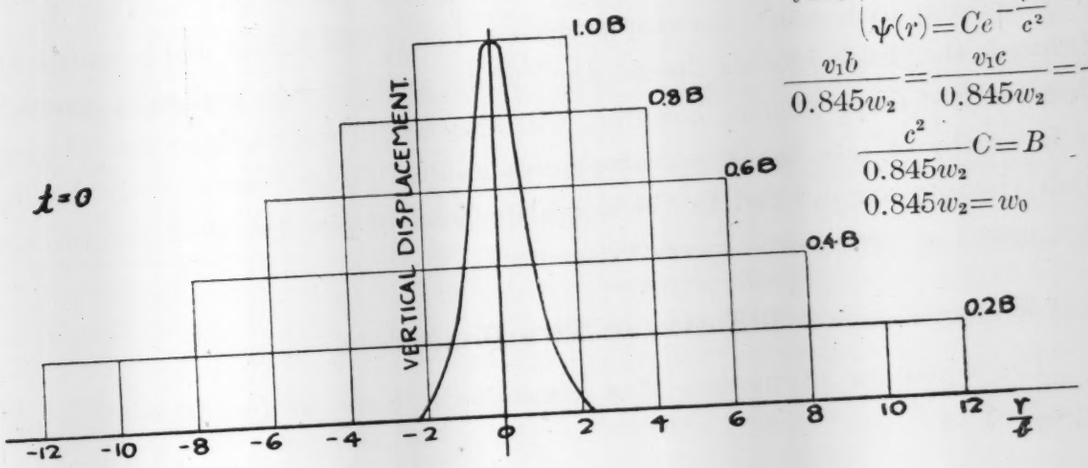

$$t=0 \quad \begin{cases} \varphi(r)=Be^{-\frac{r^2}{b^2}} \\ \psi(r)=Ce^{-\frac{r^2}{c^2}} \end{cases}$$

$$\frac{v_1 b}{0.845 w_2}=\frac{v_1 c}{0.845 w_2}=\frac{1}{5}$$

$$\frac{c^2}{0.845 w_2}C=B$$

$$0.845 w_2=w_0$$

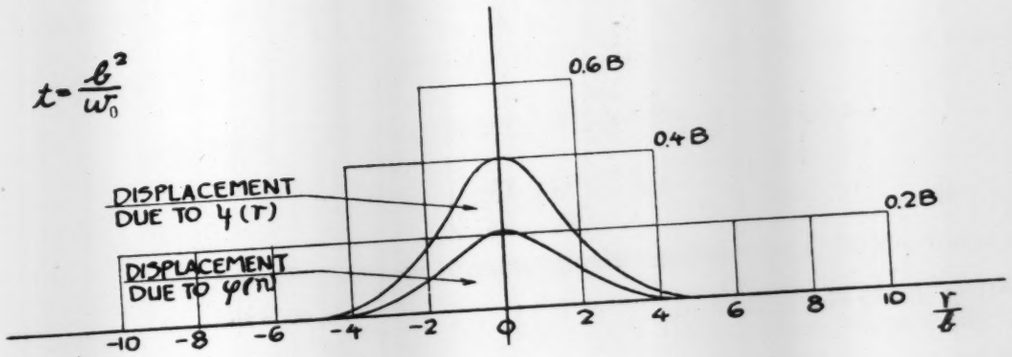

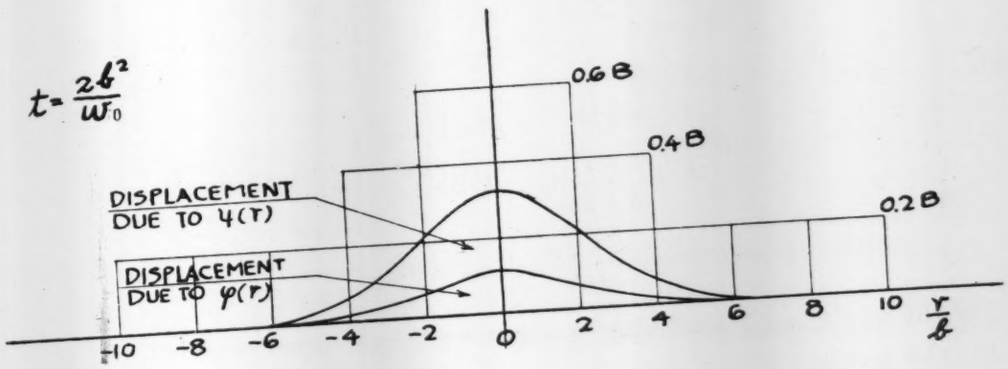

Calculated results of vertical displacements of a certain case, in which initial surface displacement and velocity are given, are plotted in Fig. 1. It will be seen that, while the displacements due to the initial displacement are diffused, the displacements due to the initial velocity are gradually excited; these excited displacments, however, will also be diffused in the course of time. It is worthy of note that the disturbances applied on an elastic body having high viscosity are diffused in the neighbourhood of the disturbed portion, not propagated as progressive waves.

Diffusion in Two Dimensions.

—The equations of motion of a visco-elastic body in two-dimensions are expressed by

$$\frac{\partial^2 \Delta}{\partial t^2}=\left(\frac{\lambda+2\mu}{\rho}+\frac{\lambda'+2\mu'}{\rho}\frac{\partial}{\partial t}\right)\left(\frac{\partial^2 \Delta}{\partial x^2}+\frac{\partial^2 \Delta}{\partial y^2}\right), \quad \cdots\cdots\cdots (21)$$

$$\frac{\partial^2 \varpi}{\partial t^2}=\left(\frac{\mu}{\rho}+\frac{\mu'}{\rho}\frac{\partial}{\partial t}\right)\left(\frac{\partial^2 \varpi}{\partial x^2}+\frac{\partial^2 \varpi}{\partial y^2}\right), \quad \cdots\cdots\cdots\cdots (22)$$

where

$$\left.\begin{aligned}\Delta&=\frac{\partial u}{\partial x}+\frac{\partial v}{\partial y},\\ 2\varpi&=\frac{\partial v}{\partial x}+\frac{\partial u}{\partial y},\end{aligned}\right\}, \quad \cdots\cdots\cdots\cdots\cdots\cdots (23)$$

u, v=horizontal and vertical displacements respectively.

Writing Δ and ϖ in (21) and (22) in the forms $\Delta=\Delta_1 e^{-\alpha y}\begin{Bmatrix}\cos pt\\ \sin pt\end{Bmatrix}$ and $\varpi=\varpi_1 e^{-\beta y}\times\begin{Bmatrix}\cos pt\\ \sin pt\end{Bmatrix}$ respectively and solving the resulting equations, we get

$$\Delta=Ae^{-w_1 h^2 t-\alpha y}\begin{Bmatrix}\cos fx\\ \sin fx\end{Bmatrix}\begin{Bmatrix}\cos pt\\ \sin pt\end{Bmatrix}, \quad \cdots\cdots\cdots\cdots\cdots (24)$$

$$2\varpi=Be^{-w_2 k^2 t-\beta y}\begin{Bmatrix}\sin fx\\ \cos fx\end{Bmatrix}\begin{Bmatrix}\cos \mathrm{pt}\\ \sin pt\end{Bmatrix}, \quad \cdots\cdots\cdots\cdots (25)$$

in which

$$\alpha^2=f^2-h^2, \qquad \beta^2=f^2-k^2,$$

$$h^2+\frac{\rho p^2}{\lambda+2\mu}, \qquad k^2=\frac{\rho p^2}{\mu},$$

$$w_1=\frac{\lambda'+2\mu'}{2\rho'}, \qquad w_2=\frac{\mu'}{2\rho'}.$$

Displacement (u_1, v_1) answering to Δ in (24) and satisfying, $\varpi=0$, is expressed by the forms,

$$u_1 = A\frac{f}{h_2}e^{-w_1h^2t-\alpha y}\begin{Bmatrix}\sin fx\\ \cos fx\end{Bmatrix}\begin{Bmatrix}\cos pt\\ \sin pt\end{Bmatrix}, \quad \ldots\ldots\ldots\ldots (26)$$

$$v_1 = A\frac{\alpha}{h^2}e^{-w_2h^2t-\beta y}\begin{Bmatrix}\cos fx\\ -\sin fx\end{Bmatrix}\begin{Bmatrix}\cos pt\\ \sin pt\end{Bmatrix}. \quad \ldots\ldots\ldots\ldots (27)$$

Displacement (u_2, v_2) answering to ϖ in (25) with the condition, $\Delta=0$, is given by the forms

$$u_2 = -B\frac{\beta}{k^2}e^{-w_2k^2t-\beta y}\begin{Bmatrix}\sin fx\\ \cos fx\end{Bmatrix}\begin{Bmatrix}\cos pt\\ \sin pt\end{Bmatrix}, \quad \ldots\ldots\ldots\ldots (28)$$

$$v_2 = -B\frac{f}{k^2}e^{-w_2k^2t-\beta y}\begin{Bmatrix}\cos fx\\ -\sin fx\end{Bmatrix}\begin{Bmatrix}\cos pt\\ \sin pt\end{Bmatrix}. \quad \ldots\ldots\ldots\ldots (29)$$

The conditions at the surface are satisfied, if the following equations hold at $y=0$,

$$\lambda\Delta + 2\mu\frac{\partial v}{\partial y} + \frac{\partial}{\partial t}\left(\lambda'\Delta + 2\mu'\frac{\partial v}{\partial y}\right) = 0, \quad \ldots\ldots\ldots (30)$$

$$\mu\left(\frac{\partial v}{\partial x} + \frac{\partial u}{\partial y}\right) + \mu'\frac{\partial}{\partial t}\left(\frac{\partial v}{\partial x} + \frac{\partial u}{\partial y}\right) = 0, \quad \ldots\ldots\ldots (31)$$

where $u=u_1+u_2$ and $v=v_1+v_2$.

Putting $\frac{\lambda}{\mu}=\frac{\lambda'}{\mu'}$ and pursuing the same line of treatment as before, we find the expressions of the elementary displacement as below:—

$$\left.\begin{aligned} u &= Ce^{-\cdot845\,w_2f^2t}(3.55e^{-\cdot847fy} - 2.04e^{-\cdot393fy})\begin{Bmatrix}\cos fx\\ \sin fx\end{Bmatrix}\begin{Bmatrix}\cos pt\\ \sin pt\end{Bmatrix},\\ v &= Ce^{-\cdot845\,w_2f^2t}(-3.01^{-\cdot847fy} + 5.21e^{-\cdot393fy})\begin{Bmatrix}\sin fx\\ -\cos fx\end{Bmatrix}\begin{Bmatrix}\cos pt\\ \sin pt\end{Bmatrix}.\end{aligned}\right\} \ldots (32)$$

In this, use has been made of (26), (27), (28), (29), (30) and (31).

Generalising this we obtain the expressions of u and v for an initial surface displacement $v=\varphi(x)$ and an initial surface velocity $\frac{\partial v}{\partial t}=\psi(x)$. Thus we have

$$\left.\begin{aligned} u &= \frac{1}{2.20\pi}\int_0^\infty e^{-\cdot845\,w_2f^2t}(3.55e^{-\cdot847fy} - 2.04e^{-\cdot393fy})\cos fv_0t\,df\\ &\qquad \times\int_{-\infty}^{\infty}\varphi(\lambda)\sin f(x-\lambda)\,d\lambda\\ &\quad + \frac{1}{2.20\pi}\int_0^\infty e^{-\cdot845\,w_2f^2t}(3.55e^{-\cdot847fy} - 2.04e^{-\cdot393fy})\frac{\sin fv_0t}{fv_0}\,df\\ &\qquad \times\int_{-\infty}^{\infty}\psi(\lambda)\sin f(x-\lambda)\,d\lambda,\\ v &= \frac{1}{2.20\pi}\int_0^\infty e^{-\cdot845\,w_2f^2t}(-3.01e^{-\cdot847fy} + 5.21^{-\cdot393fy})\cos fv_0t\,df\end{aligned}\right\} \ldots (33)$$

FIG. II

(a) $t=0$

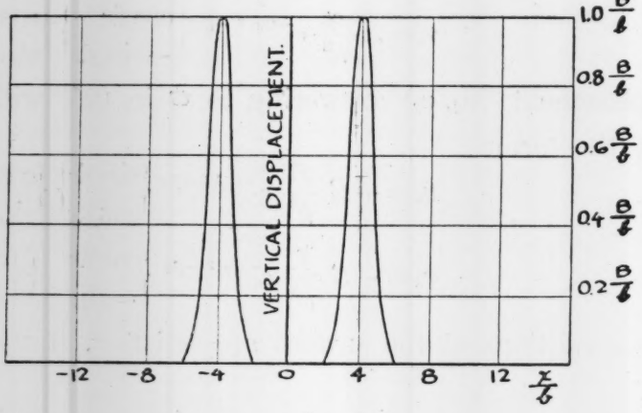

(b) $t=\frac{b^2}{\omega_0}$

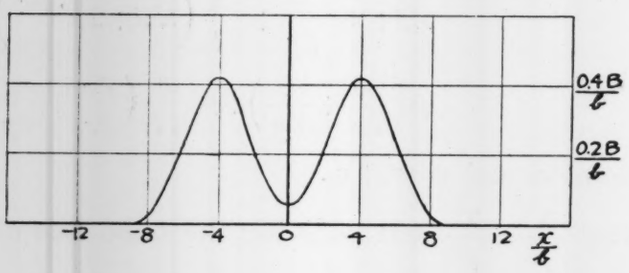

(c) $t=\frac{2b^2}{\omega_0}$

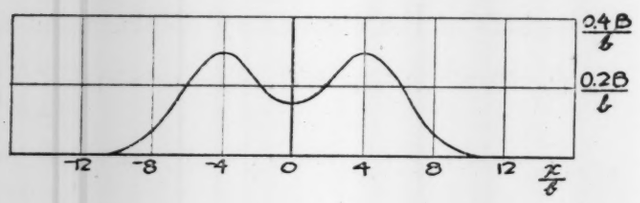

(d) $t=\frac{3b^2}{\omega_0}$

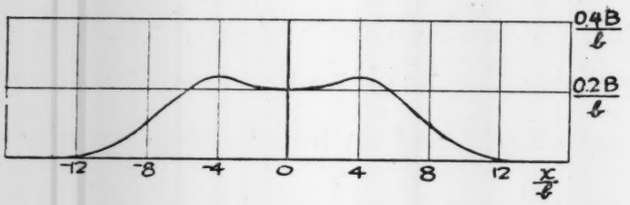

(e) $t=\frac{4b^2}{\omega_0}$

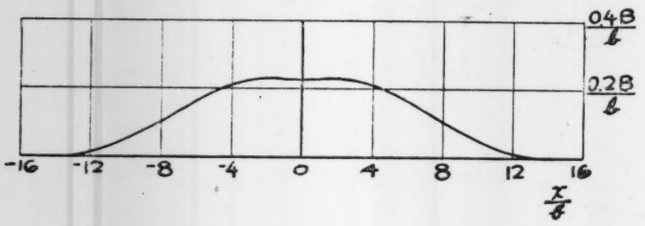

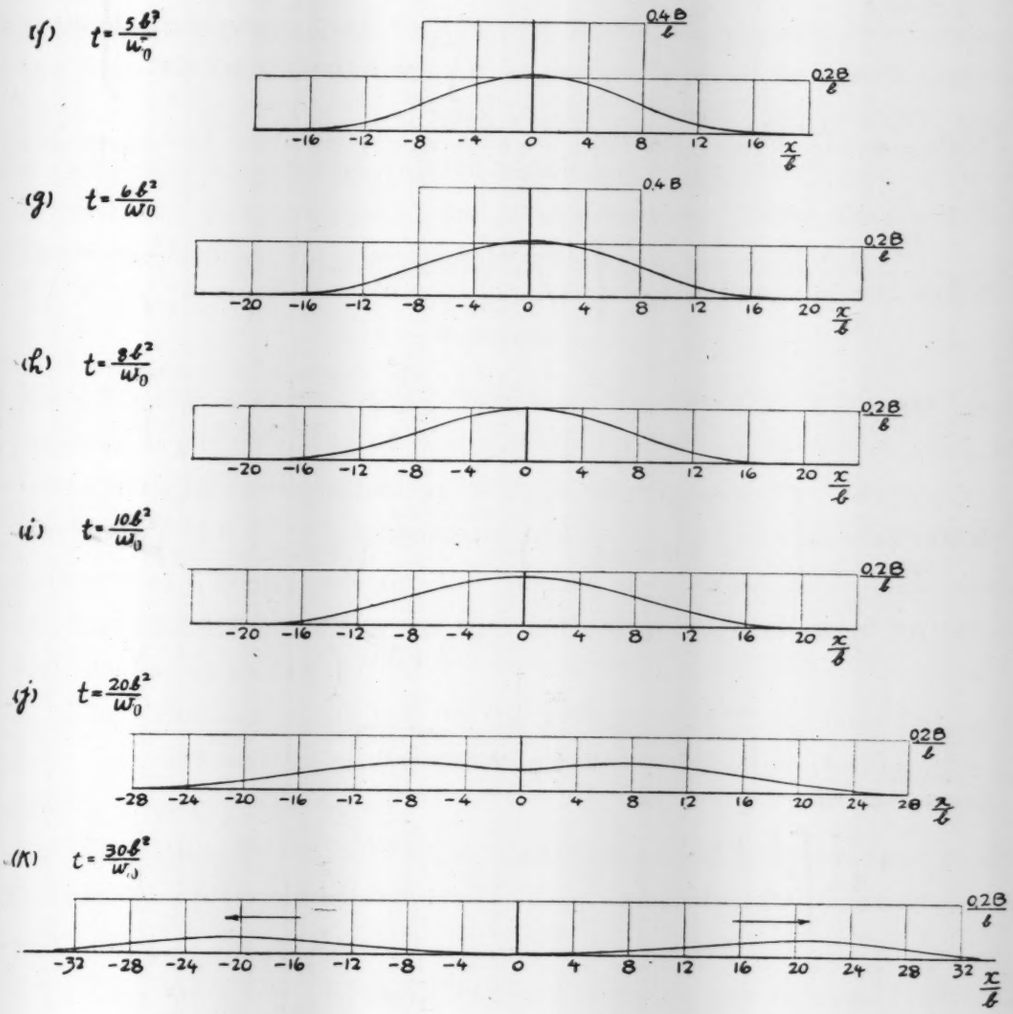

$$\left.\begin{aligned} &t=0\\ &\varphi(x)=\frac{B}{b}e^{-\frac{x^2}{b^2}}\\ &\varphi(x)=0 \end{aligned}\right\}$$

$$\frac{v_1 b}{0.845 w_2}=\frac{1}{b}$$

$$0.845 w_2=w_0$$

$$\times\int_{-\infty}^{\infty}\varphi(\lambda)\cos f(x-\lambda)\,d\lambda$$

$$+\frac{1}{2.20\pi}\int_0^{\infty}e^{-\cdot845\,w_2 f^2 t}(-3.01\,e^{-\cdot847 fy}+5.21\,e^{-\cdot393 fy})\frac{\sin fv_0 t}{fv_0}\,df$$

$$\times\int_{-\infty}^{\infty}\psi(\lambda)\cos f(x-\lambda)\,d\lambda.$$

Putting $\varphi(\lambda)=\frac{B}{b}e^{-\frac{\lambda^2}{b^2}}$, $\psi(\lambda)=\frac{C}{c}e^{-\frac{\lambda^2}{c^2}}$ and evaluating the integrals in the case of $y=0$, we find

$$v_0=\frac{1.51\,B}{2.20\times 2\sqrt{\pi}\sqrt{4\times.845\,w_2t+b^2}}\left[\frac{(x+v_0t)+(x-v_0t)}{\sqrt{.845\,w_2t+\frac{b^2}{4}}}-\frac{1}{2\cdot3}\frac{(x+v_0t)^3+(x-v_0t)^3}{\left(.845\,w_2t+\frac{b^2}{4}\right)^{\frac{3}{2}}}\right.$$

$$\left.+\frac{1}{3.4.5}\frac{(x+v_0t)^5+(x-v_0t)^5}{\left(.845\,w_2t+\frac{b^2}{4}\right)^{\frac{5}{2}}}-\cdots\right]$$

$$+\frac{1.51\,C}{2.20\times 2\sqrt{\pi}\,v_0}\left[\frac{1}{2}\frac{(x+v_0t)^2-(x-v_0t)^2}{\left(.845\,w_2t+\frac{b^2}{4}\right)}-\frac{1}{2.3.4}\frac{(x+v_0t)^4-(x-v_0t)^4}{\left(.845\,w_2t+\frac{b^2}{4}\right)^2}\right.$$

$$\left.+\frac{1}{3.4.5.6}\frac{(x+v_0t)^6-(x-v_0t)^6}{\left(.845\,w_2t+\frac{b^2}{4}\right)^3}-\cdots\right].$$

$$v_0=\frac{B}{2\sqrt{4\times.845\,w_2t+b^2}}\left[e^{-\frac{(x+v_0t)^2}{4\times\cdot845\times w_2t+b^2}}+e^{-\frac{(x-v_0t)^2}{4\times\cdot845\times w_2t+b^2}}\right]$$

$$+\frac{C}{4v_0}\left[\frac{(x+v_0t)-(x-v_0t)}{\sqrt{.845\,w_2t+\frac{b^2}{4}}}-\frac{1}{4.3}\frac{(x+v_0t)^3-(x-v_0)^3}{\left(.845\,w_2t+\frac{b^2}{4}\right)^{\frac{3}{2}}}\right.$$

$$\left.+\frac{1}{2!4^25}\frac{(x+v_0t)^5-(x-v_0t)^5}{\left(.845\,w_2t+\frac{b^2}{4}\right)^{\frac{5}{2}}}-\cdots\right].$$

.....(34)

Calculated results of vertical displacements of a certain case, in which initial surface displacement only is given, are illustrated in Fig. II. This example has been taken up for the purpose of ascertaining the way, in which two independent tremors occurring at separate regions of surface are diffused, and for the determination of the behaviours, which take place subsequently. It will be understood from the figure that two separate disturbances begin to diffuse each other at an early time. When the diffusion is prevailed, the distribution of vertical displacements of the surface is nearly trapezoidal. The

surface displacements after a short time are rather sharp at the middle part and then take gradually a flat form. Later the middle part again begins to subside; and this is followed by the division of the disturbed portion into two independent crests propagated, though very slowly, in opposite directions. This is a characteristic feature of tremors, which are diffused in two dimensions on the surface of a body with very high viscosity. Such natures will be observed in the vibrations of sands and soils, in which a number of separate disturbances are diffused and then propagated for short distances. These natures are, thus, well accounted for by the visco-elastic property of the solid body.

Summary.

We have now obtained a few results by the use of Fourier's double integral applied to the problem of the vibration of the visco-elastic solid body. The essential parts are summed up as follows:—

1. Propagation of arbitrary waves on the surface of visco-elastic body and the diffusion of like tremors on the surface of a solid with high viscosity have a close connection in a sense that both these natures stand on the same physical elements.

2. The disturbances applied on the surface of an elastic body having high viscosity, are diffused in the neighbourhood of the disturbed portion, not propagated as progressive waves.

3. While tremors due to initial displacement are diffused, tremors due to initial velocity are gradually excited; these excited displacements are also diffused in the course of time.

4. In a certain case of two-dimensional motion a pair of equal disturbances occurring at separate portions are diffused each other at an early time. The surface displacements after a short time become very like to those of a single tremor. Later the middle part of this tremor begins to subside and then the tremor is divided into two parts propagated very slowly in opposite directions.

In concluding this paper the author's thanks are due to Professors Nagaoka and Terada for their kind advices and suggestions.

April 1928.

Rayleigh-type Waves propagated along an Inner Stratum of a Body.

By

Katsutada SEZAWA and **Genrokuro NISHIMURA.**

Earthquake Research Institute.

彈性體の内部層に傳はるレーレー型波

所員 妹澤克惟
西村源六郎

表面層に傳はるレーレー型波に就ては種々の場合の計算が著者の一人に依て試みてある。又ラム教授は十年程前に板に傳はる短波長の彈性波の計算を行ひ、次に數年前にはストーンレー氏が彈性體の内部層に傳はるラブ型波を研究した。最近には松澤助教授が地殻内に弱い層の存在する事を指摘した。即ち内部層に傳はるレーレー型波は早晩誰かの手によつて計算さるべき問題であつたのであるが、地震學上でも斯く重要な意味を持つ樣になつたから著者等は勇氣を得て、この研究を行つた譯である。

計算法は表面層の場合と同樣であるが波型が層の中間面に對して相對稱の場合と斜對稱の場合とについて研究し種々の結果を得た。その重要な項目を擧れば

(1) 中間層に傳はるレーレー波は分散性を現はす。

(2) 或 L/H に對して斜對稱のものが相對稱のものよりも高傳播速度を持つ。

(3) 波動速は層に特有な横波の速度と外部媒體に特有な横波の速度との間にある。

(4) $\frac{\mu'}{\mu}$ が小になるに從て、可なり長い L/H の間略一定の速度を保つ。

(5) $\frac{\mu'}{\mu}$ が非常に小になる時はこの一定に近い速度は半無限體上のレーレー波の速度に近づく。

(6) 短波長の波動勢力は弱い中間層に集積する。

It has already been studied mathematically by one[1] of the present authors how Rayleigh-type waves propagated on the surface of stratified bodies are dispersed. The results of calculation for various ratio of wave length and thickness of the layer, besides for different ratio between the elasticity of the layer and that of the subjacent material, have also been given. Not so long ago, Professor Lamb[2] investigated the manner, in which waves of various length

(1) "Dispersion of Elastic Waves & etc.," *Bull. of the Inst.* III. (1927).

(2) Lamb, "On Waves in an Elastic Plate," *Proc. Roy. Soc.*, (1916).

are transmitted over a plate. Stoneley[1] later showed, together with some problems of elastic waves, the propagation of Love-type waves along an inner medium of a body. The hypothesis of the existence of a stratum in the earth crust has recently been shown by Mr. Matuzawa[2] to accord with the results of seismic observations. Thus by the theoretical need of obtaining Rayleigh-type waves along a stratum, which are left to be discovered by any student, and by the practical importance of seismology to explore the structure of the earth crust, the authors have been encouraged to study the present problem.

The method employed in this paper resembles to that in the investigation of Rayleigh-waves on a stratified body. It is, however, noted that the authors have considered in this paper both cases of symmetric and asymmetric waves with respect to the central plane of the stratum. The intermediate cases have, of course, been imagined. In the case of Rayleigh-waves on a stratified surface of a body one type only was to be investigated.

Solutions for Symmetrical Case.

When the axis of x is taken coincident with the centre line of a stratum lying in an infinite body and the axis of y is directed perpendicular to x-axis, the equations of motion, in two dimensions, of the outer medium are expressed by

$$\left.\begin{aligned} \rho\frac{\partial^2\Delta}{\partial t^2} &= (\lambda+2\mu)\left(\frac{\partial^2\Delta}{\partial x^2}+\frac{\partial^2\Delta}{\partial y^2}\right), \\ \rho\frac{\partial^2\varpi}{\partial t^2} &= \mu\left(\frac{\partial^2\varpi}{\partial x^2}+\frac{\partial^2\varpi}{\partial y^2}\right), \end{aligned}\right\} \quad \cdots\cdots\cdots\cdots (1)$$

in which

$$\left.\begin{aligned} \Delta &= \frac{\partial u}{\partial x}+\frac{\partial v}{\partial y}, \\ 2\varpi &= \frac{\partial v}{\partial x}-\frac{\partial u}{\partial y}, \\ u, v &= \text{components of displacement parallel to } x\text{- and } y\text{-axes respectively}, \\ \rho &= \text{density}, \\ \lambda, \mu &= \text{Lamé's elastic constants}. \end{aligned}\right\} \quad \cdots (2)$$

(1) Stoneley, "Elastic Waves at Surface of Separation ...," *Proc. Roy. Soc.*, (1924).

(2) Matuzawa, "Propagation of Love-waves along Trebly Stratified Body," *Proc. Physico-Math. Soc. of Japan*, March 1928.

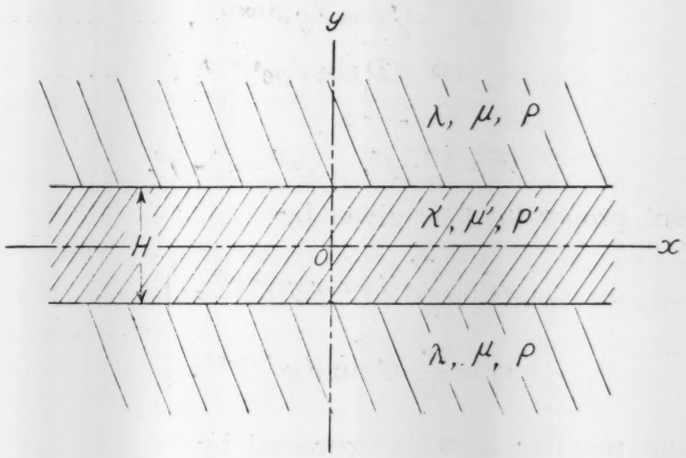

The solutions of (1) for the outer medium can be expressed by

$$\Delta = Ae^{\pm ry+i(pt-fx)}, \quad \cdots\cdots (3)$$

$$2\varpi = Be^{\pm sy+i(pt-fx)}, \quad \cdots\cdots (4)$$

$\pm$ being taken for each outer medium on the negative and positive sides of y-axis. While it is restricted that

$$\left.\begin{aligned} r^2 &= f^2 - h^2, & s^2 &= f^2 - k^2, \\ h^2 &= \frac{\rho p^2}{\lambda + 2\mu}, & k^2 &= \frac{\rho p^2}{\mu}. \end{aligned}\right\} \quad \cdots\cdots (5)$$

Displacement (u_1, v_1) answering to Δ in (3) and satisfying $\varpi = 0$ is given by

$$\left.\begin{aligned} u_1 &= \frac{if}{h^2} Ae^{\pm ry+i(pt-fx)}, \\ v_1 &= -\frac{r}{h^2} Ae^{\pm ry+i(pt-fx)}. \end{aligned}\right\} \quad \cdots\cdots (6)$$

Displacement (u_2, v_2) obtained from the value of ϖ in (4) and fulfilling the condition, $\Delta = 0$, is expressed by

$$\left.\begin{aligned} u_2 &= \frac{s}{k^2} Be^{\pm sy+i(pt-fx)}, \\ v_2 &= \frac{if}{k^2} Be^{\pm sy+i(pt-fx)}. \end{aligned}\right\} \quad \cdots\cdots (7)$$

The equations of motion of the stratum are expressed by

$$\left.\begin{aligned} \rho' \frac{\partial^2 \Delta'}{\partial t^2} &= (\lambda' + 2\mu') \left(\frac{\partial^2 \Delta'}{\partial x^2} + \frac{\partial^2 \Delta'}{\partial y^2} \right), \\ \rho' \frac{\partial^2 \varpi'}{\partial t^2} &= \mu' \left(\frac{\partial^2 \varpi'}{\partial x^2} + \frac{\partial^2 \varpi'}{\partial y^2} \right). \end{aligned}\right\} \quad \cdots\cdots (8)$$

where ρ', λ', μ' are density and Lamé's elastic constants of this stratum.

The solutions of (8) can be written by

$$\Delta' = C \cos r'y\, e^{i(pt-fx)}, \quad \cdots\cdots\cdots\cdots\cdots \quad (9)$$

$$2\varpi' = D \sin s'y e^{i(pt-fx)}, \quad \cdots\cdots\cdots\cdots\cdots \quad (10)$$

in which

$$r'^2 = h'^2 - f^2, \qquad s'^2 = k'^2 - f^2.$$

Displacement proper to Δ' is given by

$$\left.\begin{aligned} u_1' &= \frac{if}{h^2} C \cos r'y e^{i(pt-fx)}, \\ v_1' &= \frac{r'}{h^2} C \sin r'y e^{i(pt-fx)}. \end{aligned}\right\} \quad \cdots\cdots\cdots\cdots\cdots \quad (11)$$

Displacement peculiar to ϖ' is expressed by

$$\left.\begin{aligned} u_2' &= \frac{s'}{k^2} D \cos s'y e^{i(pt-fx)}, \\ v_2' &= \frac{if}{k^2} D \sin s'y e^{i(pt-fx)}. \end{aligned}\right\} \quad \cdots\cdots\cdots\cdots\cdots \quad (12)$$

Solutions for Asymmetric Case.

In like manner the solutions for the asymmetric case can be obtained. The expressions of the dilatation, distortion and displacements of the outer medium are of the same forms as in the former case. Those of the stratum are expressed by

$$\left.\begin{aligned} \Delta' &= C \sin r'y e^{i(pt-fx)}, \\ 2\varpi' &= D \cos s'y e^{i(pt-fx)}, \\ u_1' &= \frac{if}{h^2} C \sin r'y e^{i(pt-fx)}, \\ v_1' &= -\frac{r'C}{h^2} \cos r'y e^{i(pt-fx)}, \\ u_2' &= -\frac{s'D}{h^2} \sin s'y e^{i(pt-fx)}, \\ v_2' &= \frac{if}{h^2} D \cos s'y e^{i(pt-fx)}. \end{aligned}\right\} \quad \cdots\cdots\cdots\cdots\cdots \quad (13)$$

Boundary Conditions.

Now the boundary conditions are given by the following equations,

$$\left.\begin{aligned} u_1 + u_2 &= u_1' + u_2', \\ v_1 + v_2 &= v_1' + v_2', \end{aligned}\right.$$

$$\left.\begin{aligned} \lambda\Delta+2\mu\frac{\partial}{\partial y}(v_1+v_2)&=\lambda'\Delta'+2\mu'\frac{\partial}{\partial y}(v_1'+v_2'),\\ \mu\left[\frac{\partial}{\partial y}(u_1+u_2)+\frac{\partial}{\partial x}(v_1+v_2)\right]&=\mu'\left[\frac{\partial}{\partial y}(u_1'+u_2')+\frac{\partial}{\partial x}(v_1'+v_2')\right]\end{aligned}\right\}\quad\ldots\ (14)$$

at $y=\pm\frac{H}{2}$, where H is thickness of the layer.

Putting the values of $\Delta, u_1, u_2, v_1, v_2, \Delta', u_1', u_2', v_1', v_2'$ from (3), (6), (7), (9), (11), (12), (13) in the conditions (14) at the boundaries and eliminating A, B, C, and D, it follows,

$$\begin{vmatrix} i, & \frac{s}{f}, & i, & \frac{s'}{f} \\ \frac{r}{f}, & -i, & \frac{r'}{f}X, & iY \\ \left(\frac{\lambda}{\mu}\frac{h^2}{f^2}-2\frac{r^2}{f^2}\right), & 2i\frac{s}{f}, & \left(\frac{\lambda'}{\mu}\frac{h'^2}{f^2}-\frac{2\mu'}{\mu}\frac{r'^2}{f^2}\right), & 2i\frac{\mu'}{\mu}\frac{s'}{f} \\ 2i\frac{r}{f}, & \left(1+\frac{s^2}{f^2}\right), & 2i\frac{\mu'}{\mu}\frac{r'}{f}X, & -\frac{\mu'}{\mu}\left(1-\frac{s'^2}{f^2}\right)Y \end{vmatrix}=0,\quad\ldots(15)$$

where $X=\tan\frac{r'H}{2}$ and $Y=\tan\frac{s'H}{2}$ for symmetric type,

$X=-\cot\frac{r'H}{2}$ and $Y=-\cot\frac{s'H}{2}$ for asymmetric type.

Solving the above determinantal equation by tentative methods for the cases $\mu=2\mu'$ and $\mu=8\mu'$, in which $\lambda=\mu$, $\lambda'=\mu'$ and $\rho=\rho'$, the authors have obtained the relations between the velocity and $\frac{L}{H}$, L being the wave length. The illustrated diagrams on the next page give these relations. In (A) the domain indicated by the hatched lines give the velocity of propagation of waves for $\frac{\mu'}{\mu}=\frac{1}{2}$ and for different ratios of L/H. This shows that waves of the asymmetric type are propagated more quickly than those of the symmetric type. Each waves of the intermediate types have the velocity which is represented by a certain point of the hatched part. Waves, whose velocity is greater than $\sqrt{\frac{\mu}{\rho}}$, cannot exist, because of the nature that very large amplitudes of the motion at infinite distance from the stratum must be then induced and they must require an infinite energy. A significant fact is that the velocity of propagation of every case is limited between those of distortional

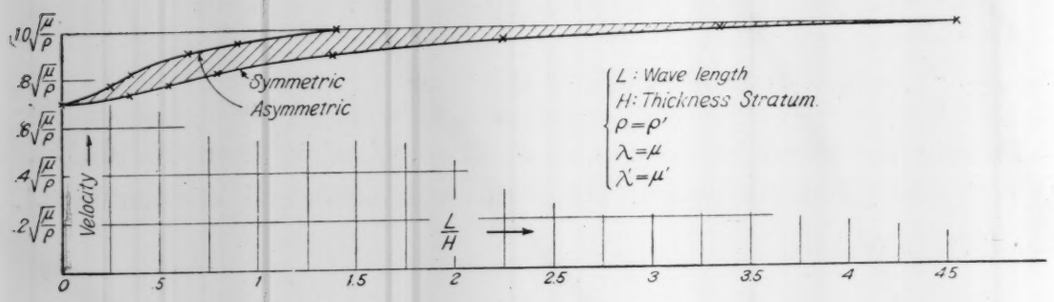

(A) $\left(\frac{\mu'}{\mu}=\frac{1}{2}\right)$

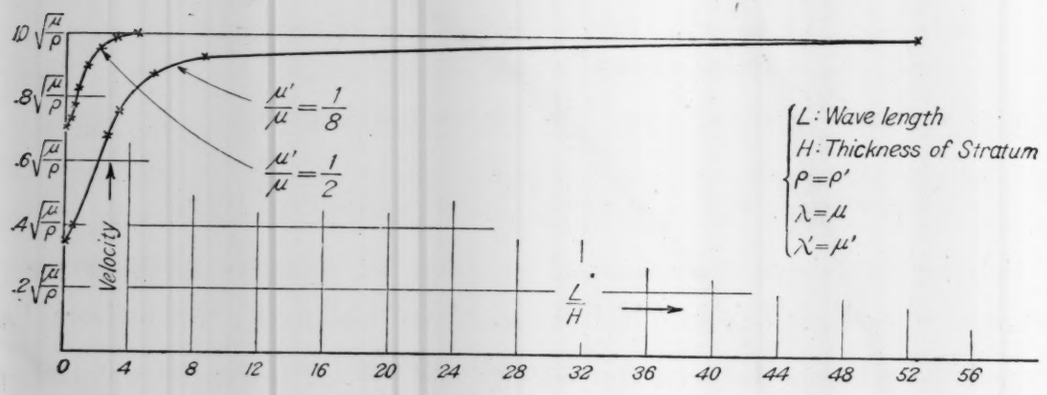

(B) (Symmetrical Case)

[The results in the upper diagrams, together with those results written in Bull. III, has been computed in very strict manners. The application of a tentative method to the numerical solutions of complicated equations involving implicit quantities gives very often much better results than those obtained by the use of the ordinary method of treating algebraic equations.]

waves in the stratum and the outer medium. Not less important is the fact that smaller ratio of $\frac{\mu'}{\mu}$ gives longer range of L/H, in which approximately constant velocities of propagation are obtained. It is imagined from the figure that, when $\frac{\mu'}{\mu}$ tends to be very small, the constant value approaches the velocity of Rayleigh-waves on a semi-infinite solid body.

The diagram and the foregoing solutions will, again, tell us, though implicitly, that the energy of waves of short length accumulates in the vicinity of such a weak stratum; this may have some importance on the problem of seismic radiation, as well as on the problem of vibration of constructive materials.

Résumé.

(1) Rayleigh-type waves propagated along an inner stratum of an elastic body can be classified into two elementary types. According as the wave forms are symmetrical or asymmetric about the central plane of the stratum, the waves may be named symmetric or asymmetric type.

(2) Rayleigh-type waves propagated along an inner stratum show generally dispersive nature.

(3) The asymmetric type has velocity higher than that of the symmetrical type for some values of L/H.

(4) Velocities of propagation of the waves along a stratum are limited between those of distortional waves in the stratum and the outer medium.

(5) Smaller ratio of $\frac{\mu'}{\mu}$ gives longer range of L/H, which keeps approximately constant values of the velocity of propagation.

(6) As $\frac{\mu'}{\mu}$ tends to be very small, the constant value above mentioned approaches the velocity of propagation of Rayleigh-waves on a semi-infinite solid body.

(7) Energy of waves of short length accumulates in the vicinity of a weak stratum.

In conclusion, the authors are indebted to Professor Suyehiro, the Director of the Institute, who has allowed them to complete this investigation at leisure.

April 1928.

Experiments on the Effect of an Irregular Succesession of Impulses upon a Simple Vibrating System.

By

Torahiko TERADA and **Ukitirô NAKAYA.**

不規則なる衝撃群に因る振動系の運動に關する實驗

所員 寺田寅彦

理化學研究所 中谷宇吉郎

摘要

一定の固有振動週期を有する振動系に、不規則な間隔をもつて、多數の衝撃が相次いで與へられた時に、其振動系が如何なる運動をするであらうかといふ事は、地震學上に於ても興味ある問題である。此問題に就て著者の一人は、十餘年前に、若干理論上の考察をして其結果を發表して置いた。今、此處では、此の問題に關する實驗を行つて、前に得た理論上の結果と比較し、又實驗的摸型によつて得られる運動を地震の運動等と比較して見たのである。

振動系としては振子を用ゐ、其れに、二つの互に反對な方向から散彈の流れを衝突させ、その衝撃によつて生ずる振子の運動を、地震計と同樣な裝置で自記させた。

此の運動の平均の運動エネルギーの數値を記象から求めるには、小野博士が地球磁場變化の度を表示する爲に用ゐた mean variability の方法を採用した。此の量が衝撃の毎秒回數や、各衝撃の運動量や、又振子の減衰率等の變化によつて如何に變化するかを實驗し、其結果が理論から期待される關係と如何なる程度迄一致するかを試驗した。

振子の片側に毎秒衝突する散彈の數 n が數百乃至數千といふ場合には、平均運動エネルギー I_0 と n との關係は全然理論と一致しない。I_0 と減衰率との關係は、質的には略一致するが、量的には一致しない。此れは n が大きいと振子の有效質量並に減衰率が著しく變るといふ事によつて說明される。併し、此の場合でも、散彈の運動量と I_0 との關係は略理論と一致する。

次に n が十或は二十位の場合に就て實驗して見ると、此場合には I_0 と n 及減衰率との關係は大體に於て理論の示す通りになる事が確かめられた。

以上の實驗で得た振子運動の記象は、此れを各種地震波の記象や又潮汐副振動其他種々な自然界の運動の記象と比較すると、殆んど區別の付かない程類似したものがある。此の事實は地震記象の意義を解釋する際にも、又地震計の作用を考察する際にも考慮しなければならないことであらうと考へられる。

In 1917, one of the present authors published a paper[1] on some theoretical considerations regarding the behaviour of a simple resonator acted upon by an irregular succession of discontinuous impulses. For the case when the duration of a single impulse is small compared with the intervals of successive impulses and a great number of such impulses takes place before the initial amplitude is sensibly damped, an expression for the mean kinetic energy of the resonator was derived. Thus, when the equation of motion for the natural vibration is

$$m\ddot{x}+f\dot{x}+kx=0$$

the mean kinetic energy is given by

$$I_0=\frac{a^2Q^2}{4m\alpha t_0}$$

where a is the amplitude of a single impulse considered as constant and t_0 the mean interval of the impulses. α is the measure of damping given by

$$\alpha=\frac{f}{2m}.$$

Q is a function of the natural frequency given by β where

$$\beta^2=\frac{k}{m}-\frac{f^2}{4m^2},$$

as well as of the duration τ of the single impulse, the function differing according to the form of the pulse.

The ideal case treated in the above theory may be applied to the case of a physical pendulum of which the suspended mass is subjected to an irregular succession of impacts by a stream of some granular substance such as shots or sand directed upon it. It is, however, diffiicult to see to what degree of approximation the assumption made for the ideal case is fulfilled in this actual case, especially when the number of grains colliding per unit time becomes large and the mutual independence of the elementary pulses cannot be insured. An experimental study of the problem seems, therefore, not without interest, especially in connection with some fundamental problem of seismology.

These considerations led the present authors to undertake a series of experiments in this line. Though the method and apparatus used are of a

(1) Proc. Tokyo Math.-Phys. Soc., [ii] **9** (1917), 142; the promised publication of the results of further investigation has been reserved on account of the lack of immediate application, as our conception on the nature of X-rays has since that time been greatly modified. For the problems as are concerned in the present paper, however, the result given in the paper cited seems to be sufficient for an approximate discussion.

provisory nature and the results obtained are still fragmentary, we may be allowed to give a brief account of them in the following.

The experiments were made in two series, the first with a large number of grains impinging on the pendulum in unit time and the second with a small number. Our descriptions of the experiments will therefore be conveniently divided into two parts.

I. Experiments with Large Number of Impulses per Unit Time.

(a) *Apparatus.*

For a preliminary experiment, a physical pendulum consisting of a lead bob and a brass rod was subjected to impact of two streams of fine sand directed on two opposite sides of the bob and the motion of the rod was recorded on a smoked paper covering a rotating drum, by means of a light style attached to the rod. The amplitudes of irregular oscillations of the pendulum thus excited were too small to be subjected to the method of analysis intended. Stream of water was also tried instead of sand without success. Finally, we decided upon the use of ordinary gun shots as the most suitable material for our present purpose.

The pendulum No. I used in the earlier part of the first series of experiment was a simple brass rod suspended by an iron pin attached perpendicular to the rod near the upper end of the rod, the pin playing the rôle of a knife edge, resting upon a plane support. Near the lower end of the pendulum rod a pair of thin iron plate was attached in diametrally opposite positions for receiving the impacts and serving as the targets of the two streams of shots respectively. This plate was bent in a form of semi-cylinder, with its axis parallel to the rod and its concave side outward, in order to avoid the lateral scattering of the impinging shots. After a few trial experiments made with this pendulum, another pendulum No. II (Fig. 1) was constructed, for which a knife edge K was replaced for the pin of No. I. The natural period of the pendulum was 1.48 sec. A pair of liquid dampers D was also provided for, by means of which the rate of damping could be adjusted through a wide range by using different kinds of liquid, or by varying the dimension of the vane. The semi-cylindrical receivers or targets S were retained. The shots were fed from the funnel F and directed upon the receiver S by means of a conduit

Fig. 1.

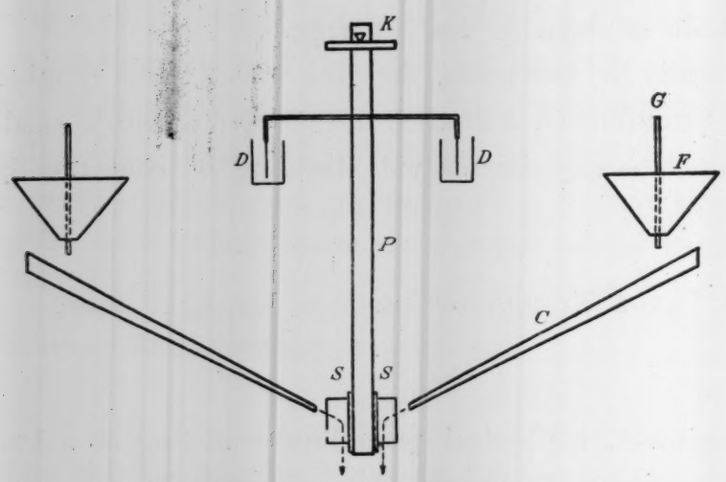

K, Knife edge; *P*, pendulum rod;
D, damper; *S*, semi-cylindrical receiver;
C, conduit; *F*, funnel; *G*, glass rod.

C with a fixed inclination of about 22°. The velocity of the shots impinging upon *S* could be varied by displacing the funnel *F* along the length of the conduit. A difficulty was felt in sending out a nearly uniform stream of grains from the mouth of the funnel upon the conduit, as the grains are apt to stop their own outlet when the aperture is made too small and if the aperture be widened the flow became too large. This difficulty could be avoided by inserting a thin glass rod *G* in the funnel as shown in Fig. 1 and by giving it an oscillating motion in the vertical direction. The motion was given by hand with an average frequency of 3–6 vibrations per second. It was verified later by special experiments that the variation in the frequency of motion of the glass rod produces no sensible change in the numerical results of the experiments.

For recording the motion of the pendulum, a thin aluminium rod was attached to the pendulum rod *P* near *S*. The end of this aluminium rod carried a light style taken from a seismograph of Omori type, which recorded the motion upon the smoked paper covering a revolving drum, also borrowd from a seismograph.

The shots used were mainly of two kinds:

No.	Mass of a single grain
5	0.15 gr.
12	0.024 gr.

The shot No. 12 was used only in a few earlier experiments; in the later experiments, No. 5 was chiefly used.

(b) *Methods of Numerical Reduction of the Results of Experiments.*

In order to obtain an approximate measure of the magnitude of the

impulse due to the collision of a single grain of shots, it is needed to determine the velocity with which it impinges upon the pendulum. As it suffices for the present purpose to know an approximate relative measure of the momentum of the grain, we determined the average velocity of the stream of grains at the outlet of the conduit by estimating the mean horizontal distance a traversed by the stream during its fall from the muzzle of the conduit to the floor below. If the height of the muzzle above the floor be h, the distance between the foot of the muzzle and the foot of the stream be a and the angle of inclination of the conduit be θ, the muzzle velocity v_0 will be given by

$$v_0^2=\frac{g\,a^2}{2\cos\,\theta\,(h\cos\theta-a\sin\theta)},$$

where g is the acceleration due to gravity. The horizontal component will be given by $v_0\cos\theta$, if desired.

As already mentioned, the velocity was varied by varying the distance l between the outlet of the funnel supplying the shots into the head of the of the conduit and the muzzle of the conduit facing the pendulum target. The result of experiment showed that the velocity is approximately independent of the number of grains n flowing per unit time when the number is varied from 300 to 450 per sec. The relation between l and v_0 may be tabulated as follows:

l (cm.)	v_0 (cm/sec.)
48	143
28	117
15	88

Though a more detailed investigation regarding the relation between l and v_0 will of itself form an interesting theme for some technical physicists, we were for the present satisfied with obtaining thus an approximate *relative* measure of the momentum transmitted to the pendulum by the impact of a single grain.

A discussion regarding the details of the actual mechanism of collision of a stream of grains upon a given form of the receiver such as here used is by no means an easy matter. We assume, therefore, simply that each grain transmits a momentum proportional to Mv_0 where M is the mass of a single grain, and proceed to see empirically in which way the motion of the pendulum is governed by Mv_0, n and the logarithmic decrement.

The damping ratio κ of the pendulum was measured by the ratio of the successive swings in alternate directions. It is related with α above defined and the natural period of oscillation T by the equation

$$\alpha T = 2 \log \kappa$$

The values of κ obtained in different sets of our experiments was 1.00, 1.15, 1.72, 10, 100 and ∞ respectively. The latter two numbers are of course very roughly estimated. For the aperiodic case, a mixture of water glass with water was used for the damping liquid instead of paraffin used in other cases.

For a measure of the mean kinetic energy of the pendulum excited by the impact of the stream of shots we adopted the "mean variability" of the displacement of the pendulum. The concept of the mean variability of a physical quantity y depending on another x was introduced by Dr. S. Ono[1] as a convenient measure of the activity of disturbance in the terrestrial magnetic field, or of any physical quantity subjected to a similar fluctuation. Thus, the variability of y referred to a definite interval of x, say l, is defined by the integral

$$V_l = \frac{1}{l} \int_0^l \left(\frac{dy}{dx} \right)^2 dx.$$

The mean value $\overline{V}$ of this quantity for different intervals throughout a certain range of x is called the mean variability of y in that range.

In the present case, taking y for the displacement of the pendulum as a funtion of time x, $\overline{V}$ is proportional to the mean kinetic energy, as the vibrating mass of the pendulum is kept constant.

In Ono's paper cited, a very simple method is given for evaluating the mean variability from the graph representing $y=f(x)$. A transparent paper or plate ruled with a number of parallel lines with a constant interval p is placed upon the graph such that the ruled lines are parallel to the axis of x. The number of the points of intersection of the curve with the equidistant parallel lines is counted, including the point at which the curve comes into contact tangentially with one of the parallel lines. Let this number be denoted by R for a range of x extending over a length of τ. The variability for the range τ is then given by the expression

(1) S. Ono, Ann. Rep. Centr. Met. Obs. Jap., Magnetic Observation for the Year 1916; Jap. Journ. Astr. Geoph., **3** (1925), 11.

$$\overline{V}=\frac{2R^2p^2}{\tau^2}.$$

The mean value of $\overline{V}$ for a number of intervals may be taken as the mean variability for those intervals. The numerical factor of the above expression may deviate from 2 in some extraordinary cases, but seems to be approximately equal to 2 in most cases of fluctuation in kindred natural phenomena.

In order to apply the above method in our case, we used a glass plate ruled with equidistant parallel lines with the interval $p=2$ mm. for the most cases except for a few records with small amplitude of vibration, in which case another plate with $p=1$ mm. was used. For a number of records, mean R per unit time was counted with each of the two plate and it was found that the product Rp is very nearly independent of p, though with a tendency to be slightly greater for the smaller p. Thus, for example, the ratios of two R's obtained with the two values of p were 2.14, 2.12 and 2.02 for the three records examined.

In order to obtain $\overline{V}$ for one second, we must count the actual number R for each second and calculate the mean value of R^2 for a number of data. As the calculation is not simple, we took the mean value of R per second from the record extending over several ten seconds and replaced $(\overline{R})^2$ for $\overline{R^2}$, as it may be shown that the two quantitities are approximately proportional in ordinary cases.[1] In any case, we may conveniently take $(\overline{R})^2$ obtained with a constant p as an approximate measure proportional to the mean kinetic energy of the pendulum, i. e. $I_0 \propto (\overline{R})^2$.

From (1), we have

$$I_0=C\frac{a^2}{\alpha t_0},$$

where C is a constant inversely proportional to the pendulum mass. If the number of impulses, or of the grains impinging per second be n, we have $t_0=1/n$. Since a is proportional to the mean velocity v_0 for a given mass of the single grain and α to $\log \kappa$ as already mentioned, we obtain

$$I_0=C'\frac{v_0^2 n}{\log \kappa},$$

where C' is a constant proportional to the square of the mass of a single

(1) Usually $\overline{R^2}\fallingdotseq 2(\overline{R})^2$; See Ono's paper, loc. cit.

grain. This value of I_0 will be proportional to $(\bar{R})^2$ or $\bar{R}^2$ as above determined from the experimental records.[1]

The methods for evaluating v_0 and κ have already been described. n could be estimated approximately from the time required for streaming out a known total mass of shots and the mean mass of a single grain.

(c) *Results of Experiments.*

In the earlier part of the experiments some test has been made regarding the effect of the mass M of the single grain, using the shots No. 5 and 12. It was found, for example, that comparing the two cases with $M=0.15$, $n=700$ and $M=0.024$, $n=2000$, the disturbance of the pendulum is decidedly larger for the former case. The proportionality between $\bar{R}^2$ and $M^2 n$ could, however, not be confirmed. This experiment was, however, made before the final improved form of the apparatus was decided upon and wants a future revision.

In Table I we give a summary of the results of the experiments carried out with the apparatus described in a previous section, using various combinations of the values of n, κ and v_0 or Mv_0, available.

TABLE I.

Number of records used	κ	n	Mv_0	$\bar{R}$	$\bar{R}^2$
10	1.00	300	21	7.24	52.4
,,	,,	320	18	5.43	29.5
,,	,,	340	13	4.32	18.7
,,	,,	490	21	5.87	34.5
,,	,,	510	18	4.05	16.4
,,	,,	525	13	3.21	10.3
10	1.15	305	21	5.81	33.8
,,	,,	355	18	3.46	12.0
,,	,,	470	21	4.07	16.6
,,	,,	470	18	3.62	13.1
10	1.72	295	21	2.87	8.2
5	10	320	21	1.94	3.8
5	100	320	21	1.68	2.8
10	,,	470	21	1.90	3.6
,,	,,	620	21	1.51	2.3

(1) The theoretical case treated was that of one-sided impulses, i. e. a was all of the same sign, while in the case of our present experiment the shots were directed upon the pendulum from two opposite sides so that the impulses consisted of nearly equal numbers of positive and negative ones. It will, however, be evident that the expression for I_0 still holds for this case, provided we take for n the total number of the shots impinging on both sides of the pendulum.

The result will be seen to be far from agreeing with the thereotical relation. In the following we will, therefore, examine in what respect the discrepancy is brought about.

Firstly, we will examine the relation between R and κ. Arranging the data according to the magnitude of κ, we obtain Table II below.

TABLE II.

κ	$\log_{10}\kappa$	$\bar{R}^2$ $n \fallingdotseq 300$	$\bar{R}^2$ $n \fallingdotseq 500$
1.00	0.000	52.4	34.5
1.15	0.061	33.8	16.6
1.72	0.235	8.2	—
10.	1.00	3.8	—
100.	2.00	2.8	3.6

The relation is plotted in Fig. 2. It will be seen that the mean variability decreases with the increasing logarithmic decrement. The apparent deviation from the theoretical hyperbolic form may be understood if we consider that the effective magnitude of damping will be much greater when the pendulum is moving among the stream of granular mass than in the case of free vibration

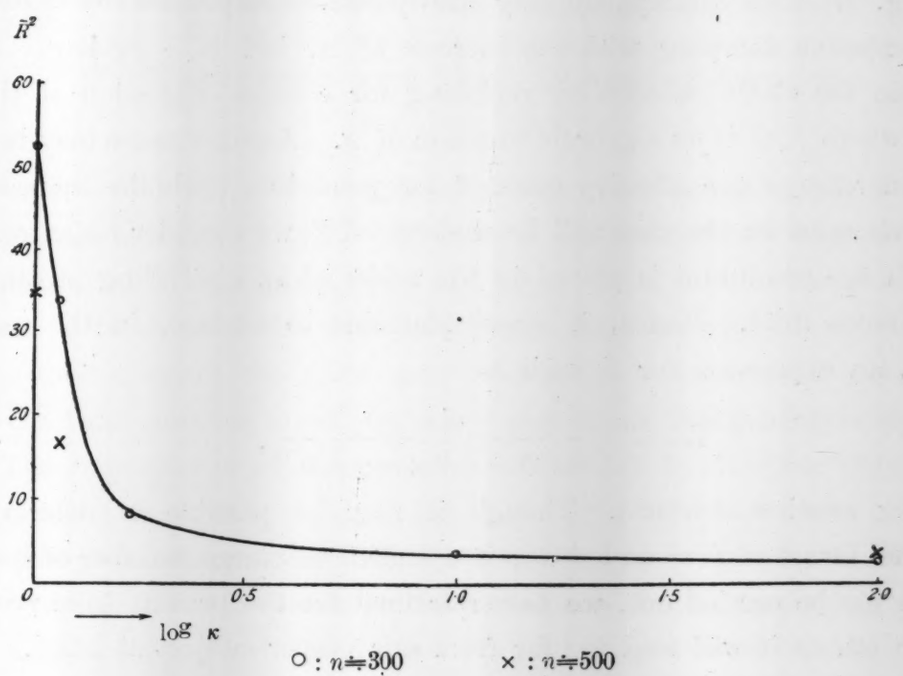

○ : $n \fallingdotseq 300$ × : $n \fallingdotseq 500$

Fig 2.

without the impinging shots and that the value of κ here used was, of course, determined for the latter case.

Next, the effect of varying n will be seen from Table III.

TABLE III.

κ	Mv_0	$\bar{R}$ $n\fallingdotseq 300$	$\bar{R}$ $n\fallingdotseq 500$	Ratio of $\bar{R}$ $(n\fallingdotseq 300)/(n\fallingdotseq 500)$
1.00	22	7.24	5.87	1.25
	18	5.43	4.05	1.34
	13	4.32	3.21	1.34
1.15	22	5.81	4.07	1.43
	18	3.46	3.62	0.96
100	22	3.39	3.80	0.89

Here, the most striking deviation from the theoretical relation is found. Thus, while a linear increase of the mean variability with increasing n is expected, the experimental results show an inverse relation, especially for the case of small damping. It is to be noted that for $\kappa=1.00$ the ratio of the variabilities for the two cases with $n=300$ and 500 is nearly independent of the value of Mv_0. For a large value of κ, the above ratio seems to decrease and becomes less than unity as expected from the theory. This relation may also be seen from Fig. 2. This discrepancy may also partly be explained by the increase of the effective damping with the increase of n, but it is evidently difficult to explain the above relation by replacing for κ some expression of the form $\kappa+f(n)$ where $f(n)$ is an algebraic function of n. Another cause may be sought in the increase of the effective mass of the pendulum with the increase of n. That such must be the case will be understood if we consider an extreme case in which the pendulum is placed in the midst of two colliding streams of a dense viscous fluid. Hence, it seems plausible to assume, in the case with large n, an expression for I_0 such as

$$I_0=C''\frac{v_0^2\, n}{[m+\phi(n)]\log[\kappa+f(n)]},$$

C'' being another constant. Though it may be possible to determine the functional forms of $f(n)$ and $\phi(n)$, if a sufficiently large number of systematic experiments be carried out, we have refrained for the present from proceeding any further, as it will lead too far from our proper subject at hand.

Lastly, the relation between Mv_0 and $\bar{R}$ will be shown by Table IV.

Table IV.

$\kappa=1.00$		
	Mv_0	13 : 18 : 22 = 1 : 1.39 : 1.69
$\bar{R}$	$n\fallingdotseq 300$	4.32 : 5.43 : 7.24 = 1 : 1.25 : 1.67
	$n\fallingdotseq 500$	3.21 : 4.05 : 5.87 = 1 : 1.26 : 1.83
$\kappa=1.15$		
	Mv_0	18 : 22 = 1 : 1.22
$\bar{R}$	$n\fallingdotseq 300$	3.46 : 5.81 = 1 : 1.68
	$n\fallingdotseq 500$	3.62 : 4.07 = 1 : 1.12

It will be seen that the two quantities are roughly proportional to each other at least for the case of smaller damping.

Thus far, we have seen that when the number of shots impinging on the pendulum is of the order of several hundreds to thousands per second the result of the simple theoretical calculation does not hold even approximately. The examination of the nature of discrepancy observed has shown that the swarm of grains seems to play a part of something like an atmosphere of very dense gas surrounding the vibrating mass, thus conspicuously affecting the effective mass as well as the damping of the system. In short, the assumption does not hold that each grain of shots acts as a discrete impulse independent of others. Thence, we proceeded to carry out another series of experiments with a decidedly smaller n than in the above, as will be described in the following.

II. Experiments with Small Number of Impulses per Unit Time.

In this second series of experiment n was to be varied within a range of small numbers between 5 and 20. In order to obtain suffiently large amplitudes of the pendulum it was necessary to use larger shots than in the previous experiments. The shots chosen were of 0.6 mm. diameter with the mass $M=1.24$ gr. The total mass of the shots used in a series of experiment was 2600 gr. so that the total number impinging upon one side of the pendulum was about 1050. The frequency n of the impulses was found by dividing this number by the number of seconds required for discharging this total mass.

As the grain diameter of the shots was large, it was found difficult to obtain a regular flow by means of the funnel used in the previous experiment so that a different method was devised for supplying a nearly uniform stream of shots. Referring to Pl. XII, Fig. 3 and 4, an endless band B of rubber is set

in a slow uniform motion by means of the two cylinders C revolving on their parallel axes, over which the band plays the part of a machine belt. The motion is regulated by means of a motor M and a reducing gear R. The shots S which is supplied by hand to the rear end of the moving band, fall through the pair of symmetrically placed conduits D into the "distributor" R. The latter is a rectangular shallow box of which the bed plate is studded with nails at the net points of 1.5 cm. square mesh. This devise was introduced to disperse any coherent group of shots which might be formed during their passage through the conduit. The shots were then guided to the pendulum P by means of the short canal T of which the muzzle was directed to the receiver V of the semi-cylindrical form as in the previous experiment. The motion of the pendulum was then recorded on the smoked paper covering the drum M by means of the needle N. A shows the damper.

Two kinds of pendulums were used. One of them No. II was of a brass rod with a mass of about 1.05 kg. As the mass of the grain of shot increased, the transverse vibration of the pendulum rod became conspicuous and appeared superposed on the record. Hence, another pendulum No. III was made of iron tube with 1.65 kg. mass. The most experiments were made with this latter one. In the following the results of experiments carried out with the pendulum No. III will be given graphically by Fig. 5—8. The abscissae represent the numbers of shots impinging on each side of the pendulum per second and the ordinates the quantities $(\overline{R})^2$ which is proportional to the mean variability or the mean kinetic energy. The points corresponding to the different values of κ are distinguished by the different marks ○ and ×.

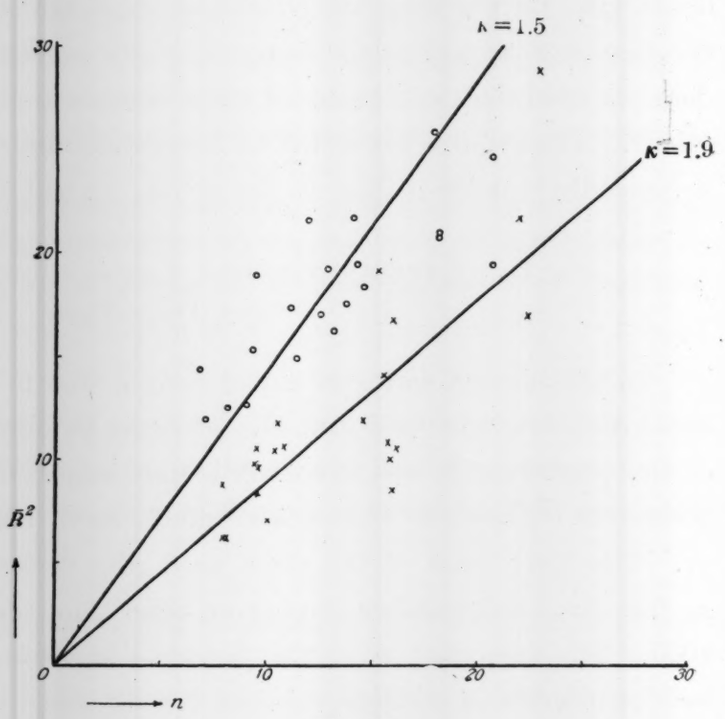

Fig. 5.

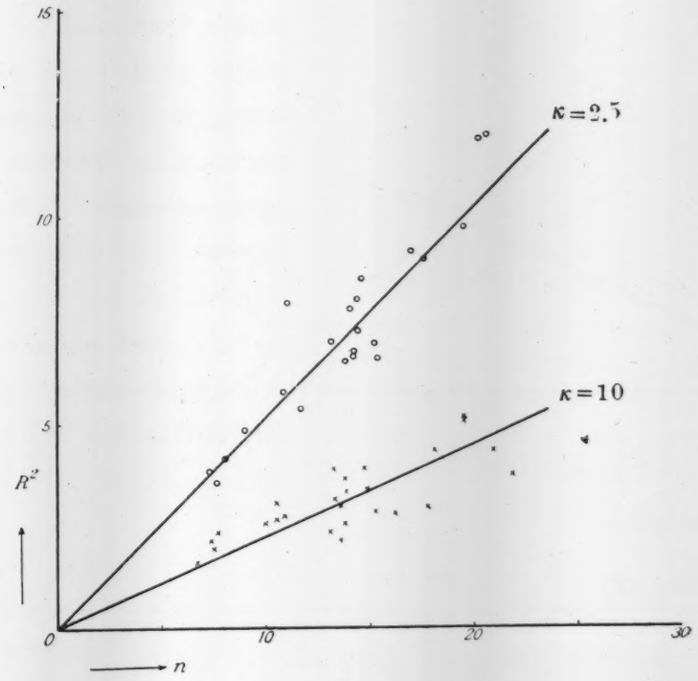
15
10
5
0
10
20
30
n
R^2
κ=2.5
κ=10

Fig. 6.

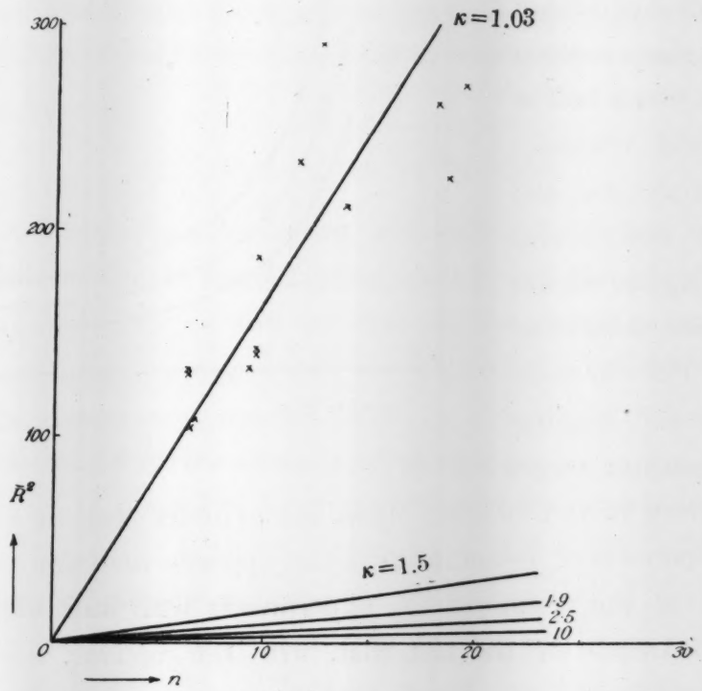
300
200
100
0
10
20
30
n
R^2
κ=1.03
κ=1.5
1·9
2·5
10

Fig. 7.

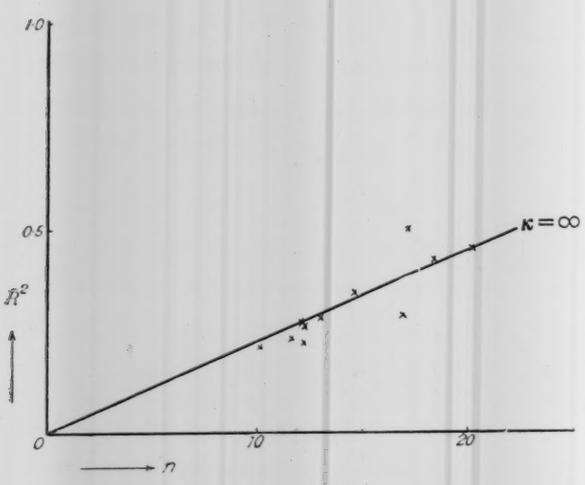

Fig. 8.

The straight lines are drawn by rough estimation. Though the points plotted are considerably scattered, it will be seen that the proportionality between n and $(\bar{R})^2$ holds approximately. From the above figures, the relation between the logarithmic decrement and $(\bar{R})^2$ may be obtained as shown in Fig. 9. An approximate hyperbolic trend of the curves for different values of n will be noted.

Thus the relation

$$\text{Mean variability} \propto \frac{n}{\log \kappa}$$

which does not hold in the case with large n, is found to hold approximately in the present case with small n.

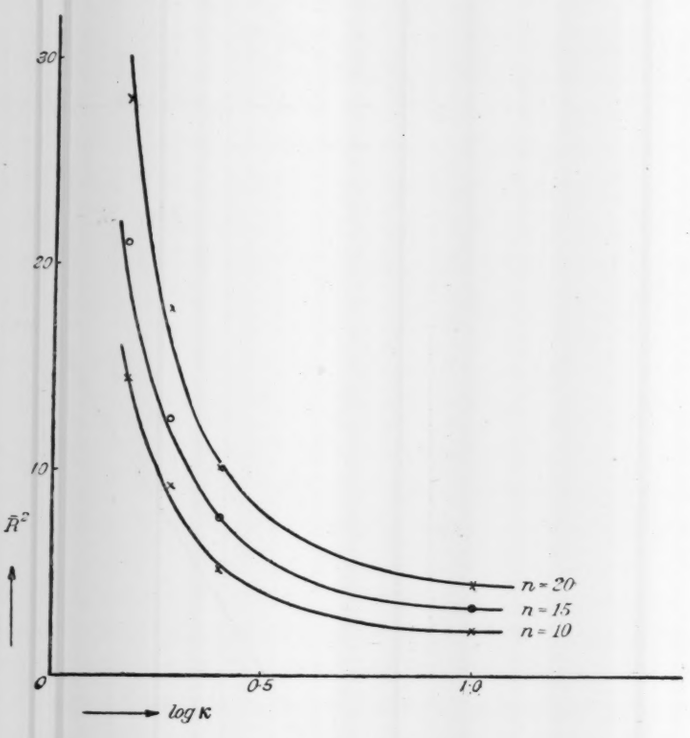

Fig. 9.

In a series of experiment, another kind of shots receiver was used which was a hollow cylinder attached coaxially with the pendulum rod and provided with two lateral holes for receiving the stream of shots from the mouths of the canals T. The shots entering the holes and impinging on the pendulum target were reflected from it and collided upon the cylinder wall of the receiver imparting the components of momentum in the opposite direction. Fig. 10 shows the comparison of the results of the experiments with and without the cylindrical receiver. Inspite of the fact that, with the receiver, the effective value of n may be considered to be larger than without it, the actual value of the

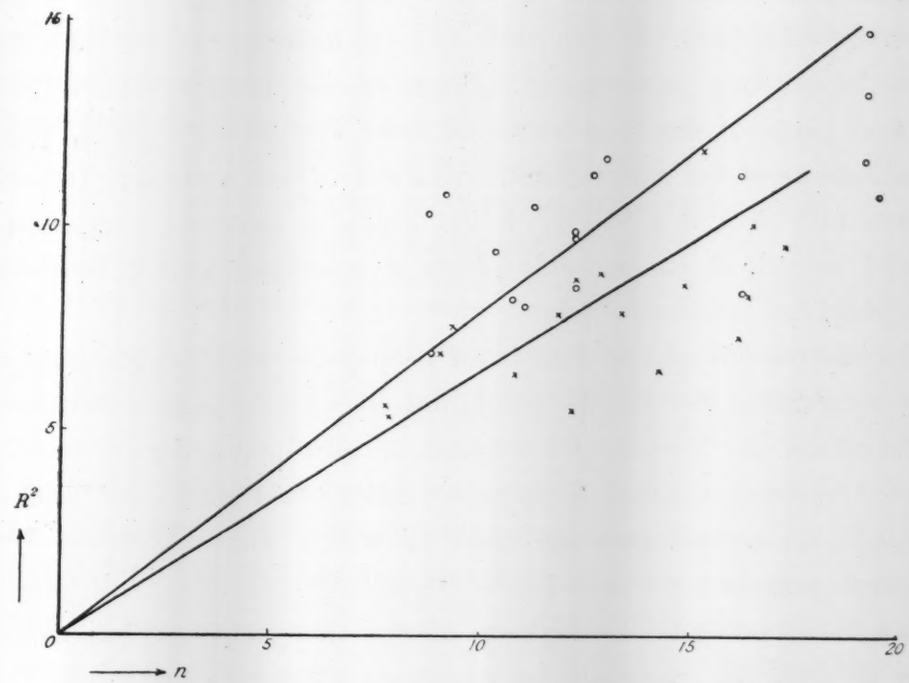

Fig. 10. ○ : without receiver.
× : with " .

mean variability is decidedly smaller in the former case than in the latter. This fact may probably be explained partly by an increase in the effective mass of the pendulum and perhaps also partly by the presence of a regular time relation between the direct impact of a shot and the second opposite impact after its reflection.

III. Character of Motions.

Thus far, we have been concerned with the quantitative relation between the mean kinetic energy of the vibrating system and the quantities specifying the nature of the system as well as that of the exciting impulses. In the following, we will spend a few words on the general qualitative characters of motion of such system and discuss them in connection with those of some kindred motions found in the domain of seimology.

Pl. XIII, Fig. 11 illustrates some specimens of the records obtained with the pendulum No. III with different values of n and κ. It will be seen that among the irregular motions recorded the natural period of the system appears always conspicuous. This is evident even in the case with very large damping (Fig. 11, lowest graphs). Those who are familiar with the records of

seismographs will easily perceive the most striking analogy of forms between the motions of the earth as recorded by the instruments and the motions of the pendulum here investigated. Some of the present records resemble the principal parts of the long waves of some distant earthquake, while the others reminds as of the microseismic vibration of the ground. Experienced seismologists may feel at a loss to decide which is the natural and which is the artificial record, if two suitable pieces of matching records be shown for connoisseuring.

In the other fields of the domain of geophysics there are also many kinds of motion resembling that of the pendulum here investigated. We may cite, among the others, the secondary undulation of tides appearing on mareograms, especially of stations situated in bays or gulfs[1] and also the "seiches" of some lakes.[2] These are also the cases in which some oscillators with definite natural periods are excited into irregular oscillations with fluctuating amplitudes. Our present investigation shows that such oscillations may be caused by an irregular succession of impulses, where no "resonance" in the ordinary sense of the word is possible.

Returning to our records shown in the above figures we may remark that besides the natural period of the pendulum a real "spectrum" of different periods is revealed, some of them greater and the others less than the natural one. If we pick up as is usual in the case of natural phenomena, a number of more or less regular trains of waves and determine their average periods, we will obtain a long list of different values. If we sort out the numbers thus obtained into groups by this or that choice we may obtain a number of "apparent proper periods" which in reality have nothing to do with the true natural periods of the vibrating system at hand.

These considerations will be sufficient for warning us againt drawing a hasty inference regarding the natural period from the results of an analysis of the kind above stated. For the discrimination of the true period some procedure is necessary. The periodogram method of Schuster may be one of the criterion, but it must fail when the natural period is gradually varying or when the damping is considerable. A practicable method in such case seems to obtain

(1) Many interesting examples of mareograms will be found in the paper "Secondary Undulations of Oceanic Tides" by K. Honda and others, Journ Coll. Sci., Tokyo, **24** (1908).

(2) See Journ. Coll. Sci., Tokyo, **28**, Art. 5 (1911).

a more or less complete spectrum of frequency curve from a sufficiently large number of records and search for the conspicuos frequency maxima. We must, however, be cautious in that case not to be deceived by the "periodicity" due to chance[1] of the frequency curve.

IV. Bearing of the Results of the Experiments on Seismometry.

Seismographs in common use are some or other kinds of oscillating system with definte natural periods and damping coefficients. The building within which the seismograph is installed may be another system. Again the portion of the earth crust may also have its own natural mode of vibration. If then a proper succession of a large number of discrete impulses be given to these systems the seismograph will probably record an irregular train of waves quite similar to those obtained in our experiment and thence also similar to actual seismograms. Here seems to arise some questions of fundamental importance on the true nature of the seismic waves as well as on the reliable method of seismometry.

Though the present investigation has led to no positive conclusion regarding these problems, the above may be of some significance in pointing out one of the lines of inquiry to be taken up seriously for the future development of seismology.

The experiments were carried out in the Labaratory of the Institute of Physical and Chemical Research, Tokyo. Our best thanks are due to Prof. Okochi, the Director of the Institute, for allowing us the use of the laboratory room and its installations necessary for the present experiments.

Summary.

A physical pendulum is excited into an irregular oscillation by the impact of two streams of shots impinging upon it from the opposite sides. The motion recorded is studied with respect to its mean kinetic energy as a function of the velocity and the number of the colliding shots and also of the logarithmic decrement of the pendulum. The results of experiments are compared and

(1) See T. Terada, Proc. Tokyo Math. Phys. Soc., **8** (1916), 492.

found approximately agreeing with those expected from the theory, in the case when the number of collision per second is small. When the number is very large some discrepancies are observed which may be explained by the increase in the effective mass as well as the effective damping of the pendulum on account of the swarm of shots surrounding the vibrating mass.

It is pointed out that the general formal characters of the motion of the pendulum here studied are essentially similar to that of some or other types of motion of the earth as recorded by seismographs. An important bearing of this fact upon the fundamental problems of seismology is briefly suggested.

Fig. 3.

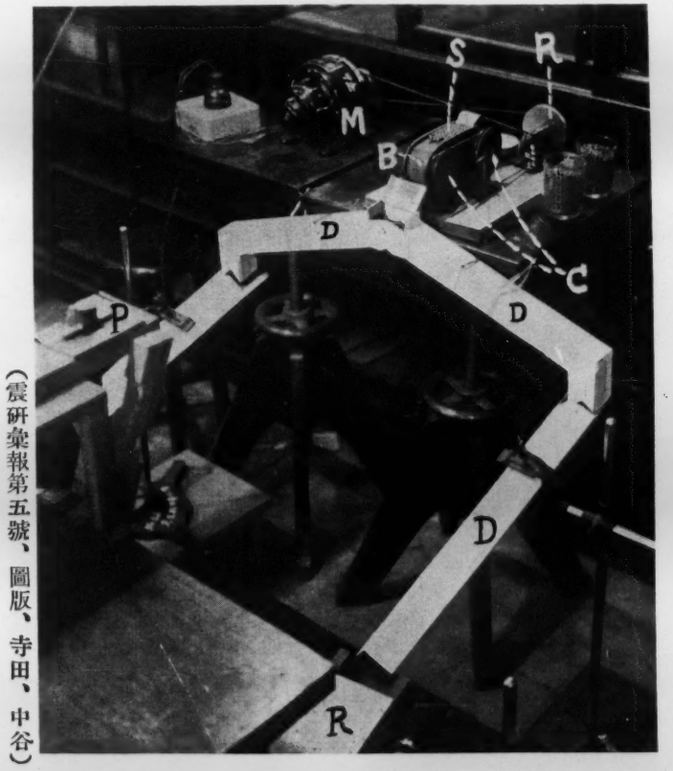

Fig. 4.

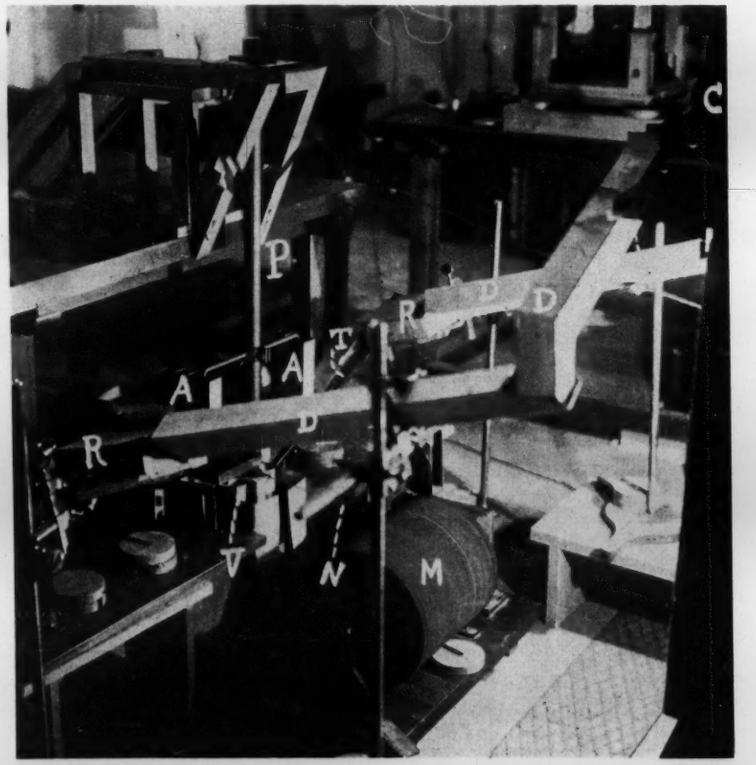

(震研彙報第五號、圖版、寺田、中谷)

Terada and Nakaya : Experiments on the Effect of Impulses etc.

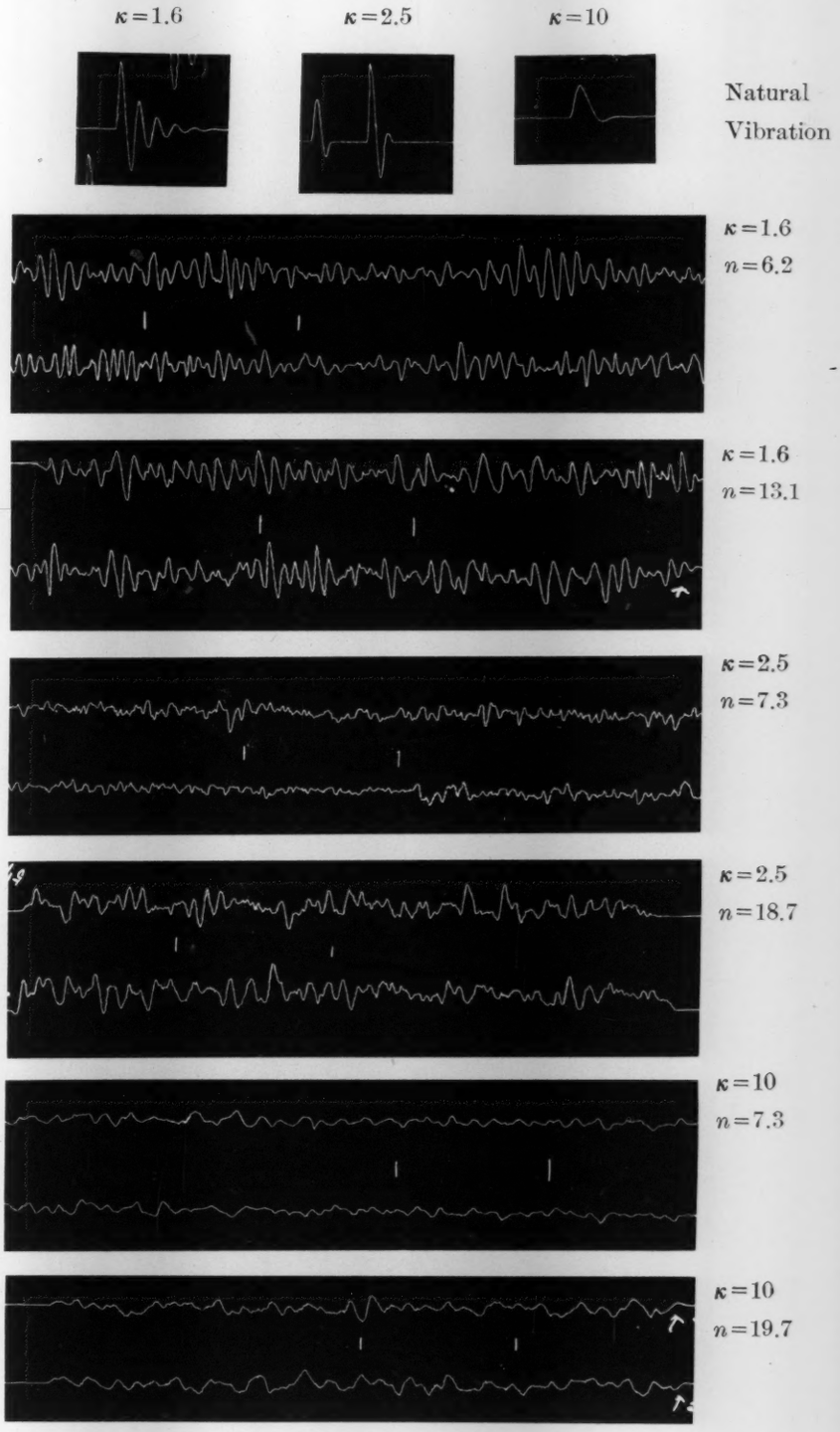

Fig. 11.

Terada and Nakaya : Experiments on the Effect of Impulses etc.

奥丹後半島の地形發達史

所員 多田文男

Physiographic History of the Oku-Tango Peninsula

By

Fumio TADA

Earthquake Research Institute

(Abstract)

The Oku-Tango Peninsula makes a two-cycled mountainland from the standpoint of its physiographic history. Low relief of its central plateau represents the cycle of erosion of the former age and maturely dissected hills along its margin show that of the present time.

The characteristic of the present cycle is the occurrence of blocking movements, by which the surface of the former cycle has been uplifted to the present altitude and has formed the major tectonic feature of the peninsula. There are two types of fault in this region: one running from northwest to southeast, the other from northeast to southwest.

Blocking movements in the present cycle have taken place neither continuously nor simultaneously, but have made a series of intermittent occurrences. Among them, latest three minor ones are distinctly observable in the topography of the peninsula. The first is a differential upheaval which is well explained by coastal terraces, the second, a slight submergence known from the shoreline of rias type, and the third, a tilting of land blocks represented by the recent Oku-Tango earthquake on March 7, 1927. In these minor episodes, we have found that the movements have been carried on always in the same sense, namely, blocks of land have been tilted up in their southeastern or northeastern side.

緒　　言

奥丹後半島の地體構造と奥丹後地震との關係に就いては既に山崎博士(1)、津屋學士(2)等によつて詳細な議論が發表せられて居るが、筆者も亦此地方の地形發達

(1) 山崎直方、多田文男: 昭和二年の奥丹後地震（地形學的考察）
地震研究所彙報 第四號 昭和三年 159–177 頁

(2) 津屋弘達: 奥丹後半島の地質構造に就いて（豫報）
同　　上　139–158 頁

史を調査して諸氏と略々同様な結論に達した。卽ち奥丹後地震は此半島を形造つた造山運動の一繼續事項であつて、古き斷層線なる郷村斷層と山田斷層とに沿ふて塊裂運動の行はれた爲起つたのであり、その塊裂運動の性質も地質時代の夫と同じ性質を有して居る事を知つたのであつた。よつて一地方が曾つて受けた地殻運動の歷史竝びにその性質を調査する事は地震研究上徒事でない事と考へる。本篇に於ては此半島の地形に現はれた地殻運動の歷史を古き時代より現今に至る迄順を追ふて述べる事とした。

第　一　輪　廻

奥丹後半島の中央部には廣い地域を占めて低起伏の山地が發達して居る。此山地の高さは 500 m 乃至 700 m であつて、その峯線は等高性を帶び、平坦な斷面を示して居る。特に此地方の北部にある太鼓山附近と、東南部にある世屋村附近

第一圖　奥丹後半島の斷面圖

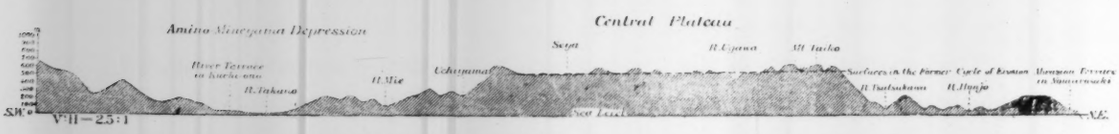

Fig. 1. Projected profile of the Oku-Tango Peninsula.

とでは地形が著しく平坦であつて、3 平方粁の地域に 120 m 以下の起伏を見るのみである。そして此低起伏の山地を流れて居る河流は 60/1000 と云ふが如き緩漫な縱斷面と平衡發達に近い橫斷面とを有し幅の廣い谷床を流れて居る。

かくの如き低起伏のある事は此地方が現今より 400 m 以上低かつた時代に地殻運動の平靜であつた期間があり、その間に久しく侵蝕作用が働いて、此地方一體の山地が晩壯年的地貌に化した事を示して居るのである。今半島中央部の低起伏山地を中央高臺と呼び、此地貌の造られた平靜時代を假に第一輪廻と稱することにする。

第一輪廻の侵蝕面の分布は第三圖に示した通りであつて、斑點をなして各所に散在して居る。その高さは一定でなく、太鼓山に於ては 600 m、世屋村地方に於ては 450–550 m であるが、碇峠と神主地方とに於ては 300–400 m となり、小原山の頂上にては 380 m となつて居る。此の如く低起伏の山地が異なつた高さに存する事は第一輪廻中に廣く發達した低起伏面が次の輪廻中の塊裂運動の際差別ある隆起を行つた爲である。

此低起伏の地貌は花崗岩、古期安山岩竝に下部新第三紀層より成る地方の山頂に認められる。從つてその形成せられた時期は津屋學士の5或は 6[1] の時代以後であらう。而して津屋學士の謂はれる F_1, F_2 なる斷層による斷層地形は此靜止時代に行はれた侵蝕によつて破壞せられて居て今日之を窺ふ術を得ない。

第 二 輪 廻

中央高臺の周圍には起伏の極めて大いな且、壯年的に開析せられた地帶があり、中央高臺の上の低起伏山地との間に著しい地形的不整合を示して居る。卽ち此周圍の山地を切刻んで居る河流は急な縱斷面と激しい上昇的發達をなした橫斷面とを有して居り、その上流部にある平衡に近い河流との間に地形的不連續點を有して居る。第二圖は中央高臺より發し、北流して直ちに日本海に注ぐ宇川と、東流して若狹灣に注ぐ世屋川との流路の傾斜を示した圖であるが、上流部の傾斜が中流部の夫より却つて緩漫な事を示して居る。

第二圖　宇川と世屋川との流路の傾斜（‰ を以て表はす）
I. 宇川　1. 成谷　2. 木子谷　3. 駒倉谷　II. 世屋川

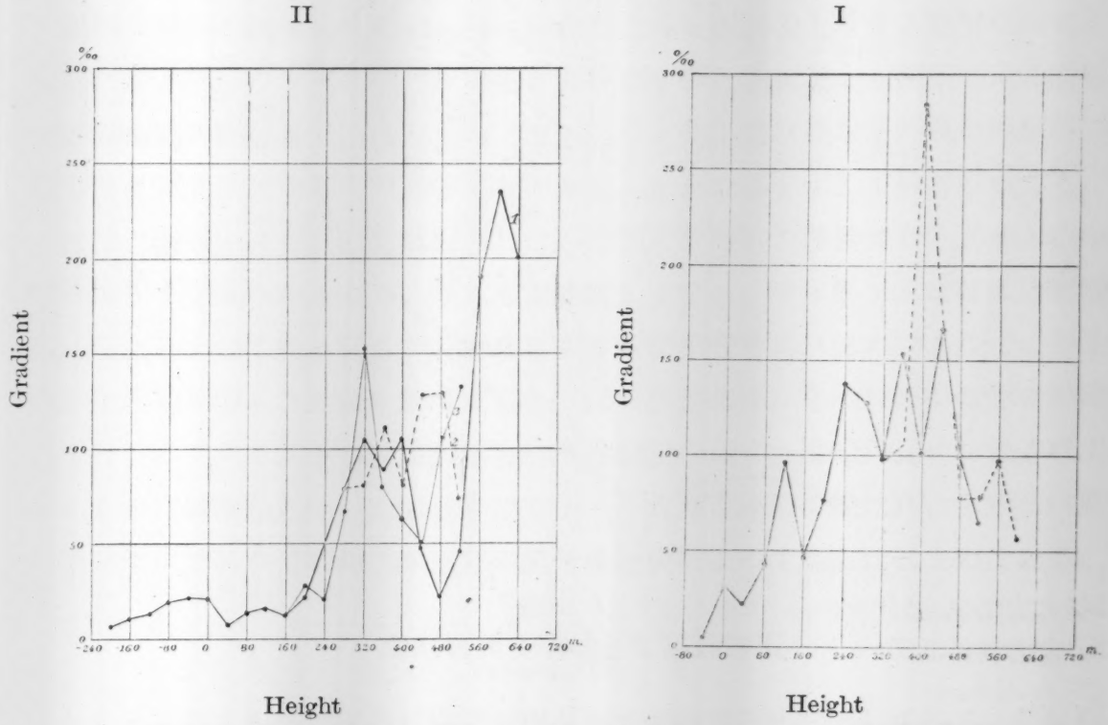

Fig. 2. Gradients of Longitudinal Profiles of R. Ugawa and R. Seya

(1) 前揭 144 頁

斯くの如く中央高臺の周圍に壯年的に開析せられた山地のある事は第一輪廻後地殻運動の激しい時代があつて侵蝕作用の回春が行はれた事を示すのである。假に此地殻運動の盛なりし時代を第二輪廻と呼ぶ事とする。

第二輪廻中に行はれた地殻運動は主として塊裂運動であつた。その斷層系統はその走向から見て二種類に分たれる。その一は西北より東南に走る斷層であつて山崎博士[1]が若狹灣に對して同心圓狀に走るものとされた斷層であり、その二は東北より西南に走るもの、則ち山崎博士が若狹灣に對して放射狀に走るものとされた斷層である。第三圖は此等の斷層中落差の大で、地形學的に明瞭なるものを記入した圖である。奥丹後半島は此等の斷層によつて、多くの地塊に分たれ、今日見るが如き主要な地形軀幹を形造るに至つたのである。

第三圖　奥丹後半島の地形的斷層構造

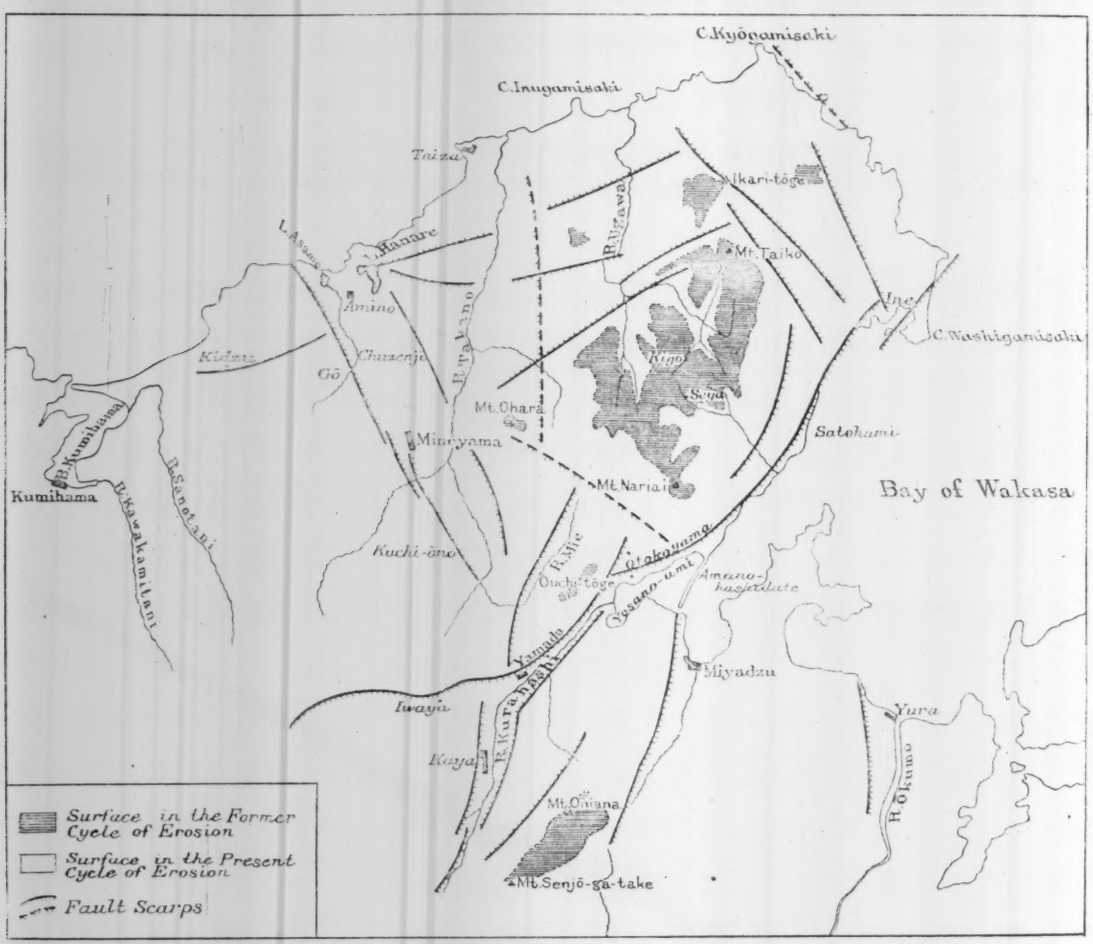

Fig. 3. Map showing the Distribution of Erosion Surfaces and of Major Geomorphologic Faults in the Oku-Tango Peninsula

此半島の地形學的斷層構造を更に詳しく述べて見ると、奥丹後半島はその西端を圓山川に沿ふた斷層によつて限られ、その東南端を若狹灣の西岸より倉梯川と岩屋川との流域を經て出石に達する地溝帶によつて限られた地塊である。而して此地塊は更に網野より峯山に通ずる地溝によつて磯砂山地塊と中央高臺との二つの地塊に分たれて居る。此二つの地塊は又更に西北より東南に走る斷層によつて小地塊に分たれて居るのであつて、磯砂山の地塊は久美濱陷落地帶によつて東西二部に分たれ、その東の地塊は又東北東より西南西に走る斷層、例へば網野驛より木津に至る斷層或は菱山峠を横ぎる斷層等によつて更に小地塊に分かたれて居るのである。一方中央高臺は其の周圍を總て斷層によつて圍まれた地壘であつてその隆起した頂上に低起伏の侵蝕面を戴き、その陷落せる部分に依遲ヶ尾山の如き火山を戴いて居るのである。

此等の地塊の區分は第四圖によつて略知る事が出來る。此圖は一般地形圖によつて此地方を4平方粁づつの正方形の區域に分ち、その各地域中の最高點一點づつを摘記し、その最高點を基として等高線を畫いたものであつて、一種の切峯面である。此圖示法によつて侵蝕作用による高さの變化をある程度迄除き得て塊裂運動による直接の高さの變化を容易に知る事が出來るのである。

此等二種類の斷層系統の中、特に明瞭で且高い斷層崖を有する斷層は西北より東南に走る斷層の中東北側に斷層崖を向けたものと、東北より西南に走る斷層の中、東南側に斷層崖を向けたものとであつて、此事實は此半島の各地塊が第二輪廻中常に西北或は西南に傾動する傾向を有して來た事を示して居るのである。

此第二輪廻中に行はれた塊裂運動は一時的に行はれた運動でなくて多くの小運動の集りより成つたもので、今日も尙連續して居る。津屋學士も此時代の斷層を F_3, F_4 に分かつて居られるが、此は更に多くに小分せられるのであつて、半島の主要な地貌が造られた後に於てすら、三回の傾動作用があつた事が地形に記錄されて居るのである。その一は隆起を伴つた傾動作用で、海岸段丘に記錄されて居り、その二は沈降を伴つた傾動作用でリヤス式海岸地形に現はれ、その三は最近の傾動作用であつて昭和二年三月の奥丹後地震によつてあらはれたのである。

海岸段丘に現はれた傾動作用

奥丹後半島の西北側海岸には之を緣どつて海岸段丘が發達して居る。第五圖は

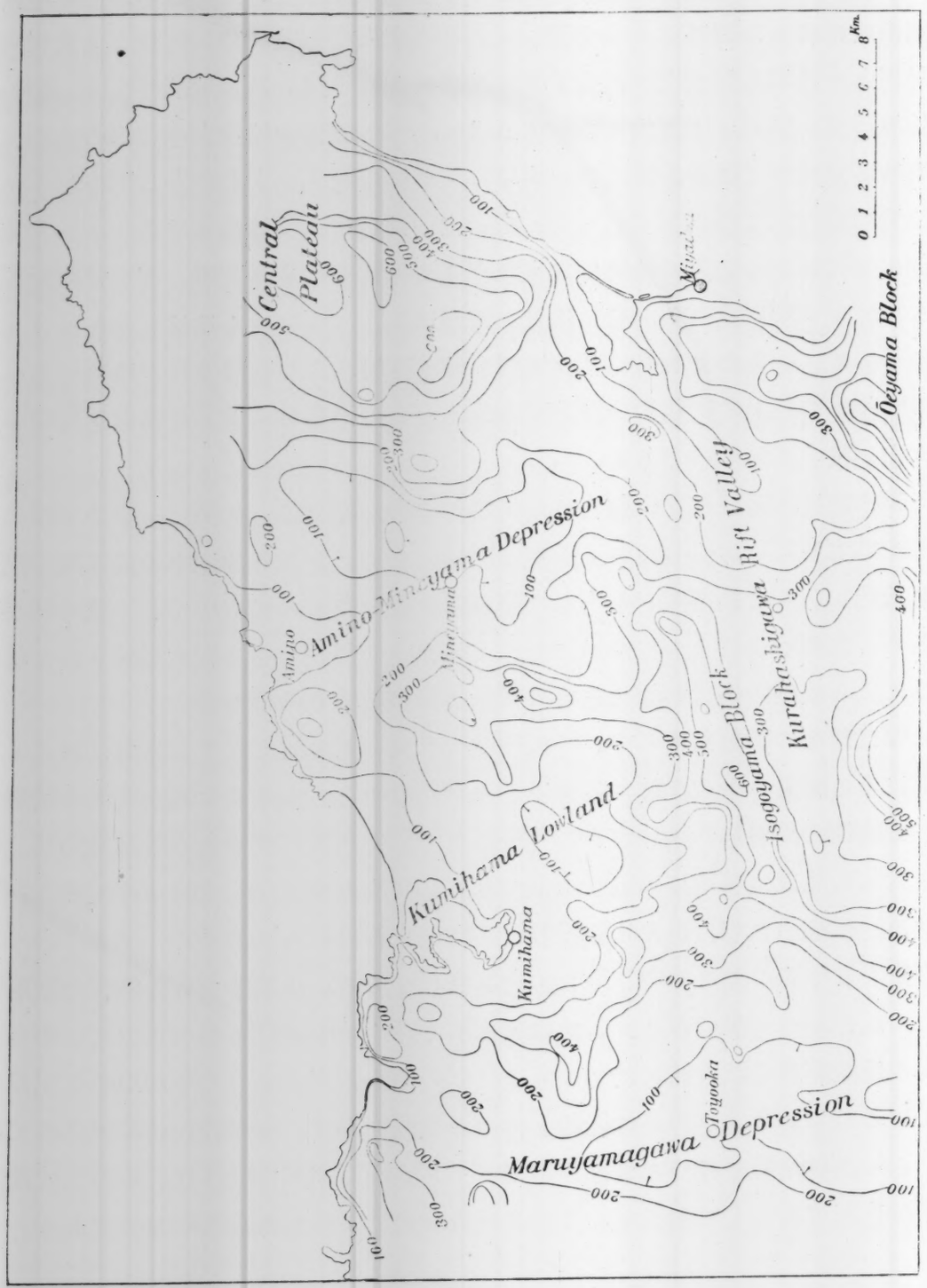

第四圖　奥丹後半島の切峯面

Fig. 4. Summit Level of the Oku-Tango Peninsula

此段丘の分布とその高さとを示した圖である。今之を西南より東北に向つて追跡して見る事としやう。

久美濱低地帶には久美濱灣を圍ぐつて 7–10 m の高さを有する隆起した海岸平野が存して居る。此海岸平野を造る砂層の中には有孔蟲の遺骸が含まれて居り、此が舊き時代の久美濱灣中の堆積物なりし事を明にして居る。

久美濱灣の西部には蒲井より大向に至る間に 8–10 m の高さにて 20–40 m の幅を有する海蝕段丘があり、又灣の東部なる箱石にも同高の海蝕臺地があるが、此は砂丘の砂によつて蔽はれて居て明瞭でない。

濱詰より淺茂川に至る海岸では丘陵が直ちに海に迫つて居て 50–60 m の懸崖をなし、その基部には洞窟或は離礁が造られて居る、此はレトログレッションの激しい事を示して居るのであるが、尙一部には 10 m の高さの海蝕段丘が斑點をなして發達して居る。磯はかゝる段丘の上に發達した部落である。

小濱より掛津を經て三津に至る海岸には砂丘が發達して居て邱陵地の斜面を厚く被ふて居るが海崖に於ける觀察によれば、狹く且低い乍らも海蝕段丘が存して居るやうである。三津より間人をに至る間には 20–30 m の高さの海蝕段丘が認められる。竹野川を越えて東北に行けば、段丘の巾は次第に廣くなり竹野筆石竝びに此代で 300 m, 中濱で 400 m となり、尾和では 500 m に達して居る。此より巾は次第に減じ袖志では400 m となり、經ケ岬に至つて全くなくなつて居る。段丘の高さも亦東北に行くに從つて高くなり、竹野及び此代で 40 m, 中濱で 50 m となり袖志では 60 m に達して居る。

此間、段丘の幅は犬ケ岬、文珠ケ鼻の如き突出部に於ては狹く入江の部に於ては廣い。此は入江の部に於ては後の山地より川によつて運ばれる扇狀地層が厚く堆積して居て海蝕作用を弱めて居る爲である。

經ケ岬を廻ぐつて東北側の海岸に出ると、此海岸の北西部は斷層海岸であつて 100 m を超えた斷崖が急に迫つて居てその下に段丘が發達して居ないが、本庄より南して、新井崎に至る間には狹い乍ら高さ 60–80 m の海蝕段丘が認められる。

更に鷲ケ岬を圍ぐつて東南側の海岸に出ると、此海岸も亦斷層海岸であつて、その斷層崖下には海蝕段丘がない。而して、此斷層海岸より東側には舞鶴に至る迄沈降性の海岸地形を見るのみである。

第五圖　奥丹後半島に於ける海岸段丘及河成段丘の分布圖

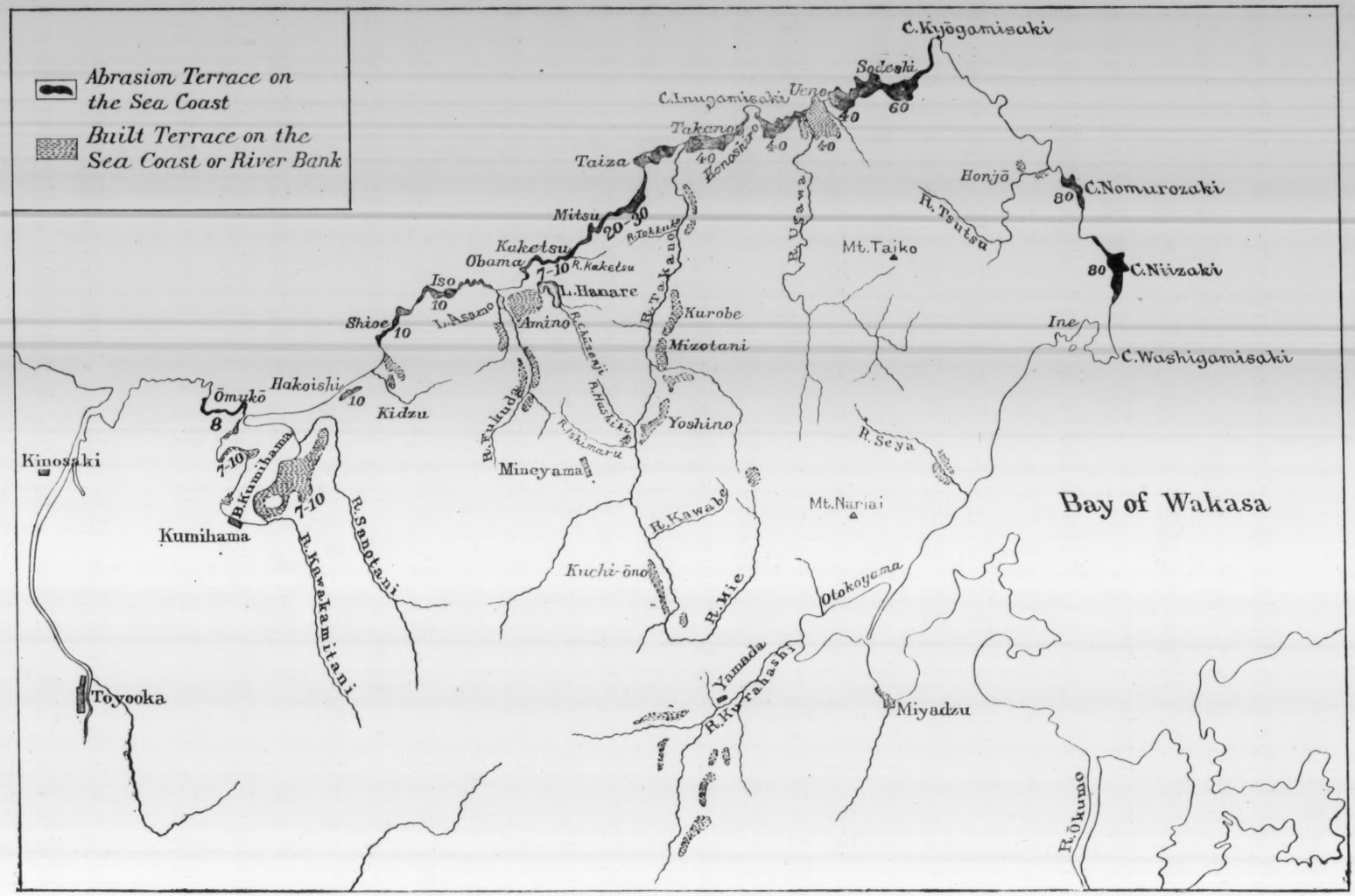

Fig. 5. Map showing the Distribution of Coastal and River Terraces.

(Heights of Terraces are shown in meter.)

之を要するに、半島の西北側海岸には一帶に海岸段丘が發達して居るが、その高さも幅も東北方で大きく、西南に向ふに從つて次第に減じて居る。東北側海岸には一部に海蝕段丘を認めるのみであり、東南側の海岸には全く之を認め得ないのである。

此等の海岸段丘は數回の隆起運動の量とその間に挾まれた沈降運動の量との總和の爲に現今見るが如き分布をなしたものであつて、從つて一部には數階の段丘の認められゝ所もある。而も此運動の結果として、半島の首部の地塊が東北側の斷層海岸を軸として西南に傾動し、東南側斷層海岸を軸として西北に傾動した事が推知されるのである。只現在の高さによつて隆起量を數量的に決定する事が出來ない。それは海蝕崖直下は一般に厚い扇狀地によつて蔽はれて居て、その下の海蝕段丘の眞の高さを知り難い爲である。

海岸地形に記錄された隆起運動は河流の沿岸にも記錄されて居る。第五圖に示すやうに、竹野川其他の河流の流域には河成段丘が認められる。此河成段丘の高さによつても隆起の性質が知られる筈であるが資料が不足であつて結論を得るに至らない。

此半島では西北に向て流れる川と東南に向て流れる川との縱斷面の間に著しい對照が見られる。卽ち前者例へば福田川、竹野川の如き河の縱斷面には不連續點の著しいものが見出されないが、後者例へば男山川或は世屋川の如き川の縱斷面には傾斜の不連續點が數個所に見出される。此事實も亦半島が東南側海岸の斷層を軸として西北に傾動した事を示して居るのである。

又東北より西南に流れる河流はその侵蝕力を强ふし、西南より東北に流れる河流はその侵蝕力を弱めて居る。第六圖は竹野川の支流の中、西南より東北に流れる川と福田川の支流中東北より西南に流れる川との縱斷面を比較した圖であるが

第六圖　竹野川と福田川との縱斷面

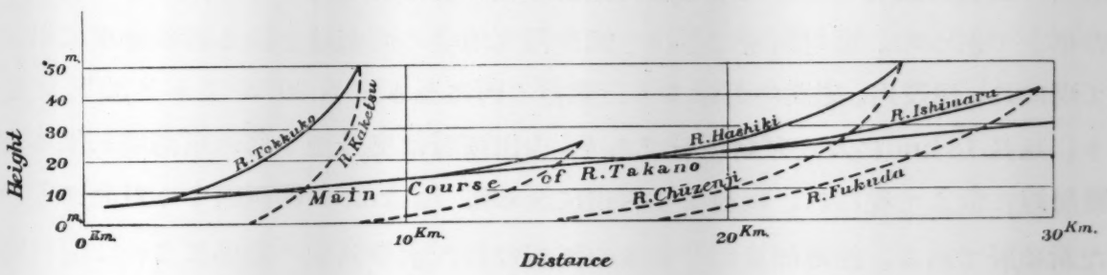

Flg. 6. Longitudinal Profiles of R. Takano and R. Fukuda

後者は前者に比して急な傾斜を有し、前者の頭部を奪取しつゝあるのである。此も半島が西南に傾動した爲、後者が侵蝕の回春を起せる爲である。

リヤス型海岸に現はれた沈降運動

海岸段丘を形造つた隆起のあつた後、奥丹後半島は更に小量の沈降運動を受けて居る。久美濱陷落地帶は此沈降の爲に溺谷となつた土地で久美濱灣はその溺谷の殘跡である。淺茂湖平野も離湖平野も又竹野川の最下流部も曾つて溺谷であつた。溺谷の奥行は沈降の量と沈降前の河の傾斜とによつて決定せられるが略同じい傾斜を有して居た此等の河川に於て、溺谷の奥行の深さは久美濱地方で最も深く東北に行くに從つて次第に淺かつたもののやうであり、沈降の量は數量的に此を言ふを得ないが西南で大であつた事が推知されるのである。

竹野川は緩漫な流路をもつて居り、その中流部にある峯山地方では下流部よりの沖積平野の巾が却つて廣く、且低濕であつてその沖積土中には濕地植物が埋沒されて居り、曾つて此中流地方が沼澤地であつた事を示して居る。此事實も亦下流より中流部に向つた、即ち、西南に向つた傾動があつた事を示して居るのである。第四圖の切峯面を見ると峯山地方に 100 m 以下の低地があるがその出口は現在の竹野川の下流にはない。此は隆起運動、沈降運動を通じて半島が西南に傾動した事を暗示して居るのである。此様な現象は若狹灣より鳥取地方に至る迄一般に見られる現象であつて、佐野谷川の上流にも圓山川の上流にも、又由良川の上流にも夫々その下流地方に比し切峯面の低い地帶が存して居る。此は海岸地方より川の上流地方に向つて傾動の行はれた事を指示して居るのである。

奥丹後地震に伴なつた地變

昭和二年三月七日の地震によつて現はれた地變の主なものは鄉村斷層と山田斷層との二條の斷層の生じた事と鄉村斷層以西の海岸が隆起して海蝕段丘が現はれた事とであつた。鄉村斷層は峯山—網野陷落地帶の西南端を限る舊斷層線に沿ふて現はれ、淺茂川、磯間の海岸より三重村の西に至る迄 N 30°W より S 30°E に走り、延長 18 km に及んだ新斷層であり、山田斷層は奥丹後半島の東南端を限る舊斷層線に沿ふて現はれ、幾地より男山に至る迄 7.5 km の間西南より東北に走つた新斷層である。陸地測量部[1]によつて行はれた水準側量の結果によれば鄉村斷

(1) 丹後震災地水準測量第一回報告　地區研究所彙報　第 3 號 167 頁

層の西南側の地塊即ち磯砂山地塊と、山田斷層の西北側の地塊即ち中央高台の地塊とが各々斷層を界として隆起をなして居るが、その隆起の量は斷層の近くで大きく之を遠ざかるに從つて漸次小となつて居る。

又西北側の海岸では、此地震の結果、鄉村斷層の西南側の地塊が隆起して曾つて水中にあつた岩礁が、水上に現はれて第二の海蝕段丘を形成した。此隆起の量も斷層に近い所で最も大きく 80 cm に達して居るが、西南に離るゝに從つて小となり、久美濱灣にては何等の變化も認められない。

此等の事實は今回の地震によつても半島の內磯砂山地塊が鄉村斷層を軸として西南に傾動し、中央高台の地塊が山田斷層を界として西北に傾動せる事を語つて居るのである。

結　　論

かくの如く奥丹後半島の地形發達史を研べて來て、筆者は第二輪廻中に行はれた塊裂運動が常に同一の性質を有して居る事を學び得た。卽ち東北或は東南に斷層崖を向けた斷層が最も多く且つ明瞭な事から見て西南或は西北に傾動した地塊の多い事を知り、海岸段丘の分布から見てこの段丘を造つた隆起運動が西南への傾動を伴つた事を知り、更にリヤス式の海岸地形から見て次で起つた沈降運動も同樣の傾動せるを知り、最後に今回の地震の結果起つた塊裂運動と同樣な傾動作用であつた事を知つたのである。故に一地方が受ける地殼運動にはその土地によつて一定の習性があるやうに考へられる。從つて、一地方の受けた地殼運動の性質とその土地に起る地震に伴ふ地變との間には密接な關係があるのであらう。

支壁式鐵筋混凝土堰堤の耐震法に就て

所員 物部長穂

New Method of Improving the Seismic Stability of Reinforced Concrete Dams

By

Nagaho MONONOBE

Earthquake Research Institute.

In this paper the author proposed a new method of improving the seismic stability of reinforced concrete dam with buttress walls. He uses a number of horizontal struts, each of which spans over the canyon, connecting the buttress walls. Both ends of each strut are to be rigidly anchored to the side slopes of the canyon, in most cases at footings of buttress walls. Horizontal component of seismic force acting on the dam is to be transmitted to the anchores by the struts, of which larger part is in compression and another in tension.

The author studied statical properties of this type of structure and made it clear that the horizontal deflection of buttress walls due to seismic force is remarkably decreased and the material provided against the danger is considerably saved.

(一) 在來の支壁式堰堤

支壁式堰堤は上流面に設けたる傾斜又は直立遮水壁（第一圖 a）と之れを支持する直立支壁（第一圖 b）とを以て其の主體となす。現今各國に廣く使用さる型式に於ては遮水壁は鐵筋混凝土造にして、徑間四米乃至十五米の單支版又は拱版の多數の徑間より成り、其の兩端は支壁上流面に支持せられ以て池水の壓力に耐へ、支壁は堤の方向に直角に配置され其の上流端は鉛直に對し三十五度乃至四十五度の傾斜を、下流端は二十度以下の傾斜をなせる三角形の大直立壁にして、壁厚は上部より下部に增大し、米國に於ては 0.3 米（頂部）乃至 1.6 米（底部）を用ひ、其の水壓に依る彎折を防止せんが爲め、所々に水平支材（第一圖 c）を配置し、各支材の端に當り支壁に少量の竪鐵筋を配置するを常とするも、歐洲特に伊國に於ては其の厚さ一般に大にして、

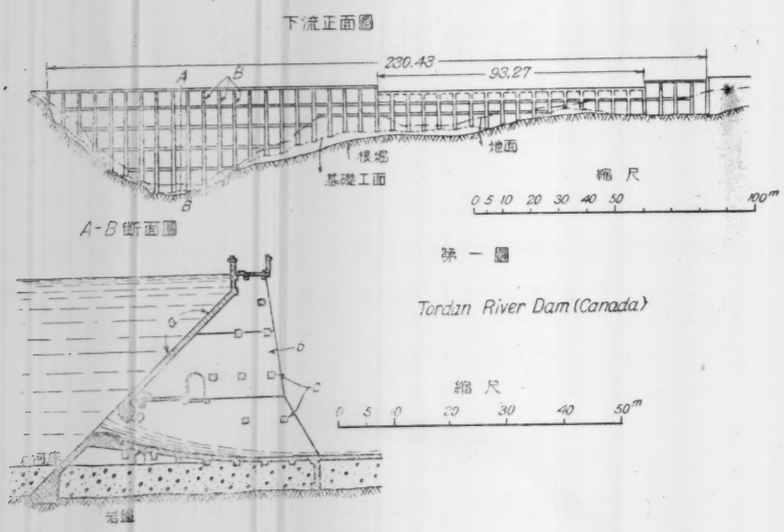

テイルチオ堰堤に於ては、底部に於て 7.7 米の厚さに達し、全く鐵筋を使用せざるものとす。而して使用混凝土は 1:2:4 乃至 1:3:6 の配合にして、稍〻厚き支壁は 1:3:6 の配合を用ふるを常とす。

此種堰堤に於ては、遮水壁上の池水の重量を利用して、堤全體の安定を保持するものなるを以て、自體の重量に依て安定を保つべき重力式堰堤に比し、堤體に使用する材料極めて少量にして、通常の場合に於ては、僅かに後者の $\frac{1}{3}$ 乃至 $\frac{1}{2}$ に過ぎず、從て其の工費も著しく廉にして、重力式の 70％ 乃至 80％ を超えず、從て今日迄歐米各國に於て築造せられたるもの極めて多數に上り、其の高さも 60 米（二百尺）に達せり。

今其の著名なるもの〻寸法及材料等を列擧すれば第一表及第二表の如し。

第一表　世界著名鐵筋混凝土堰堤

場所名	國洲名	築造年月	最大高 (m)	全長 (m)	徑間 (m) (支壁心々)	遮水版型式	徑間數
La Prele	Wyoming	1909	45.6	110.0	5.5	單支版	20
Guayabal	Porto Rico	1911	36.6	602.5	5.5	同	72
Tordan	Canada	1913	38.4	230.6	5.49	同	42
Combamala	Italy	1916	38.0	99.0	5.5	同	17
Cisco	Texas	1923	30.0	330.0	5.4	同	61
Tordan	Canada	1927	38.5	211.0			
Gem Lake	California	1916	34.13	213.4	12.2	拱	17
Tirso	Sardinia	1922	69.5	283.0	15.0	同	18
San Dieguite	California	1918	41.5	228.6	7.25	同	23

Vöhrenbach	Baden	1925	82.59	145.0	10.8	同	13
Little Rock	California	1924	52.0	220.0	7.3	同	28
Venina	Italy	工事中	53.0	—	—	同	—
Mignano	,,	,,	51.6	—	—	同	—
Camplioccili	,,	,,	65.0	—	—	同	—
Suviana	,,	,,	87.0	180.0	—	同	—
Aaensire	Norway	,,	55.0	123.0	—	同	—

第二表　使用材料表

貯水池	La Prele.	Tordan	Combamals	Cisco	Gem Lake	Vöhrenbach	Little Rock Creek	Tordas
Volume of Concrete (m^3)	17100	16000	12000	43000	6522	11000	20000	20000
Steel (ton)	400	380	170	1000	74	150	526	380
Concrete の配合 遮水壁	1:2:4	1:2:4	—	1:2:4	1:2:4	1:2.4:3.6	—	—
Concrete の配合 支壁	1:3:6	1:3:6	—	1:2:4	1:2.5:5	1:3.3:6	—	—
Reinforce. kg/m^3 of Concrete	23.5	23.8	14.0	23.2	11.4	13.6	26.3	19.0
% of Reiforcement	0.3	0.3	0.18	0.3	0.15	0.17	0.33	0.24

上述の如く支壁式鐵筋混凝土は堰堤は重力式に比し著しく經濟的にして、特に使用材料少量なるを以て、材料の運搬に不便なる遠隔高地に有利なるのみならず、工事期間を著しく短縮し得るを以て工事を急施する場合に適し、從て其の力學的計算の煩雜なるにも拘らず近年其の築造益々多きを加へ特に伊國に最も多く、目下築造中のスビヤナ堤の如きは高さ 87 米（二百八十七尺）に達せり。

而して使用材料の少量なるに依り重力式に比し構造著しく纖細複雜に而も高度の應力を用ふるに拘はらず、設計法の合理的なるに依り築造後不幸倒壞の災を惹起したるもの極めて少なく、何れも地盤及基礎の不適當に依るものにして、堤それ自身の構造上の缺點に基因せるものを見ず。

即ち此種堰堤は其の高さ、應力に順應する優良なる材料と施工とを用ふるに於ては、重力式と同樣の安全にして確實なる貯水池壁たるや明かにして、本邦に於ても大震以前に築造されたるものに、函館市水道貯水池、信越電力中津川調整池等あるも今日何等の不安あるを聞かず。

（二）支壁式堰堤の耐震性

然るに在來の鐵筋混凝土堰堤は、大地震の災厄を經驗せざる歐米諸國に於て發

達せるものにして、其の設計法を視るも何等耐震上の考慮を爲さず。而して堤長に直角なる方向に於ては、元來强大なる水壓を支持し、尙多大の餘裕を有するを以て、此方向に襲來する地震力に對しては、多少の强度增進に依りて、容易に對抗し得る事明かなるも、堤長に平行なる方向に於ては、常時何等の外力を受けざるを以て、細長にして殆んど鐵筋を有せざる高壁を建て列ね、僅かに水平細支材を配置して水壓による支壁の彎折に備ふるに過ぎず。斯の如き構造に於ては一朝堤長に平行又は斜の方向に襲來する大地震に際會しなば、併立せる支壁の倒壞を惹起するの虞れ大にして、我國の如き地震國に於ては、耐震上特別の改良を施さざるに於ては其の築造は極めて危險なりと云はざるべからず。而て地震の作用に依る堤長に平行なる水平分力に對し支壁の安定を增大せんには、次の二原理に依る事を得べし。卽ち、

(1) 建築構造の如く構造物の各部分に作用する水平力を構造主體の內力として直下の地盤に傳達すること。

(2) 支壁を連續して特別の水平支材を設け構造主體に作用する水平力を水平に兩岸の岩盤に傳達すること、

而して今日我國に於ける此種構造物に對して監督官廳は堅硬なる岩盤上に築造さるゝ場合に於ても、凡ての方向に對し重力の $\frac{1}{8}$ の水平力に對し安全に耐抗し得る事を要求せるを以て、若し (1) の原理に依れば、堤體の質量過大ならざる場合にありては多數の支壁に直交する鐵筋混凝土造竪壁及水平壁（建築物の各階床）を用ひ、所謂壁式建築物と同樣の工法を用ひ而も堤高の變ずる點毎に耐水的伸縮裝置を施し、構造物の高さの差に因る水平撓度の不同に備へざるべからず。

然るに堰堤に於ては其の使用目的上必要なる壁體は單に直立支壁と上流面に於ける傾斜遮水壁とに過ぎず、而も後者は溫度の昇降に因る內力及龜裂の發生を輕減せんが爲め單支版を用ひ、其の支端には伸縮目地を置くを常とせるを以て、上記の如く竪壁及水平壁を使用するは單に耐震のみの目的を以て其の工費を、現時歐米に用ひらるものゝ約二倍に增嵩せしむると事なり、其の經濟上の特徵を全く滅却するは到るものとす。

次に矢張り (1) の原理に依り、支壁と之に直交する多數の堅剛なる水平支材とに依り、架構（架構建築の柱と桁）を組立て、各部材の彎曲と直應力（主として彎曲應力）に依りて、水平地震力に耐抗せしめんとすれば、使用材料並に工事費

に於ては前者に比し稍〻有利なりと雖も、重力の$\frac{1}{8}$程度の水平力に耐抗せんには尙殆んど支壁容積に匹敵する材料を之に使用せざるべからざる事となり、其の工事費も現在歐米の實例に比し 60％位の增加を來し、而も其の構造上次の如き看過し得ざる重大缺點を有する事となる。

(a) 谷の兩側斜面に於て架構の高さ急變するを以て均一水平力に對し、同一水平線上の各點撓みは、谷中央の架構に於て著しく大にして、谷岸に於ては零なるを以て、堰堤全體として考ふる時は水平力は兩岸の支壁に集中作用し、其の根部の破壞を免れ能はざる事。

(b) 支壁特に其の上部の水平撓み過大にして單支遮水版に於ては兩端の伸縮目地に依て漏水又は破壞を防止し得ず、拱版に於ては其の起拱點の强制變位過大なる爲め破壞又は龜裂を免れざる事。

(三) 架構式鐵筋混凝土堰堤に於て均一水平加速度の作用に因て生ずる水平撓度

前節 (a) に擧げたる缺點は矩形谷か又は兩端鉛直壁體に終る池壁にして、全長を通じ壁高同一なる場合支材を其の終端に於て滑動せしむる構造に依りて之れを防止する事を得べしと雖も、壁高稍〻大なる場合にありては支材に多大の材料を使用するも尙遮水版兩端の目地幅に對して過大の水平撓みを起すべく今日の實例にては兩端の目地幅は最大 10 mm にして之れにアスファルト、タール、ペーパー等を塡充するを以て、漏水する事なくして移動し得る水平撓みは、兩端を合して即ち版一徑間に對して、10 mm を以て限度と看做さゞるべからず。依て架構式原理に依る支壁堰堤（又は池壁）に於て、堰堤の高さ、支壁及水平支材の間隔、支壁と水平支材の材料容積比等の種々の値に對する、堤頂に於ける水平變位卽ち支壁の最大撓度を略算せんとす。

第 二 圖

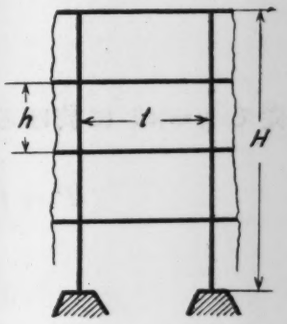

以下の計算に於て、（第二圖參照）

l ..... 支壁の間隔

h ..... 水平支材の間隔

$H=mh$ ..... 支壁の總高

b ..... 支壁の幅

t ……支壁の厚さ

t_1 ……水平支材の厚さ及幅

今支壁の側面形狀は三角形をなし其の頂點 (Virtual crown) は堤頂上$\frac{h}{2}$ の所に位するものと假定すれば、堤頂上の混凝土容積は、大體に於て堤頂橋梁のそれと同一程度のものとなる。依て Virtual crown を座標の原點にとり、y 軸を鉛直下向にとれば、y なる位置に於ける支壁の幅 (b) は略 y に等しく、其の壁厚 (t) も y の簡單なる函數を以て表す事を得るを以て、歐米の實例に徴し、支壁の寸法を次式の如く定め、充分なる鐵筋を以て之を補强するものとす。卽ち、

$$b=y \qquad t=0.35\,(1+0.1\,y)\cdots\cdots\text{in metre}$$

今支壁材料の重量を 2.5 tons/m^3 とすれば、y なる位置に於て高さ 1 m の部分の重量 (w) は次式を以て表はさる。

$$w=2.5\times0.35\,(1+0.1\,y)\,y=0.875\,(1+0.1y)\,y\cdots\cdots\text{in tons.}$$

今地震に依り堤體の各部に其の重量の k 倍の水平力が作用するものとすれば、上記の部分に作用する水平力 (p) は kw にして、遮水壁と支壁との重量比は、普通單支版に於て 0.4～0.5 拱に於て $\frac{1}{3}$ なるを以て、總高 29 m に迄對し 0.4, 30 m 以上に對し 0.3 とし、尙耐震上の必要より多數の水平支材を用ふるものとすれば、$h=l$ により、h の間隔に一群の水平支材を配置するを便とするを以て、

$y=nh$ (n は任意の整數) に於て、支壁の水平斷面積を A_w, 此の位置に交はる水平支材群の總鉛直斷面積を A_b, とすれば、兩者の重量比は大體、A_b/A_w を以て表はさる。從て

$y=nh$ なる位置に於て、高さ 1 m に作用する水平力 (p) は、次式を以て表はす事を得。

$$p=0.875\left(1+0.4\frac{A_b}{A_w}\right)ky\left(1+\frac{1}{10}y\right)$$

從て $y=nh$ に於ける支材群に作用する總水平地震力 (P_n) は

$$P_n=\int_0^{nh}p\,dy=0.875\left(1.4+\frac{A_b}{A_w}\right)k\int_0^{nh}y\left(1+\frac{1}{10}y\right)dy$$

$$=0.875\left(1.4+\frac{A_b}{A_w}\right)k\,\frac{n^2h^2}{2}\left(1+\frac{nh}{15}\right)$$

次に　I_w ....支壁斷面の慣性能率（但し重量及水壓に依る壓力大なるを以て全斷面を有效と看做す）

I_b ....水平面上の全支材の斷面積（A_b）の慣性能率、但し著しき應張力の發生あるを以て、混凝土厚さの $\frac{2}{3}$ を有效とし、其の總幅を b_1 とし且つ剛性を大ならしむる爲め、$t_1=1.5\,t$ とす。

然る時は

$$I_w=\frac{bt^3}{12}=3.57\times10^{-3}nh\left(1+\frac{nh}{10}\right)^3\cdots\cdots\cdots\text{in } m^4$$

$$I_b=b_1\frac{t^3}{12}=\frac{1}{12}b_1t^3\cdots\cdots\cdots\cdots\cdots\cdots\text{in } m^4$$

今 β を以て支材と支壁との剛度比を表はせば

$$\beta=\frac{I_b}{l}\ \frac{I_w}{h}=\frac{I_b}{I_w}=\frac{b_1}{b}$$

$$\frac{A_b}{A_w}=\frac{1.5\,b_1t}{bt}=\frac{1.5\,b_1}{b}=1.5\,\beta$$

次に γ を以て支壁斷面の環動半徑 $\sqrt{I_w/A_w}$ を表はし、$S=\left(\frac{\gamma}{h}\right)^2$ と置けば $H=mh$ なる高さを有する堰堤の堤頂水平變位 δ は大略次式に依りて算出するを得。

$$\delta=\sum_{n=1}^{m}\frac{P_n\,h^3}{12\,E\,I_{wn}}\cdot\frac{1+\beta_n}{\beta_n}(1+36\,S_n)$$

茲に E は混凝土の彈性係數にして、1.4×10^6 tons/m^2.

I_{wn}, β_n 及 S_n はそれぞれ $y=nh$ に於ける I_w, β 及 S の値を表はす。

上記の撓度計算式は（內藤多仲氏耐震構造論 P. 63）此種構造物に對しては、一の略近似式に過ぎざるも、本節の如く單に支壁上部の水平撓みが、遮水版兩端の調節し得る程度なるや否やを窺知せんが爲めには充分なるものと認む。尙 β と A_b/A_w 卽ち水平支材と支壁との材料比との關係は第三表に示すが如し。

第三表　β, $\frac{1+\beta}{\beta}$ 及 $\frac{A_b}{A_w}$ の關係

$\beta=$	1	$\frac{1}{2}$	$\frac{1}{3}$	$\frac{1}{4}$
$\frac{1+\beta}{\beta}=$	2	3	4	5
$\frac{A_b}{A_w}=$	1.5	0.75	0.5	0.375

上記の方法に依りて算出せる δ の値は第四表に示すが如し。

第四表　　堰堤撓み (δ) ($m.m$) の表

$k=0.2$　　H＝堰堤の高さ (m)

β＝水平支材の剛度/支壁の剛度

(1)　$h=l=5\,m$

H in m	5	10	15	20	25	30	35	40	45	50	55	A_b/A_w
$\beta=1$	2.8	5.4	8.1	10.2	12.4	14.5	16.4	18.3	19.7	21.9	23.5	1.5 (實施不可能)
$\beta=\frac{1}{2}$	3.2	6.2	9.2	11.6	14.2	15.6	18.7	20.8	22.5	24.8	26.7	0.75 (實施困難)
$\beta=\frac{1}{3}$	3.6	7.1	10.3	13.1	15.9	18.6	21.0	23.5	25.2	28.0	31.0	0.50 (同　上)
$\beta=\frac{1}{4}$	4.2	8.4	12.1	15.4	18.7	21.9	24.6	27.5	29.7	33.0	35.4	0.375

(2)　$h=l=6\,m$

H in m	6	12	18	24	30	36	42	48	54	60	A_b/A_w
$\beta=1$	4.3	8.7	12.9	16.8	20.2	23.4	26.3	29.4	32.2	34.5	1.5
$\beta=\frac{1}{2}$	5.0	10.0	14.6	19.0	23.0	26.7	30.0	33.3	36.4	39.3	0.75
$\beta=\frac{1}{3}$	5.6	11.3	16.6	21.5	26.0	30.1	33.8	36.3	41.1	44.4	0.50
$\beta=\frac{1}{4}$	6.5	13.2	19.7	24.9	30.0	34 8	39.4	43.7	47.6	51.6	0.375

(3)　$h=l=8\,m$

H in m	8	16	24	32	40	48	56	64	A_b/A_w
$\beta=1$	7.9	15.2	21.6	27.3	32.6	37.3	41.6	45.8	1.5
$\beta=\frac{1}{2}$	11.7	22.6	32.1	40.7	48.4	55.3	61.5	68.0	0.75
$\beta=\frac{1}{3}$	13.2	25.5	36.3	46.0	54.3	62.4	70.0	76.7	0.50
$\beta=\frac{1}{4}$	14.1	27.2	39.5	49.1	58.2	66.4	74.0	81.4	0.375

(4)　$h=l=10\ m$

H in m	10	20	30	40	50	60	70	A_b/A_w
$\beta=\left\{\begin{matrix}1\\ \frac{1}{2}\\ \frac{1}{3}\\ \frac{1}{4}\end{matrix}\right\}\delta\ m.m.$	18.8	26.7	48.4	60.0	70.6	80.0	88.7	1.5
	22.7	42.0	58.3	72.6	85.0	96.0	107.0	0.75
	25.5	47.5	66.0	82.0	96.0	109.0	121.0	0.50
	30.0	55.3	77.0	95.7	112.2	128.0	142.0	0.375

第四表に示せる計算は、堰堤の撓みを出來得るだけ小ならしめんが爲め、現在工法の十數倍乃至數十倍の水平支材を使用せる場合を掲げたるものにして、事實支壁の 30 % 以上の斷面の支材を使用することは經濟上は勿論、施工上も極めて不利なるものとす。今假りに遮水壁の頂部に於て最大 10 mm の水平撓みを許すものとするも、$h=l=5\ m.$　$A_b/A_w=\frac{1}{2}$

として辛じて 16 m 高さに及ぶことを得べし。卽ち在來の原理に依る支壁式堰堤は、其の撓度の過大なる點のみに於ても、耐震上極めて不適當なるものと云はざるべからず。若し支壁の厚さを增大し、之れに比例して支材斷面を增せば、若干撓みを低減するを得と雖も、之れを半減するためには、約 1.5 倍の材料を使用せざるべからず。

（四）　堤長に平行なる水平分力を水平支材に依りて兩岸に傳達する方法

此方法に依れば種々新なる構造原理を用ふる事となり、其の概要を述ぶれば次の如し。（第三圖參照）。

（1）　堰堤の方向に平行なる地震力は、支壁を連結して一直線上に岸より岸に達する多數の水平支材列の直應力に依て兩岸に傳達す。

（2）　支材列の兩端は重量に依る摩擦

第三圖

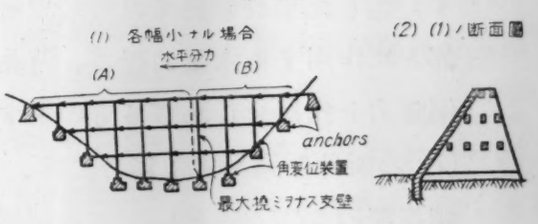

力又は特殊の裝置に依り確實に鎭定するを要す。此種堰堤は谷の岩盤特に堅硬なる場合に築造するを常とするを以て、鎭定方法はさしたる困難を生ぜず、且直上支壁の重量を利用するものとす。

（3） 支材列の兩端を確實に固定する時は、其の一側（A）に直壓力、他側（B）に應張力作用するを以て此等に依る A 部の彈性短縮と、B 部の彈性伸長との同一なる如き位置に於ける支壁に最大撓みを生じ、これより兩岸に近づくに從て、支壁の撓みは漸次減少し、鎭定部に於て零となる。

（4） 支材はこれに作用する應壓力及應張力の何れにも對抗し得る强さを有するものとし、且つ架構式と全然反對に剛度の過大ならざるを可とす。應力は端に最大にして中央に至るに從て漸減するも、施工の便宜と、支壁の最大撓みを低減するとの爲め、全長に亘りて最大應力に對抗し得る如き斷面を用ふるを可とす。

（5） 上記の原理に據る耐震支材に於ては、其の斷面の大さ及鐵筋量を適當に決定する事に依りて、支壁の大部分をして殆ど彎曲作用を受けしめざる事を得るも、其の下端は基礎に固定され其の水平變位を制止さるゝを以て、最下の水平材の下部の支壁は、角變位を强制せらる。從て壁底に於て微少の角變位を爲し得る裝置を設けざる可らず。

（6） 谷幅著しく廣き場合は、支材の斷面を著しく大ならしめざる限り、中央部に於て支材の伸縮過大となり從て支壁の水平變位も過大となるを以て、數徑間の間、支壁間を堤に平行なる壁（又は構）に依て剛に連結し、剛性極めて大にして、兩側の支材に依りて傳達さるゝ水平力に對し、殆んど撓みを生ぜざる如き直立堤體を形成せしめ、其の兩側に於て支材端を固定す。而して剛性部の長さ即ち壁又は構を以て連結すべき支壁の數は高さ、二剛性部の支材列の長さ等に依て理論的に定むるものとす。

（7） (6) の場合遮水壁を固定版となし、連結壁の一に利用する事を得るものとす。但し此場合に於ては外端支壁の兩側に於て、剛性部と、普通の柔性壁部とに作用する水壓に因る、彎曲力率及剪力を正しく平衡せしめ、支壁に偏壓力を作用せしめざるものとす。

（8） (7) の要件を滿足する爲めには、柔性部の單支版の有效徑間を、剛性部の純徑間の 57.7 % とし、其の兩端は支壁より突出せる肱木版に依りて單支

せしむ。卽ち此突出長は上記純徑間の 30～35％ となる。水壓は同水深に於ては常に同一なる特性を有するを以て、斯く支壁突出部に依りて支承するも、兩側不平衡の危險なく、而も單支版の厚さを過大ならしむる事なくして支壁の間隔を大ならしめ、從て其數を著しく減じ多大の材料節約を爲し得るものとす。

(9) 本堰堤に用ふる水平支材は在來式の如く大なる剛度を要せざるを以て、應張力の爲めの鋼材は少數の稍大なる斷面の釘又は鐵骨を使用し得、且つ支壁接合部の剛性を要求ぜざるを以て、支壁築造後鋼材を足場として、支材の混凝土工を行ふ事を得。

(10) 斜方向の地震力により支壁の歪む事を防止し、地震力を堤に直角及平行なる二分力に分立して作用せしむる爲めには、支材を適當なる間隔の水平面內に配置し、一水平面內に存する支材は、之れを水平綾構又は剛なる方形枠を以て連結す。但し方形枠を形成せしむる場合は、水平支材は水平面に於て大なる剛性を有せしむるものとす。

上記の如く種々新なる工法を用ふるに於ては、支壁式堰堤の經濟上の特徵を減却する事なくして、堤長に平行なる水平分力に對し確實に耐抗し得べく、以下順を追ふて靜力學上より之を說明せんとす。(8) 及 (9) の原理に依り、支壁の間隔を大にし、其の數を減じ得るを以て、以下の計算例に於ては其の間隔を 10 m と定めたり。單位は m 及 metric ton を用ふるも鋼材斷面積は cm^2, 變位は $m.m.$ を用ふ。

(五) 剛性部と柔性部との割合

今 N 徑間に對して m 徑間を剛構造とし、n 徑間を柔構造とし、N 徑間全體に作用する水平力を凡て剛構造部に負擔せしむる時、堤の高さと、其の頂の撓みとの關係を算出せんとす。

第　四　圖

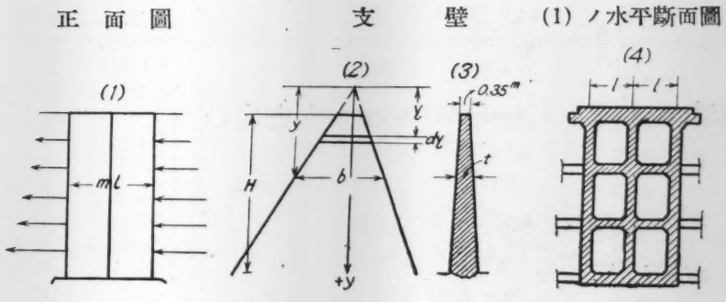

(三) の計算と同樣支壁の厚さを次の如く定む

$$t=0.35\left(1+\frac{y}{10}\right)\qquad b=y$$

$$A\text{（斷面積）}=tb=0.35\,y\left(1+\frac{y}{10}\right)$$

$$I=2\,tb\left(\frac{ml}{2}\right)^2=\frac{0.7}{2}\,m^2l^2\left(y+\frac{y^2}{10}\right)$$

茲に支壁は水壓に依り强大なる壓力を受くるを以て、地震力に依り彎曲力率を受くるも、應張力を發生せざるを以て、全斷面を有效と看做して I を算定す。((三) の撓度計算參照)

$+y$ に於て高さ 1 m 當りの一徑間分の堤の重量は

$$2\times0.35\,wy\left(1+\frac{y}{10}\right)=0.7\,wy\left(1+\frac{y}{10}\right)$$

但し新型式の堤に於ては柔性部の支材は小斷面積にて足るも、剛性部の連結壁の重量は著しく大なるを以て、總重量を支壁の二倍と假定す。

次に水平分力を各部重量の k 倍とすれば、

$F=+y$ に於て N 徑間に依る高さ 1 m 當りの水平地震力

$$=kN\times0.7\,wy\left(1+\frac{y}{10}\right)$$

M_y=水平地震力に依る y 斷面の彎曲力率

$$=\int_0^y(y-\eta)\,Fd\eta$$

$$=0.7\,kNw\int_0^y(y-\eta)\,\eta\left(1+\frac{\eta}{10}\right)d\eta=\frac{0.7\,kwN}{120}(20\,y^3+y^4)$$

然るに y に於ける撓み (δy) と My と Iy の關係は、次の微分方程式に依て表はさる。

$$\frac{d^2\delta y}{dy^2}=\frac{M_y}{EI_y}$$

茲に E は混凝土の彈性係數にして、1,400,000 tons/m^2 と定む。

依て

$$\frac{d^2\delta y}{dy^2}=\frac{kwN(20\,y^3+y^4)}{30\,Em^2l^2\left(y+\frac{y^2}{10}\right)}$$

$$=\frac{kwN}{3\,E\,m^2l^2}\left\{y^2+10\,y-100\,\frac{1000}{y+10}\right\}$$

上記の微分方程式を解き堰堤の高さを H として、

$$y=H+5 \text{ に於て } \left[\frac{d\,\delta y}{dy}\right]_{H+5}=0 \text{ 及 } [\delta y]_{H+5}=0$$

なる二條件に依りて積分常數を定むれば

$$[\delta y]_{y=5}-[\delta y]_{y=H+5}$$

は所要の堤頂に於ける水平撓み (δ) なり。卽ち

$$\delta=\frac{10^4\,kwN}{36E\,m^2l^2}\times\left\{\begin{array}{l}3\left(\frac{H+5}{10}\right)^4+2\left(\frac{H+5}{10}\right)^3-9\left(\frac{H+5}{10}\right)^2\\-18\left[\log_e\,(H+15)-\left(\frac{H+5}{10}\right)-\frac{12}{18}\right]\\+\left(\frac{5}{10}\right)^4+2\left(\frac{5}{10}\right)^3-6\left(\frac{5}{10}\right)^2\\+18\,[\log_e\,15-1]\end{array}\right\}$$

依て

$k=0.2$　　$w=2.5\ \text{tons}/m^3$

$N=10$　　$l=10\ m$

$E=1.4\times10^6\ \text{tons}/m^2$

とし、δ を $m.m.$ にて表せば

$$\delta=\frac{1}{100.8\,m^2}\left\{\begin{array}{l}3\left(\frac{H+5}{10}\right)^4+2\left(\frac{H+5}{10}\right)^3-9\left(\frac{H+5}{10}\right)^2\\-18\left[\log_e\,(H+15)-\frac{H+5}{10}\right]+41.56\end{array}\right\}$$

上式に依り H 及 m の種々の値に對し、δ を算出すれば次表の如し、

第　五　表

$H=$	10	20	30	40	50	10	metres
$m=1$	0.122	1.14	4.58	12.70	28.5	55.6	$m.m$
2	0.031	0.29	1.14	3.18	7.13	13.9	,,
3	0.014	0.13	0.51	1.41	3.17	6.2	,,
4	—	0.07	0.29	0.80	1.78	3.50	,,
5	—	—	0.18	0.51	1.14	2.22	,,
6	—	—	0.13	0.35	0.79	1.55	,,

($\delta=$)

(六) 剛性部の安定

(A) 滿水時の安定

$$W_1=\text{剛性部の總重量}=\int_0^{H+5} 0.7\,w\,m\,y\left(1+\frac{y}{10}\right)dy$$

$$=0.7\times 2.5\,m\left(\frac{1}{2}+\frac{H+5}{30}\right)(H+5)^2$$

$i+j=1.0$

$i=$上流側の傾斜

$j=$下流側の傾斜

第　五　圖

正面圖　(1)　　側面圖　(2)

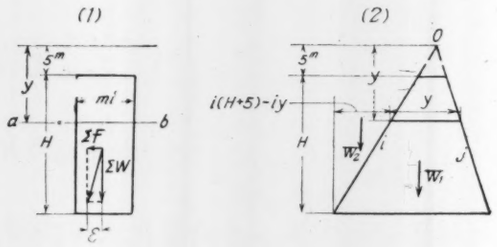

$W_2=$遮水壁直上の池水の重量

$$=\int^{H+5} w_0\,m\,l\,i\{(H+5)-y\}\,dy$$

$$=\frac{1}{2}\,m\,l\,i\,H^2$$

茲に水の重量を $1.0\ \text{ton}/m^3$ にとる、

$$M_y=\frac{0.7\,k\,w\,N}{120}(20\,y^3+y^4)$$

$$\therefore\quad E=\text{偏心距離}=\frac{M_y}{W_1+W_2}$$

$$=\frac{kN(H+25)(H+5)}{120\,m\left\{\left(\frac{1}{2}+\frac{H+5}{30}\right)+\frac{l}{3.5}\,i\left(\frac{H}{H+5}\right)^2\right\}}$$

今 $E=\frac{1}{4}\,ml$ として安定上必要なる m の値を求むれば、

$$m^2=\frac{kN(H+25)(H+5)}{30\,l\left\{0.5+\frac{H+5}{30}+\frac{l}{3.5}\,i\left(\frac{H}{H+5}\right)^2\right\}}$$

前例の如く $k=0.2$ $N=1.0$ $l=10\,m$ とし尙 $i=0.9$ とすれば

$$m^2=\frac{2\left(\frac{H}{10}+2.5\right)\left(\frac{H}{10}+0.5\right)}{3\left\{0.5+\frac{H+5}{30}+\frac{10\times 0.9}{3.5}\left(\frac{H}{H+5}\right)\right\}}$$

H の種々の値に對する所要 m の値を算出すれば、第六表の如し、

第　六　表

$H(m)=10$	20	30	40	50	60
$m=$ 1.28	1.59	1.90	2.20	2.48	2.76

(*B*)　空虚時の安定

池水及堆砂皆無なる場合は絶無にして、而も水壓の作用なきを以て、底面の壓力は極めて小なりと雖も、今假りに反力の偏心距離を $\frac{1}{2}ml$ とし、卽ち外圍支壁の中心に反力を作用せしむる爲めに必要なる m の値を求むるに、

水壓は零なるを以て、(*A*) の場合に於て、$W_2=0$ と置き

$$E=\frac{ml}{2}=\frac{kN(H+25)(H+5)}{120\,m\left(\frac{1}{2}+\frac{H+5}{30}\right)}$$

前同様に $k=0.2$　$N=10\,m$　$l=10\,m$ とすれば

$$m^2=\frac{0.2\times10\,(H+25)\,(H+5)}{600\left(0.5+\frac{H+5}{30}\right)}=\frac{\left(\frac{H}{10}+2.5\right)\left(\frac{H}{10}+0.5\right)}{2+\frac{H}{10}}$$

H の種々の値に對する所要 m の値を算出すれば次表の如し、

第　七　表

$H(m)=10$	20	30	40	50	60
$m=$ 1.33	1.68	1.96	2.21	2.43	2.63

但し岩盤に埋め込み混凝土を塡充するか、又は床版にて聯結すれば安定を考慮するに及ばず。

(七)　剛性部の彎曲應力

空虚の場合は剛性部支壁に應張力を發生するを以て、鉛直鐵筋の挿入を要す。今外緣の支壁のみを以て彎曲應力に耐抗するものとし、重量に依る壓力は小なるを以て之れを除外し、代ふるに混凝土の許容應壓力を低く、鋼の應張力を多少高くとる。

$f_c=450$ tons/m^2 (常時 300 tons/m^2 とし地震の場合
50 % を增せば 450 ton/m^2 なり)

$f_s=18{,}000$ tons/m^2 (常時 12,000 tons/m^2 の 50 % 增し)

第六圖
剛性部水平斷面圖

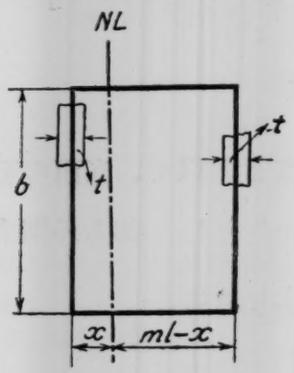

$$\frac{f_c}{x}=\frac{f_s}{n(ml-x)}$$

$$\therefore \quad x=\frac{1}{4}ml$$

$$M=\frac{3.5}{120}(20y^2+y^3)$$

$$b=y \qquad t=0.35(1+0.1y)$$

p_s≡混凝土斷面積に對する鐵筋斷面積の %

$$\frac{p_s}{100}btf_s(ml-x)=M$$

$$\therefore \quad p_s=\frac{(2+0.1y)\left(\frac{y}{10}\right)^2}{1.62ml(1+0.19)}$$

若し $l=10m$ ならば

$$p_s=\frac{(2+0.1y)\left(\frac{y}{10}\right)^2}{16.2(1+0.1y)}\cdot\frac{1}{m}$$

上式に依り種々の y の値に對する p_s を算出すれば次表の如し。

第八表　所要鐵筋量 p_s %

$H(m)=$	10	20	30	40	50	60
$y(m)=$	15	25	35	45	55	65
$m=1$	1.998	0.486	0.924	1.48	2.14	2.96
$m=2$	0.100	0.244	0.462	0.74	1.08	1.48
$m=3$			0.320	0.50	0.72	0.80
$m=4$				0.38	0.54	0.74
$m=5$					0.44	0.60

結局剛性部の安定は滿水時偏心距離を $\frac{1}{6}\sim\frac{1}{5}$ にとり。支壁に鉛直鐵筋を挿入すれば可なり。但し鐵筋の % は下流端に於て、平均量 (p_s) の二倍位とし、上流に向ふて漸次 % を減じ、支壁頭部に於て更に $2p_s$ に增す。

(八) 柔性部の最大撓み

支壁、遮水壁及水平支材に作用する水平地震力は、全部水平支材に依りて剛部又は鎭定に傳達するを以て、支壁の撓みは、一列の兩端に於て實地上零にして、中間に於て最大値を生ず。

先づ（七）の場合の如く、地震時に於ける混凝土及鋼の許容應力を

$$f_c=450\ \text{tons}/m^2 \qquad f_s=18{,}000\ \text{tons}/m^2$$

と定む。f_s に比し f_c の割合に小なるは、施工の不完全を重視せる爲めにして、450 tons/m^2 は

$$45\ kg/cm^2 \quad \text{卽ち} \quad 643\ lb/in^2 \quad \text{にして、}$$

橋梁に於ける常時彎曲應力、建物に於ける震度 0.1 の場合の彎曲應力と同一なり。上記の許容應力に於て自重其の他の彎曲作用に對する餘裕を有せしむる爲め、張力は全部鋼、壓力は全部混凝土のみに依て耐抗するものとす。

次に全長 Nl 中に於て一端より $n_1 l$ の部分の支材に應壓力、他端より $n_2 l$ の部分の支材に應張力の作用するものとすれば、兩部の總伸長又は壓縮が同一なる爲めには、

$$\frac{450}{E_c}n_1 l=\frac{18{,}000}{E_s}n_2 l \qquad \therefore \qquad \frac{n_2}{n_1}=\frac{3}{8}$$

第七圖 水平支材

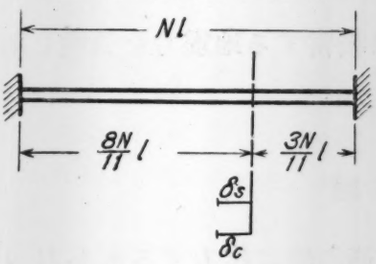

今一列中の全支材に同一斷面同一鋼材を使用するものとすれば、抗壓支材に於ける平均應力 f_{cm} は

$$f_{cm}=\frac{1}{2}\left(f_c+\frac{f_c}{\frac{8N}{11}}\right)=\frac{f_c}{2}\left(1+\frac{11}{8N}\right)$$

(Buttress wall の數は $N+1$ なり)

同樣に抗張材の平均應力 f_{sm} は

$$f_{cm}=\frac{f_s}{5}\left(1+\frac{11}{3N}\right)$$

然る時は支壁の最大撓み δ は

$$\delta=\delta_c=\delta_s=\frac{f_c}{2E_c}\left(1+\frac{11}{8N}\right)\frac{8N}{11}l=\frac{f_s}{2E_s}\left(1+\frac{11}{3N}\right)\frac{3N}{11}l$$

$$=\frac{450}{2\times1.4\times10^6}\left(\frac{8N}{11}+1\right)l\ \text{in metre}=\frac{450}{2.8\times10^3}\left(\frac{8N}{11}1+\right)l\ \text{in } m.m$$

若し地震による最大撓みを 10 $m.m$ に制限すれば

$$10=\frac{450}{2.8\times10^3}\left(\frac{8N}{17}+1\right)l \qquad \therefore \qquad N=\frac{85}{l}-\frac{11}{8}$$

若し $\delta=10\ m.m$ として Nl を大にするには、

fc 及 fs を同一割合に小にすれば可なり。若し Nl を 1.5 倍となさんとすれば、

$$f_c=300\ \text{tons}/m^2 \qquad f_s=12{,}000\ \text{tons}/m^2$$

とし之れに依りて最大應力に對する斷面を定むれば可なり。

又 Nl を不變として δ を增減せんとすれば、f_c 及 f_s を同割合に增減すれば可なり。

若し剛性部又は鎭定裝置に於て支材の壓力に依り δ_{0c}. 全張力に依り δ_{0s} だけの變位を生ずる時は上記の計算は次の如くに變ず。

$$\delta=\delta_c+\delta_{0c}=\delta_s+\delta_{0s}=\frac{f_c}{2E_c}\left(1+\frac{11}{8N}\right)\frac{8N}{11}l+d_{0c}$$

$$=\frac{f_s}{2E_c}\left(1+\frac{11}{3N}\right)\left(\frac{8N}{11}\right)+\delta_{0s}$$

普通 N が正しく 8:3 の兩部に分割し得ざるを以て、實際の n_1 及 n_2 は算出値の小數點以下を必ず切り上げ、δ_{0c} 及 δ_{0s} の影響に備へ且つ安定の爲め、支材は混凝土の最小抗壓强度の 70% に於て全柔性部長、卽ち Nl に相當する地震力を負擔し得、鋼材は其の彈性限度に於て、$\frac{1}{2}Nl$ に相當する地震力を負擔し得る如き斷面を用ふれば充分安全なりとす。

(九) 水平支材の斷面積

第八圖　水平支材應力圖

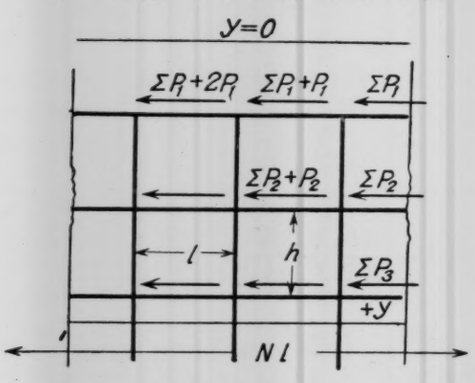

y に於ける單位高の堤に作力する水平力 P は

$$P=\lambda\,(a+Ab/Am)\,ky\left(1+\frac{y}{10}\right)$$

$$\lambda=0.35\times2.5$$

故に $y=\left(n-\frac{1}{2}\right)h$ に於ける水平面內支材群に於て一徑間に對する水平力は次の如し、

$$P_n=\int_{(n-1)h}^{(n)h}Pdy=\int_{(n-1)h}^{(n)h}\lambda\left(a+\frac{A_b}{A_w}\right)ky\left(1+\frac{y}{10}\right)dy$$

$$=\lambda\left(a+\frac{A_b}{A_w}\right)k\left\{\frac{h^2}{2}(2n-1)+\frac{h^3}{30}(n^3-\overline{n-1^3})\right\}$$

今　　$a+\frac{A_b}{A_w}=2.0$　　$k=0.2$　　とすれば

$$P_n=35\left\{\left(\frac{h}{10}\right)^2\left(n-\frac{1}{2}\right)+\frac{1}{3}\left(\frac{h}{10}\right)^3(n^3-\overline{n-1}^3)\right\}$$

一水平面内の支材列の最大應力は次の如し。

$$\text{最大應壓力}=\Sigma P_{nc}=\int_0^{\frac{8N}{11}}\int_{(n-1)h}^{(nh)}\lambda\left(a+\frac{A_b}{A_w}\right)ky\left(1+\frac{y}{10}\right)dy\,dN$$

$$=35\times\left\{\left(\frac{h}{10}\right)^2(n-0.5)+\left(\frac{h}{10}\right)^3\frac{1}{3}(n^3-\overline{n-1}^3)\right\}\frac{8N}{11}$$

$$\text{最大應張力}=\Sigma P_{ns}=35\left(\frac{3N}{11}\right)\left\{\left(\frac{h}{10}\right)^3(n-0.5)+\left(\frac{h}{10}\right)^3\frac{1}{3}(n^3-\overline{n-1}^3)\right\}$$

故に

Ac＝一水平面内に於ける支材の混凝土斷面$=\frac{\Sigma P_{ns}}{f_c}$ in m^2

As＝　　,,　　鋼材斷面$=\frac{\Sigma P_{ns}}{f_s}$ in m^2

今前數節の例の如く、　$l=10\,m$,　$h=10\,m$,　$\delta=10\,m.m$,

$Nl=10$　$l=100\,m$,　$f_c=450\,\text{tons}/m^2$,　$f_s=18{,}000\,\text{tons}/m^2$

として、A_c 及 A_s を算出すれば次の如し。

第　九　表　　一水平面内に於ける支材總斷面積

總堤高　(m)＝	10	20	30	40	50	60	70
堤頂よりの距離 (m)＝	0	10	20	30	40	50	60
$A_c(m^2)$ ＝	0.63	2.90	6.67	11.97	18.95	27.1	36.8
$A_s(\overline{cm}^2)$ ＝	59.1	271	625	1124	1740	2540	3440
A % ＝	0.93	0.93	0.93	0.93	0.93	0.93	0.93
Ac/A_w ＝	0.221	0.221	0.221	0.221	0.221	0.221	0.221
F_c ＝	212	975	2250	4040	6310	9110	12400
鎭定力 F_s (tons) ＝	79.6	366	843	1516	2370	3420	4650

卽ち水平撓度を最大 10 $m.m$ に限定するも所要支材の容積は、支壁のそれの 22 % を以て足り、鐵筋量も約 1 % 以て充分なりとす。　（完）

新築中の議院建築物の震動驗測 （第二回）

所員 今村明恒
助手 岸上冬彦

On the Vibration of the Imperial Diet Building. (*Second report.*)

By

Akitune IMAMURA and **Fuyuhiko KISHINOUYE.**

(Abstract)

About three years ago, one of the writers measured with his new tromometers (the 25 th year-type) the vibrations of the Imperial Diet Building, which has been, and still is, in course of construction. (Bull. Earthq. Research Inst., Tokyo Imp. Univ., I, pp. 14-21.) It was then nothing but two isolated frames, having, besides the underground floor, four floors with a total height of about 22.7 meters. These two parts will be called the northern and the southern wings; they were later connected by a central spired structure consisting of eight floors and having a total height of about 67.8 meters. (See Fig. 1.) Soon after the completion last July of these frames and that of the concrete ground floor, the same tromometers were again brought and installed on the underground, on the 5 th and on the 8 th floors and 25 earthquakes were observed with them during the two subsequent months. (See Table II.) On Oct. 20 th the instruments, which had been installed on the ground and the 8 th floors, were removed into the 3 rd floor of N and S wings and 6 earthquakes were observed with them during the two subsequent weeks. (See Table III.) The results of observations may be summarized as follows:—

I. Free vibrations of the structure. (See Fig. 2.)

1) The whole structure, with the exception of the central spired part, vibrates with a period of about 0.4 sec. and an amplitude of about 0.03 mm. at maximum.

2) The N-S component vibrations of the spired part show, for the most part, a period of about 0.7 sec. on the 5 th and on the 8 th floors with amplitudes of about 0.02 mm. and 0.034 mm. respectively. This seems to suggest that the tower vibrates in this direction with the upper end free and the other end fixed—perhaps fixed at the level of the roofs of the N and S wings of the structure.

3) The E-W component vibrations of the spired structure show, for the most part, a period of about 0.38 sec. with an amplitude of 0.01 mm. on the 5th floor, whereas on the 8th floor they show a period of about 0.78 sec. with an amplitude of 0.03 mm. This suggests that the central spired structure makes in the transverse direction of the building a complex motion consisting of a vibration with the lower end fixed and the upper end free, together with another one with both ends fixed.

II. Vibrations due to earthquakes.

1) When the period of earthquake motion approaches 0.4 sec., the structure shows a phenomenon of resonance. (See Fig. 3.)

2) The greater the deviation of the period of earthquake motion from 0.4 sec., the more do the N-S component vibrations of the different floors approach each other in magnitude; when the earthquake motion is large enough and its period is equal to one second, the ratios of amplitudes on the 8th, the 5th and the underground floors are approximately 3:2:1.

3) When the earthquake motion is small and its period approaches 0.4 sec., the central spired building shows in a E-W direction larger vibrations on the 5th floor than on the 8th floor. (See Fig. 4.) This would suggest that the predominant vibration of the spired building in this direction is of the type with both ends fixed.

4) When the earthquake motion is large enough, the spired building shows that the higher the floor the greater is the vibration. This would suggest that the predominant vibration of the structure is that of the type with the lower end fixed and the upper end free.

大正十四年に帝國議院の本建築が中央部を殘して、貴族院及び衆議院の各鋼骨組立を終つたので、著者の一人は大正十四年式簡單微動計を以て建築物の比較驗測を行ひました。その結果は東京帝國大學地震研究所彙報第一號に「地震計測整備の一班」と云ふ題の下に載つて居ります。

昭和二年夏には議院の鋼骨の組立が完了したので、當局の依賴により第二回の驗測を同年八月から十一月までの間に於て實施致しました。その方法は前回の場合と同樣に致しました。驗測に用ひる器械は全部大正十四年式簡單微動計に揃へる豫定でありましたが、丹後地震の餘震調査等の爲に、三臺の中一臺は大森式（改良型）を用ひました。

1. 大正十四年式簡單微動計 No. 1, 倍率 50
2. ,, No. 2, ,,
3. 大森式簡單微動計（改良型), ,,

器械の常數は第一表に示してあります。

第一圖 議院建築物略圖

Fig. 1. Sketch of the Imperial Diet Building.

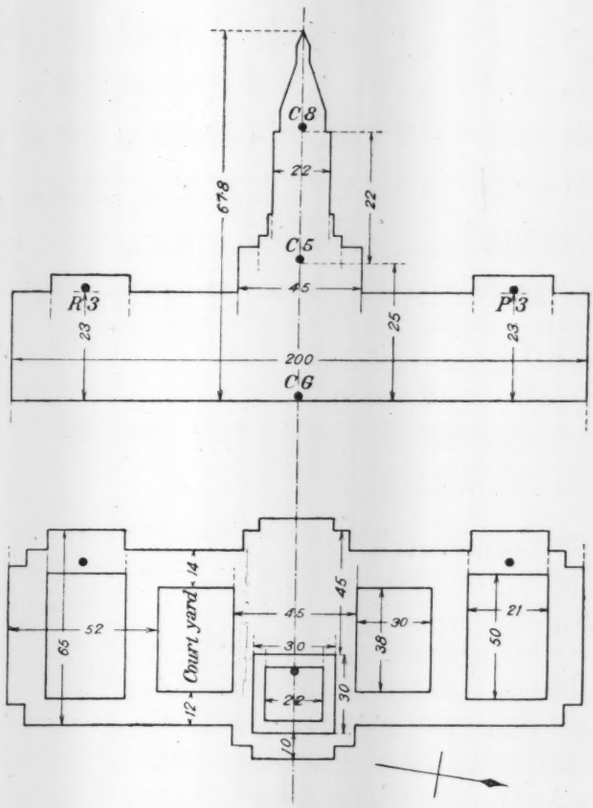

長さの單位....米 Number indicates length in meter.

觀測位置....黑點 Dot, the position of observation.

此の大森式は複式描針の構造を十四年式と同樣にして、微動を描くに適當にしたものであります。建築物に据付ける前に、地震學教室に於て比較檢査をしました。その結果週期の短い時、即ち近距離地震、地面の人爲的震動では器械の異なる爲の影響は無いと考へられましたので、比較驗測には週期の大きいものを用ひることは避けました。十四年式二臺は如何なる震動でも殆ど等しく記錄しました。（大森式及び十四年式簡單微動計に就いても前記の論文に記述されて居ります。）

八月六日驗測開始。十四年式 No. 1 を中央の塔の八階、大森式を塔の五階、十四年式 No. 4 を地階の三個所に建築物の方向と平行に据付けました。後に記す驗測結果には此の方位が用ひてありまして、南北動とは建築物の長い方向、東西動とは短い方向を指すのであります。塔の各階の間隔は下の如くであります。（第一圖）

地階	一階	二階	三階	四階	五階	六階	七階	八階
4.4 m	4.9	5.8	5.9	4.2	4.4	12.5	5.5	

塔の五階は貴衆兩院の最上層よりも一段高い所であります。

五階に於て建築物の自己振動と考へられる微動が東西動と南北動とで週期が異なるので（第一圖)、九月二日に五階にあつた大森式を 90° 方向を變へて見まし

た。その結果器械による差異でないことが判りました。

十四年式と大森式とは構造上大いなる差がありますので、念の爲に九月十二日に十四年式 No. 4 を五階に、大森式を地階に移しました。建築物の自己振動は器械を換へても前同様に表はれました。中央部の驗測は八月六日に開始したことを前に述べて置きましたが、凡そ二個月の間に一通りの地震觀測が出來上りました。其の中二十五回のものに關する驗測の結果が第二表に纏めてあります。

斯くして中央部の驗測を終りましたから、十月二十日に五階の十四年式 No. 4 は其の儘にして、大森式を貴族院三階に、十四年式 No. 1 を衆議院三階に移しました。此の二個所は大正十四年に驗測されてありますが、中央部によつて連結された爲に其れが如何に變化したかを調べる爲でありました。二週間位で驗測を終へ、其結果は第三表にある様に六回の地震驗測として纏めてあります。

十一月二日驗測を終りました。約三個月間建築工事場の方々に種々援助を受けたことを此の機會に於て厚く御禮申上げます。

第 一 表 TABLE I

微動計の常數 Constants of Tromometers

CG: 中央塔の地階 Underground of the central tower
C5: ,, の五階 Fifth floor of ,, ,, ,,
C8: ,, の八階 Eighth floor of ,, ,, ,,

位置 Place	器械 Instrument	月日 Date	成分 Component	T_0	ε	r
1.						
CG	1925-type Portable Tromometer No. 4	VIII 11-12	EW NS	7.79 s 7.89	0.13 0.16	1.72 3.13
C5	Improved Omori's Portable Tromometer	VIII 7-8	EW NS	4.23 4.14	0.06 0.11	0.33 0.14
C8	1925-type Portable Tromometer No. 1	VIII 7-8	EW NS	7.69 7.33	0.26 0.23	4.13 4.71
2.						
CG	1925-type Portable Tromometer No. 4	IX 11-12	EW NS	6.72 6.71	0.14 0.15	2.01 3.21
C5	Improved Omori's Portable Tromometer	IX 11-12	EW NS	3.31 3.23	0.14 0.10	1.01 0.78
C8	1925-type Portable Tromometer No. 1	IX 11-12	EW NS	6.55 6.19	0.15 0.11	6.58 5.08

3.

CG	Improved Omori's Portable Tromometer	IX 29-30	EW NS	3.98 3.96	0.12 0.07	0.51 0.33
C5	1925-type Portable Tromometer No. 4	IX 29-30	EW NS	6.56 5.98	0.12 0.17	3.56 2.45
C8	1925-type Portable Tromometer No. 1	IX 29-30	EW NS	5.52 5.74	0.25 0.24	4.52 4.67

R3: 衆議院三階 Third floor of the House of Representatives

P3: 貴族院三階 ,, ,, ,, ,, ,, ,, Peers

4.

R3	1925-type Protable Tromometer No. 1	XI 1-2	EW NS	4.28 4.93	0.17 0.24	1.16 7.29
C5	1925-type Portable Tromometer No. 4	XI 1-2	EW NS	6.00 5.78	0.12 0.14	4.01 3.61
P3	Improved Omori's Portable Tromometer	XI 1-2	EW NS	3.43 3.58	0.03 0.06	0.61 0.65

第 二 表 TABLE II

中央塔の地階、五階及び八階に於ける地震觀測表 Observations of earthquakes at underground, fifth floor and eighth floor of the central tower.

數字は微動計に記錄された儘の全振幅 Figures indicate the double amplitude in mm ×50.

括弧の中の數字はその時の週期 Figures in parentheses indicate the period of observedmovement in sec.

ゴシックの數字は振幅の比 Gothic figures indicate the ratio of amplitudes of each component.

(1) 八月七日十時四十分二十三秒 微震

VIII 7: 10 h 40 m 23 s. Slight

震原 東京の東三十六粁 初期部 九・三秒

Origin: 36 km E of Tokyo. Dur. p. t. =9.3 s

	主要部第一波 S		主要部三秒目 3 s after S	
	EW	NS	EW	NS
CG	9.9 (0.69) **1**	24.4 (1.46) **1**	10.7 (0.17) **1**	7.0 (0.35) **1**
C5	27.0 (0.22) **2.7**	19.4 (0.51) **0.8**	77.7 (0.36) **7.3**	69.9 (0.36) **10.0**
C8	38.7 (0.40) **3.7**	>50.0 (——) **>2.1**	82.6 (0.40) **7.7**	——

(2) 八月八日二十一時五十五分四十二秒 微震（無感）
VIII 8: 21 h 55 m 42 s. Slight (unfelt)
震原 東京灣口 初期部 八・四秒
Origin: at the entrance of Tokyo Bay. Dur. p. t.=8.4 s

	主要部第一波 S		主要部一秒目 1 s after S	
CG	0.2 (0.33) **1**	0.5 (0.33) **1**	1.3 (0.33) **1**	0.5 (0.33) **1**
C5	4.2 (0.26) **21.0**	——	7.5 (0.39) **5.8**	——
C8	1.5 (0.34) **7.5**	1.0 (0.341) **2.0**	3.5 (0.56) **2.7**	2.0 (0.67) **4.0**

(3) 八月十二日五時五十三分四秒 微震
VIII 12: 5 h 53 m 04 s. Slight
震原 東京の北東三十五粁 初期部 九・三秒
Origin: 35 km NE of Tokyo. Dur. p. t.=9.3 s

	主要部第一波 S		主要部第二波 Next to S		主要部六秒目 6 s after S	
CG	1.5 (0.31) **1**	3.0 (0.32) **1**	1.3 (0.32) **1**	3.3 (0.32) **1**	2.0 (0.32) **1**	1.5 (0.32) **1**
C5	11.5 (0.40) **7.7**	5.7 (0.66) **1.9**	16.0 (0.40) **12.3**	11.8 (0.66) **3.6**	41.9 (0.40) **21.0**	12.3 (0.53) **8.2**
C8	7.4 (0.51) **4.9**	9.8 (0.82) **3.3**	4.9 (0.51) **3.8**	19.3 (0.82) **5.8**	10.0 (0.71) **5.0**	17.4 (0.72) **11.6**

(4) 八月十四日二十時五十七分四十八秒 微震
VIII 14: 20 h 57 m 48 s. Slight
震原 東京の北東五十五粁 初期部 八・一秒
Origin: 55 km NE of Tokyo. Dur. p. t.=8.1 s

	主要部第一波 S		主要部七秒目 7 s after S	
CG	0.3 (0.36) **1**	0.4 (0.36) **1**	0.2 (0.27) **1**	0.2 (0.27) **1**
C5	0.9 (0.43) **3.0**	0.5 (0.54) **1.3**	3.9 (0.35) **20.0**	1.7 (0.43) **8.5**
C8	0.6 (0.50) **2.0**	0.6 (0.50) **1.5**	1.8 (0.40) **9.0**	2.0 (0.69) **10.0**

(5) 八月十九日二十一時四十三分四十一秒 微震
VIII 19: 21 h 43 m 41 s. Slight
震原 鹿島沖 初期部 一七・七秒

Origin: off the coast of Hitati. Dur. p. t.=17.7 s

	主要部第一波 S		主要部十秒目 10 s after S	
CG	2.0 (0.92) **1**	1.9 (0.35) **1**	1.2 (0.46) **1**	0.9 (0.46) **1**
C5	11.2 (0.56) **5.6**	3.5 (0.56) **1.8**	36.2 (0.45) **30.1**	12.1 (0.79) **13.4**
C8	6.4 (0.46) **3.2**	6.6 (0.74) **3.5**	20.2 (0.83) **16.8**	20.2 (0.83) **22.5**

（6） 八月三十一日十七時四十五分三十五秒 微震（無感）

VIII 31: 17 h 45 m 35 s. Slight (unfelt)

震原 東京附近 初期部 五・五秒

Origin: Near Tokyo. Dur. p. t.=5.5 s

	主要部第一波 S		主要部第二波 Next to S	
CG	0.5 (0.39) **1**	0.5 (0.48) **1**	0.6 (0.39) **1**	0.3 (0.48) **1**
C5	4.9 (0.37) **9.8**	1.7 (0.73) **3.4**	5.6 (0.37) **9.3**	2.4 (0.73) **8.0**
C8	1.8 (0.46) **3.6**	2.8 (0.82) **5.6**	2.2 (0.46) **3.7**	3.3 (0.82) **11.0**

（7） 八月三十一日二十二時十五分三十三秒 微震 〔圖版參照〕

VIII 31: 22 h 15 m 33 s. Slight [See Plates]

震原 東京の北東五十粁 初期部 九・八秒

Origin: 50 km NE of Tokyo. Dur. p. t.=9.8 s

	主要部第一波 S		主要部第二波 Next to S		主要部四秒目 4 s after S	
CG	4.1 (0.85) **1**	4.4 (0.85) **1**	4.3 (0.50) **1**	8.4 (0.50) **1**	1.7 (0.30) **1**	4.5 (0.40) **1**
C5	7.2 (0.69) **1.8**	5.4 (0.92) **1.2**	6.8 (0.69) **1.6**	15.5 (0.92) **1.8**	48.3 (0.57) **28.2**	23.7 (0.92) **5.3**
C8	10.7 (0.75) **2.6**	7.3 (0.85) **1.7**	15.8 (0.75) **3.7**	19.4 (0.85) **2.3**	17.0 (0.75) **10.0**	23.4 (0.85) **5.2**

（8） 九月四日十二時三十二分二十四秒 微震（無感）

IX 4: 12 h 32 m 24 s. Slight (unfelt)

震原 東京灣 初期部 四・八秒

Origin: Tokyo Bay. Dur. p. t.=4.8 s

	主要部第一波 S		主要部二秒目 2 s after S	
CG	0.9 (0.27) 1	0.6 (0.27) 1	0.5 (0.27) 1	0.7 (0.27) 1
C5	1.1 (0.26) 1.2	1.7 (0.53) 2.8	7.3 (0.39) 14.6	3.8 (0.53) 5.4
C8	2.7 (0.52) 3.0	3.0 (0.73) 5.0	5.0 (0.84) 10.0	5.1 (0.84) 7.3

(9) 九月五日四時十六分四秒　　微震（無感）
IX 5: 4 h 16 m 0.4 s.　　Slight (unfelt)
震原　東京附近　　初期部　五•四秒
Origin: Near Tokyo.　　Dur. p. t. = 5.4 s

	主要部第一波 S		主要部四秒目 4 s after S		主要部六秒目 6 s after S	
CG	0.3 (0.22) 1	0.2 (0.33) 1	0.1 (0.22) 1	0.2 (0.22) 1	0.3 (0.33) 1	0.2 (0.33) 1
C5	1.5 (0.33) 5.9	0.6 (0.65) 3.0	6.3 (0.44) 63.0	1.1 (0.55) 5.5	4.5 (0.44) 15.0	1.0 (0.55) 5.0
C8	1.0 (0.60) 3.3	0.5 (0.70) 2.5	1.5 (0.40) 15.0	1.3 (0.30) 6.5	2.9 (0.40) 9.7	1.0 (0.30) 5.0

(10) 九月五日九時三十三分十五秒　　弱震
IX 5: 9 h 33 m 15 s.　　Moderate
震原　那珂川口　　初期部　一四•三秒
Origin: The mouth of Nakagawa.　　Dur. p. t. = 14.3 s

	主要部第一波 S		主要部第二波 Next to S	
CG	3.5 (1.10) 1	13.3 (1.00) 1	29.8 (1.10) 1	20.9 (0.90) 1
C5	25.4 (1.02) 7.3	10.8 (0.76) 0.8	67.4 (0.89) 2.3	43.5 (0.64) 2.1
C8	40.0 (0.62) 11.4	17.6 (0.49) 1.3	106.8 (0.62) 3.6	72.0 (0.49) 3.5

(11) 九月六日七時三十九分四十四秒　　弱震
IX 6: 7 h 39 m 44 s.　　Moderate
震原　東京の四南四七十七粁　　初期部　九•三秒
Origin: 77 km WSW of Tokyo.　　Dur. p. t. = 9.3 s

	主要部第一波 S		主要部二秒目 2 s after S	
CG	4.6 (0.68) 1	9.2 (0.68) 1	6.0 (0.42) 1	12.6 (0.51) 1
C5	5.5 (0.36) 1.2	13.8 (0.60) 1.5	34.1 (0.36) 5.7	80.3 (0.60) 6.4
C8	18.2 (0.94) 4.0	——	11.7 (0.42) 2.0	——

(12) 九月七日十九時三十三分三十五秒 弱震

IX 7: 19 h 33 m 35 s. Moderate

震原 東京の北四十一粁 初期部 八・八秒

Origin: 41 km N of Tokyo. Dur. p. t. = 8.8 s

	主要部第一波 S		主要部第二波 Next to S		主要部四秒目 4 s after S	
CG	12.7 (1.04) 1	8.0 (0.70) 1	14.7 (1.04) 1	9.9 (0.70) 1	14.5 (0.35) 1	15.0 (0.35) 1
C5	40.7 (0.36) 3.2	59.1 (0.60) 7.5	60.7 (0.36) 4.1	64.5 (0.60) 6.5	87.5 (0.72) 6.0	>17.0 (0.83) >11.3
C8	28.5 (0.79) 2.2	49.1 (0.69) 6.1	63.6 (0.79) 4.3	59.3 (0.69) 6.0	47.7 (0.69) 3.3	133.0 (0.79) 8.9

(13) 九月十三日十三時五十六分十三秒 弱震

IX 13: 13 h 56 m 13 s. Moderate

震原 東京の東北東四十六粁 初期部 九・四秒

Origin: 46 km ENE of Tokyo. Dur. p. t. = 9.4 s

	主要部第一波 S		主要部第二波 Next to S	
CG	18.1 (0.50) 1	8.7 (0.61) 1	12.6 (0.50) 1	16.6 (0.61) 1
C5	34.8 (0.49) 1.9	21.8 (0.69) 2.5	42.8 (0.49) 3.4	45.9 (0.69) 2.8
C8	27.7 (0.37) 1.5	30.3 (0.61) 3.5	24.1 (0.37) 1.9	55.3 (0.61) 3.3

(14) 九月十六日二十三時五分二十三秒 微震

IX 16: 23 h 05 m 23 s. Slight

震原 東京灣 初期部 七・三秒

Origin: Tokyo Bay. Dur. p. t. = 7.3 s

	主要部第一波 S		主要部一二秒目 12 s after S	
CG	0.2 (0.12) **1**	0.6 (0.12) **1**	0.4 (0.48) **1**	0.4 (0.36) **1**
C5	——	1.6 (0.58) **2.7**	——	1.2 (0.50) **3.0**
C8	0.7 (0.50) **3.5**	1.0 (0.61) **1.7**	1.0 (0.45) **2.5**	1.8 (0.81) **4.5**

(15) 九月十八日七時二十二分十秒　微震
IX 18: 7 h 22 m 10 s. Slight
震原　東京の南西六十二粁　初期部　七・三秒
Origin: 62 km SW of Tokyo. Dur. p. t. = 7.3 s

	主要部第一波 S		主要部四秒目 4 s after S		主要部二九秒目 29 s after S	
CG	2.8 (0.37) **1**	1.4 (0.62) **1**	2.5 (0.37) **1**	0.3 (0.25) **1**	2.7 (0.36) **1**	4.4 (0.49) **1**
C5	9.3 (0.48) **3.3**	2.8 (0.57) **2.0**	18.9 (0.48) **7.6**	5.2 (0.86) **17.3**	15.9 (0.89) **5.9**	11.7 (0.78) **2.7**
C8	8.7 (0.66) **3.1**	4.5 (0.66) **3.2**	23.7 (0.96) **9.5**	8.3 (0.86) **27.7**	33.5 (0.89) **12.4**	13.5 (0.78) **3.1**

(16) 九月十八日十八時十九分五十二秒　微震
IX 18: 18 h 19 m 52 s. Slight
震原　東京の北北東三十八粁　初期部　八・三秒
Origin: 38 km NNE of Tokyo. Dur. p. t. = 8.3 s

	主要部第一波 S		主要部第二波 Next to S		主要部一一秒目 11 s after S	
CG	2.4 (1.00) **1**	——	3.8 (0.87) **1**	——	2.9 (0.50) **1**	——
C5	13.7 (0.40) **5.7**	4.5 (0.61) **1**	23.1 (0.40) **6.1**	3.4 (0.61) **1**	24.9 (0.40) **8.9**	7.4 (0.61) **1**
C8	13.4 (0.89) **5.6**	7.2 (0.71) **1.6**	16.3 (0.8) **4.8**	10.4 (0.71) **3.1**	17.8 (0.80) **6.1**	10.5 (0.62) **1.4**

(17) 十月五日九時二十七分五十七秒　微震（無感）
X 5: 9 h 27 m 57 s. Slight. (unfelt)
震原　東京の南西四十粁　初期部　七・〇秒
Origin: 40 km SW of Tokyo. Dur. p. t. = 7.0 s

	主要部第一波 S		主要部二秒目 2s after S	
CG	1.6 (0.21) 1	0.5 (0.21) 1	1.6 (0.38) 1	1.2 (0.19) 1
C5	9.5 (0.38) 5.9	——	11.0 (0.47) 6.9	——
C9	2.6 (0.30) 1.6	6.7 (0.69) 13.4	6.5 (0.58) 4.1	6.2 (0.67) 5.2

(18) 十月七日二十三時二十六分三十二秒 微震

X 7: 23 h 26 m 32 s. Slight

震原 東京の北東四十二粁 初期部 七・二秒

Origin: 42 km NE of Tokyo. Dur. p. t. = 7.2 s

	主要部第一波 S		主要部九秒目 9s after S	
CG	0.7 (0.35) 1	0.5 (0.35) 1	0.6 (0.46) 1	0.4 (0.35) 1
C5	1.7 (0.18) 2.4	——	19.3 (0.37) 32.2	——
C8	1.3 (0.46) 1.9	2.1 (0.69) 4.2	7.0 (0.46) 11.7	4.0 (0.46) 10.0

(19) 十月十一日十時十三分二十秒 弱震

X 11: 10 h 13 m 20 s. Moderate

震原 鹿島沖 初期部 一七・五秒

Origin: Off the coast of Hitati. Dur. p. t. = 17.5 s

	主要部第一波 S		主要部第二波 Next to S	
CG	0.6 (1.00) 1	0.3 (1.00) 1	39.6 (0.75) 1	22.1 (0.50) 1
C5	31.0 (0.55) 51.7	29.4 (1.10?) 98.0	12.1 (0.55) 0.3	32.8 (1.10?) 1.5
C8	37.5 (1.22) 62.5	35.5 (1.13) 118.3	34.4 (1.22) 0.9	43.3 (1.13) 2.0

(20) 十月十二日二時三十八分五十三秒 弱震

X 13: 2 h 38 m 53 s. Moderate

震原 東京灣 初期部 八・八秒

Origin: Tokyo Bay. Dur. p. t. = 8.8 s

	主要部第一波 S		主要部第二波 Next to S		主要部一〇秒目 10 s after S	
CG	——	8.2 (1.00) 1	——	15.1 (0.57) 1	——	2.0 (0.23) 1
C5	6.7 (0.18) 1	15 8 (0.72) 1.9	10.2 (0.18) 1	34.8 (0.72) 2.3	27.5 (0.18) 1	59.1 (0.63) 29.6
C8	7.6 (0.28) 1.1	22.7 (0.75) 2.8	11.0 (0.37) 1.1	44.6 (0.75) 3.0	22.0 (0.84) 0.8	81.9 (0.84) 41.0

(21) 十月十三日十七時四十一分五十八秒 微震
X 13: 17 h 41 m 58 s Slight
震原 東京の南南東二十粁 初期部 八・七秒
Origin: 20 km SSE of Tokyo. Dur. p. t.=8.7 s

	主要部第一波 S		主要部四秒目 4 s after S	
CG	0.7 (0.46) 1	0.5 (0.57) 1	0.7 (0.35) 1	0.6 (0.46) 1
C5	1.7 (0.48) 2.4	0.7 (0.80) 1.4	6.5 (0.32) 9.3	1.5 (0.40) 2.5
C8	1.0 (0.43) 1.4	1.1 (0.85) 2.2	2.9 (0.43) 4.1	1.9 (0.64) 3.2

(22) 十月十四日十九時七分二十六秒 微震
X 14: 19 h 07 m 26 s. Slight
震原 東京附近 初期部 五・六秒
Origin: Near Tokyo. Dur. p. t.=5.6 s

	主要部第一波 S		主要部第二波 Next to S		主要部二秒目 2 s after S	
CG	1.7 (0.52) 1	2.6 (0.26) 1	2.1 (0.39) 1	2.5 (0.26) 1	1.6 (0.51) 1	0.9 (0.26) 1
C5	2.4 (0.33) 1.4	4.0 (0.33) 1.5	6.0 (0.33) 2.9	8.0 (0.42) 3.2	16.8 (0.42) 10.5	6.8 (0.50) 7.5
C8	5.0 (0.46) 3.0	6.2 (0.56) 2.4	7.4 (0.37) 3.5	9.8 (0.74) 3.9	8.0 (0.37) 5.0	10.2 (0.74) 11.3

(23) 十月十四日二十三時二十七分十四秒 微震（無感）
X 14: 23 h 27 m 14 s. Slight (unfelt)
震原 東京の南西三十九粁 初期部 五・二秒
Origin: 39 km SW of Tokyo. Dur. p. t.=5.2 s

	主要部第一波 S		主要部第二波 Next to S	
CG	0.3 (0.22) 1	0.5 (0.34) 1	0.5 (0.22) 1	0.5 (0.34) 1
C5	1.7 (0.19) 5.7	0.5 (0.29) 1.0	1.6 (0.19) 3.2	0.5 (0.29) 1.0
C8	1.3 (0.38) 4.3	1.4 (0.29) 2.8	1.5 (0.38) 3.0	2.0 (0.57) 4.0

(24) 十月十四日二十三時四十六分五十一秒 微震（無感）
X 14: 23 h 46 m 51 s. Slight (unfelt)
震原 東京附近 初期部 三・七秒
Origin: Near Tokyo. Dur. p. t. = 3.7 s

	主要部第一波 S		主要部第二波 Next to S	
CG	0.5 (0.35) 1	0.6 (0.24) 1	0.7 (0.35) 1	0.3 (0.24) 1
C5	1.4 (0.29) 2.8	1.1 (0.57) 1.8	1.4 (0.29) 2.0	1.7 (0.57) 5.7
C8	0.20 (0.50) 4.0	1.7 (0.50) 2.8	3.0 (0.50) 4.3	2.6 (0.61) 8.7

(25) 十月十六日二時十五分四十七秒 微震（無感）
X 16: 2 h 15 m 47 s. Slight (unfelt)
震原 東京附近 初期部 四・四秒
Origin: Near Tokyo. Dur. p. t. = 4.4 s

	主要部第一波 S		主要部第二波 Next to S		主要部四秒目 4 s after S	
CG	0.3 (0.24) 1	0.4 (0.24) 1	0.5 (0.24) 1	0.6 (0.24) 1	0.2 (0.36) 1	0.2 (0.24) 1
C5	1.2 (0.18) 4.0	1.0 (0.27) 2.5	1.2 (0.18) 2.4	0.3 (0.27) 0.5	7.5 (0.27) 37.5	1.5 (0.62) 7.5
C8	0.7 (0.39) 2.3	1.0 (0.39) 2.5	1.1 (0.39) 2.2	1.6 (0.39) 2.7	1.0 (0.30) 5.0	1.7 (0.69) 8.5

第三表 TABLE III.

貴族院三階、衆議院三階及び中央塔五階に於ける地震觀測表 Observations of earthquakes at the third floors of the House of Peers and Representatives and fifth floor of the central tower.

(1) 十月二十二日五時四十六分四十七秒 微震（無感）
X 22: 5 h 46 m 47 s. Slight (unfelt)

震原　東京の南二十粁　初期部　四・五秒
Origin: 20 km S of Tokyo.　Dur. p. t.=4.5 s

	主要部第一波 S		主要部第二波 Next to S		主要部三秒目 3 s after S	
	EW	NS	EW	NS	EW	NS
R3	0.8 (0.39) 1	1.2 (0.30) 1	1.2 (0.39) 1	1.5 (0.30) 1	1.5 (0.49) 1	0.8 (0.39) 1
C5	0.7 (0.40) 0.9	0.5 (0.30) 0.4	0.2 (0.40) 0.2	1.2 (0.30) 0.8	2.2 (0.20) 1.5	1.0 (0.50) 1.3
P3	0.3 (0.40) 0.4	0.7 (0.40) 0.6	0.4 (0.40) 0.3	1.4 (0.40) 0.9	1.0 (0.40) 0.7	1.5 (0.40) 1.9

(2) 十月二十四日五時十九分五十八秒　微震
X 24: 5 h 19 m 58 s.　Slight
震原　東京の南西二十粁　初期部　六・〇秒
Origin: 20 km SW of Tokyo.　Dur. p. t.=6.0 s

	主要部第一波 S		主要部第二波 Next to S	
R3	12.0 (0.51) 1	4.7 (0.41) 1	24.2 (0.41) 1	12.5 (0.51) 1
C5	11.8 (0.48) 1.0	12.0 (0.46) 2.6	14.1 (0.46) 0.6	9.3 (0.46) 0.7
P3	8.5 (0.57) 0.7	15.5 (0.57) 3.3	13.6 (0.57) 0.5	24.2 (0.57) 1.8

(3) 十月二十四日十三時十四分九秒　微震
X 24: 13 h 14 m 09 s.　Slight
震原　手賀沼附近　初期部　七・四秒
Origin: Near Teganuma.　Dur. p. t.=7.4 s

	主要部第一波 S		主要部第二波 Next to S	
R3	3.7 (0.70) 1	3.5 (0.49) 1	7.8 (0.40) 1	5.8 (0.40) 1
C5	5.0 (0.56) 1.4	2.7 (0.56) 0.8	8.9 (0.56) 1.1	6.6 (0.68) 1.1
P3	3.8 (0.62) 1.0	3.4 (0.62) 1.0	6.8 (0.62) 0.9	7.5 (0.62) 1.3

(4) 十月二十五日十五時二分二十九秒 弱震
X 25: 15 h 02 m 29 s. Moderate
震原 東京灣 初期部 九・五秒
Origin: Tokyo Bay. Dur. p. t. = 9.5 s

	主要部第一波 S		主要部第二波 Next to S	
R3	27.7 (0.54) 1	31.8 (0.40) 1	40.4 (0.54) 1	60.3 (0.40) 1
C5	35.2 (0.47) 1.3	32.4 (0.57) 1.0	75.5 (0.47) 1.9	>48.5 (0.57) >0.8
P3	17.4 (0.59) 0.7	34.0 (0.59) 1.1	47.0 (0.59) 1.2	76.0 (0.59) 1.3

(5) 十月二十九日四時五十一分四十八秒 微震
X 29: 4 h 51 m 48 s. Slight
震原 東京の東北東六十五粁 初期部 一一・三秒
Origin: 65 km ENE of Tokyo. Dur. p. t. = 11.3 s

	主要部第一波 S		主要部第二波 Next to S		主要部二秒目 2 s after S	
R3	2.2 (0.46) 1	1.4 (0.46) 1	1.9 (0.46) 1	1.0 (0.46) 1	3.5 (0.46) 1	1.9 (0.46) 1
C5	2.2 (0.65) 1.0	1.8 (0.65) 1.3	1.8 (0.65) 1.0	1.9 (0.65) 1.9	15.5 (0.26) 4.4	2.3 (0.52) 1.2
P3	1.6 (0.53) 0.8	1.3 (0.53) 0.9	1.0 (0.53) 0.5	1.1 (0.53) 1.1	3.8 (0.27) 1.1	3.6 (0.39) 1.9

(6) 十一月二日六時十四分九秒 微震
XI 2: 6 h 14 m 09 s. Slight
震原 東京の北五十九粁 初期部 八・九秒
Origin: 59 km N of Tokyo. Dur. p. t. = 8.9 s

	主要部第一波 S		主要部第二波 Next to S		主要部六秒目 6 s after S	
R3	1.4 (0.50) 1	1.0 (0.50) 1	1.0 (0.50) 1	1.1 (0.50) 1	2.8 (0.50) 1	3.0 (0.50) 1
C5	1.0 (0.31) 0.7	0.3 (0.31) 0.3	1.6 (0.31) 1.6	0.8 (0.31) 0.7	3.1 (0.31) 1.1	1.3 (0.42) 0.4
P3	0.5 (0.41) 0.4	0.8 (0.41) 0.8	0.6 (0.41) 0.6	1.5 (0.41) 1.4	3.1 (0.55) 1.1	3.4 (0.55) 1.1

次に驗測結果の概要を述べます。

微動計に就いて

微動計の自己振動週期は、第一表にあります様に時と共に次第に小さくなりました。殊に器械の位置を變へた後は、振子の支點をなす圓錐形の部分を取換へたり種々の注意をしましたが、据付の時は滿足な結果を見せても間もなく週期は小さくなつてゐました。併し此の週期の差は本問題では測定値に影響しないと考へられます。又晝間に針が傾いて外れてしまふことが多くて困りました。五階、八階では溫度が上ると北東の方が低くなる様に現はれましたが、之は鋼骨の膨張の爲か、器械に原因があるか未だ明らかでありません。併し夜中には針は傾きませんでした。又地階でも全く傾きませんでした。針が傾く所では記象が重なる爲に晝間の地震は殆ど測定が出來ませんでした。

第二圖　建築物の自己振動週期の頻度
Fig. 2. Frequency-distribution of the self-vibration period of different floors.

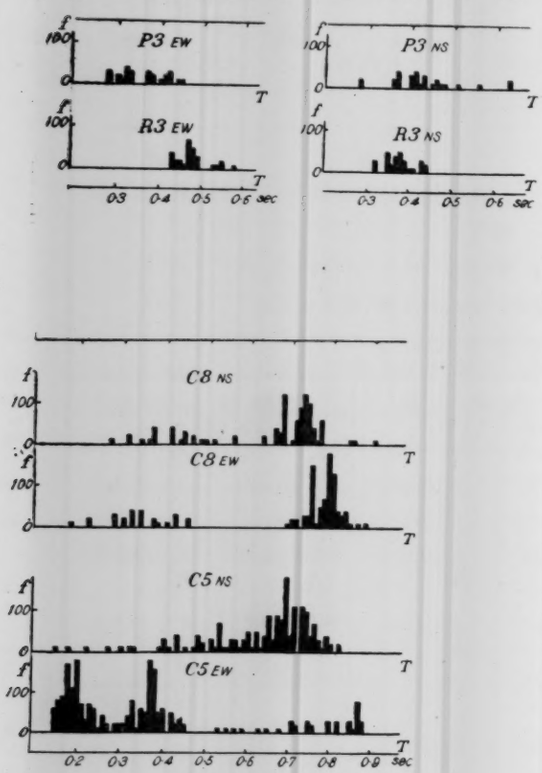

T....自己振動週期 self-vibration period
f ....同上頻度frequency of the same estimated per 0.01 sec.

此の驗測された週期に於ては 0.01 秒の桁は餘り信を置き難いことを斷つて置きます。

建築物の自己振動（第二圖）

地階は既にコンクリートで固めてあつた爲か、建築物の自己振動と思はれるものは全く現はれませんでした。地階で脈動を描いてゐるとき、上部ではその振幅の大さに比例して大きく振動し、脈動のないときは自己振動の振幅は小さくはなるが無くなることはありません。

中央塔の五階の東西動は週期が 0.37–0.38 s が多く、之が見えない時は 0.18–0.20 s が現はれます。又 0.2 s 位の小振動の重なつた 0.8 s 位の週期の振動も見えましたが、之は餘り明らかでありません。振幅は殆ど 0 から 0.008 mm まで

變はり、週期の大きい 0.8 s 位のものは 0.014 mm 位までになることがありました。晝間は他の所も、比較的週期の短い、振幅の大きい振動が現はれました。此は工事場の種々の機關の運轉や自動車、荷車等の影響に由ることが大きいものと思はれます。

五階の南北動は週期 0.65–0.75 s、振幅は 0–0.02 mm で稀には 0.04 mm 位になりました。一般に振幅は東西動よりも大きく現はれました。

中央塔の八階の東西動は週期 0.75–0.80 s 振幅は 0.32 mm まで、南北動は週期 0.68–0.74 s、振幅 0.034 mm まででありました。卽ち東西動と南北動とは殆ど等しくあります。

貴衆兩院の三階では器械の据付期間に暴風がなかつたことも一因でありませうか、一般に振幅は小さくありました。衆議院の東西動は週期 0.43–0.49 s で振幅は 0–0.006 mm、晝間には 0.03 mm 位に大きくなりました。南北動は週期 0.35–0.39 s、振幅 0–0.004 mm、晝間 0.012 mm、の振動がありました。貴族院の東西動は 0.32–0.42 s、0–0.006 mm、晝間 0.018 mm、南北動は 0.37–0.43 s、0–0.004 mm、晝間 0.024 mm でありました。大正十四年の驗測の時は貴衆兩院の自己振動週期は平均 0.66 s でありましたが、今回は約 0.4 s で前回よりも小さくなつて居ります。此の結果は前回には貴衆兩院が別々であつたのに、今回は中央部によつて接續され、鋼骨の組立が完成した爲に構造物の剛度を增し、又地階及び一階が一部分コンクリートで固められたことに因ると考へられます。

第三圖　五階と地面との振幅の比

Fig. 3. Ratio of amplitudes of vibration on the fifth floor and the ground.

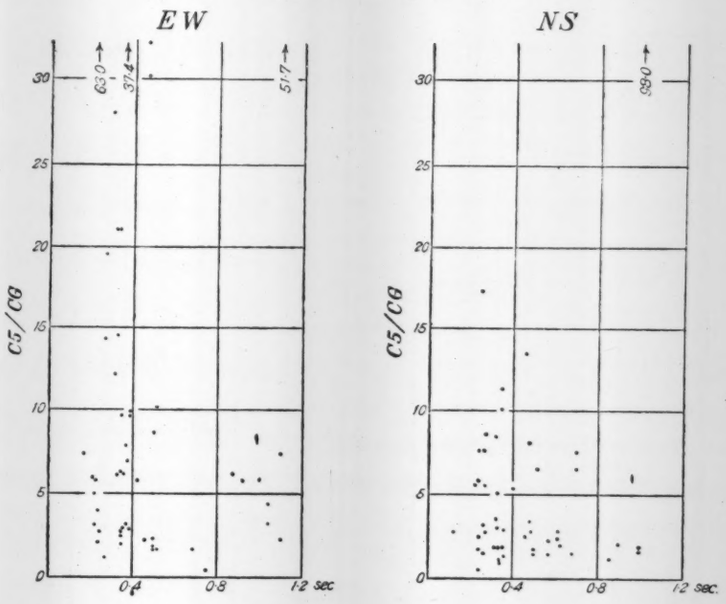

C5/CG....五階と地上との振幅比 Ratio of amplitudes.

T_{CG} .....地上の震動週期 Period of the vibration on the ground.

第四圖　八階と五階との振幅の比

Fig. 4　Ratio of amplitudes of vibration on the eighth and fifth floors.

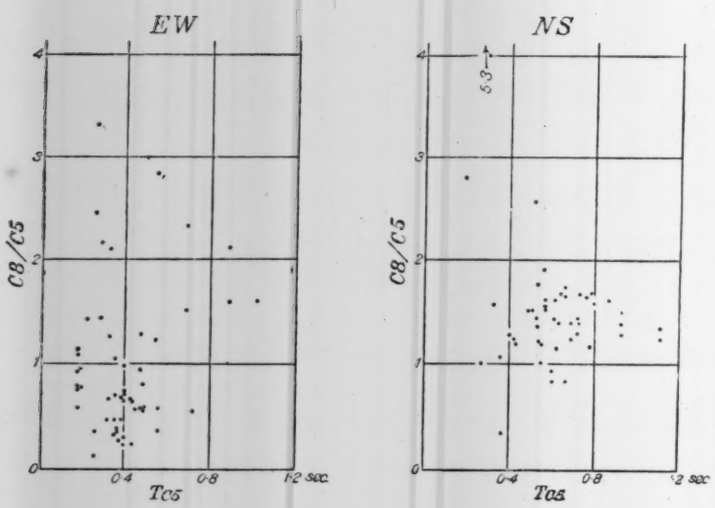

$C8/C5$....八階と五階との振幅比 Ratio of amplitudes.

T_{C5}.....五階の震動週期 Period of vibration on the fifth floor.

第五圖　八階と地上との振幅の比

Fig. 5.　Ratio of amplitudes of vibration on the eighth floor and the ground.

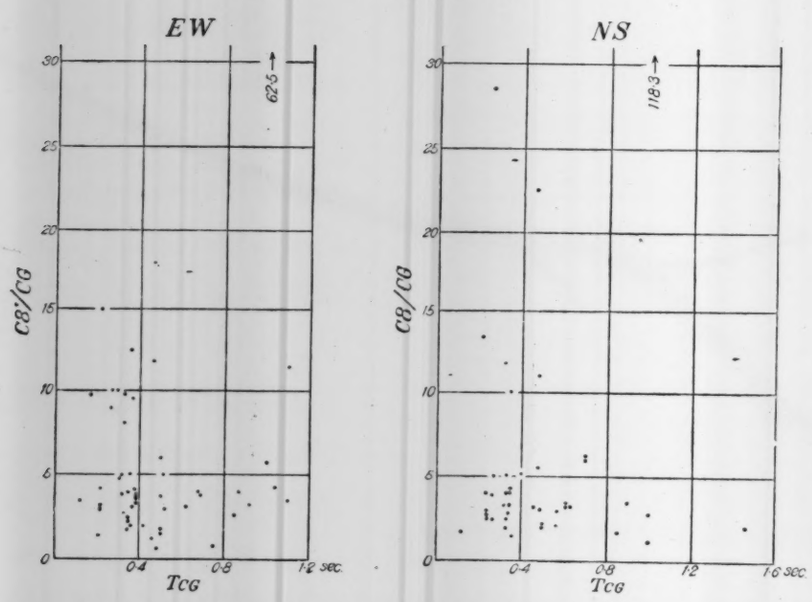

$C8/CG$....八階と地上との振幅比 Ratio of amplitudes.

T_{CG}.....地上の震動週期 Period of vibration on the ground.

地震による震動の驗測結果

地階にある微動計の地震記象と本郷の地震學教室内の同型の器械の記象とを比較するとその間に差は認められませんでした。

議院の塔の三個所では初動及び主要動の初めには、互に振動の相 (Phase) に差は認められませんでしたが、中間の主要動では違つて居りました。それは五階及び八階では地震動の週期に無關係に構造物の自己振動を混じ、主要動では特に著しく其の自己振動が現はれる爲でありませう。

中央部の東西動については地震動の週期が 0.3–0.4 s といふ五階の自己振動週期に近いときに、五階の振幅は地階よりも遙かに大きくなりますが (第三圖)、其

第六圖 地震に因る震動週期の頻度
Fig. 6. Frequency-distribution of the periods of vibrations due to earthquake.

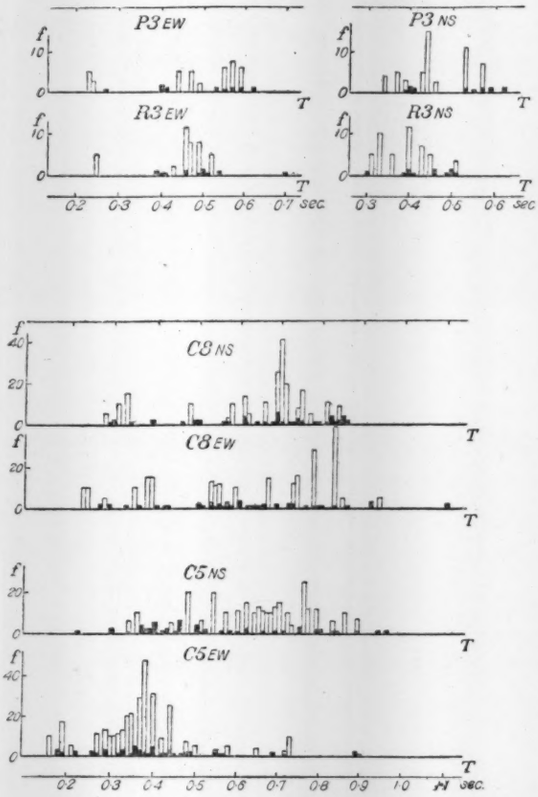

f 空柱 blanc column....最大地動に於ける震動週期の頻度 Frequency of vibration periods at max. earth's movement.

f 黑柱 blackened column....第二、三表に於ける地震動週期の頻度 Frequency of vibration period in Tab. II and III.

T....震動週期 vibration period.

の時八階は五階よりも却つて振幅の小さいことが一般であります（第四圖）。八階の週期については振幅の小さい時は五階の自己振動週期に等しい 0.4 s が現はれますが、振幅が大きくなると八階の自己振動週期 0.8 s が現はれます（第五圖、第六圖）。恰も棒の振動に於て一端固定他端自由の場合と兩端固定の場合との基本振動が現はれるものゝ様でありまして振動大なるとき第一の場合となり振動小なるとき第二の場合となるらしく思はれます。

次に南北動に就いては四階の振幅は地階よりも數倍大きく、その時週期は 0.6–0.7 s になり、八階の週期は 0.7 s 位で振幅は五階よりも更に大きくなり、塔は一端固定、他端自由の棒の基本振動の形をなすかと考へられます。

中央の塔では東西動の週期が場所によつて異なるのが著しいことであります。此事は中央塔と四階以下の部分との接續個所に於て東西の方向と南北の方向とが構造の安定上幾分の差異あることを示すものの様でありまして特に注目すべき點である様に感じました。

長週期の遠方地震では塔も地面と同様に震動しました。

貴族院、衆議院の三階では地震の時の週期は 0.5 s で、振幅は塔の五階とも大體等しい様であります。それ故、塔以外の部分は一體となつて震動すると思はれます。唯地震の時の週期が自己振動週期よりも 0.1 s 許り大きいのは測定の誤差によるのかも知れませんが少し注意をひきます。（第五圖、第六圖）

要するに、貴衆兩院では前回には構造は相等しいのに振動が異なつてゐたのは、その地盤が異なる爲であつたのでありませう。それが今回は中央部で十分に強く連結され又地階がコンクリートで固められたので全體として振動して、各〻の地盤の影響が無くなつた様に思はれます。

昭和三年八月三十一日二十二時十五分三十三秒ノ微震ノ記象

Registers of Earthquake of VIII 31:22^{h} 15^{m} 33^{s}

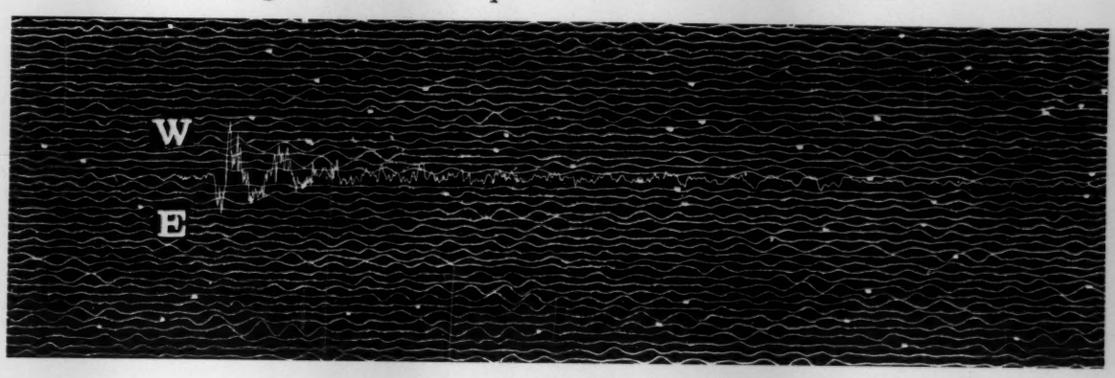

C G

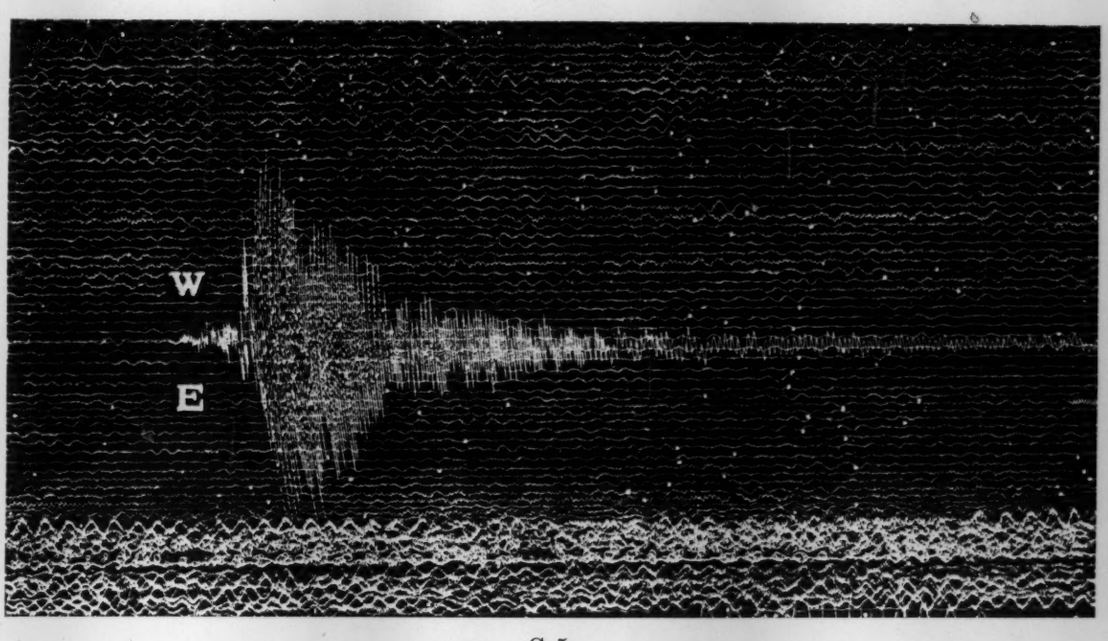

C 5

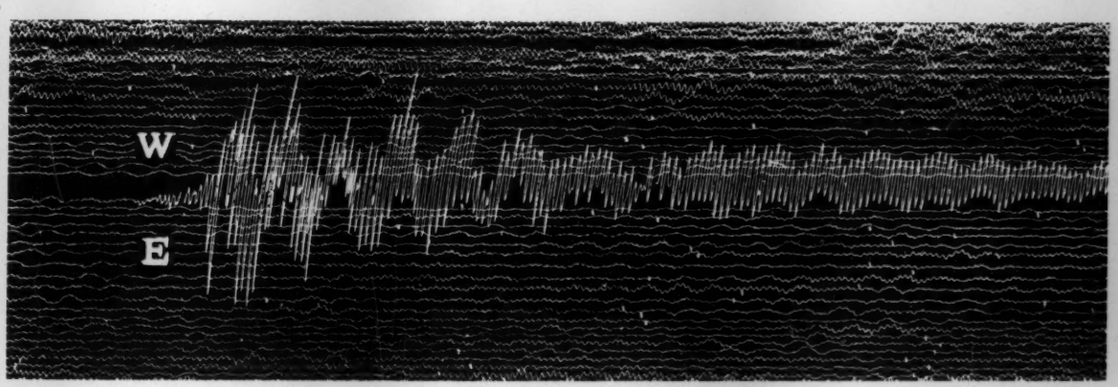

C 8

（震研彙報第五號、圖版、今村、岸上）

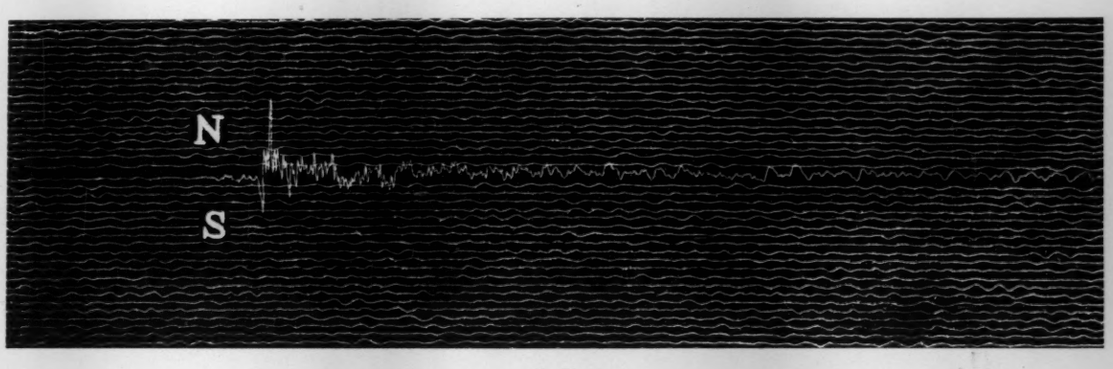

C G

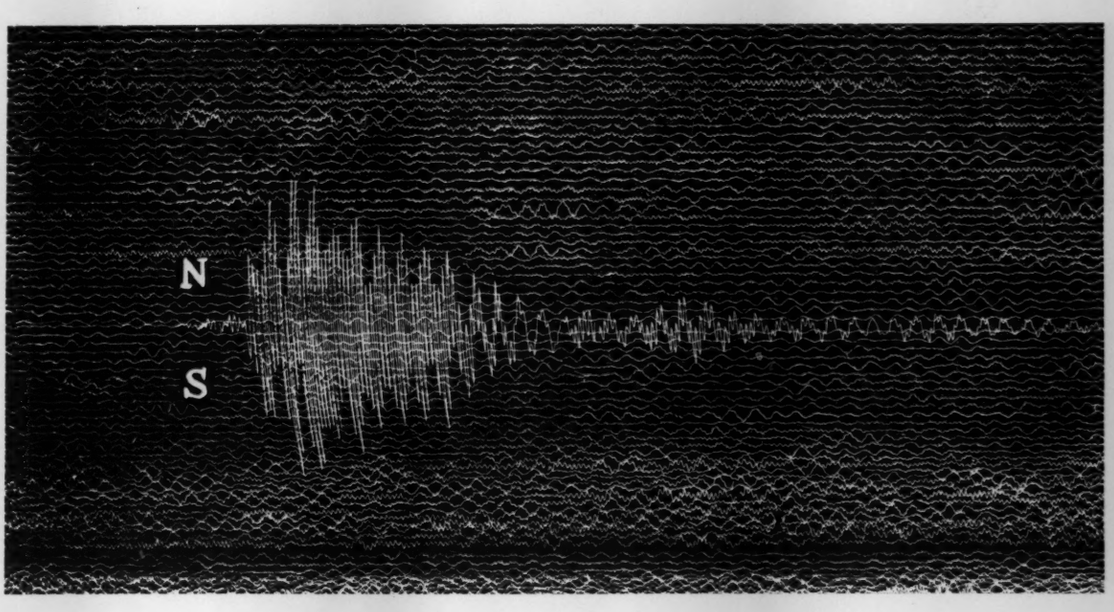

C 5

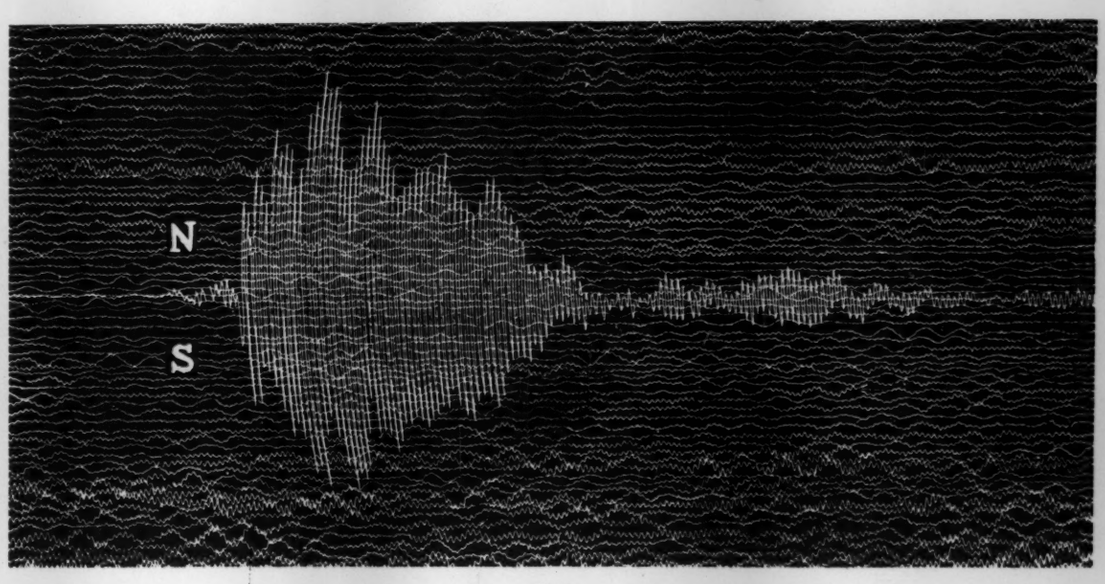

C 8

（震研彙報第五號、圖版、今村、岸上）

日 本 海 溝 の 形

（昭和三年一月海軍水路部刊行の同圖より轉載）

Form of the Japan Trench.

(Reproduced from the Chart issued by the Hydrographic Department, I. J. N.)

The Hydrographic Department of the Imperial Japanese Navy recently published a bathymetric chart giving the form of the "Japan Trench", revised with the data obtained by the sounding works carried out in 1926-27, which is reproduced in the annexed Chart (Pl. XVI), with the permission of the Department.

The following points are to be remarked:

1. The part of the trench with the depth above 6000 m. has become decidedly narrower than in the earlier chart.
2. A depth above 9000 m. has been found to E. of Idu Islands.
3. The depth formerly reported as $\overline{9950}$ off Nozimazaki could not be verified,

The Director.

最近に海軍水路部より昭和三年一月刊行の「日本海溝の形」と名くる近海深度圖を寄贈されたり。同圖は地震學者にとりても有益なるものと認め、同部の承認を得て此處に轉載する事とせり。

所　長

FORM OF THE JAPAN TRENCH (Depth in metres)

Red figures denoté soundings made by the "Mansyû" in 1926—27.

[Hydrographic Department, Imperial Japanese Navy.]

[Bull. Eqk. Res. Inst., Vol. 5. Pl. XVI.]

日本海溝の形 1927 XI 海軍大佐 重松良一 描畫

本圖は最近までの資料により描きたるものなり。南方諸島に沿ふ新水深は1926年10月軍艦滿洲(艦長重松良一)の測量其の他の新水深は1927年8.9月同艦(艦長海軍大佐 佐藤英夫)の測量による。(圖中赤色數字は新水深)

注意すべき要點

1. 6000m より深き溝が著しく狹くなりしこと。
2. 伊豆諸島の東側に 9000m より深き個所のあること。
3. 誉て野島崎沖合に $\overset{\bullet}{9950}$ と報ぜられしところは見當らぬこと。

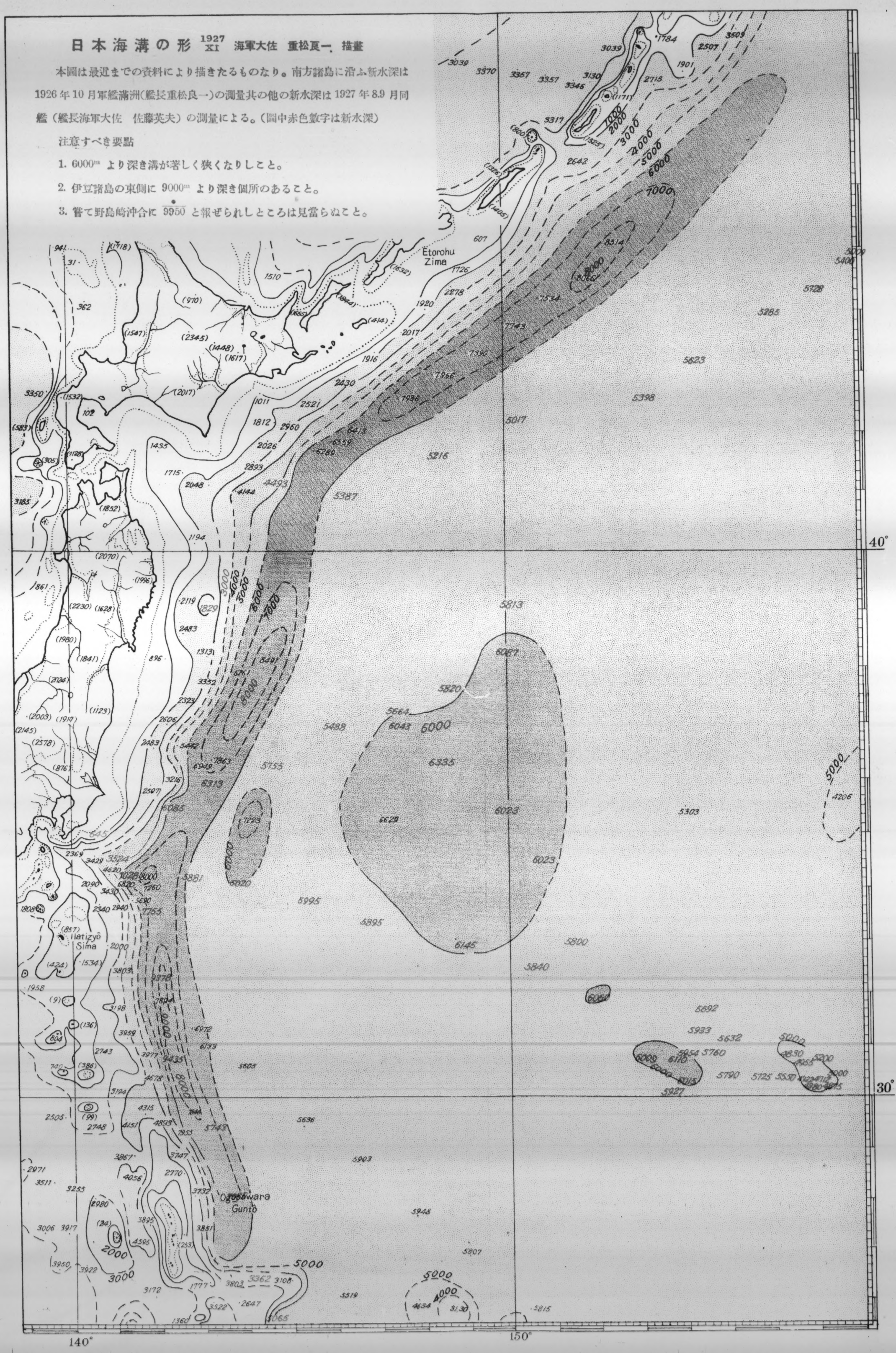

丹後震災地一等水準測量第二回及第三回檢測成果比較要圖

陸地測量部

Comparison of the Results of the Second and Third Precise Levellings in the Region Disturbed by the Tango Earthquake.

By

Hitosi OMURA, Major General, The Land Survey Department.

The comparison of the first and second precise levellings after the Tango Earthquake has already been reported in Vol. 4 of this Bulletin. The levelling work was resumed for the third time along the same route in order to detect any further vertical displacement. The result of comparison of the data of the second and third levellings is summarized in the synoptic map reproduced in the annexed Plate (Pl. XVII).

The time and duration of the field work for the two levellings are as follows:

The second levelling: June 1–July 31, 1927.

The third levelling: March 3—April 20, 1928.

(The dates for the second levelling given in Bull. 4 are to be corrected as above.)

丹後震災後に於ける第一回及第二回水準測量成果比較は既に彙報第四號に報告したり。本年更に引續き同一經路に就き第三回の檢測を行ひたるにより其成果を第二回の成果と比較し別紙要圖に圖示して參考に供す。

第二回並第三回檢測作業の期間左の如し。

第二回： 昭和二年六月一日より七月三十一日迄

第三回： 昭和三年三月三日より四月二十日迄

彙報第四號所載の第二回測量期間は上の通訂正)

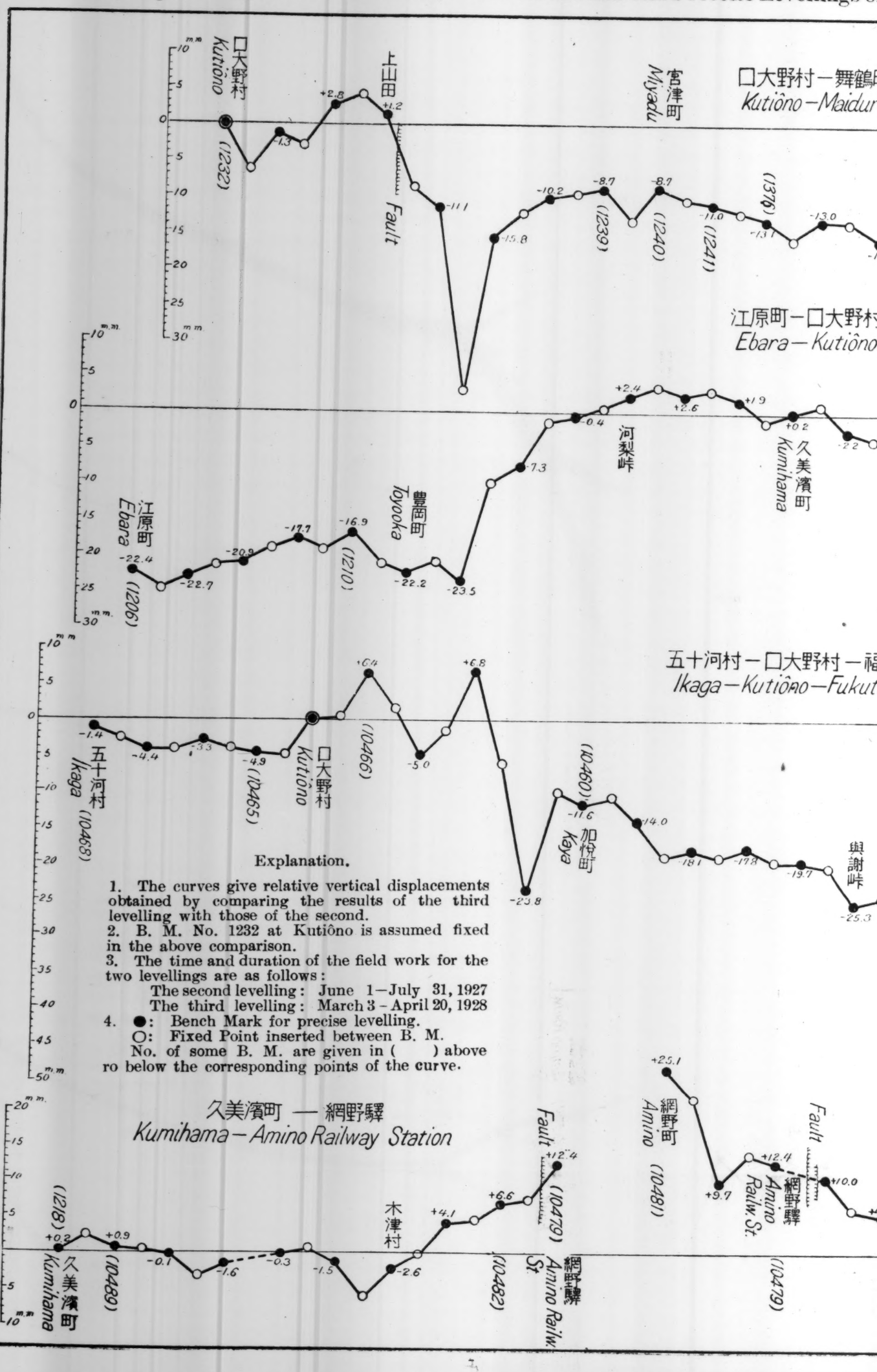
口大野村
Kutiôno
(1232)
宮津町
Miyadu
口大野村－舞鶴
Kutiôno－Maidur
Fault
江原町－口大野村
Ebara－Kutiôno
江原町
Ebara
(1206)
豊岡町
Toyooka
(1210)
河梨峠
久美濱町
Kumihama
五十河村－口大野村－福
Ikaga－Kutiôno－Fukut
五十河村
Ikaga
(10468)
(10465)
(10466)
(10460)
加悦町
Kaya
與謝峠
Explanation.
1. The curves give relative vertical displacements obtained by comparing the results of the third levelling with those of the second.
2. B. M. No. 1232 at Kutiôno is assumed fixed in the above comparison.
3. The time and duration of the field work for the two levellings are as follows:
The second levelling: June 1—July 31, 1927
The third levelling: March 3 - April 20, 1928
4. ●: Bench Mark for precise levelling.
○: Fixed Point inserted between B. M.
No. of some B. M. are given in ( ) above ro below the corresponding points of the curve.
久美濱町 — 網野驛
Kumihama－Amino Railway Station
(1218)
(10480)
木津村
(10481)
網野町
Amino
(10479)
網野驛
Amino Railw. St.
(10482)

丹後震災地一等水準測量第二回及第三回檢測成果比較要圖

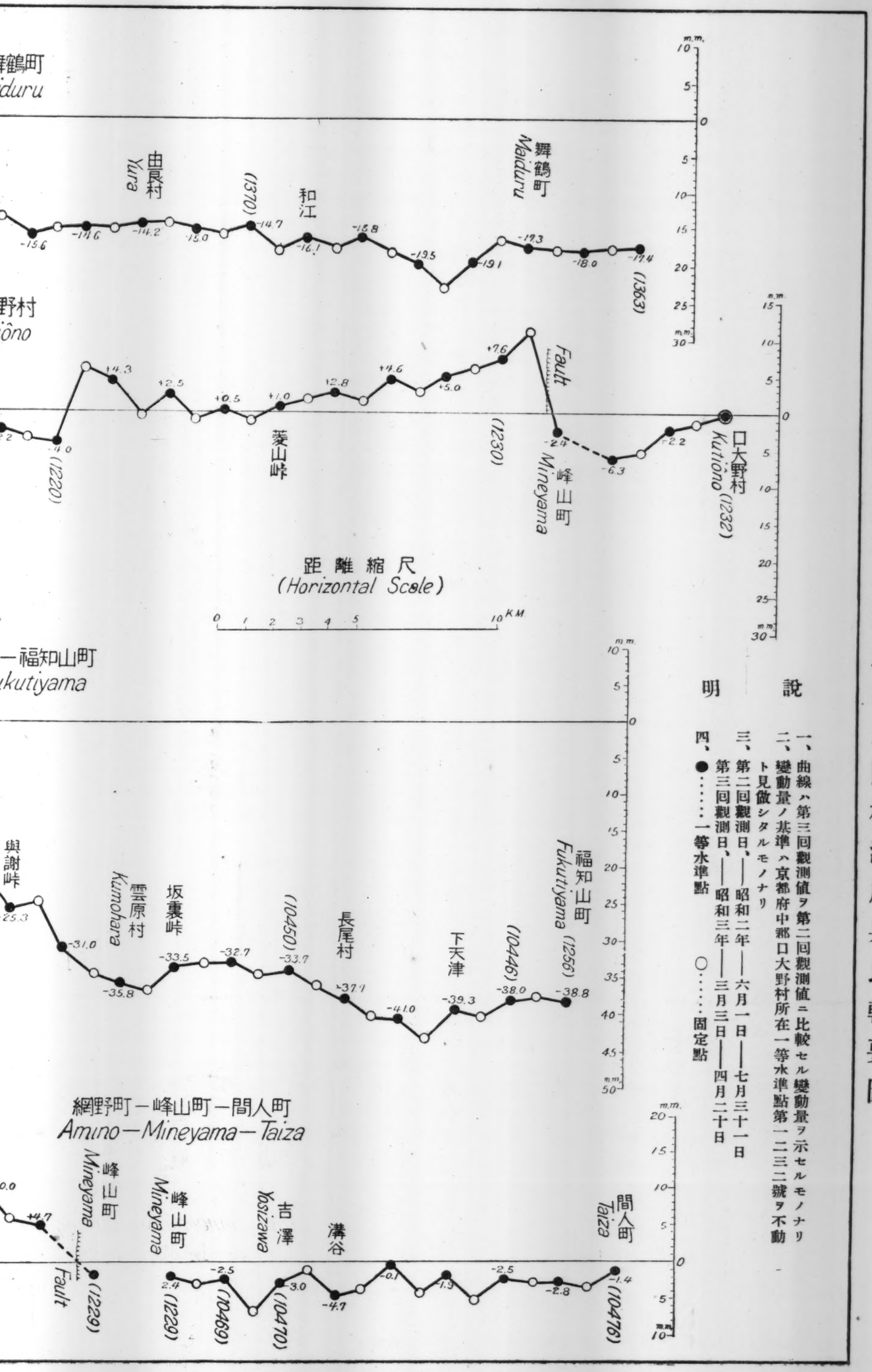

說明

一、曲線ハ第三回觀測値ヲ第二回觀測値ニ比較セル變動量ヲ示セルモノナリ

二、變動量ノ基準ハ京都府中郡口大野村所在一等水準點第一二三二號ヲ不動ト見做シタルモノナリ

三、第二回觀測日、——昭和二年——六月一日——七月三十一日

第三回觀測日、——昭和三年——三月三日——四月二十日

四、●……一等水準點　○……固定點

═所　報═

○ 談 話 會 記 事

第二十三回談話會（昭和三年二月二十一日）

1. 熔融シリカ製重力偏差計（豫備報告）	所員	坪井忠二
1. 丹後地震ノ餘震觀測調査報告（第二報）鄉村、山田ノ兩斷層ニ就テ	囑託	那須信治
1. 關東ニ於ケル氣壓勾配ノ長週期變化ト地震發生トノ關係	所員	井上宇胤
1. 東京及其近傍ニ於ケル地表傾斜變化觀測	所員	石本巳四雄
1. 彈性波ノ廻折ニ就テ	所員	妹澤克惟
1. 內部層ニ傳ハル彈性波ノ安定	所員	妹澤克惟
1. 長岡市西方强震調査補遺 附、但馬及丹後地震記象ニ對スル一見解	所員	松澤武雄
1. 關東大地震ニヨリ柱模灣底ニ生ジタル起伏ニ就テ	所員	長岡半太郎

第二十四回談話會（昭和三年三月二十日）

1. 丹後地震ニ於ケル地殼變動ニ就テ	所員 所員	寺田寅彥 宮部直巳
1. 關東地震ト海面	所員 囑託	寺田寅彥 山口生知
1. 關東地震ト河川ノ水位	囑託	山口生知
1. 越後西部ニ於ケル慢性的傾動	所員	山崎直方
1. 議院建築振動調査	所員 所員	今村明恒 岸上冬彥
1. 關東大地震前東京ニ於ケル土地ノ傾斜ニ就キテ	所員	今村明恒
1. 越後新潟地方精密水準測量ノ結果ニ就キテ	所員	今村明恒
1. 關東地震ニ就キテ	所員	長岡半太郎

第二十五回談話會（昭和三年四月二十四日）

1. 丹後震災三角測量ニ就テ 1. 同第三回一等水準測量ノ成果ニ就テ	三角科長 陸地測量師	青柳和夫 梅本豐吉
1 關東地方復舊高程測量ノ結果ニ就テノ研究	陸地測量師 工兵中尉	武藤勝彥 熱海景良
1. 東京水準網ノ垂直變動ニ就テ	工兵中尉 陸地測量師	熱海景良 武藤勝彥
1. 東京ヨリ興津、甲府ヲ經テ東京ニ復歸スル水準環線ノ垂直變動ニ就テ	工兵中尉 陸地測量師	熱海景良 武藤勝彥
1. 昭和三年三月二十三日荒川上流地震前後ニ於ケル傾斜變化	所員 囑託	石本巳四雄 辻光之助
1. 半無限體上ノ震動ノ擴散ニ就テ	所員	妹澤克惟
1. 丹後地震ト地殼變動（前回ノ續）	所員 所員	寺田寅彥 宮部直巳
1. 關東地震ニ就キテ（第三） （イ）岩漿分化（magmatic differentiation） （ロ）地震ノ周期ニ就テ	所員 所員	長岡半太郎 白井俊明

第廿六回談話會 （昭和三年五月廿二日）

1. 水準原點ノ眞高改訂ニ就テ — 陸地測量部
1. 關東地方ニ於ケル地塊ニ生ジタル傾斜ト垂直變動トノ關係ニ就テ — 陸地測量師 武藤勝彦
1. 三鷹村天文臺ニ於ケル傾斜變化ト氣溫トノ關係ニ就テ — 囑託 辻光之助
1. 四點觀測カラ地震波ノ速度ト震源ノ位置トヲ求メル一方法ニ就テ — 所員 高橋龍太郎
1. 鈴鹿山脈ノ成生 — 所員 多田文男
1. 丹後地方地殼變動（第三報） — 所員 寺田寅彦／所員 宮部直巳／所員 東庄三郎
1. 火山ノ形ニ就テ — 所員 寺田寅彦／所員 東庄三郎
1. 高溫蒸氣ト「鹽化ナトリウム」ノ作用ニヨル岩石ノ變化實驗結果 — 所員 長岡半太郎
1. 大洋底ノ平坦ニシテ安定ナル理由ト其沿岸ノ地震 — 所員 白井俊明

第二十七回談話會 （昭和三年六月十九日）

1. コンクリートノ長期腐蝕試驗 — 所員 內田祥三／濱田稔
1. 法文經第二號館鐵骨架構ノ振動觀測 — 所員 內田祥三／武藤清
1. 丹後地方地表傾斜變化ト餘震群ノ移動ニ就テ — 囑託 那須信治
1. 地震ノ S 波ノ傳播狀況 — 所員 松澤武雄
1. 變位ガ方位的ニ或分布ヲナス「レーレー」波ノ傳播（第一報） — 所員 妹澤克惟
1. 近海低氣壓ト海水面トノ關係 — 囑託 山口生知
1. 氣壓ト海水面 — 所員 寺田寅彦
1. 地震ト海底變動 — 所員 寺田寅彦
1. 震源ノ位置ヲ求メル作圖法ニ就テ — 中央氣象臺技師 和達清夫
1. 食鹽ト蒸氣ニテ變化シタル岩石ノ密度ノ變リ — 所員 長岡半太郎
1. 關東地震ト富士火山帶及ビ千島群島等ノ成因 — 所員 白井俊明

第二十八回談話會 （昭和三年七月三日）

1. 往復的歪力ニヨリ裂罅ノ生成 — 所員 藤原咲平
1. 附地震帶相互活動及餘震ニ關スル一考察 — 所員 高山威雄
1. 橫壓ニヨル砂層ノ破壞 — 所員 寺田寅彦／所員 宮部直巳
1. 島孤ノ形狀ニ就テ — 所員 寺田寅彦
1. 塔狀體ノ減衰振動及振動頻度ノ最高限度ニ就テ — 所員 末廣恭二
1. 震源ノ大サ — 所員 長岡半太郎
1. 盤梯山爆發ニ類スル現象 — 所員 長岡半太郎
1. 變位ガ方位的ニ或ル分布ヲナス「レーレー」波ノ傳播（第二報球面上ノ問題其他） — 所員 妹澤克惟
1. 逆振子微動計製作ト本所研究所建物ノ振動測定 — 所員 石本巳四雄／所員 高橋龍太郎

1. 大震ノ初期ニ現ハル緩漫ナル波動ノ一解釋 1. 關西地震帶活動ノ前後ニ於ケル地盤變動ニ就テ	所員	今村明恒

○ 出　張

昭和三年二月廿二日學術上取調ノ爲メ三重縣下ヘ出張	所員	多田文男
昭和三年二月廿四日地表傾斜觀測ノ爲メ新潟縣下ヘ出張	助手	高橋龍太郎
昭和三年三月廿日火山地質調査ノ爲メ山梨縣下ヘ出張	理學士	市來政兼
昭和三年三月廿九日地震事項調査ノ爲メ神奈川縣下ヘ出張	所員	今村明恒
昭和三年五月一日地震觀測用務ノ爲メ茨城縣下ヘ出張	助手	井上宇胤
昭和三年五月一日地表傾斜觀測ノ爲メ茨城縣下ヘ出張	所員	石本巳四雄
昭和三年五月廿二日學術上取調ベノ爲メ新潟長野二縣下ヘ出張	助手	坪井忠二
昭和三年五月廿三日地震事項調査ノ爲メ千葉縣下ヘ出張	所員 助手	多田文男 岸上冬彥
昭和三年六月廿七日地震事項取調ベノ爲メ千葉縣下ヘ出張	理學士	波江野清藏
昭和三年七月九日學術上取調ノ爲メ和歌山縣下ヘ出張	所員	多田文男
昭和三年七月九日地殼運動調査ノ爲メ高知縣下ヘ出張	理學士	渡邊光
昭和三年七月十九日火山地質調査ノ爲メ東京府下神津島及靜岡縣下ヘ出張	助手	津屋弘逵
昭和三年七月廿日火山地質調査ノ爲メ長野縣下ヘ出張	理學士	山田節三
昭和三年七月廿七日地震事項調査ノ爲メ和歌山縣下ヘ出張	所員	今村明恒
昭和三年八月四日地表傾斜觀測ノ爲メ京都府及和歌山縣下ヘ出張	所員	石本巳四雄
昭和三年八月四日地震事項調査ノ爲メ大阪府及和歌山縣下ヘ出張	囑託	那須信治
昭和三年八月六日傾斜計觀測ノ爲メ神奈川縣下ヘ出張	助手	高橋龍太郎
昭和三年八月十一日地表傾斜觀測ノ爲メ新潟縣下ヘ出張	助手	高橋龍太郎

昭和三年八月二十一日印刷
昭和三年八月二十四日發行

編纂兼發行者　東京帝國大學地震研究所

東京市神田區南神保町十六番地
印刷者　岩波茂雄

東京市神田區美土代町二丁目一番地
印刷所　三秀舍

東京市神田區南神保町十六番地
賣捌所　岩波書店

BULLETIN OF

THE EARTHQUAKE RESEARCH INSTITUTE

TOKYO IMPERIAL UNIVERSITY

August, 1928. Vol. V.

Contents

Papers Contributed

Observations of some of recent Earthquakes and their Time-Distance Curves. (Part I) (in English) ..... T. Matuzawa

Report of Inspection of the Strong Etigo Earthquake, Oct. 27, 1927. (in Japanese) ..... T. Matuzawa

On the Horizontal Shift of the Dislocation accompanied by the Recent Destructive Earthquakes in the Kwantô District and in Tango Province. (in Japanese) ..... A. Imamura, F. Kishinouye

On the Correlation between the Long Period Fluctuation of Barometric Gradient and the Occurrence of Earthquakes in Kwantô District, Japan. (in English) ..... W. Inouye

On the Diffraction of Elastic Waves. (in English) ..... K. Sezawa

On the Diffusion of Tremors on the Surface of a Semi-infinite Solid Body. (in English) ..... K. Sezawa

Rayleigh-type Waves propagated along an Inner Stratum of a Body. (in English) ..... K. Sezawa, G. Nishimura

Experiments on the Effect of an Irregular Succession of Impulses upon a Simple Vibrating System. (in English) ..... T. Terada, U. Nakaya

Physiographic History of the Oku-Tango Peninsula. (in Japanese) ..... F. Tada

New Method of Improving the Seismic Stability of Reinforced Concrete Dams. (in Japanese) ..... N. Mononobe

On the Vibration of the Imperial Diet Building. (Second report) (in Japanese) ..... A. Imamura, F. Kishinouye

Reports

Form of the Japan Trench. (in Japanese) (Reproduction) ..... Hydrographic Department

Comparison of the Results of the Second and Third Precise Levelling in the Region Disturbed by the Tango Earthquake. (in Japanese) ..... Land Survey Department

Institute Notes

(For the papers written in Japanese or in occidental languages, the abstracts are given in occidental languages or in Japanese respectively)